Development and Implementation of Early Detection Systems for Ground Movement
[Vermont Agency of Transportation Project Assignment 05-01]

Final Report

prepared for

Christopher C. Benda, P.E.
Program Development/Materials and Research
Vermont Agency of Transportation
1 National Life Drive
Montpelier, VT 05633-5001

by

Jeffrey D. Lloyd, Don J. DeGroot, P.E. and Alan J. Lutenegger, P.E.
Department of Civil and Environmental Engineering
University of Massachusetts Amherst
Amherst, MA 01003

7 July 2008

SUMMARY

The primary objective of this project was to study an unstable natural slope to determine if geotechnical engineering ground instrumentation can be used as an effective means of conducting remote automated slope monitoring and provide for early warning of slope instability. The Geotechnical Engineering Group at the University of Massachusetts Amherst (UMass Amherst), in collaboration with the Vermont Agency of Transportation (VTrans), instrumented an unstable natural slope located in Waterbury Center, VT. Instrumentation consisting of in-place-inclinometers, vibrating wire pressure transducers and a rain gage were installed together with an automated data acquisition and logging system in late Fall 2005. The instruments were monitored remotely from UMass Amherst between 2006 and spring 2008 using a PC desktop server, cellular connection, and data acquisition/database software. In situ tests conducted during the field drilling operations and laboratory tests conducted on samples collected from the site were used to determine a representative soil profile for the slope. This information was used in combination with water table elevation data to conduct limit equilibrium stability analyzes of the slope.

During the approximately two of years of monitoring the instrumentation, which consisted of automatically recording multiple daily readings and storing them on the server at UMass Amherst, the instrumentation were found to work well. Only a few periodic problems were encountered which were solved after a site visit to troubleshoot the problem. There were difficulties interpreting the inclinometer data in large part because they were not installed until several months after the inclinometer casing and some significant slope movement had already occurred.

The remote data acquisition and database management software were also found to work well and provide an easy to use, versatile system that can be simultaneously used for multiple projects. Furthermore, access and visualization of the data can readily be provided from any internet connection via a user and password protection system.

The site characterization program and stability analyzes showed that a relatively thin silty clay layer is the critical zone controlling movement of the Waterbury Center slope. Instrumentation data and field observations showed that slope movement can often be tied directly to the elevation of the ground water table. Thus in the absence in reliable inclinometer data for this project, readings from the instrumentation monitoring the groundwater table elevation can be used to set triggers for an early warning system. Specific values for these triggers can be set using individual instrumentation readings and/or any combination of readings or computed values to set different alarms levels (e.g., green, yellow, and red). These functions are straight forward to implement in the software system and alarms can be sent out using a variety of communication options (e.g., email, page).

It is concluded that the instrumentation, data acquisition and software systems used in this project are well suited for conducting remote, automated monitoring/detection of ground movement. However, a significant challenge for any project using such a system will be making a determination of what values or combination of factors should be used to set the alarm triggers. It is likely that the triggers will have to be tuned for each specific project as data are collected and more is learned of the ground response to key events (e.g., heavy rain, construction, etc.) so as to balance receiving the appropriate warning when merited but also avoiding too many false alarms.

TABLE OF CONTENTS

LIST OF TABLES

LIST OF FIGURES

LIST OF SYMBOLS

Symbol	Meaning	Units
a_1	High level alarm yellow threshold value	m (ft.)
a_2	High level alarm red threshold value	m (ft.)
b_1	Rate of change alarm yellow threshold value	m/min (ft./min)
b_2	Rate of change alarm red threshold value	m/min (ft./min)
c_1	Time history alarm yellow threshold value	m (ft.)
c_2	Time history alarm red threshold value	m (ft.)
AI_{HL}	High level alarm input	-
AI_{RC}	Rate of change alarm input	-
AI_{TH}	Time history alarm input	-
c'	Effective stress cohesion	kPa (psf)
F	Ground water table elevation factor	-
e_0	Initial void ratio of trimmed specimen	-
H_H	Highest ground water table elevation in monitoring well	m (ft.)
H_L	Lowest ground water table elevation in monitoring well	m (ft.)
H_t	Ground water table elevation at time of current reading	m (ft.)
N	Standard Penetration Test blows per 0.3 m (1 ft.)	-
S_t	Sensitivity	-
s_u	Undrained shear strength	kPa (psf)
s_{ur}	Remolded undrained shear strength	kPa (psf)
s_u/ σ'_{v0}	Normalized peak undrained shear strength	-
u	Pore pressure	kPa (psf)
w	Water content	%
w_n	Natural water content	%
α_{HL}	High level alarm weight	-
α_{RC}	Rate of change alarm weight	-
α_{TH}	Time history alarm weight	-
ΔH	$H_H - H_L$	m (ft.)

ΔL	Horizontal displacement	mm (in.)
Δ_{tc}	Time period for rate of change alarm	minutes
Δ_{th}	Time period for time history alarm	minutes
ε_{vc}	Vertical consolidation strain	%
ϕ'	Effective stress friction angle	°
γ_t	Total unit weight	kN/m^3 (pcf)
γ_d	Dry unit weight	kN/m^3 (pcf)
σ'_p	Preconsolidation stress	kPa (psf)
σ'_{vc}	Vertical consolidation effective stress	kPa (psf)
σ'_{v0}	In situ vertical effective stress	kPa (psf)
σ_{v0}	In situ vertical total stress	kPa (psf)
τ_h	Horizontal shear stress	kPa (psf)

1.0 INTRODUCTION

1.1 BACKGROUND

The movement of unstable slopes can create unsafe conditions and costly damage to property and infrastructure. Installation and monitoring of ground instrumentation such as inclinometers is typically used to observe slopes and ideally to provide a precursor to unsafe conditions. However, traditional monitoring of slopes using instrumentation and site visits to record instrumentation data is personnel and time intensive. This can result in infrequent readings and reduces the likelihood of early detection of potentially serious slope movement. This is further exacerbated for sites in remote locations that are either difficult to access or time consuming to reach. A potentially economical and reliable solution to this problem is to implement an automated monitoring system that incorporates ground instrumentation, data acquisition equipment, cellular technology and server based data reporting. Furthermore, the system can be used to set triggers based on individual instrumentation readings or various combinations of such, which when activated can send out alarms to key personnel. Together such a combination of hardware and software can provide for an automated early warning system.

This report presents the results of a project conducted with the Vermont Agency of Transportation (VTrans) that investigated the application of automated monitoring of field instrumentation for an unstable natural slope and implementation of an early warning system.

1.2 PROJECT OBJECTIVES

The primary objective of the project was to study an unstable natural slope to determine if geotechnical engineering ground instrumentation can be used as an effective means of conducting remote automated slope monitoring and provide for early warning of slope instability. Within the scope of this primary objective, key project goals were to: 1) identify a test site with a potentially unstable slope, 2) select appropriate instrumentation, data logging equipment, and data management software, 3) install the instrumentation at the test site and automate the data logging, and 4) analyze the recorded data and implement an automated system for slope monitoring and near real-time early warning of slope movement.

1.3 PROJECT TASKS

The following project tasks were proposed to fulfill the objectives noted in the previous section:

Task 1: Selection of Test Site.

Identify a test site together with VTrans that consists of an unstable natural slope for installation of instrumentation and data acquisition equipment.

Task 2: Evaluation and Selection of Measurement Methods.

Review current instrumentation systems available and their associated costs. Based on the selected test site and in consultation with an instrumentation vendor, select a modular instrumentation and data acquisition system suitable for this project and that can also be used for future VTrans projects.

Task 3: Installation of Monitoring System.

Together with VTrans, install the field instrumentation and data acquisition equipment at the selected test site. Instrumentation should include in-place inclinometer strings, open-standpipe piezometers, a barometer, a rain gauge and a data logger system.

Task 4: Remote Monitoring of Instrumentation

Implement the hardware and software required to set-up a remote monitoring and database management system. The system will need to automatically download the instrumentation data, store and process the data, and display the data on a server at UMass Amherst and simultaneously be made available on the internet (via password access).

Task 5: Site Characterization

Together with VTrans, conduct a site characterization program consisting of in situ and laboratory tests. The primary purpose of the site characterization program is to provide geotechnical engineering design parameters (e.g., effective stress friction angle and cohesion) for the key soil units at the site. These data are to be used to conduct a numerical analysis of the stability of the slope.

Task 6: Instrumentation Data Analysis and Numerical Analysis

Analyze the instrumentation data to investigate data trends that could potentially serve as precursors of unstable slope conditions. These data should be analyzed in conjunction with numerical analysis of slope stability using a limit equilibrium program. Investigate relationships among the slope factor of safety, ground water table elevation and inclinometers readings. Determine if these data can be used to develop triggers and hence alarms for early warming of slope movement.

Task 7: Summary of Lessons Learned and Recommendations

Synthesize the project results into a final report and provide VTrans with a summary of lessons learned and recommendations for implementation of automated monitoring of instrumentation data for early warning of slope movement for future projects.

1.4 PROJECT ORGANIZATION

This project was funded by VTrans under the title "*Development and Implementation of Early Detection Systems for Ground Movement*," Vermont Agency of Transportation Project Assignment 05-01. The project was approved for funding with an initial start date of 10 March 2005 with an eighteen month duration. Total project budget equaled $104,953, which included approximately $36,500 for instrumentation, hardware and software. The original project proposal was prepared by Professor Jason T. DeJong of UMass Amherst and who also served initially as the project Principal Investigator (PI). Professor DeJong resigned his position at UMass Amherst effective August 2005 and Professor Don J. DeGroot was thus approved as the project PI and Professor Alan J. Lutenegger as the Project Co-PI. Professor DeGroot returned from his sabbatical in September 2005 and assumed his role as Project PI at that time.

The project proposal originally planned for installation of an instrumentation package for the St. Johnsbury Railroad Slope Area project but during the initial months of the project this site was no longer available for testing. The original instrumentation order (from Geokon Inc.) was cancelled and subsequently needed to be re-ordered in the Fall 2005. The instrumentation was installed at the Waterbury Center site during December 2005 to January 2006. As a result of these delays a no-cost extension was approved by VTrans until June 2007. At the end of this no-

cost extension the instrumentation was left on site and UMass Amherst continued to collect and analyze the data until April 2008.

This report is the final report for the project. Chapter 2 presents a brief summary of background information and prior research on slope monitoring and automated recording of geotechnical instrumentation. This information was in part used as a basis for describing the instrumentation selected for monitoring the Waterbury Center site, the methods for instrumentation data recording, and methods for data management. Chapter 3 describes the equipment and methods used to install the instrumentation system, data acquisition system, and the field and laboratory testing program. A site location, description and geologic history are presented in Chapter 4 together with a developed representative site soil properties profile based on this information and results of the in situ and laboratory site characterization testing programs. Chapter 5 presents examples of data collected from the Waterbury site instrumentation and interpretation of that data. Results of the slope stability analysis are presented in Chapter 6 and are used for the basis of proposing a methodology for using the data to develop an early warning system. Chapter 7 concludes the report with lessons learned on this project regarding the instrumentation, data logging, and data storage and visualization aspects. Additional recommendations based on recent developments in field instrumentation are also given.

2.0 SUMMERY OF LITERATURE

This chapter presents a brief summary of background information and prior research on slope monitoring and automated recording of geotechnical instrumentation. The traditional inclinometer method, justification and methods for instrumentation data recording, and methods for data management are covered.

2.1 TRADITIONAL SLOPE MONITORING

The movement of unstable slopes can create unsafe and costly damage to property and infrastructure. Monitoring of unstable slopes has traditionally been a time and labor intensive activity using hand inclinometers and open standpipes.

Dunnicliff (1988) described inclinometers as a "gravity-sensing transducer designed to measure inclination with respect to vertical." Traditional inclinometer systems (Figure 2.1) include a permanently installed guide casing which can be made of PVC, aluminum, fiberglass, or steel, and is grooved to control the orientation of the transducer probe. A portable readout box is attached to the transducer probe with a graduated electrical cable, allowing for the depth of the probe to be known. The transducer probe incorporates guide wheels to align its orientation within the casing.

During a survey of the inclinometer, the transducer probe is lowered to the bottom of the casing and then is raised incrementally as additional readings are made. Typical increments are 0.5 m (1.6 ft.) or 0.61 m (2 ft.) (Furlani et al. 2005).

Since measurements are taken at the site by technicians, labor costs can be high, often including travel to and from the site. Sites in remote areas may be measured infrequently, leading to the potential that important slope movement information is missed.

2.2 AUTOMATION OF GEOTECHNICAL INSTRUMENTATION

In an effort to increase performance and efficiencies while reducing costs, the geotechnical instrumentation industry has been moving towards an "intelligent" construction site which requires that more continuous data be delivered to users (Furlani et al. 2005). In the past, cost had largely dominated the automation of instrumentation. Marr (1999) argued that

automation could only be roughly justified when there is a "large number of sensors (more than 50), the need for readings to be taken more than once a day, the need for all readings to be taken within seconds of each other, and difficult site access," either for safety or long access time. However, developments in information technologies, computers, and the internet have increased the reliability of automation and lowered costs. By 2005, Marr (2005) updated the justification for automation of instrumentation to situations where the "number of sensors exceeds 50, where significant changes can occur within one week, where access to the instruments requires more than one person, or where the travel distance to the site exceeds a one-hour drive." Further, Marr (2005) summarized the reasons to automate instrumentation as:

- Reducing the time to obtain and evaluate data
- Provide automated warning
- Get data from remote or dangerous locations
- Record more readings
- Take readings where rate of change is too fast for manual approaches
- Measure different parameters at the same time
- Improve reliability of data
- Lower cost of monitoring

Automation of traditional inclinometers has often been accomplished with In-Place Inclinometers (IPIs), incorporating a fixed string of sensors that do not require on-site manipulation while being installed in traditional grooved casing (Furlani et al. 2005). Figure 2.2 presents a typical IPI installation. Each IPI string is usually made up of multiple gravity sensing transducers (e.g., tilt meter) connected together by rigid connecting tubing. A pivot at each sensor allows for displacement to occur, with each sensor measuring its change in tilt relative to the pivot below. Since each IPI string is dedicated to one borehole throughout the monitoring period, multiple IPI strings must be used for each project, rather than one traditional hand inclinometer. This can make IPI equipment expensive (Bennett et al. 2007, Furlani et al. 2005).

The main component of an automated data acquisition system is a datalogger. Kane and Beck (2000) described the datalogger as a small computer with a voltmeter and memory. The datalogger "can be programmed to output specific voltages over certain durations, read voltages, and store values." The datalogger is usually installed at the site in a protective enclosure to protect it from the environment. Instruments are either directly wired to the datalogger or

through a multiplexer, allowing for up to 16 instruments to be wired to one port on the datalogger, increasing the instrument capacity of the datalogger. Some multiplexers can be connected in series to each other, further increasing instrumentation capacity.

Many dataloggers use 12V DC power, supplied by internal and external batteries. Power requirements can vary depending on the type and number of instruments installed and the type of datalogger communication. At sites where grid power is available, the external battery can be replaced by hardwired external power. Typical remote installations will use a 12V deep cycle marine battery, trickle charged by one or multiple solar panels (Ding et al. 2000, Kane and Beck 2000).

Reliable communication to the datalogger is of importance once the data collection has been automated. Many commercially available dataloggers have numerous communication options available. Table 2.1 outlines the options available for Campbell Scientific dataloggers (Campbell Scientific 2006). Where frequent access to the site by a technician is possible, or where monitoring data is not needed regularly, direct access to the datalogger by a laptop to download the data is available. This option is also useful for site maintenance visits regardless of the primary communication method. A direct telephone connection to the datalogger has traditionally been the most reliable, but in the case of remote dataloggers, this option is not always available (Kane and Beck 2000). Radio modems using a variety of spectrums are available for both short and long ranges, and in addition to requiring a transceiver at both ends often need direct line of sight between antennas (Campbell Scientific 2006, Ding et al. 2000, Kane and Beck 2000).

Radio modem to telephone modem bridges are available, creating a radio link from the datalogger to the nearest telephone connection, potentially reducing the radio network infrastructure requirements. Gaining in popularity is cellular phone based communications, sharing the remote application benefits of radio communications with the ease of telephone communications. Using a cellular modem at the datalogger and a standard telephone modem at the office, a communication link can be created for remote data downloading and datalogger programming (Campbell Scientific 2006, Ding et al. 2000, Kane and Beck 2000, Simeoni and Mongiovi 2007).

2.3 DATA MANAGEMENT

Automation of instrumentation can lead to the creation of large amounts of data. One instrument polled every two hours over a period of a year will collect over 4300 readings. A robust hardware and software system to store, process, and display the data is required.

The traditional method of data management has included the binary or text file generated by the datalogger, which is usually imported into a spreadsheet for manipulation and plotting. The data files can accumulate over time, and the spreadsheet file can become large and overwhelm the processing capability of the computer. Working with old data could involve investigative work to find the relevant data among many files before results can be achieved (Thorarinsson 2007).

Drawing from the experience of industrial Supervisory Control And Data Acquisition (SCADA) systems, relational database programs that conform to the Structured Query Language (SQL) standard have gained acceptance for geotechnical datalogging (Kosnik 2007, Thoranrinsson 2007). Kosnik (2007) explains that "relational databases are specifically designed for storing and searching large datasets." Since the "SQL standard provides a clear and widely-supported abstract method of interacting with the database … data may be retrieved from the database by date range, by event type, or for time periods in which a particular threshold is exceeded on one of the measured channels." The use of a database removes the manual and time-consuming task of looking for specific data using the traditional method of data files.

All database programs need a user interface for user input and graphical data display. Many systems incorporate a graphical site interface similar to SCADA systems where the latest measured values of instruments are displayed over a background map, flow diagram, or photograph (Thorarinsson 2007). When alarms are incorporated, the background color of each measured value can change from green to yellow or red, allowing the operator to quickly determine the status of the instrumentation (Thorarinsson 2007).

Of interest to geotechnical engineers are the trends of recorded data over time. The database user interface should be capable of quickly generating charts over time periods of weeks, months, years, or any user-specified time period (Kosnik 2007, Thorarinsson 2007). Thorarinsson (2007) also notes that the graphs should be able to display results from several variables at once, such as data from multiple similar instruments. Adjustable scales on the axes

such as inverse, logarithmic, fixed or auto-scale, as well as adjustable colors and icons, are important graphing features.

The use of auto scale on a graph axes can highlight instrument errors where the default error value can be significantly different than actual readings. The use of automatic data validation, either by the user-interface program or during data importing to the database, can be useful to clean the data (Thorarinsson 2007).

Depending on the datalogger programming, the data imported into the database may be raw instrument readings. Conversion into engineering units is necessary for understanding of the instrumentation. Thorarinsson (2007) discusses the ability of the user-interface program to create a "virtual variable," a variable that is "calculated as a function of a variable already in the database." The instrumentation result in engineering units could be a virtual variable of the raw data value from the datalogger, streamlining the datalogger programming. In addition, new values can be calculated from separate readings, for example wind chill is a function of air temperature and wind speed.

The greatest change for the user-interface program has been the development of an internet component. Viewing the data required a separate copy of the user-interface program on every computer used, and a connection through the local area network to the database. Users outside of the local network may have limited or no access (Thorarinsson 2007). The addition of an internet component gives access to the data for all users regardless of location, as well as the potential to give access to clients or the general public. Adding internet access could be through commercial stand-alone clients, custom software, or be included with the datalogger/database/user-interface software package (Kosnik 2007, Thorarinsson 2007). Access control is an important part of the software, giving different access levels to different users, for example managers having access to several projects and technicians only having access to parts of a selected project.

2.4 EXAMPLE CASE HISTORIES

There are several published case histories about the use of instrumentation for slope stability monitoring or related work. Table 2.2 summarizes some of these case histories.

Hawkes and Marr (1999) discuss the data acquisition and geotechnical instrumentation on Boston's Central Artery/Tunnel Project. The project involved "one of the most extensive

geotechnical instrumentation systems ever deployed." Using a balance of technicians and electronic equipment, data was analyzed and distributed to project engineers within 24hrs of data collection. Although automated data collection systems are designed to reduce manpower, collect large quantities of data, and provide rapid reporting, on the Central Artery/Tunnel Project it was not financially feasible "because of the large cost of installing and maintaining such a system in a large congested construction environment."

Xiaoli et al. (2000) present results on using automated geotechnical instrumentation to monitor slopes in an Australian open pit mine. Extensometers and other instruments such as inclinometers, tilt meters, and piezometers, were connected to a datalogger and linked to a central computer via radio modems. Over a period of four years, the results indicate that the system was accurate and reliable, providing data 24 hours a day in all weather conditions.

O'Connor et al. (2001) used geotechnical instrumentation to monitor subsidence of I-70 in Pennsylvania due to underground mining. Time domain reflectometry (TDR) and GPS-based surveying were used to monitor ground deformation as mining activity passed underneath the highway. Tiltmeters were connected to a datalogger that automatically collected and stored measurements. The datalogger also compared measurements with pre-determined threshold values and automatically sent out alarm phone calls to alert key personal of a situation. The authors found that "installation of the instrumentation required oversight by experienced personnel during the startup stage." They also found that the automated monitoring allowed them to continuously monitor a 300 m long section of interstate but concentrate visual monitoring at critical locations identified by the instrumentation.

Kane et al. (2004) present an automated coastal bluff monitoring and alert system. Since bluff failure could occur at any point along a 1000 m stretch of active railroad track, a horizontal TDR array was used. Because of the large length of slope to be monitored, traditional tiltmeters or IPIs were deemed impracticable. The TDR array was continuously monitored through dataloggers and in the event of measured deformation an automated telephone call was made to key personnel. As the TDR was used to determine deformation events to raise an alarm and not the magnitude of deformation, the authors found that "TDR-based monitoring has excellent potential safeguarding railroads and highways."

Dennis et al. (2006) looked at using TDR as a replacement for inclinometers to monitor shallow failures in engineered cut slopes and embankments. Along a stretch of I-540 in

Arkansas, four field sites were instrumented with both TDR and inclinometers. It was found that TDR to monitor slope movements remotely is a feasible alternative to the more labor intensive methods such as surveying and inclinometer readings, and that "a complete TDR system can be created and installed for less money than the purchase price of a probe type inclinometer and datalogger." However, although laboratory and field results indicate that there is a strong correlation between the reflected energy measured in TDR cables and deformation, the correlations measured in the lab were different than those measured in the field, thus it was not possible to use the TDR data to compute actual deformation of the slope.

Lollino et al. (2006) used an Automatic Inclinometer System (AIS), piezometers, and rain gauges to determine a correlation between heavy rainfall events and slope movement of the Montalido di Cosola landslide in Italy. Through detailed analysis, a time lag between heavy rainfall and slope movement was determined. Using this time lag, the AIS could be scheduled to take additional readings during expected times of slope movement, creating an early warning system.

Bennett et al. (2007) discussed state-of-the-art micro-machined electromechanical sensors (MEMS) to measure 2D soil acceleration and 3D ground deformations. The MEMS accelerometers were assembled into Wireless Shape Acceleration Arrays (WSAA) for installation in the field. WSAAs are able to begin automated data transfer almost immediately after installation, providing full 3D position and orientation data at intervals of 305 mm to depths of up to 100 meters, providing significant time savings compared with a traditional inclinometer reading.

Kosnik et al. (2007) presented case studies of several automated remote monitoring projects Northwestern University's Infrastructure Technology Institute (ITI) has developed and deployed. Using a variety of instrumentation at the different projects, including TDR, remote total stations, and geophones, all the projects used a common web based interface to analyze, store, and display the collected data. The web based interface helped "maximize the usefulness of remote monitoring" and the authors recommend such a system for future instrumentation projects.

Simeoni and Mongiovi (2007) discussed the installation of an automated monitoring system at the Castelrotto landslide in Italy. Automated in-place-inclinometers were installed and combined with periodic manual probe inclinometer readings. A statistical procedure for

comparing the automated data with the periodic manual readings was developed to measure the reliability of the data. Since automated monitoring is often used for early-warning systems and decisions about safety are dependent on the data collected by the instrumentation, Simeoni and Mongiovi (2007) stressed that checks on the reliability of the data is of importance.

Barendse (2008) evaluated the use of MEMS based IPI sensors known as the ShapeAccelArray (SAA) to measure vertical and horizontal ground displacement during a bridge replacement along the Champlain Canal in New York. The SAAs were found to provide "continuous ground deformation profiles in both vertical and horizontal applications utilizing autonomous remote monitoring." In addition, the vertical SAA results correlate well with the traditional probe inclinometer and the "horizontal SAA results are consistent with the predicted foundation response." Although further field trials are needed, it was concluded that the MEMS-based IPI system can be used for real-world applications.

2.5 SELECTION OF INSTRUMENTATION AND DATA LOGGER SYSTEM FOR THE WATERBURY CENTER SITE

To automate monitoring of the Waterbury Center slope for this project, two in-place-inclinometers strings were selected. To verify the reliability of the instrumentation, the second IPI string was installed outside the zone of active slope movement and a separate inclinometer casing was installed in close proximity to the IPI string to measure deformation using a traditional probe inclinometer. Two open-standpipe piezometers were installed inline with the expected slope movement to measure the ground water table. It was decided to automate the data recording by connecting the instrumentation to a Campbell Scientific CR10X-based datalogger. Given the semi-remote location, a deep cycle marine battery charged with a solar panel was selected for power input. The RS-232 serial connection was selected for datalogger communications on site and a cellular phone modem was selected to allow for remote communications with the datalogger. Multilogger software from Canary Systems was selected to program the datalogger, and was updated during the project to provide a database-based data storage and internet-based user interface system.

Table 2.1 Campbell Scientific CR10X Datalogger Communication (Campbell Scientific 2006)

Type of Communication	Description
Telephone Networks	Use landlines or cellular transceivers
Radio Frequency (RF)	UHF, VHF, spread spectrum, or meteor burst radios
Direct Links	RS-232 serial or USB connections
PDAs	Using PalmOS or Windows CE to monitor or retrieve data and transfer programs
Short Haul Modems	Local communications via RS-232
Multidrop Interface	Links a central computer to one or more dataloggers over a distance of 4000 ft.
Satellite Transmitters	Transmit data via GOES or Argos satellite systems
Ethernet Communications	Communication over a local network or the internet
Storage Modules	Store data and programs, transfer programs, and independent local backup of data
CR10KD Keyboard Display	Program, manually initiate data transfer, and display data
Other Displays	DataView Display Unit and DSP4 Heads Up Display for displaying data

Table 2.2 Summary of Geotechnical Instrumentation Case Studies

Authors	Project	Instrumentation	Summarized Findings
Hawkes and Marr (1999)	Central Artery/Tunnel	Variety	Automated system not financially feasible
Xiaoli et al. (2000)	Automated deformation measurement for slope stability of an open pit mine	Extensometers	Over an extended period, the system is accurate and reliable
O'Connor et al. (2001)	Subsidence along I-70	TDR, GPS, Tiltmeters	Experienced personnel for instrumentation installation, automated monitoring provided useful information
Kane et al. (2004)	Automated early warning for coastal bluff slope movement	TDR	TDR monitoring of slope movement has excellent potential
Dennis et al. (2006)	Slope stability along I-540	TDR	TDR cannot measure deformation, TDR less expensive than inclinometers
Lollino et al. (2006)	Montalido di Cosola landslide, Italy	Automatic Inclinometric System (AIS)	Correlation between heavy rainfall events and slope movement to enable early warning
Bennett et al. (2007)	Unstable soil slopes, CA	Wireless shape-acceleration array	Capable of easy installation and autonomous operation to provide full 3D data
Kosnik et al. (2007)	Case Studies in automated remote monitoring	TDR, remote total station, geophone	Web based interface maximizes usefulness of remote monitoring
Simeoni and Mongiovi (2007)	Castelrotto landslide, Italy	In-place inclinometers	IPIs should be checked with portable inclinometers
Barendse (2008)	Bridge replacement, Champlain Canal, NY	ShapeAccelArray (SAA)	MEMS-based IPI systems can be used for real-world applications

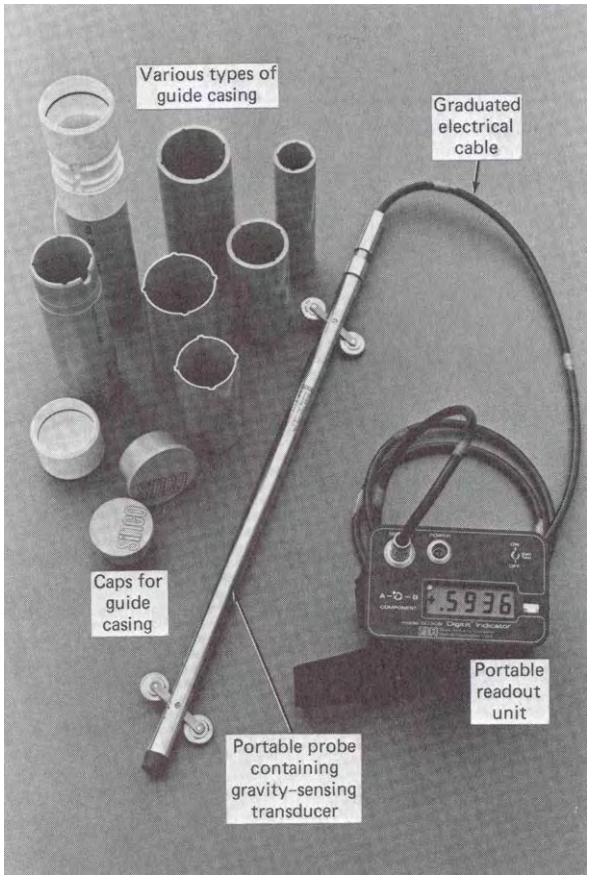

Figure 2.1 Traditional inclinometer system, including guide casing, transducer probe, and readout box (Dunnicliff 1988).

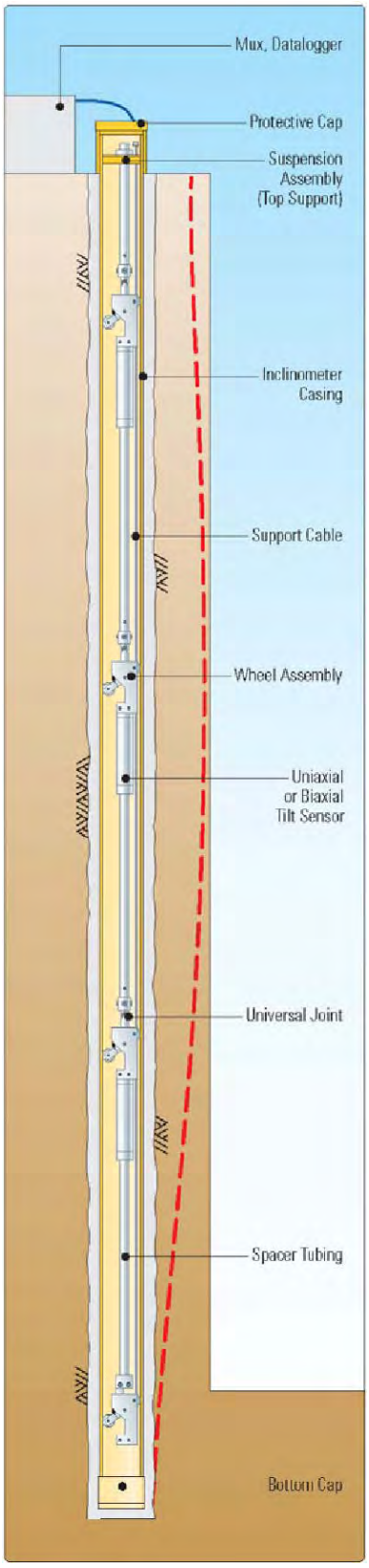

Figure 2.2 Typical IPI installation including three inclinometers (Geokon 2007).

3.0 METHODS OF INVESTIGATION

This chapter describes the equipment and methods used to install the instrumentation system, data acquisition system, and the field and laboratory testing program. Table 3.1 presents the project timeline for field work and instrumentation. The instrumentation system consists of two in-place inclinometer strings of five inclinometers each and two open-standpipe piezometers, a barometer, and a rain gauge. The data acquisition system consists of a Campbell Scientific CR10X datalogger with a cellular telephone modem for communications and a personal computer based software system for data management. Table 3.2 presents the instrumentation and data acquisition system components and cost. The field testing program, which was conducted by the Vermont Agency of Transportation (VTrans), consisted of Standard Penetration and Field Vane Tests. The laboratory testing program consisted primarily of drained direct shear and constant rate of strain consolidation tests conducted on undisturbed tube samples collected by VTrans. The laboratory tests were performed by VTrans and at the University of Massachusetts Amherst Geotechnical Engineering Laboratories.

3.1 DESCRIPTION OF INSTRUMENTATION INSTALLATION

Five borings were conducted by VTrans using a CME 45C track rig from July 12 thru August 11, 2005. Figure 3.1 presents the site location plan and Appendix A presents the VTrans boring logs and monitoring well construction diagrams. Standard 70mm (2.75 in.) PVC inclinometer casing was installed in three of the boreholes and labeled Inclinometer #1 through Inclinometer #3. Inclinometers #1 & #2 were placed within the zone of slope movement with the intention of using Inclinometer #1 for traditional hand-inclinometer readings while installing the in-place inclinometer string in Inclinometer #2. Inclinometer #3 was located outside the zone of slope movement for reference. In the remaining two boreholes, which were located inline with the zone of slope movement, 38mm (1.5 in) PVC well casing was installed. Both wells were backfilled around the casing with filter sand from the bottom to a depth of 1.52 m (5 ft.) from the ground surface and Bentonite was used for the remainder. Monitoring Well #1 is located below the road and next to Inclinometers #1 & #2, and is screened from 1.65 to 6.22 m (5.4 to 20.4 ft.), while Well #2 is located above the road and is screened from 3.05 to 7.62 m (10 to 25 ft.). Figure

3.2 shows the general site layout, with Inclinometers #1 & #2 in the foreground and Inclinometer #3 and the data acquisition system in the background.

Hand inclinometer readings were conducted by VTrans in all three inclinometer casings approximately twice a month from August to December 2005 (Appendix B). On December 19, 2005, UMass Amherst installed five Geokon 6300 series vibrating-wire in-place inclinometers (IPIs) in Inclinometer #2 (Figure 3.3) at depths below the ground surface of 0.76m (2.5 ft), 3.81m (12.5 ft), 6.86m (22.5 ft), 12.95m (42.5 ft), and 19.05m (62.5 ft). Each IPI was attached to a wheel and pivot assembly to ride the tracking groves in the casing and rigid stainless steel tubing to connect successive IPIs at a pivot. The tubing was available in 1.5m (5 ft) to 3m (10 ft) lengths and a connector was used to make longer segment lengths. Figures 3.4 and 3.5 present sketches of the installed IPI strings. Five Geokon 6300 series IPIs were installed in Inclinometer #3 at depths of 0.76m (2.5 ft), 2.29m (7.5 ft), 3.81m (12.5 ft), 6.86m (22.5 ft), and 12.95m (42.5 ft). In theory an IPI measures the change in inclination of the entire segment, known as the gauge length, and deflection is calculated with the assumption that the tubing does not touch the walls of the casing between pivot points. Post-installation zero readings were taken in both IPI strings using a Geokon GK-403 readout box.

Geokon 4500 series vibrating-wire piezometers were installed in the two monitoring wells at a depth of 6.1m (20 ft) from the top of the casing, at an elevation of 193.55 m (635 ft.) for Monitoring Well #1 and 195.07 m (640 ft.) for Monitoring Well #2. Several initial readings were taken on the day of installation using a GK-403 readout box. Prior to the installation of the data acquisition system, manual readings of the IPIs and vibrating-wire piezometers were taken five times during December 2005 and January 2006 using a GK-403 readout box.

On January 24, 2006, a Geokon series 4580 vibrating wire barometer (SN 05-12273) was installed by UMass Amherst. This barometer is used to correct the monitoring well piezometers for fluctuations in atmospheric pressure. Initial readings were taken with a GK-403 readout box before connecting the barometer to the datalogger. The 4580 series barometer is vented to the atmosphere and is susceptible to water infiltration and damage. Initially the barometer performed as expected but by late July, 2006, intermittent over-range values were being recorded with increasing frequency. On December 5, 2006, the barometer stopped working. During a field visit by UMass Amherst and Geokon on April 11, 2007, it was discovered that the barometer was full of water and ice despite being located in the protective plywood instrument box, and it was

assumed that expanding ice during the winter destroyed the vibrating wire. The barometer was returned to Geokon for repair and was reinstalled (new SN# 07-8954) in a more protective location in the instrument box on May 19, 2007. Figure 3.6 shows ice damage to the barometer.

A MetOne 385 tipping bucket rain/snow gauge was installed on July 6, 2007. Figure 3.7 shows the installed rain gauge. A custom bracket was constructed to mount the rain gauge on the solar panel support pole. Although the 385 rain gauge includes an electric heater for melting snow, this feature is not being used due to the lack of available AC power at the site. On November 12, 2007, UMass Amherst cleaned debris out of the rain gauge and changed the wiring to the datalogger. Thereafter, reliable data were continuously recorded.

3.2 DESCRIPTION OF DATA ACQUISITION SYSTEM

3.2.1 Datalogger

The data acquisition system used for this project is based around a Geokon 8020 Micro-10 datalogger coupled to two Geokon 8032 16 channel multiplexers. Figure 3.8 presents a flow diagram of the instrumentation and datalogger installation. The Micro-10 (Figure 3.9) consists of a Campbell Scientific (CSI) CR10X datalogger, 12V battery, battery charger, CSI SC32B optically isolated RS-232 interface, Geokon VWDSP, distribution board with connections for directly-connected instruments (such as the rain gauge), and a Redwing 100 cellular modem. A waterproof fiberglass Nema 4 enclosure protects the equipment from the environment. Mounted external from the enclosure was a deep cycle marine 12V battery, a Yagi cellular telephone antenna, and a solar panel to trickle-charge the batteries (Figure 3.10).

The Geokon 8032 multiplexer (Figure 3.11) was designed to interface with up to 16 instruments with temperature measurements or 32 instruments with no temperature. The multiplexer was mounted inside a waterproof Nema 4 enclosure to protect it from the environment. For this project, two multiplexers were used. One was located near Inclinometer #2 and has the five in-place inclinometers connected to it as well as the piezometer from Monitoring Well #1. The enclosure was mounted above the ground on metal fence posts. The second multiplexer was located adjacent to the datalogger and was connected to the five in-place inclinometers from Inclinometer #3 as well as the piezometer from Monitoring Well #2 and the barometer. A protective plywood box was constructed above ground to hold the datalogger and

multiplexer enclosures, as well as the marine battery and barometer. This box also serves as a support for the Yagi cellular antenna, the solar panel, and the rain gauge.

3.2.2 Remote Access

Access to the datalogger from a personal computer for programming and data retrieval can be done two ways, through a direct connection to the datalogger RS-232 interface or remotely using the cellular modem. The use of a cellular modem allows for the long distance and ease of a traditional land-line telephone system, while eliminating the need for the remote datalogger to be located near existing utilities. This can also be accomplished using radio modems, but the maximum distance between the base computer and the datalogger is limited and such connections can often be slow and unreliable.

3.2.3 Datalogger Administration

This project used the software package Multilogger from Canary Systems for datalogger programming and data retrieval. Multilogger serves as a graphical interface for datalogger programming, enabling complex datalogger configurations to be programmed and quickly updated, without the user needing to have detailed knowledge of datalogger programming. Multilogger also includes the ability to connect to the datalogger, allowing for local or remote administration and updating. The open connection with the datalogger makes real-time monitoring of the datalogger useful for programming and troubleshooting of the datalogger software and individual instruments. Multilogger is also used for data retrieval from the datalogger.

Multilogger has the ability to convert individual instrument readings into engineering units using stored calibration factors and applying appropriate corrections such as temperature. For this project, however, it was selected to have the raw digit readings from the vibrating wire instruments as the output and to have the conversion to engineering units calculated during data processing.

3.2.4 Data Management

The use of an automated datalogger allows for data to be collected and saved in a reliable manner over the long term. Data management is an important part of the data acquisition system especially when collecting, processing, and storing large data sets. This project looked at two

methods, the traditional text file and Excel spreadsheet approach, and the state-of-the-art database with a graphical web interface.

As this project was initially setup, data was downloaded manually using Multilogger approximately once every week or two. The data was saved in a comma-delineated text file and the filename was manually changed to reflect the date of the download. The new data was then added to a master Excel spreadsheet by manually copying and pasting the data from the text file. As the datalogger output raw digit readings from the instruments, the Excel file converted the readings into engineering values, applied the temperature correction, and in the case of the piezometers, corrected for atmospheric pressure using the barometer data. Several charts were setup in the Excel file for plotting the data and these charts needed to be updated to include the new data.

After a year and a half of data collection, it became apparent that this method was becoming impractical. The master spreadsheet was split into two, one for the in-place inclinometers and a second one for the monitoring wells and barometer. With the inclinometer spreadsheet exceeding 100MB in size, it was difficult to share the data file and updating the file was requiring a powerful personal computer to prevent crashes and lock-ups, outgrowing the laptop that had been used since the beginning of the project.

Starting in August, 2007, Canary Systems provided their latest in datalogger administration and data management software; a combination of MutliloggerDB, Insite, and MLWeb. Figure 3.12 presents a flow diagram of the software package. MultiloggerDB is an upgrade from the stand-alone Multilogger in that it incorporates a powerful Firebird-based database for data storage. Rather than manually downloading the data and saving it as a text file, MultiloggerDB can automatically download the data at predefined intervals and import it into the database. Additionally, data can be imported into the database manually. For this project, once MultiloggerDB was configured and running, all the previous data from the beginning of the project was imported into the database to create a complete record. When data is imported into the database, MultiloggerDB can be configured to check the data for its validity. Over-range data from the vibrating-wire instruments will typically ouput a raw digit reading of -99999. MultiloggerDB will check the data to a pre-defined acceptable range and mark data outside the range as invalid, preventing its inclusion in calculations and charts but not deleting the data. This task was previously conducted by having to write macros in the original Excel spreadsheet.

Insite is a graphical site interface for the database. For this project Insite was configured to present the user with an image of the project site (Figure 3.13) with the latest instrument readings linked to icons representing the individual instruments or instrument locations. A second project view was setup to show a profile of the in-place inclinometer strings (Figure 3.14). Clicking on an icon brings up a relevant pre-configured plot and additional files can be linked to an icon such as an image file for a picture or a .pdf for reference information. Insite was also used to enter all the necessary equations and calibration factors to convert raw digit readings into engineering units, linking "data elements" to "calculated elements" which could then be used for plots, graphical display, and alarms. Insite also includes a highly configurable plotting interface for pre-configuring plots and utilizes absolute dates for time as well as relative dates, such as 'last week' or 'last three months,' ensuring that pre-configured plots are always up to date (Figure 3.15). Quick reports and instrument reports can be pre-configured and set up to be automatically generated and emailed to a list of designated recipients. For this project, an instrument report was automatically generated on the first of the month and emailed, detailing the percent of valid readings by each instrument which is important for monitoring the reliability of the datalogger and instruments. An option to output data from the database into an Excel spreadsheet file is also available for additional flexibility. All settings and configurations made in Insite are saved to the database and are available to any copy of Insite installed on the network or to the internet through MLWeb.

MLWeb, the third piece of software in the package, creates a web server to graphically display the database on the internet, making the project available anywhere. Using a personal computer with a dedicated internet address and a customized installation of Windows XP Professional, MLWeb quickly publishes the interface created using Insite to the internet. All the icons, images, and pre-configured plots are available and are presented in an easy to navigate single page (Figure 3.16). Requests for a plot are handled by the server, generated in real time to ensure that the plot is of the most recent data, and output in a standard .pdf form (Figure 3.17) to work on a variety of computers and platforms. In addition to access to all pre-configured plots, reports, and excel files, a custom output form is available to make a custom plot, report, or excel file with options for data included and the time range. Additional options in the web interface include raw data display and lists of recently generated alarms and reports. For project security, MLWeb has the ability to make the project's web site open to everyone, or require users to login

with an administrator assigned password. SSL-based encryption is supported for a high level of internet security.

3.2.5 Multiple Dataloggers

Projects may be complex enough to require the use of multiple dataloggers and instrument setups or project managers may have multiple projects each with a datalogger. This project was limited to one datalogger but in January, 2008, a second datalogger was added to evaluate the increased complexity of such a system.

The second datalogger is a standard Campbell Scientific (CSI) CR10X coupled to a CSI AM416 Multiplexer and CSI AVW1 vibrating wire instrument interface. Initially installed on the UMass Amherst campus in the fall of 2003, this datalogger has been recording data from up to 16 Geokon 4500 series piezometers. The initial datalogger software was custom written by UMass Amherst and the datalogger was programmed to record its data to a CSI SM4M storage module which was periodically removed and the data downloaded to a personal computer. For the inclusion of this datalogger into a multiple-datalogger evaluation, a reliable remote connection needed to be created for the Multilogger server to communicate with. Using two CSI RF400 spread spectrum radio modems and a CSI COM210 phone modem, a telephone to radio link was established between the server and the datalogger. New software for the datalogger was written using MultiloggerDB.

The traditional method of data management would work well with multiple dataloggers in that each datalogger can be dialed up separately and the data can be added to its respective data file or spreadsheet. This method is also limited due to the difficulty of the traditional method dealing with large amounts of data. MultiloggerDB is designed to handle multiple dataloggers, and gives each datalogger a unique project ID number. This number is applied to all data when imported into the database. Insite takes advantage of the ID number, and all graphical interface components are also linked by project ID, keeping project-specific plots and reports separate. MLWeb takes the graphical interface of Insite one step further. On projects requiring users to log in, four levels of access are supported, Administrators, Project Managers, Technicians, and Guests. Administrators and Project Managers are able to view all projects running on the server, while Technicians and Guests are only allowed to view specific projects that they may be working on. For this evaluation, a technician was created who could only view the VTrans project, and a second was created who could only view the UMass Amherst project.

A second approach for managing multiple dataloggers and a database is that MultiloggerDB supports multiple databases. Each project can be configured with its own database, essentially creating a one-datalogger based system for each project. This second approach would also work well for large and complex projects with multiple-dataloggers. With multiple databases, each database and therefore each project would have its own web site. For this Canary Systems recommends the use of Windows Server, an operating system specifically designed for server applications and is the preferred operating system for MLWeb. Even for projects with one datalogger but a high web traffic requirement, Windows Server is the recommended platform.

3.3 IN SITU TEST METHODS AND SOIL SAMPLING

3.3.1 Standard Penetration Tests

Standard Penetration Tests were conducted by VTrans during the drilling of Inclinometers 1 and 3 in general accordance with the American Association of State Highway and Transportation Officials (AASHTO) standard T206, *Penetration Test and Split-Barrel Sampling of Soils*. Tests were carried out using a 5.08 cm (2 in.) split-barrel sampler with a hardened steel drive shoe, a soil retainer, and without liners. The hammer assembly was a 63.5 kg (140 lb.) CME automatic hammer. The automatic hammer is a fully-enclosed hammer system that incorporates a hydraulically driven continuous chain for lifting the hammer. To conduct the test, the operator threads an anvil onto the drill string and lowers the hammer assembly over the anvil. The hydraulic motor is then engaged, turning the continuous chain and lifting the hammer 76.2 cm (30 in.) before the hammer free falls within a guide tube, striking the anvil and transferring energy through the drill string to the sampler. The hammer will continue to be lifted by the chain and dropped until the hydraulic motor is disengaged. The number of hammer blows required to drive the sampler through each 15.2 cm (6 in.) increment is recorded and the SPT N-value is the sum of the blows for the second and third increment.

For this investigation, the sampler was driven for a total of 61 cm (24 in.) at which point the sampler was removed from the borehole and disassembled. The amount of soil within the sampler was measured and recorded as the recovery before a field description of the soil was made and samples collected for lab testing. The drilling on the borehole resumed until the next test depth was reached and the sampler was lowered back into the borehole. During the drilling

of Inclinometer #1 continuous SPT sampling was conducted from the ground surface until bedrock was encountered at 19.37 m (63.55 ft.). Continuous sampling is where the new testing depth is the same depth that the sampler had been driven to on the previous test; for this investigation the testing depths were every 61 cm (2 ft.) coinciding with a driving of the sampler 61 cm (2 ft.) For the drilling of Inclinometer #3 continuous sampling was conducted from the ground surface to a depth of 4.27 m (14 ft.)

3.3.2 Field Vane Test

Field Vane Tests (FVT) were conducted by VTrans during the drilling of Inclinometer #2 in general accordance with AASHTO standard T223, *Field Vane Shear Test in Cohesive Soil*. FVTs were conducted at five depths from 4.88 m (16 ft.) to 11.58 m (38 ft.) in conjunction with thin-walled tube sampling as the borehole was advanced. The vane was advanced down the borehole to the desired test depth at which point torque was applied to the vane through a gear drive at a rate not exceeding 0.1 degree per second. After reading the maximum torque applied, the vane was rapidly rotated for ten full rotations to remold the soil. Torque was then reapplied and the maximum value was recorded as the remolded torque. To determine the shear strength, the measured torque was multiplied by the vane shape constant, K, which was 9.385×10^{-7} m^3 (3.314×10^{-5} ft^3), a value calculated from the 7.62 cm (3 in.) diameter and 15.24 cm (6 in.) height of the non-tapered vane used.

3.3.3 Thin-Walled Tube Sampling

Thin-walled tubing sampling was conducted by VTrans during the boring of Inclinometers 2 and 3 in general accordance with AASHTO standard T207, *Thin-walled Tube Sampling of Soils*. The brass thin-walled tubes, also known as Shelby Tubes, had an outside diameter of 76.2 mm (3 in.) and a length of 0.91 m (36 in.). After the sample was collected, the tube was removed from the borehole, the recovery in the tube was measured, and the ends of the tube were sealed in preparation for shipment to UMass Amherst.

3.4 LABORATORY TEST METHODS

For this project, index testing consisting of grain size and liquid and plastic limit tests were conducted by VTrans. Drained direct shear and constant rate of strain consolidation tests were conducted by UMass Amherst.

3.4.1 Grain Size

Grain size tests were conducted by VTrans on samples collected from Inclinometers 1 and 3 in general accordance with AASHTO standard T88, *Particle Size Analysis of Soils*. A sieve analysis was performed on all collected samples to determine the percent gravel, sand, and fines. Hydrometer tests were conducted on 4 samples from Inclinometer #1 to determine the distribution of fine-grained particles.

3.4.2 Liquid and Plastic Limits

Liquid limit tests were conducted by VTrans on samples collected from Inclinometers 1 and 3 in general accordance with AASHTO standard T89, *Determining the Liquid Limit of Soils*. Plastic limit tests were conducted by VTrans on the same samples in general accordance with AASHTO standard T90, *Determining the Plastic Limit and Plasticity Index of Soils*. Eight samples between 6.1 m (20 ft.) and 12.2 m (40 ft.) in Inclinometer #1 and four samples between 1.8 m (6 ft.) and 4.3 m (14 ft.) in Inclinometer #3 were tested.

3.4.3 Water Content

Water contents were determined by VTrans on all samples collected from Inclinometers 1 and 3.

Water contents were determined by UMass Amherst in general accordance with American Society for Testing and Materials (ASTM) Standard D2216 *Standard Test Method for Laboratory Determination of Water (Moisture) Content of Soil and Rock*. The mass of a specimen was taken before and after being placed in a 110 ± 5 °C oven overnight and the two masses were compared to determine the water content.

3.4.4 Total and Dry Unit Weight

Total unit weights of specimens were determined by UMass Amherst based on the measured volumes and total mass of prepared direct shear (DS) and constant rate of strain (CRS) specimens. Dry unit weights were calculated using measured water content values and total unit weights.

3.4.5 Sample Extraction

Samples for DS and CRS tests were extracted from the thin-walled sampling tubes by UMass Amherst in general accordance to the method recommended by Ladd and DeGroot (2003) as outlined in Figure 3.18. The section of the sampling tube containing the desired

specimen was cut using a horizontal band saw for the clayey samples or a pipe cutter for the silty samples. A thin piece of piano wire was then inserted between the soil sample and the cut tube section, using a hyperdermic tube as needed for stiff samples. The wire was then attached to a wire saw and the tube section rotated 3 or 4 times to cut the sample away from the tube. The wire was then removed and the sample was then extruded from the cut tube section by pushing the tube section down over the top of a trimming pedestal of the same diameter as the sample.

3.4.6 Drained Direct Shear

Drained direct shear tests were conducted by UMass personnel in general accordance with ASTM D3080 *Standard Test Method for Direct Shear Test of Soils Under Consolidated Drained Conditions*. Specimens were extracted following section 3.3.2.5 Sample Extraction and hand trimmed into a right cylinder shape of 63.5 mm (2.5 in.) diameter by 25.4 mm (1.0 in.) Trimming was done in a humid room to prevent loss of moisture. Minimal sample disturbance was archived using a soil lathe together with a sharp trimming ring and sharp trimming tools. Moist top and bottom porous stones were then added to the specimen and the specimen was inserted into the shear box.

On the direct shear loading frame, the shear box is located in an open container that is used as a water bath for the specimen. Prior to the final consolidation increment water was added to the container and added as needed throughout the remainder of the test. Consolidation of the specimen to the final vertical stress was conducted by the application of dead weights in increments. The final increment to reach the target vertical stress was left acting on the specimen overnight. Three target vertical effective stresses were used for specimens trimmed from Inclinometer #3 25-27 ft. and one target vertical effective stress was used for a specimen trimmed from Inclinometer #2 19-21 ft. All consolidation strains were computed taking into account the apparatus compliance which was determined using a steel disk.

Drained shear was conducted at a constant rate of deformation equal to approximately 0.0203 mm/minute (0.0008 in./min.). Free drainage of the specimen was allowed to occur during the test. Using a dedicated data acquisition system coupled to transducers, readings of vertical and horizontal displacement and shear force were taken during the course of the shearing process. Shear was allowed to continue beyond the measured peak shear resistance.

After shearing the specimen, the shear box was manually returned to the pre-shear position. The specimen was then rapidly sheared by hand a minimum of five cycles before sitting

overnight and mechanically sheared the following morning. This process, but without the rapid hand shearing, was repeated up to two more times to measure the large displacement shear resistance. The net horizontal displacement was computed as the cumulative sum of the horizontal displacement for the repeated shear cycles.

3.4.7 Constant Rate of Strain Consolidation

Constant rate of strain consolidation tests were conducted by UMass Amherst in general accordance with ASTM D4186 *Standard Test Method for One-Dimensional Consolidation Properties of Soils Using Controlled-Strain Loading* and Sandbeakken et al. (1986). The tests were conducted using a GeoTAC personal computer based test control and data acquisition system, which includes a load frame, flow pump, CRS consolidometer cell and Sigma-1 CRS consolidation software.

Specimens were extracted following section 3.3.2.5 Sample Extraction and hand trimmed into a right cylinder shape of 63.5 mm (2.5 in.) diameter by 19.05 mm (0.75 in.) Trimming was done in a humid room to prevent loss of moisture. Minimal sample disturbance was archived using a soil lathe together with a sharp trimming ring and sharp trimming tools. Moist top and bottom porous stones were then added to the specimen and the specimen was inserted into the CRS cell. After placing the CRS cell into the load frame, an initial seating load and one or two incremental loads were applied. The cell chamber was then filled with deaired water and the specimen was back pressure saturated to a final target back pressure equal to 200 kPa (29 psi) and left to sit overnight.

Constant rate of strain loading was conducted using a nominal strain rate of 1 to 2 % per hour (2.8×10^{-6} to 5.6×10^{-6} s^{-1}) until a maximum stress of approximately 2.87 MPa (60,000 psf) at which point the test was stopped. All measurements during testing were made using load, displacement, and pressure transducers. If the test included an unload-reload loop, a constant stress period for 1 to 2 hours was first initiated prior to starting the unload phase and again prior to starting the reload phase. The target unload stress was set equal to 10% of the vertical stress acting on the specimen prior to start of the unload-reload loop.

The measured data were reduced using methods of Wissa et al. (1971; and also described in ASTM D4186 and Sandbeakken et al. 1986). All vertical strains were computed taking into account the apparatus compliance that was determined using a steel disk.

Table 3.1 Project Timeline for Field Work and Instrumentation

Date	Task	Comments
July 12, 2005 to August 11, 2005	Drilling and installation of 3 inclinometer casings and 2 monitoring wells	VTrans
August 12, 2005	Hand inclinometer readings Incl. #1, 2, & 3; monitoring well readings MW 1 & 2	VTrans
August 19, 2005	Hand inclinometer readings Incl. #1, 2, & 3; monitoring well readings MW 1 & 2	VTrans
August 26, 2005	Hand inclinometer readings Incl. #1, 2, & 3; monitoring well readings MW 1 & 2	VTrans
September 21, 2005	Hand inclinometer readings Incl. #1, 2, & 3; monitoring well readings MW 1 & 2	VTrans
September 29, 2005	Hand inclinometer readings Incl. #1, 2, & 3; monitoring well readings MW 1 & 2	VTrans
October 11, 2005	Hand inclinometer readings Incl. #1, 2, & 3; monitoring well readings MW 1 & 2	VTrans
October 28, 2005	Hand inclinometer readings Incl. #1, 2, & 3; monitoring well readings MW 1 & 2	VTrans
November 9, 2005	Hand inclinometer readings Incl. #1, 2, & 3; monitoring well readings MW 1 & 2	VTrans
December 1, 2005	Hand inclinometer readings Incl. #1, 2, & 3; monitoring well readings MW 1 & 2	VTrans
December 19, 2005	Hand inclinometer readings Incl. #1, 2, & 3; monitoring well readings MW 1 & 2. Installed IPIs and VW Piezometers	VTrans / UMass Amherst
December 26, 2005	Manual readings of IPIs and VW piezometers	UMass Amherst
January 4, 2006	Manual readings of IPIs and VW piezometers	UMass Amherst
January 13, 2005	Hand inclinometer reading Incl. #1. Manual readings of IPIs and VW piezometers. Installed multiplexers and CR10X	VTrans / UMass Amherst
January 24, 2005	Manual readings of IPIs and VW piezometers. Installed barometer.	UMass Amherst
January 25, 2006	Datalogger begins to record and store data	
January 31, 2006	Finished field installation of equipment	UMass Amherst
July, 2006	Intermittent over-range values on barometer start to occur	
August 9, 2006	Equipment inspection and service	UMass Amherst
October, 2006	Intermittent over-range values on MW-2 VW piezometer start to occur	
December 5, 2006	Barometer stops working	
February 7, 2007	MW-2 VW piezometer stops working	
April 11, 2007	Removed malfunctioning barometer. Repaired broken signal wire to MW-2 VW piezometer. Cleaned all signal wire connections to terminal boards	VTrans / UMass Amherst / Geokon
May 19, 2007	Reinstalled repaired barometer	UMass Amherst
May 30, 2007	Site inspection and manual soil sampling of shallow soils	UMass Amherst
July 6, 2007	Installed rain gauge	UMass Amherst
July 17, 2007	Start using MultiloggerDB/Insite/MLWeb	
November 15, 2007	Cleared debris from rain gauge	UMass Amherst
February 15, 2008	Turned off remote data retrieval	
June 3, 2008	Removed equipment from site	VTrans / UMass Amherst

Table 3.2 Instrumentation and Data Acquisition Components and Cost

Component:	Quantity	Cost:
Geokon – Micro 10 Datalogger	1	$5,890
Geokon – Cellular Modem	1	$1,110
Geokon – 8032 Multiplexer	2	$1,900
Geokon – 4999 Terminal Box	2	$800
Geokon – 6300 series IPIs	14	$5,600
Geokon – 6300 series wheel assembly	14	$3,520
Geokon – 6300 series connecting tubing	18	$1,620
Geokon – 6300 series support cable	180	$286
Geokon – Misc. cable	1425	$1,216
Geokon – Multiplexer cable	2	$324
Geokon – 4500 series VW piezometers	2	$960
Geokon – 4580 VW barometer	1	$625
Geokon – Multilogger	1	$895
MetOne – 385 rain gauge	1	$1,240 (2007)
Canary Systems – MultiloggerDB / Insite / MLWeb / 1 yr support	1	$3,740 (2007)
	Total:	$29,726

Notes: 1. Cost is 2005 prices unless noted.

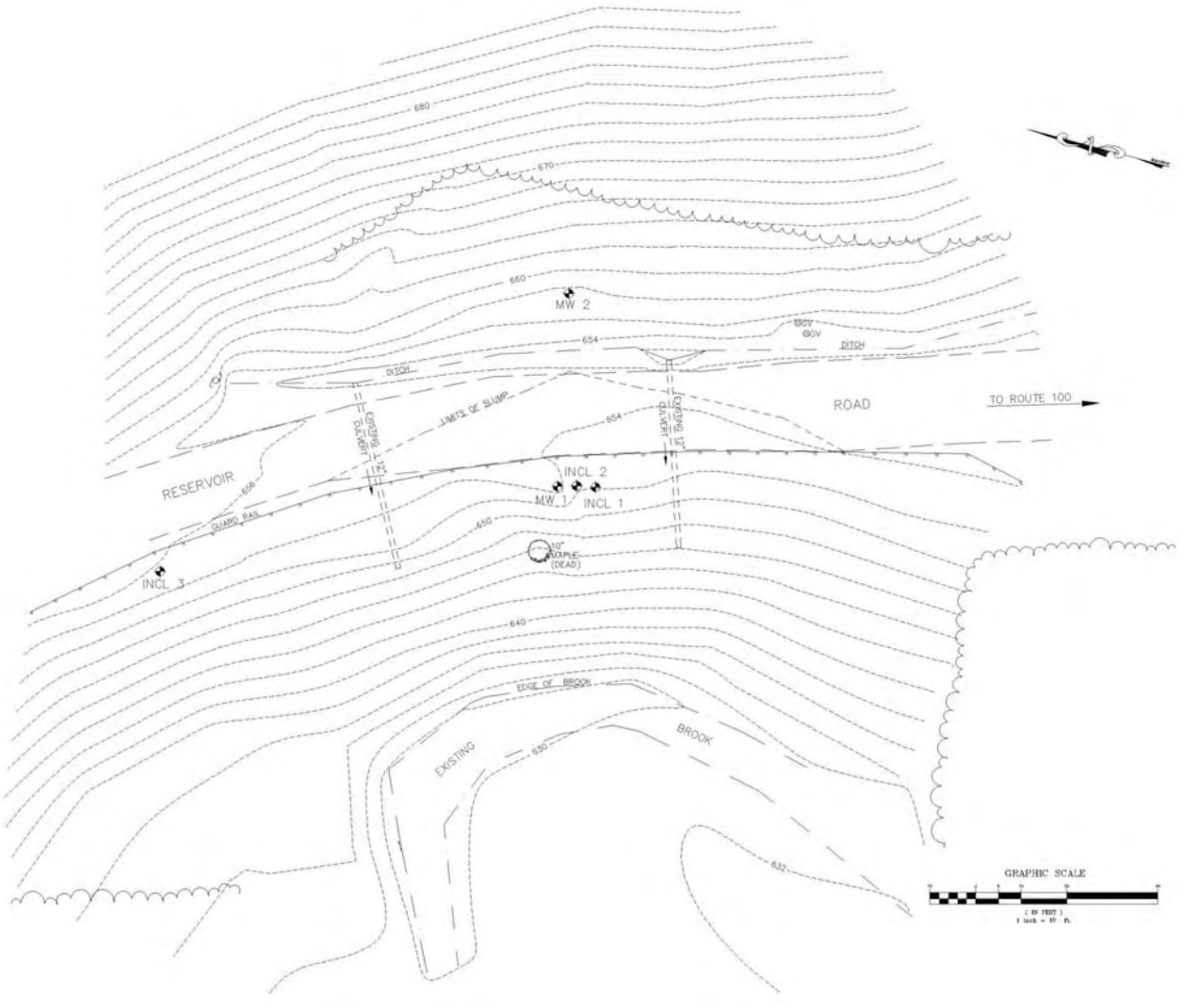

Figure 3.1 Waterbury, VT, site location plan (from Charles Grenier Consulting Engineer).

Figure 3.2 General site layout, with Inclinometers 1 & 2 in the foreground and Inclinometer #3 and the data acquisition system in the background.

Figure 3.3 Installing an IPI.

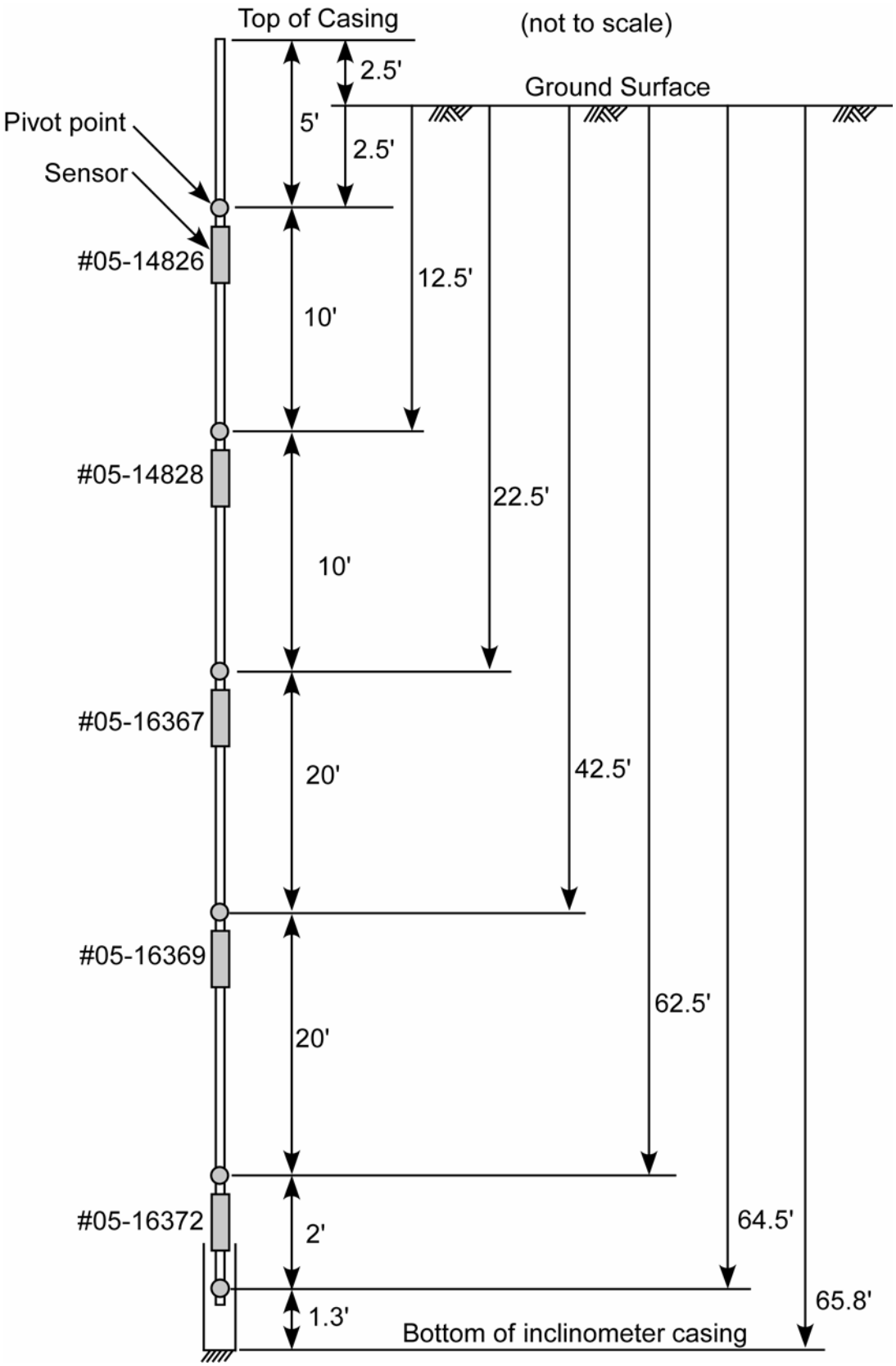

Figure 3.4 Sketch of installed IPIs in Inclinometer #2.

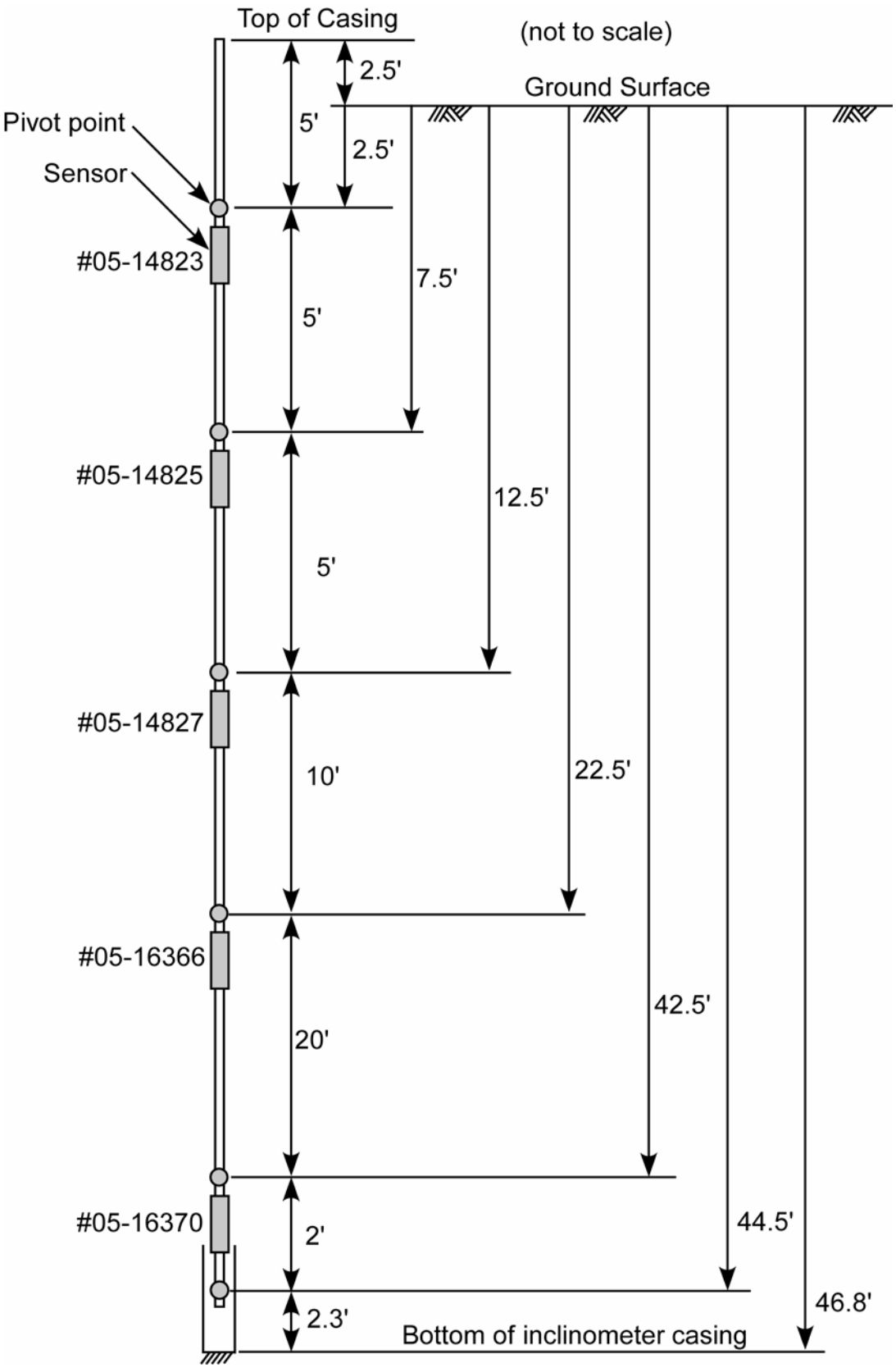

Figure 3.5 Sketch of installed IPIs in Inclinometer #3.

Figure 3.6 Ice damage inside the sealed barometer.

Figure 3.7 Installed rain gauge.

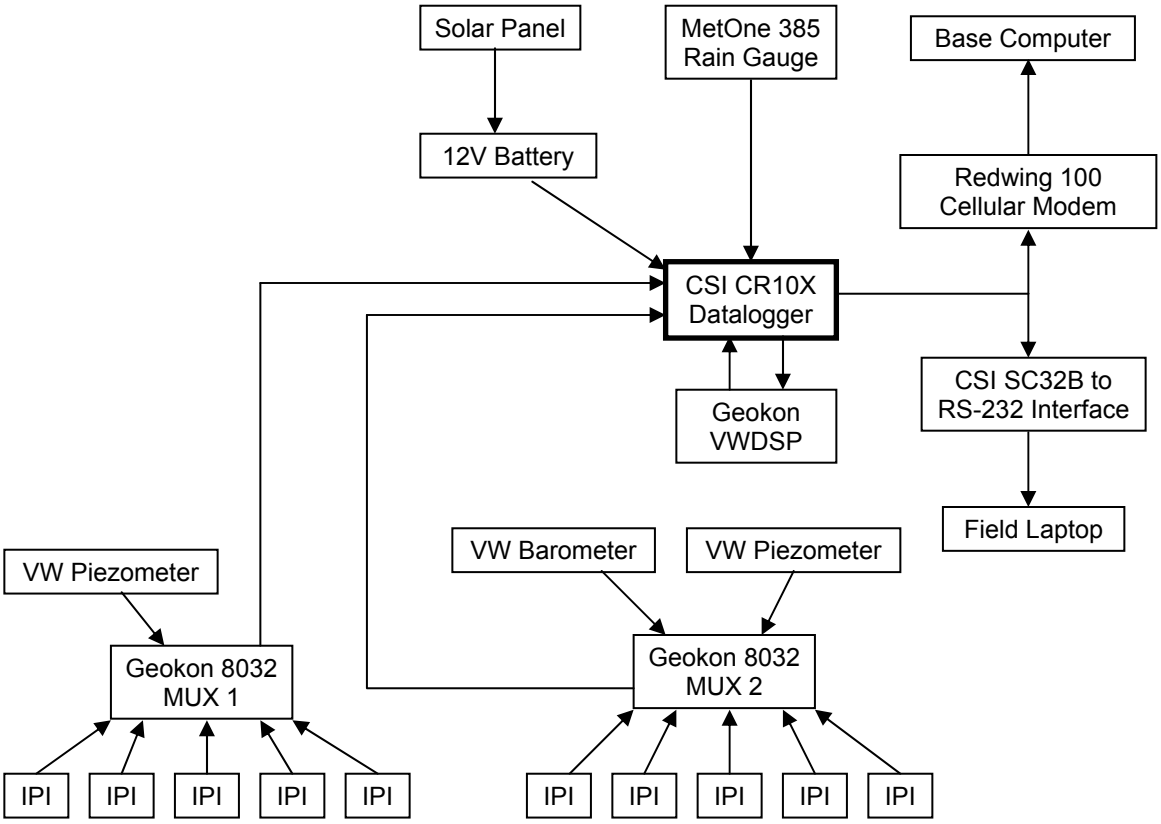

Figure 3.8 Flow Diagram of the instrumentation and datalogger installation.

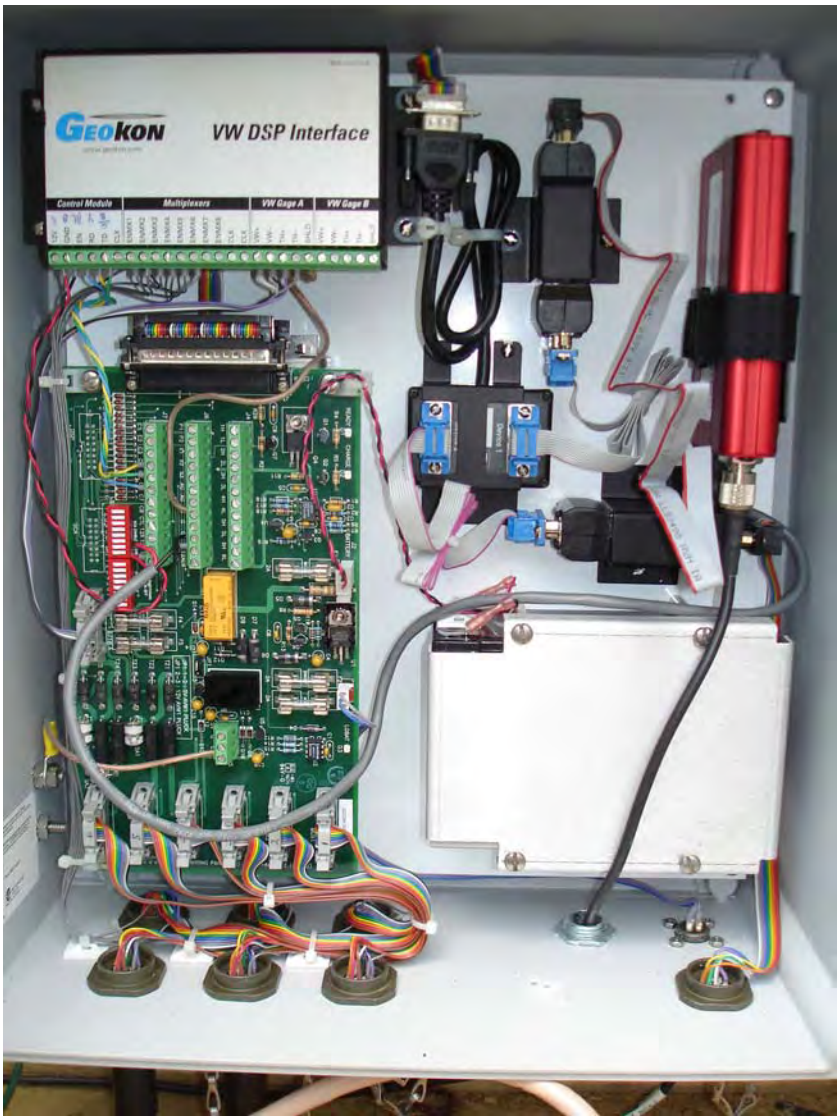

Figure 3.9 Geokon Micro-10 datalogger.

Figure 3.10 View of the data acquisition system when the protective box is open. The battery is in the front left, the multiplexer behind, and the datalogger to the right. The cell phone antenna is in the upper left and the solar panel in the upper right.

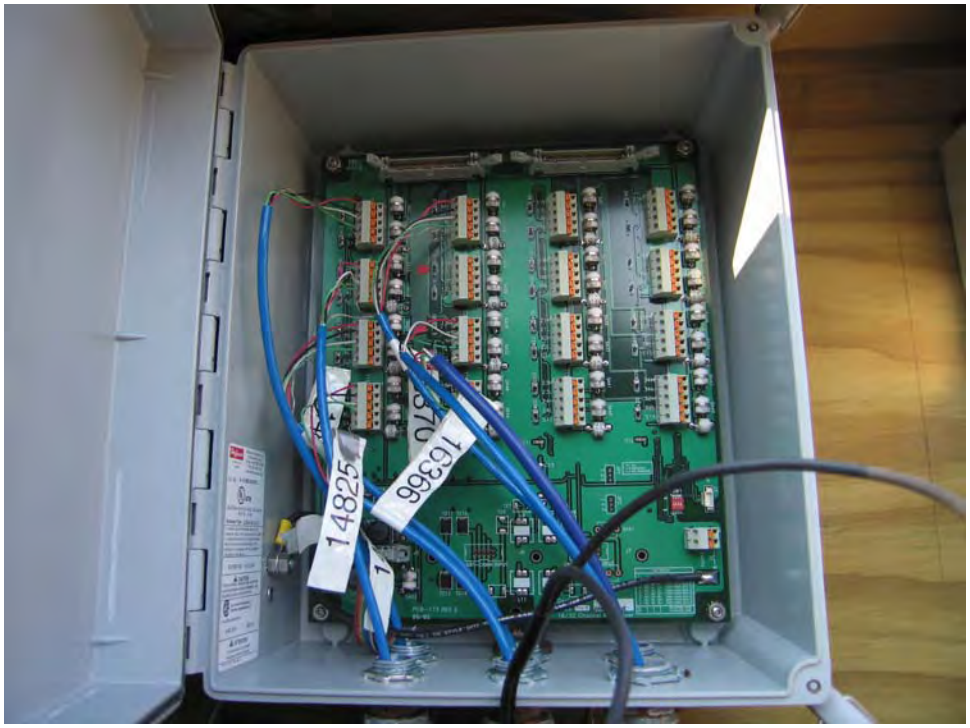

Figure 3.11 Geokon 8032 multiplexer.

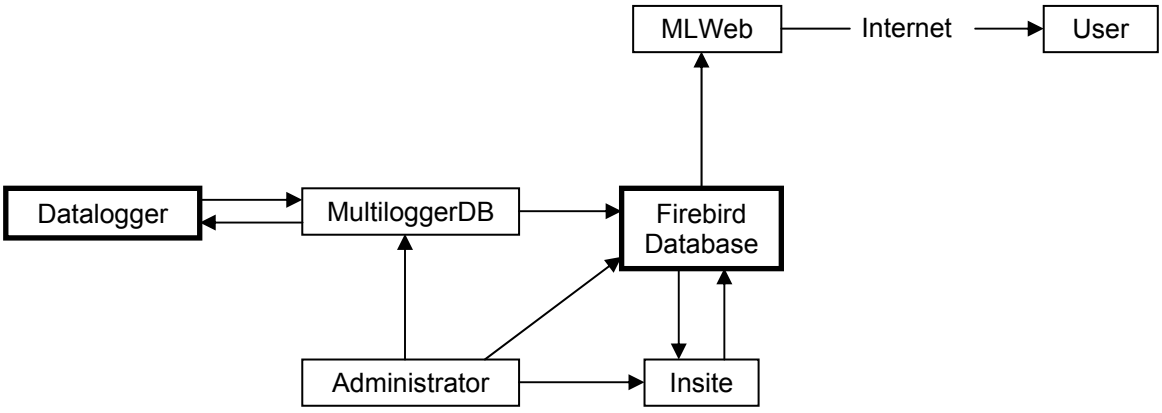

Figure 3.12 Flow diagram of MultiloggerDB software package.

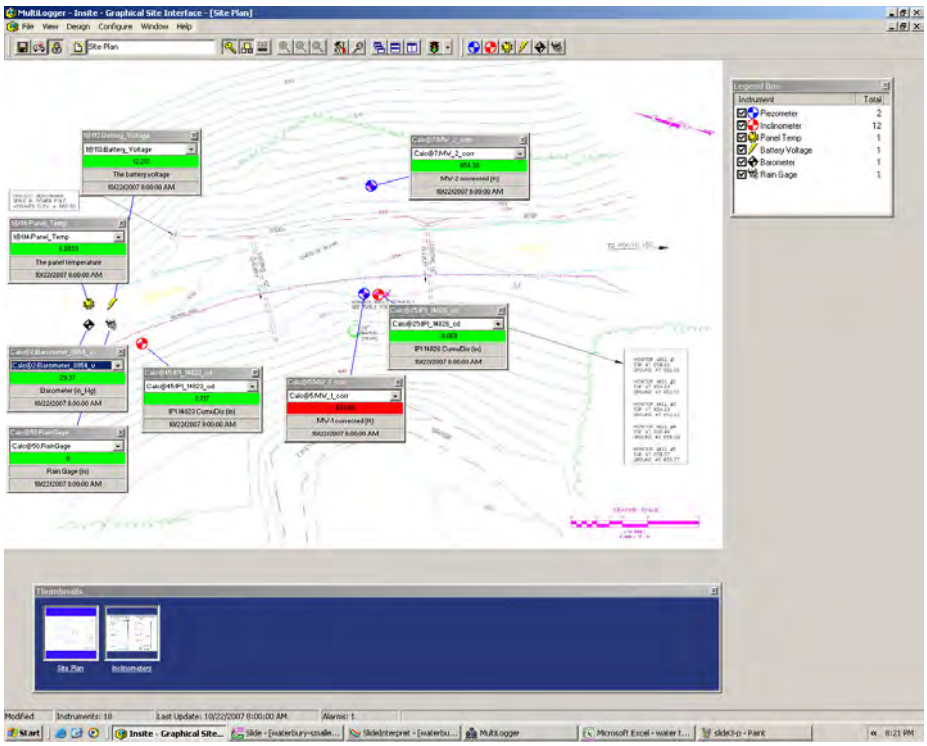

Figure 3.13 Insite project view.

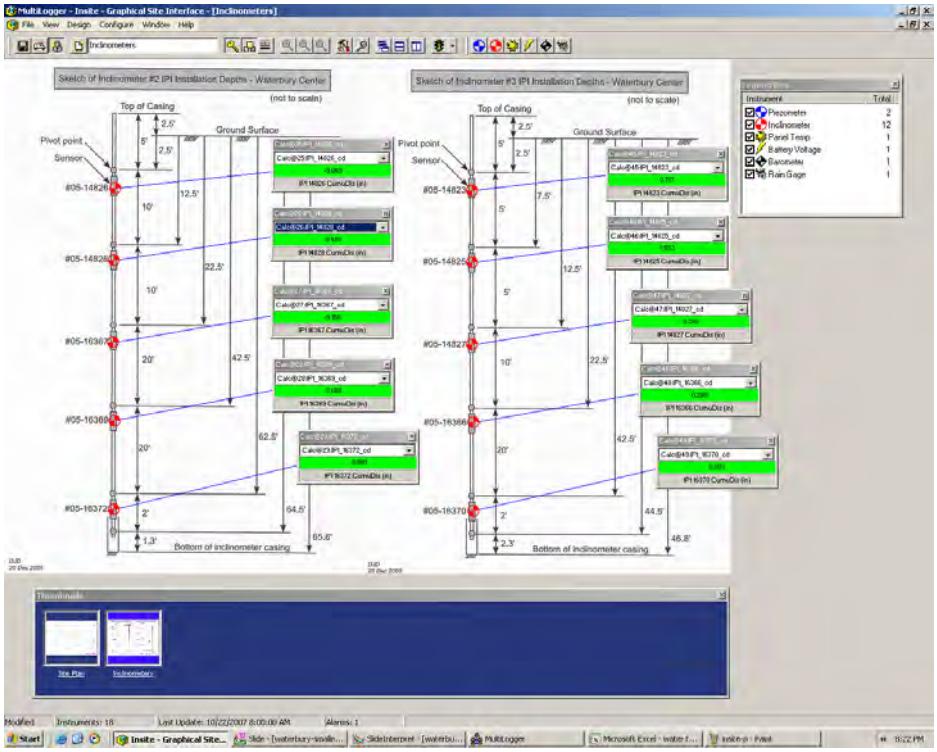

Figure 3.14 Insite IPI profile view.

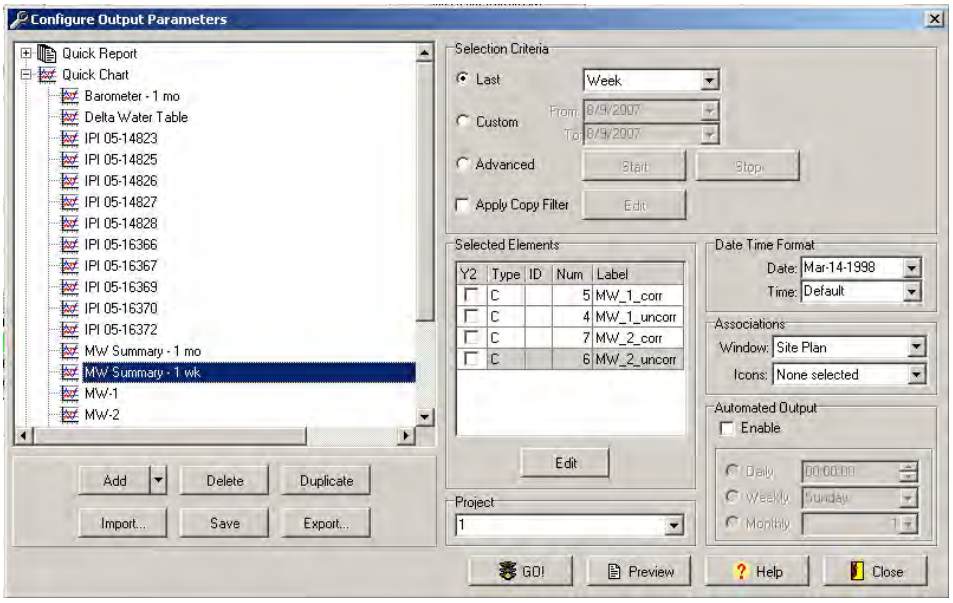

Figure 3.15 Insite plot configuration interface.

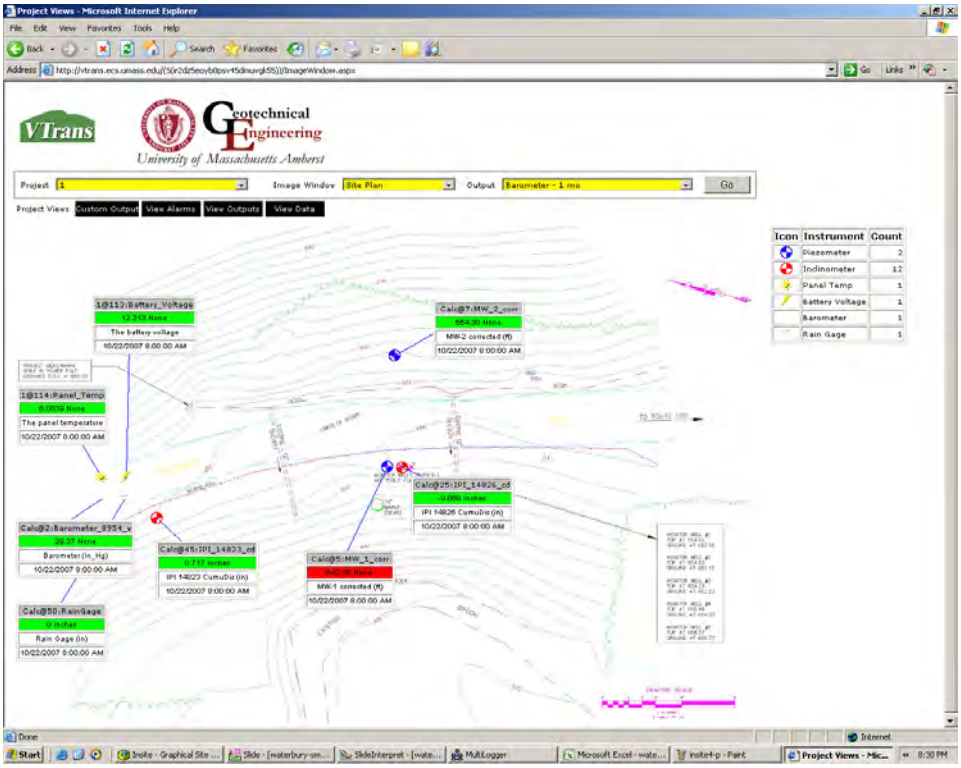

Figure 3.16 MLWeb web interface and project view.

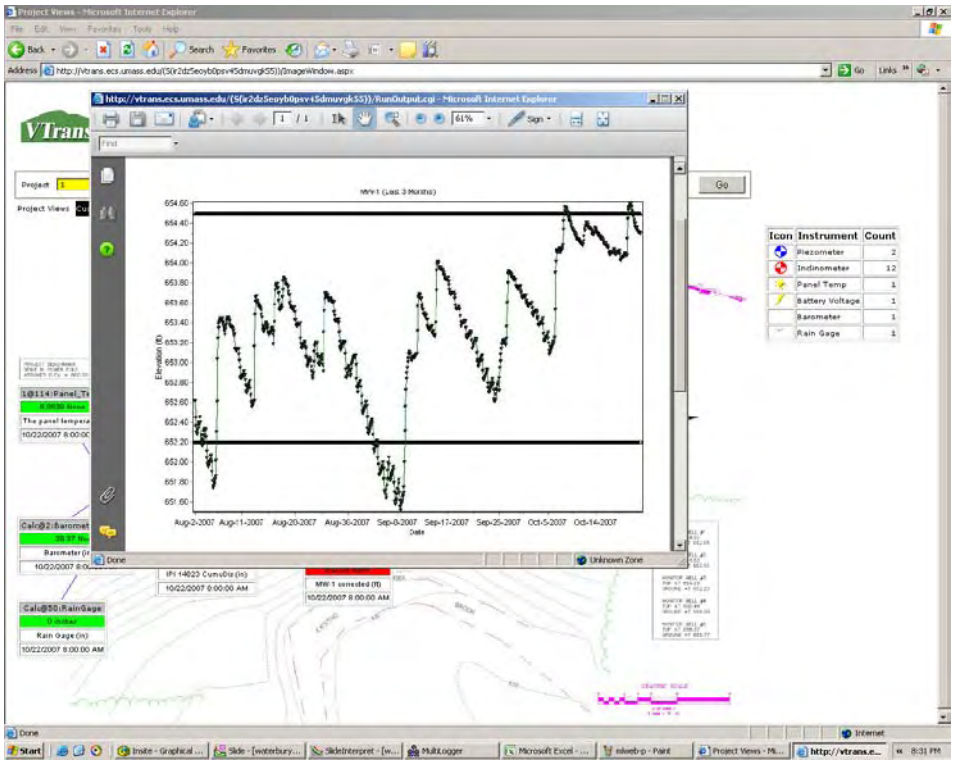

Figure 3.17 MLWeb MW-2 water elevation plot.

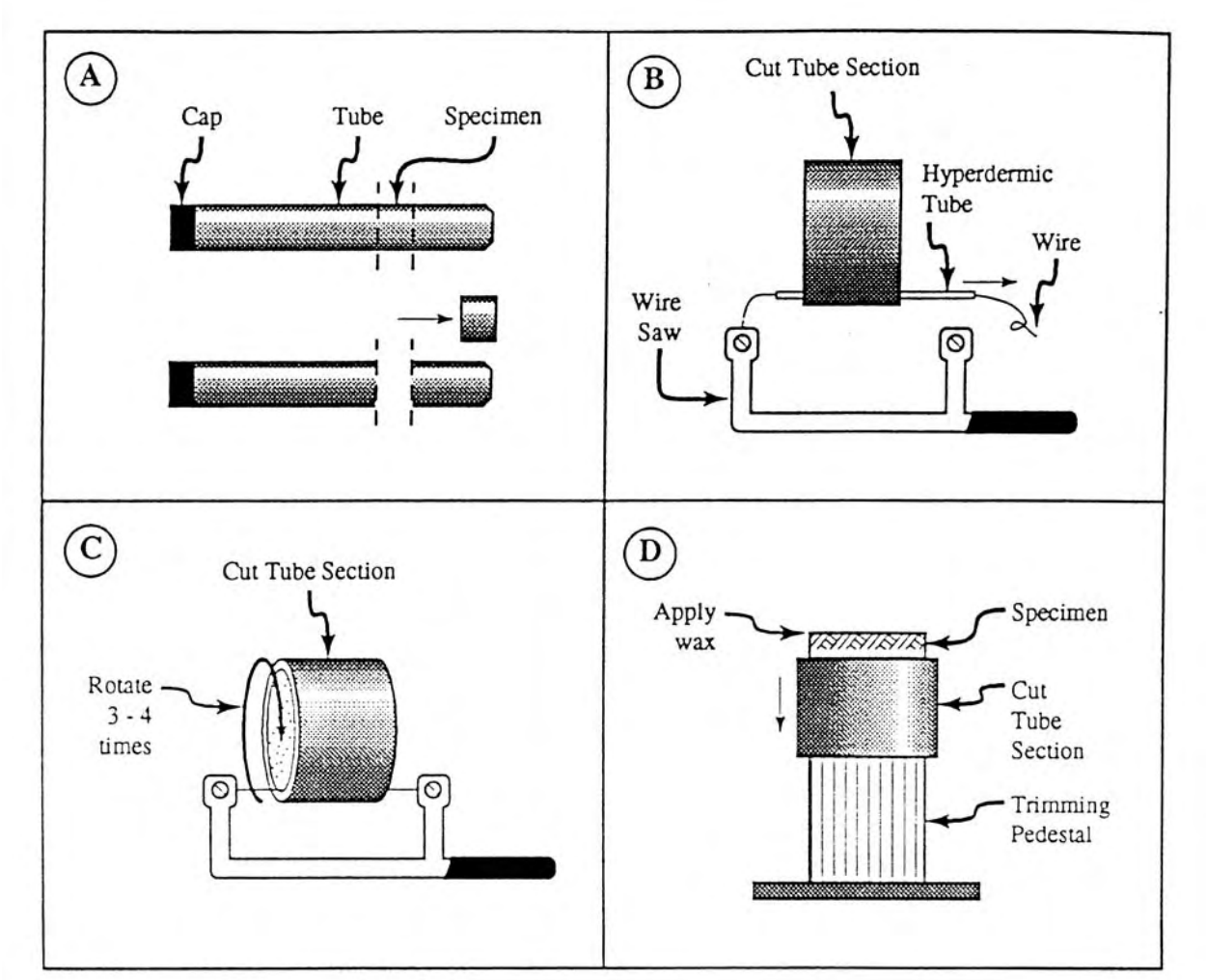

Figure 3.17 Procedure for sample extrusion for DS and CRS specimens (after Ladd and DeGroot 2003).

4.0 SITE CHARACTERIZATION

This chapter presents the site location, description, a geologic history of the Waterbury site, and a summary and interpretation of the in situ and laboratory tests. From the combination of these sources, a representative site soil profile was generated for input to the stability analysis.

4.1 SITE LOCATION AND DESCRIPTION

The Waterbury site is located on Reservoir Road, just off of Vermont Rt. 100 in Waterbury Center, VT. Figure 3.1 presents the site plan and Figure 4.1 presents a topographical map of the site. Reservoir Road is a short two-lane gravel road leading northwest (Figure 4.2) to Waterbury Center State Park and a few private residences. There is a municipal water supply line running under the uphill side of the road. The road was constructed across a slope, with the uphill side towards the northeast and the slope dropping off steeply to the southwest on the downhill side of the road. The toe of the slope forms an outer meander bend in Bryant Brook (Figure 4.3), potentially causing undercutting of the slope. The elevation of Reservoir Rd. is approximately 200 m (655 ft.) above sea level.

4.2 GEOLOGIC HISTORY

Bedrock at the Waterbury site is metamorphic, belonging to the Stowe Formation and originated during the Cambrian to Late Proterozoic period (Gale et al. 2006). During the drilling of Inclinometer 1, 2.74 m (9 ft.) of bedrock was cored and identified as unweathered black Phyllitic Schist with numerous quartz veining along foliation.

The soil at the site is primarily glaciolacustrine deposits derived mainly from the local bedrock. During the end of the Wisconsinan glaciation, glacial lakes were created throughout Vermont as the ice retreated, impounding water behind ice dams. At least three and possibly four glacial lakes have occurred at the Waterbury site, with the lake elevation becoming lower with each subsequent lake (Springston and Dunn 2006). Figure 4.4 presents the lake shorelines, with the Lake Winooski water elevation occurring around 305 m (1000 ft.), Lake Mansfield I at around 226 m (740 ft.) and Lake Mansfield II at around 198 m (650 ft.) (Springston and Dunn 2006, Stewart 1961). According to Larson (1987b), Lake Winooski drained south into the

Connecticut River valley near present day Williamstown, VT. As the ice retreated to the west-northwest down the Winooski River valley towards the Champlain valley, the meltwater was able to drain to the west through the Green Mountains near Huntington, VT, forming Lake Mansfield I. Further retreat of the ice caused a lower drain to open up close to the first, lowering the lake elevation to that of Lake Mansfield II. The last of the glacial lakes at the site drained sometime prior to the formation of the Champlain Sea 12,500 years ago (Larson 1987a).

Typical deposits formed on the lake beds are laminated and commonly varved, range from clay to silt to very fine sand, and are dark gray to gray in color (Springston and Dunn 2006). Additional deposits found locally near the site associated with Lake Mansfield I include gravel and pebbly sand overlying the lacusterine silt with a thickness of less than 3 m (10 ft.) (Spingston and Dunn 2006). Shoreline and shoaling deposits have also been found locally, consisting of pebbly fine to medium sand overlaying the lacusterine silt and occurring at the various lake water elevations (Springston and Dunn 2006). Following drainage of the glacial lakes, the lacusterine deposits have been eroded by surface water and dissected by streams and rivers, including Bryant Brook at the site.

4.3 IN SITU TESTING

In situ testing was performed by VTrans during drilling of the inclinometers and monitoring wells in July and August, 2005. Standard Penetration Testing (SPT) was conducted in conjunction with continuous sampling during drilling of Inclinometer 1 from the surface to the top of bedrock. SPTs were run in the top 4.27 m (14 ft.) during the drilling of Inclinometer 3. Figure 4.5 and Table 4.1 present the SPT results. Generally, the blow counts are low, ranging from approximately 3 to 7.

Field Vane Testing was conducted during the drilling of Inclinometer #2. Table 4.2 presents the peak and remolded undrained shear strength. The peak undrained shear strengths are low in the upper two test locations and increase with depth thereafter. Generally sensitivity values range from 1.2 to 2.8 with one value of 8.1.

4.4 LABORATORY TESTING

Liquid and plastic limit, moisture content, and grain-size tests were conducted by VTrans on samples collected during the continuous sampling of Inclinometer #1. Table 4.3 presents the

liquid and plastic limit test results and Table 4.4 presents the moisture content and grain-size test results. Figure 4.6 presents the liquid and plastic limit results plotted on Casagrande's plasticity chart. Figure 4.7 presents a profile plot of the liquid and plastic limits, natural water content, and grain-size distribution.

Drained direct shear (DS) and constant rate of strain (CRS) tests were conducted on tube samples by UMass Amherst. Figures 4.8 and 4.9 show the location of the DS and CRS tests conducted on tubes INCL #3 (25-27 ft.) and B-3 [INCL #2] (19-21 ft.).

Tables 4.5 and 4.6 present a summary of the drained direct shear tests in English and SI units including index properties, consolidation data, and shear-displacement data at peak shear stress and at large shear displacement. Figure 4.10 plots the consolidation data for all tests. Figures 4.11 through 4.14 plot the individual test shear stress-displacement data with the repeated shear cycles. Figure 4.15 plots a summary of the peak measured horizontal shear stress and the large displacement horizontal shear stress versus end of consolidation vertical effective stress for the three INCL #3 25-27 direct shear tests. The lines shown in the plot are the best-fit failure envelopes assuming a straight line fit to the data. Figure 4.16 plots the peak measured horizontal shear stress and the large displacement horizontal shear stress versus end of consolidation vertical effective stress for the test conducted on Tube B-3 [INCL #2] 19-21 ft.

Tables 4.7 and 4.8 present a summary of the CRS test specimen properties in English and SI units. Two tests were conducted on tube INCL #3 25-27 ft. and one test on tube B-3 [INCL #2] 19-21 ft. Figures 4.17 to 4.21 present plots of the compression curve and coefficient of consolidation data for each test. Coefficient of consolidation data are not available for test CRS113 on tube B-3 [INCL #2] 19-21 ft. because little to no base excess pore pressure developed during the test. Using the calculated in situ effective vertical stress from the soil profile generated in the following section, and assuming hydrostatic pore water pressure, the overconsolidation ratio (OCR) for both CRS tests is approximately 3.5.

4.5 GENERATED SOIL PROFILE

Using the boring logs, the geologic history, and the in situ and laboratory testing, a soil profile was generated for use in the stability analysis. The cross sectional profile of the slope was created by VTrans using the surveyed site plan and digitized into Slide 5.0 (as described in Chaper 6). Figure 4.22 presents the completed soil profile used in Slide 5.0 and Table 4.9

presents a summary of the soil layers and their properties. Figure 4.23 plots the vertical total and effective stress as a function of depth assuming hydrostatic pore pressures. For reference, the preconsolidation stresses estimated from the CRS tests are included. Normalized undrained shear strength from the FVT versus depth are also included.

Bedrock starts at an elevation above sea level of 179.5 m (589 ft.). Overlaying the bedrock is 1 m (3 ft.) of silt-sand-gravel with broken rock, probably a glacial till left behind by the glaciers. For stability analysis using the Mohr-Coulomb failure model, this material has an estimated unit weight of 22 kN/m^3 (140 lb/ft^3), cohesion of zero, and a phi of 45 degrees.

Starting at an elevation of 180.4 m (592 ft.) and ending at 189 m (620 ft.) is a layer of firm silt, probably deposited during the first glacial lake at the site. This material has an estimated unit weight of 18.9 kN/m^3 (120 lb/ft^3), cohesion of 7.1 kPa (150 lb/ft^2), and a $\phi' = 32$ degrees.

Above the firm silt, to an elevation of 191.4 m (628 ft.) is a layer of silty clay. It is this layer that has developed the significant movement observed by the inclinometers. It is possible this layer was deposited by a subsequent glacial lake to the one that deposited the firm silt layer below. This material has an average unit weight of 17.6 kN/m^3 (113 lb/ft^3) and a measured cohesion of 3.8 kPa (80 lb/ft^2) and $\phi' = 24.5$ degrees.

A second silt layer is above the silty clay to an elevation of 195.7 m (642 ft.). This layer is possibly a result of a third glacial lake at the site. This material has an average unit weight of 18.4 kN/m^3 (117 lb/ft^3) and a measured cohesion of 4.3 kPa (90 lb/ft^2) and $\phi' = 33.6$ degrees.

The top 3 m (10 ft.) of the soil profile, to an elevation of 198.7 m (652 ft.) is gravely sand. From the boring logs, the top 1.22 m (4 ft.) of this material has a different AASHTO classification than the lower gravely sand. This top material is probably a result of the construction and maintenance of Reservoir Rd. The lower gravely sand could also be from the road; however it is also possible that this material is part of the gravel and pebbly sand deposit associated with Lake Mansfield I that is found locally. Owing to the elevation, it could also be a shoreline deposit associated with Lake Mansfield II. The entire gravely sand layer has an estimated unit weight of 20.4 kN/m^3 (130 lb/ft^3), cohesion of zero, and a $\phi' = 35$ degrees.

There is no boring log for the installation of Monitoring Well #2, located on the uphill side of the road, to give an indication of the soil layering uphill or downhill of Inclinometer #1.

For the creation of the profile, it is assumed that the soil layers are generally parallel to the ground surface above Inclinometer #1 and flat and level below the inclinometer.

Table 4.1 Summary of Standard Penetration Test results

Depth (ft.)	Depth (m)	Blows (per 1 ft. or 0.3 m)	Recovery (% per 2 ft. or 0.6 m)
0-2	0-0.61	5	40
2-4	0.61-1.22	7	35
4-6	1.22-1.83	4	65
6-8	1.83-2.44	4	30
8-10	2.44-3.05	4	10
10-12	3.05-3.66	3	10
12-14	3.66-4.27	4	20
14-16	4.27-4.88	5	5
16-18	4.88-5.49	3	80
18-20	5.49-6.10	4	70
20-22	6.10-6.71	5	65
22-24	6.71-7.32	6	50
24-26	7.32-7.92	5	75
26-28	7.92-8.53	2	0
28-30	8.53-9.14	5	35
30-32	9.14-9.75	4	100
32-34	9.75-10.36	3	90
34-36	10.36-10.97	3	90
36-38	10.97-11.58	4	80
38-40	11.58-12.19	3	80
40-42	12.19-12.8	6	95
42-44	12.8-13.41	5	100
44-46	13.41-14.02	5	65
46-48	14.02-14.63	6	80
48-50	14.63-15.24	3	100
50-52	15.24-15.85	7	100
52-54	15.85-16.46	5	90
54-56	16.46-17.07	3	100
56-58	17.07-17.68	6	90
58-60	17.68-18.29	7	65
60-62	18.29-18.9	-	-
62-63.55	18.9-19.37	20	65
Bedrock			

Note: 1. Data from VTrans

Table 4.2 Summary of Field Vane Test results

Depth (ft)	Depth (m)	s_u Peak (psf)	s_u Peak (kPa)	s_u/σ'_{v0}	s_u Remolded (psf)	s_u Remolded (kPa)	S_t
16-18	4.88-5.49	130	6.2	0.08	113	5.4	1.2
21-23	6.4-7.01	95	4.6	0.05	45	2.2	2.1
26-28	7.92-8.53	285	13.7	0.13	155	7.4	1.8
31-33	9.45-10.06	895	42.9	0.36	110	5.3	8.1
36-38	10.97-11.58	1380	66.1	0.50	490	23.5	2.8

Notes:
1. Data from VTrans
2. $S_t = s_u/s_{ur}$

Table 4.3 Summary of liquid and plastic limits

Depth (ft)	Depth (m)	Moisture Content w (%)	Liquid Limit (LL)	Plastic Limit (PL)	Plasticity Index (PI)	Liquidity Index (LI)
20-22	6.10-6.71	33.8	29	26	3	2.6
22-24	6.71-7.32	28.2				
24-26	7.32-7.92	36.0	33	21	12	1.3
28-30	8.53-9.14	42.1	42	25	17	1.0
30-32	9.14-9.75	41.2	39	26	13	1.2
32-34	9.75-10.36	41.4	38	28	10	1.3
34-36	10.36-10.97	33.2	28	23	5	2.0
36-38	10.97-11.58	35.7	32	30	2	2.9
38-40	11.58-12.19	38.5	34	29	5	1.9

Notes:
1. Data from VTrans
2. Liquidity Index (LI) = $\frac{w - PL}{PI}$

Table 4.4 Summary of grain-size and classification results

Depth (ft.)	Depth (m)	Moisture Content (%)	Gravel (%)	Sand (%)	Fines (%)	Hydrometer (% passing 0.002 mm)	AASHTO Classification
0-2	0-0.61	5.2	35.8	52.3	11.9		A-1-b
2-4	0.61-1.22	7.6	42.2	46.2	11.6		A-1-b
4-6	1.22-1.83	8.7	25.1	57.4	17.5		A-2-4
6-8	1.83-2.44	5.9	29.4	54.3	16.3		A-2-4
10-12	3.05-3.66	31.0	3.5	7.4	89.1		A-4
12-14	3.66-4.27	33.5	8.3	18.8	72.9		A-4
14-16	4.27-4.88	33.2	18.2	30.9	50.9		A-4
16-18	4.88-5.49	37.0	3.8	14.8	81.4		A-4
18-20	5.49-6.10	34.0	0.7	5.3	94.0		A-4
20-22	6.10-6.71	33.8	0.2	4.2	95.6	59.7	A-4
22-24	6.71-7.32	28.2	0.2	6.6	93.2		A-4
24-26	7.32-7.92	36.0	0.3	2.6	97.1		A-6
28-30	8.53-9.14	42.1	0.0	1.4	98.6		A-7-6
30-32	9.14-9.75	41.2	0.0	1.0	99.0	93.0	A-6
32-34	9.75-10.36	41.4	0.0	1.0	99.0		A-4
34-36	10.36-10.97	33.2	1.4	16.5	82.1		A-4
36-38	10.97-11.58	35.7	3.4	5.3	91.3		A-4
38-40	11.58-12.19	38.5	0.0	0.8	99.2	80.3	A-4
40-42	12.19-12.8	29.7	0.0	2.9	97.1		A-4
42-44	12.8-13.41	31.3	0.3	8.6	91.1		A-4
44-46	13.41-14.02	29.7	0.0	6.1	93.9		A-4
46-48	14.02-14.63	34.3	1.5	2.8	95.7		A-4
48-50	14.63-15.24	38.8	0.0	2.0	98.0		A-4
50-52	15.24-15.85	33.1	3.0	4.3	92.7	42.3	A-4
52-54	15.85-16.46	32.2	0.0	4.7	95.3		A-4
54-56	16.46-17.07	34.0	0.0	4.1	95.9		A-4
56-58	17.07-17.68	33.4	0.0	1.6	98.4		A-4
58-60	17.68-18.29	30.8	2.0	3.0	95.0		A-4
62-63.55	18.9-19.37	10.5	46.3	30.0	23.7		A-1-b
Bedrock							

Notes:
1. Data from VTrans
2. % Gravel = % > 2.0 mm
3. 0.075 mm < % Sand < 2.0 mm
4. % Fines = % < 0.075 mm

Table 4.5 Summary of drained Direct Shear test results

Test Number	Sample Tube	w (%)	γ_t (pcf)	γ_d (pcf)	At End of Consolidation		At Maximum Shear Stress		At Large Displacement
					σ'_{vc} (psf)	ε_{vc} (%)	ΔL (in)	τ_h (psf)	τ_h (psf)
DS211	INCL#3 25-27'	45	112	77	1000	1.2	0.064	555	455
DS209	INCL#3 25-27'	39	117	84	2500	2.0	0.274	1195	1110
DS210	INCL#3 25-27'	40	117	84	4000	3.6	0.127	1925	1860
DS212	B-3 [INCL#2] 19-21'	35	117	86	2500	3.8	0.175	1750	1660

Notes: 1. w = bulk water content of entire test specimen.

Table 4.6 Summary of drained Direct Shear test SI results

Test Number	Sample Tube	w (%)	γ_t (kN/m^3)	γ_d (kN/m^3)	At End of Consolidation		At Maximum Shear Stress		At Large Displacement
					σ'_{vc} (kPa)	ε_{vc} (%)	ΔL (mm)	τ_h (kPa)	τ_h (kPa)
DS211	INCL#3 25-27'	45	17.4	12.1	47.9	1.2	1.63	26.6	21.8
DS209	INCL#3 25-27'	39	18.4	13.2	119.7	2.0	6.96	57.2	53.2
DS210	INCL#3 25-27'	40	18.4	13.2	191.5	3.6	3.23	92.2	89.1
DS212	B-3 [INCL#2] 19-21'	35	18.4	13.5	119.7	3.8	4.45	83.8	79.5

Notes: 1. w = bulk water content of entire test specimen.

Table 4.7 Summary of Constant Rate of Strain specimen properties

Test #	Sample Tube	w (%)	γ_t (pcf)	γ_d (pcf)	e_0	σ'_p (psf)	OCR
CRS 110	INCL#3 25-27’	45	111	76	1.241	7300	3.4
CRS 111	INCL#3 25-27’	37	107	78	1.200	7500	3.5
CRS 113	B-3 [INCL#2] 19-21’	31	119	91	0.856	-	-

Notes:
1. w = bulk water content of entire test specimen.
2. e_0 computed using an assumed specific gravity = 2.75.
3. σ'_p = preconsolidation stress as determined by Strain Energy Method (Becker et al. 1987).
4. OCR = σ'_p / σ'_{v0}

Table 4.8 Summary of Constant Rate of Strain specimen properties – SI units

Test #	Sample Tube	w (%)	γ_t (kN/m^3)	γ_d (kN/m^3)	e_0	σ'_p (kPa)	OCR
CRS 110	INCL#3 25-27’	45	17.4	11.9	1.241	350	3.4
CRS 111	INCL#3 25-27’	37	16.8	12.3	1.200	360	3.5
CRS 113	B-3 [INCL#2] 19-21’	31	18.7	14.3	0.856	-	-

Notes:
1. w = bulk water content of entire test specimen.
2. e_0 computed using an assumed specific gravity = 2.75.
3. σ'_p = preconsolidation stress as determined by Strain Energy Method (Becker et al. 1987).
4. OCR = σ'_p / σ'_{v0}

Table 4.9 Summary of soil profile materials and estimated properties

Elevation	Name	Unit Weight	c'	ϕ' (°)
195.7-198.7 m (642-652 ft.)	Gravely Sand	20.4 kN/m^3 (130 lb/ft^3)	0	35
191.4-195.7 m (628-642 ft.)	Silt	18.4 kN/m^3 (117 lb/ft^3)	4.3 kPa (90 lb/ft^2)	33.6
189-191.4 m (620-628 ft.)	Silty Clay	17.6 kN/m^3 (113 lb/ft^3)	3.8 kPa (80 lb/ft^2)	24.5
180.4-189 m (592-620 ft.)	Firm Silt	18.9 kN/m^3 (120 lb/ft^3)	7.1 kPa (150 lb/ft^2)	32
179.5-180.4 m (589-592 ft.)	Till	22 kN/m^3 (140 lb/ft^3)	0	45
179.5 m (589 ft.)	Bedrock	-	-	-

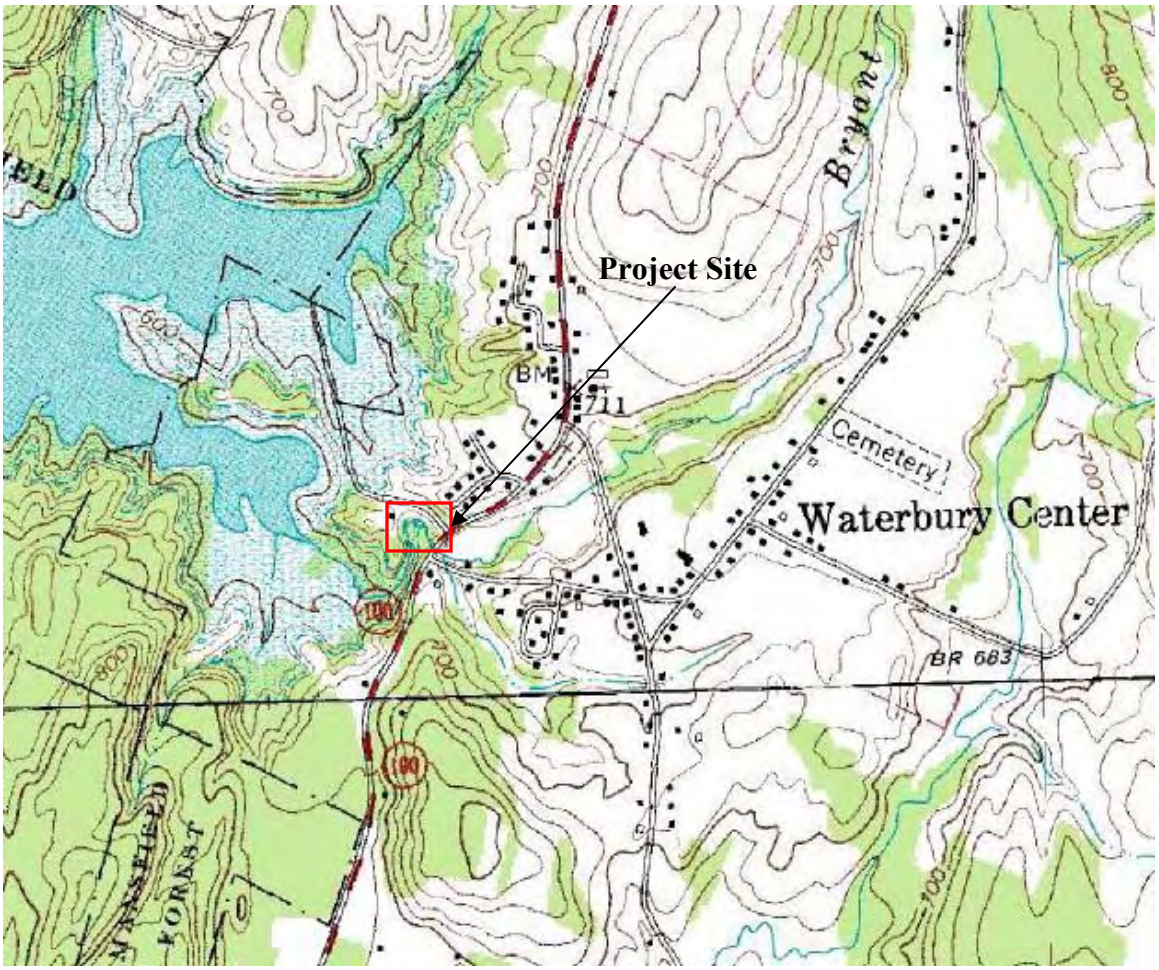

Figure 4.1 Project site location in Waterbury Center, VT. (from USGS)

Figure 4.2 Reservoir Rd. looking northwest. The datalogger and solar panel are in the background, and Incl 2 is in the middle near the tree.

Figure 4.3 Looking downhill at Bryant Brook.

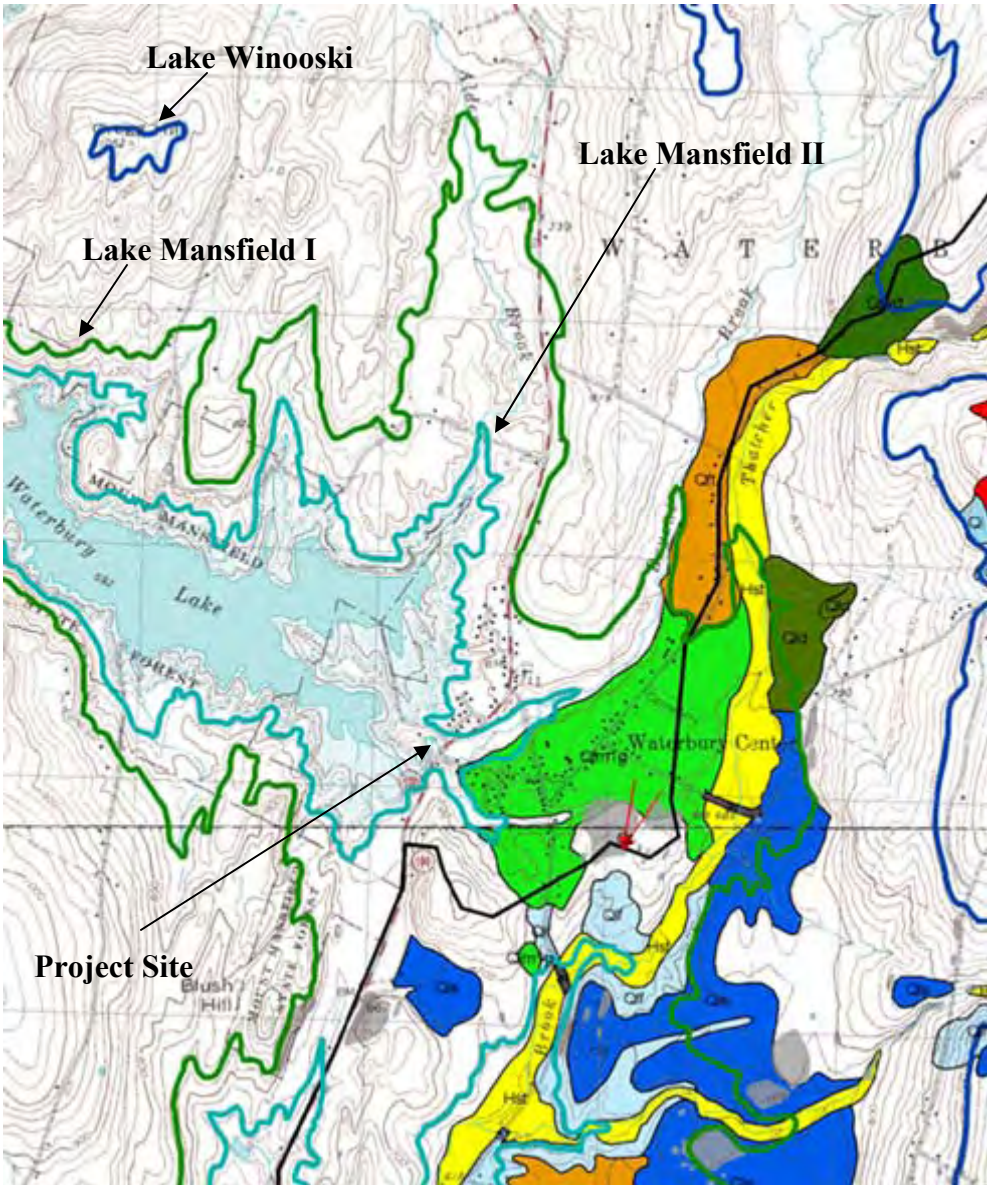

Figure 4.4 Surficial map show glacial lake shorelines (from Springston and Dunn 2006).

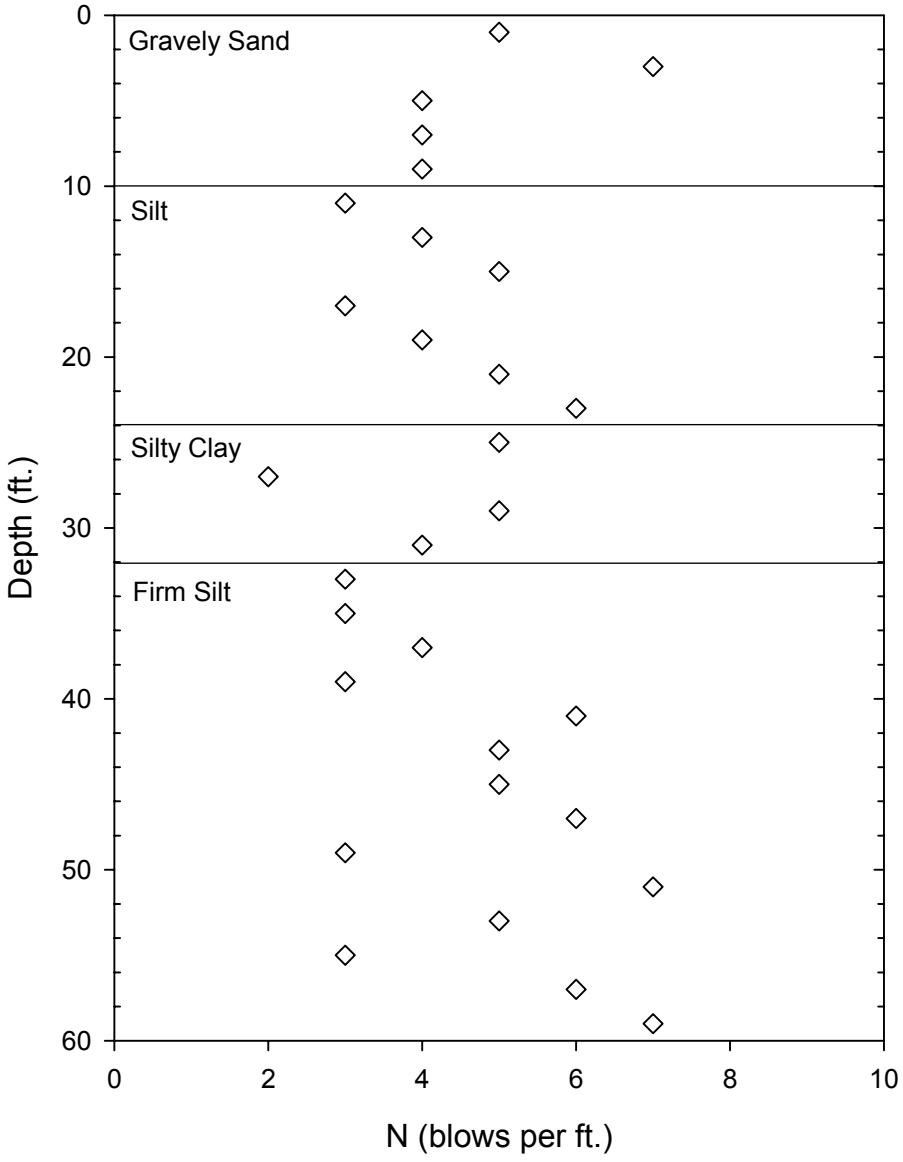

Figure 4.5 SPT blow counts versus depth for Inclinometer 1.

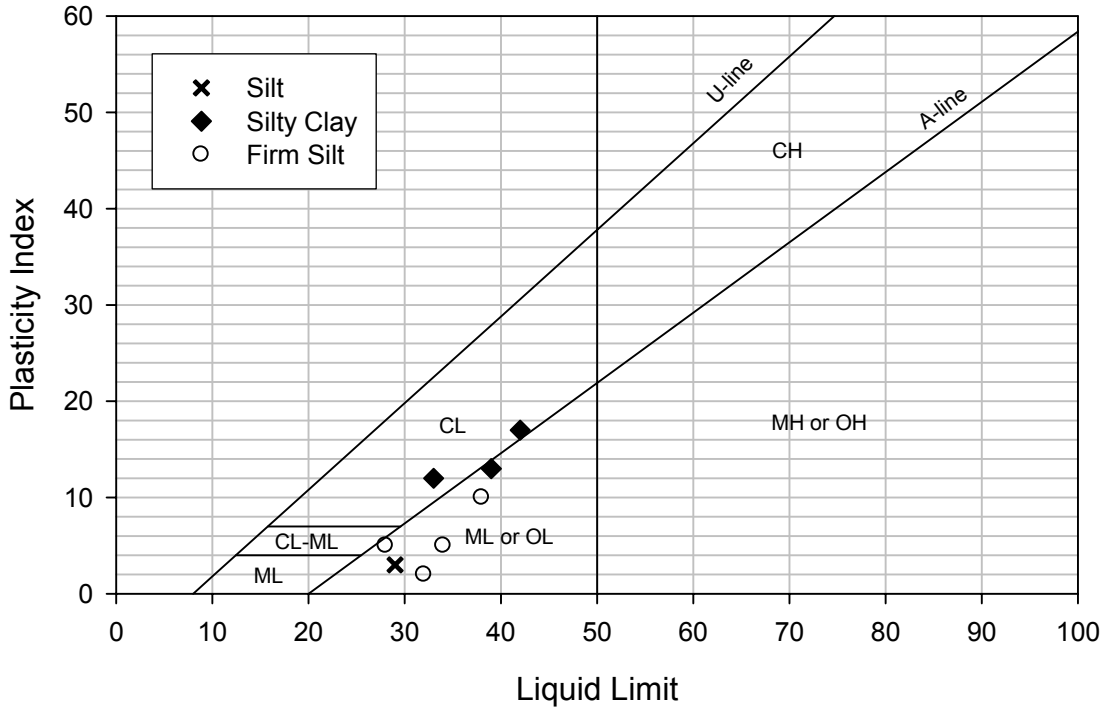

Figure 4.6 Casagrande's plasticity chart for Inclinometer 1.

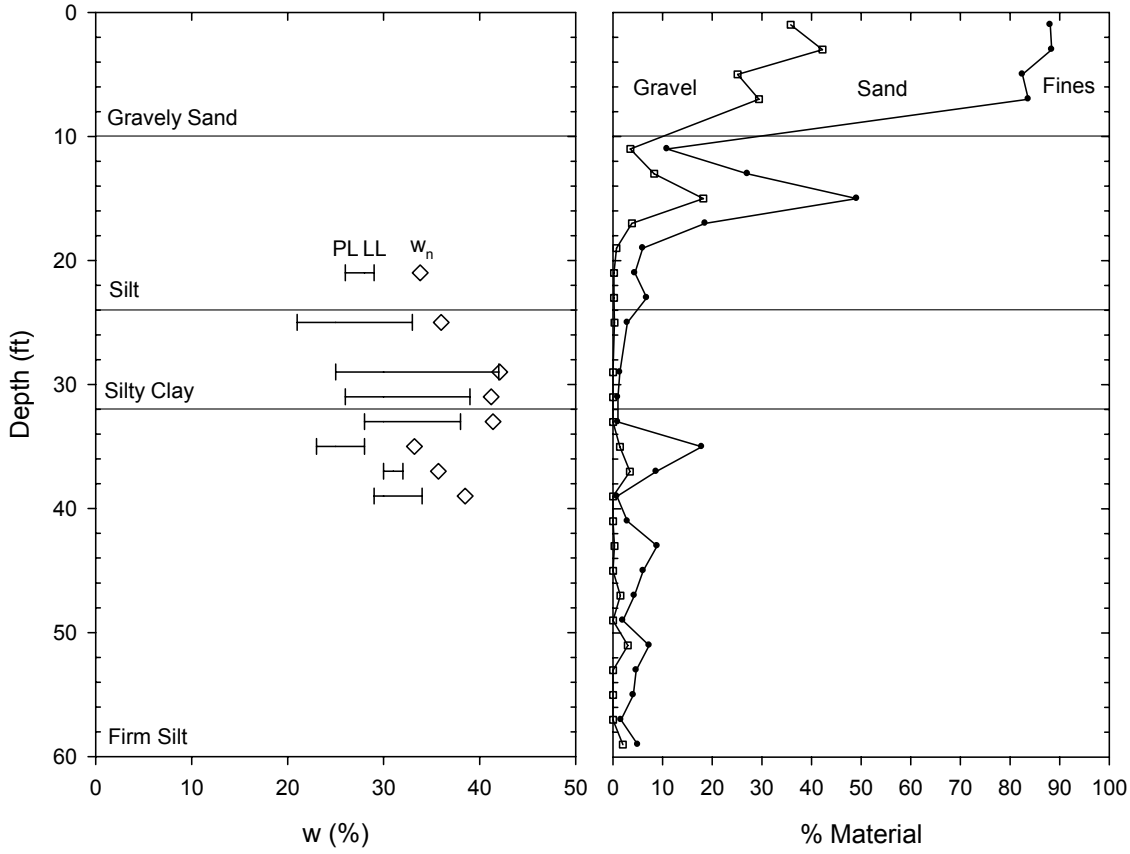

Figure 4.7 Profile plots of liquid and plastic limits, water content, and grain-size distribution of Inclinometer 1.

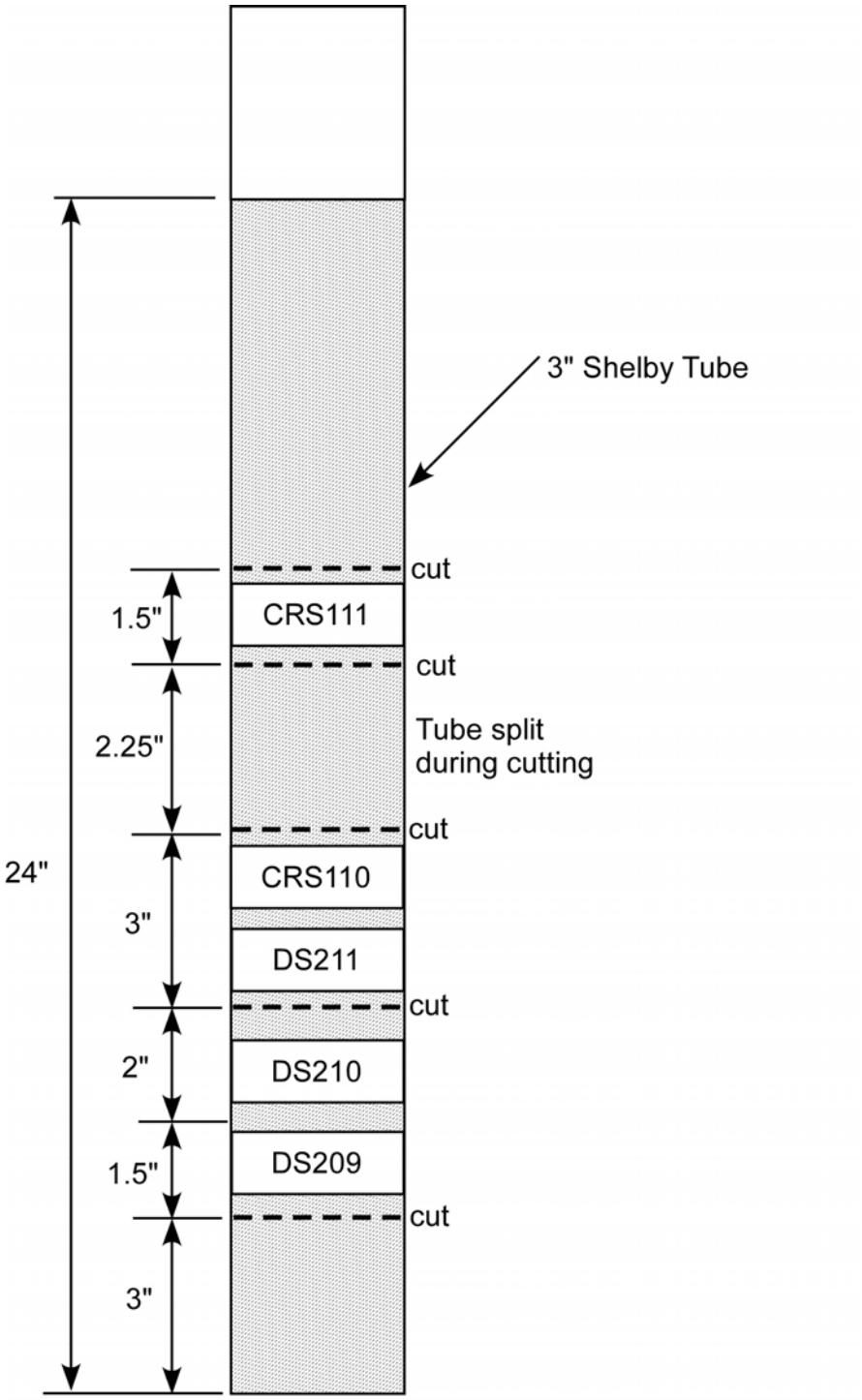

Notes:
1. Bottom of Tube Depth = 27'
2. DSxxx = Drained Direct Shear Test Number
3. CRSxxx = Constant Rate of Strain Consolidation Test Number
4. Drawing not to scale

Figure 4.8 DS and CRS specimen locations in sample tube INCL #3 (25-27 ft.).

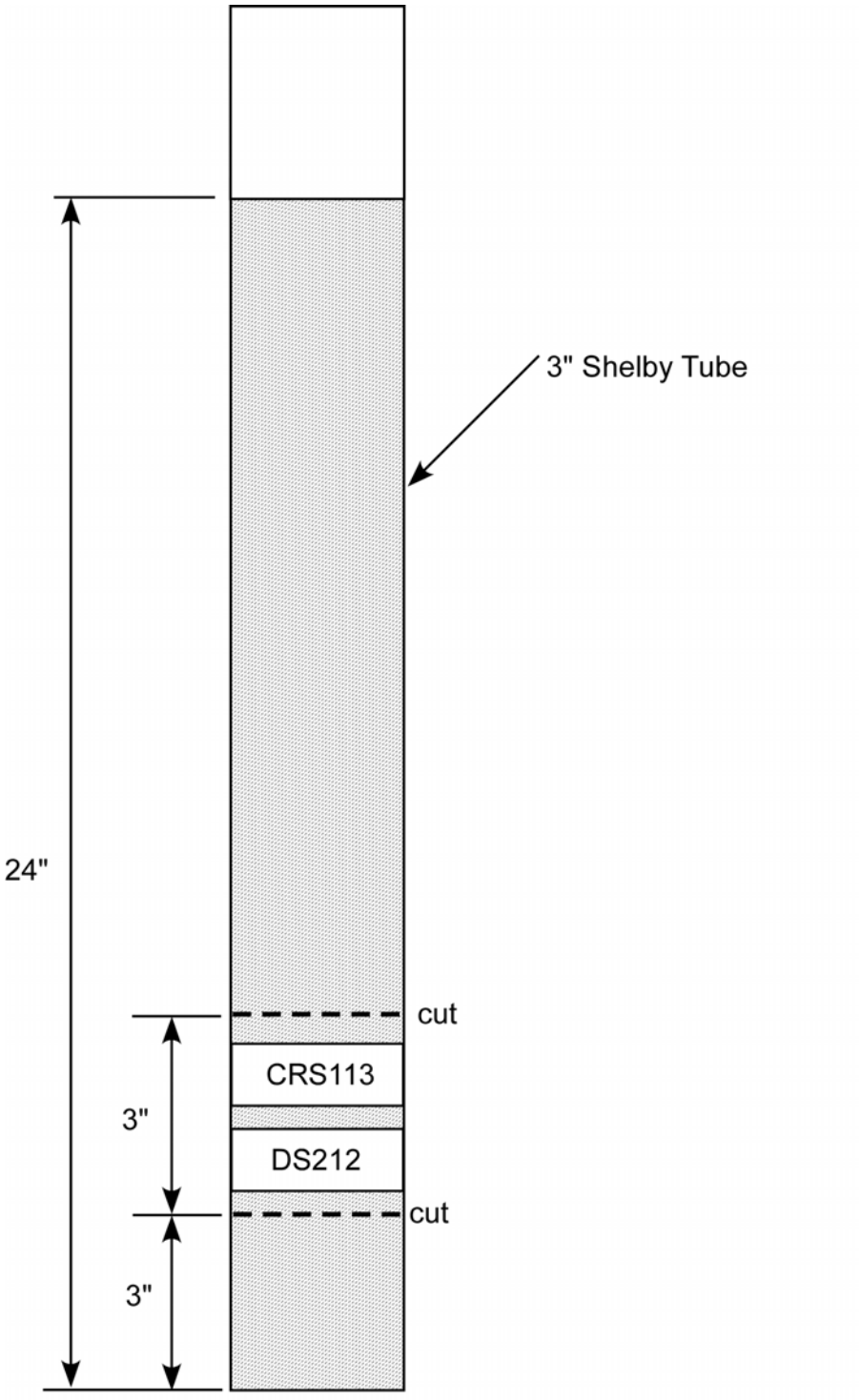

Notes:
1. Bottom of Tube Depth = 21'
2. DSxxx = Drained Direct Shear Test Number
3. CRSxxx = Constant Rate of Strain Consolidation Test Number
4. Drawing not to scale

Figure 4.9 DS and CRS specimen locations in sample tube B-3 [INCL #2] (19-21 ft.).

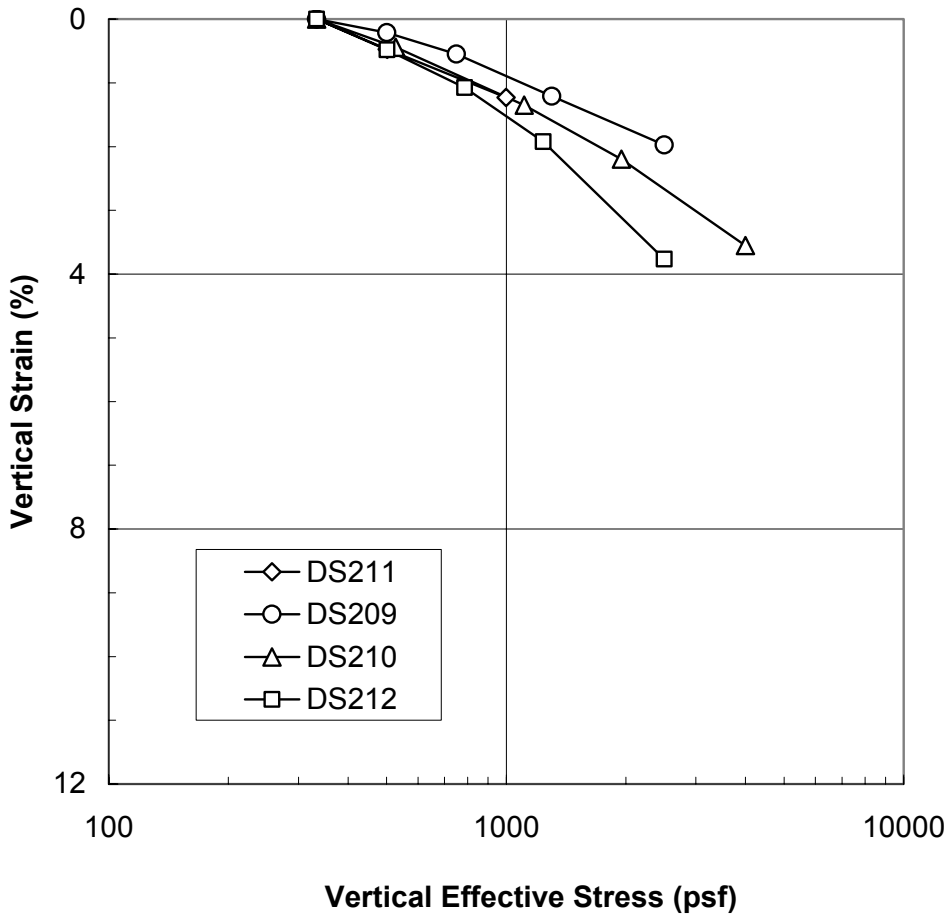

Figure 4.10 Vertical strain versus vertical effective stress for consolidation phase of the Direct Shear tests.

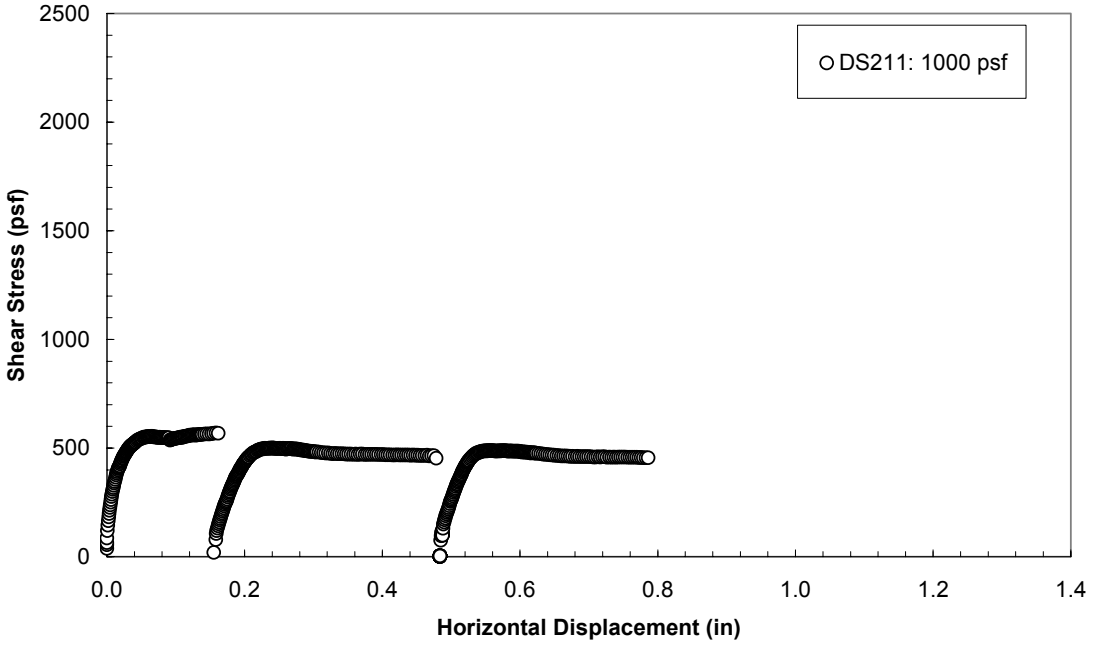

Figure 4.11 Horizontal shear stress versus horizontal displacement for drained shear phase of test DS211 on Tube INCL#3 25-27 ft. with σ'_{vc} = 1000 psf.

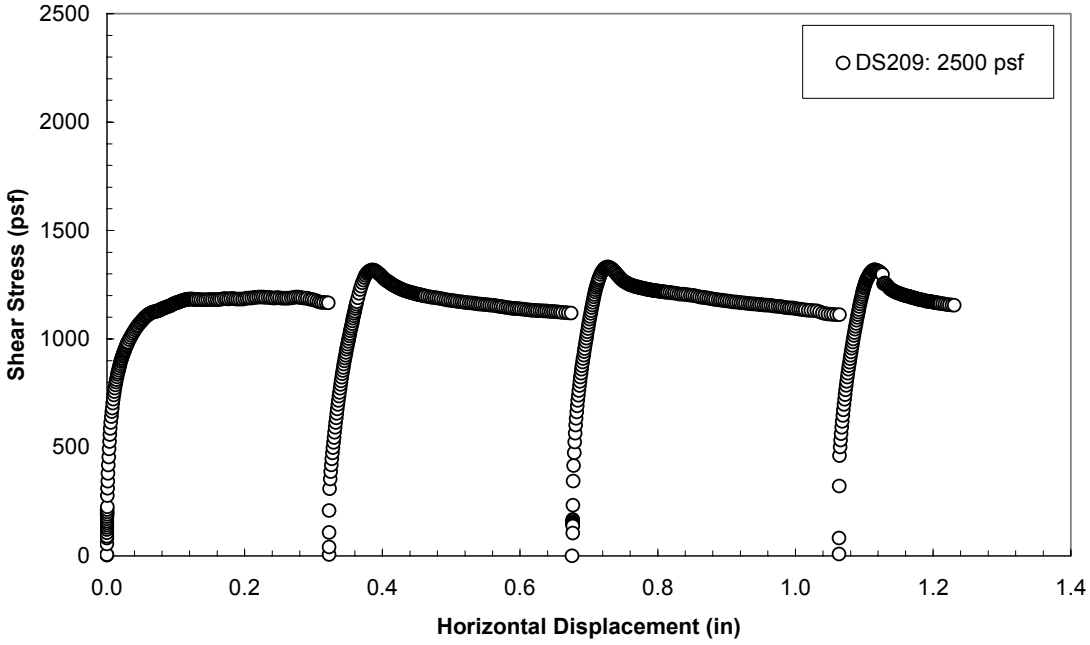

Figure 4.12 Horizontal shear stress versus horizontal displacement for drained shear phase of test DS209 on Tube INCL#3 25-27 ft. with σ'_{vc} = 2500 psf.

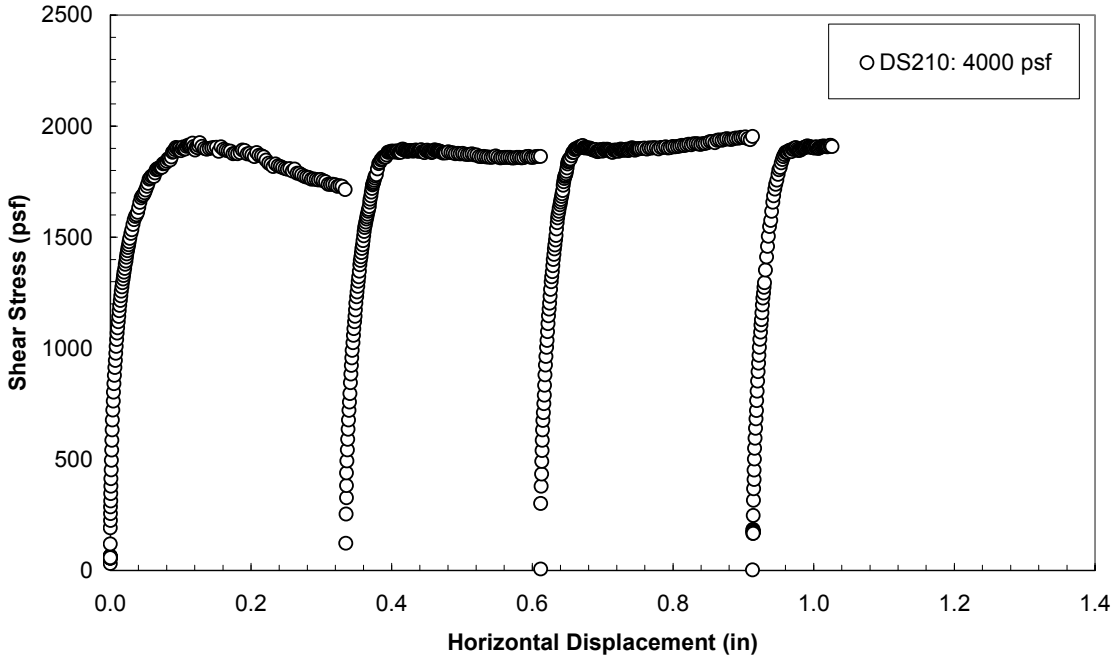

Figure 4.13 Horizontal shear stress versus horizontal displacement for drained shear phase of test DS210 on Tube INCL#3 25-27 ft. with σ'_{vc} = 4000 psf.

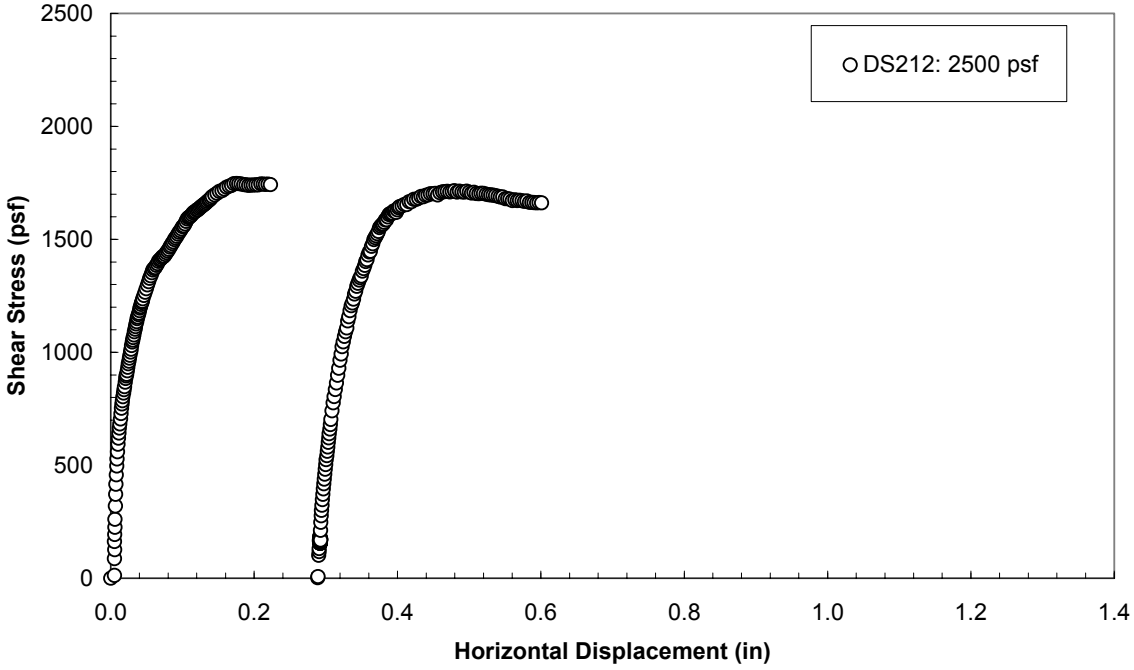

Figure 4.14 Horizontal shear stress versus horizontal displacement for drained shear phase of test DS212 on Tube B-3 [INCL#2] 19-21 ft. with σ'_{vc} = 2500 psf.

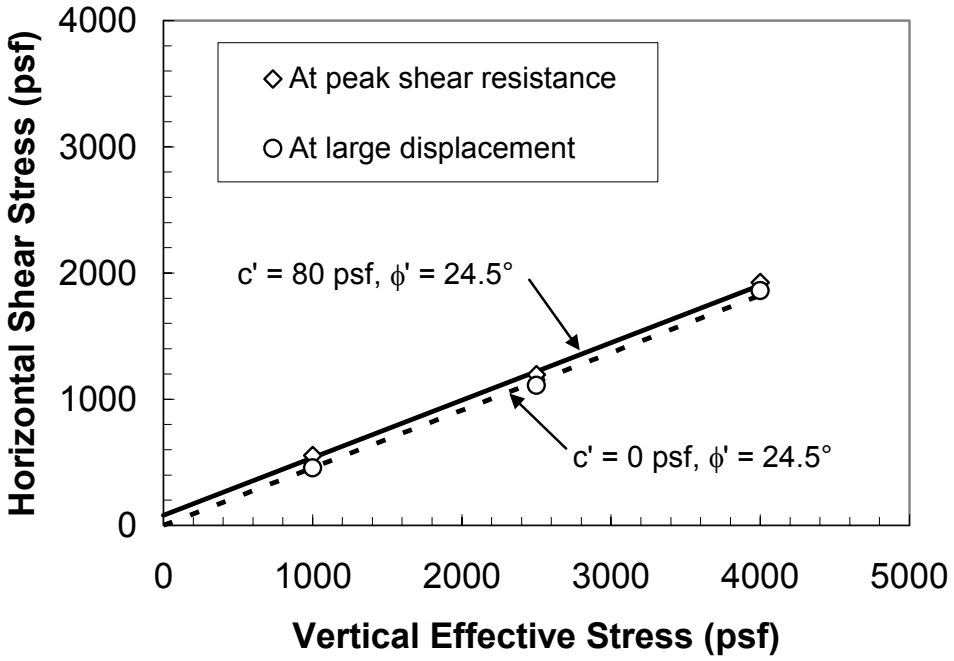

Figure 4.15 Measured horizontal peak and large displacement shear stress versus end of consolidation vertical effective stress for the Direct Shear tests on Tube INCL#3 25-27 ft.

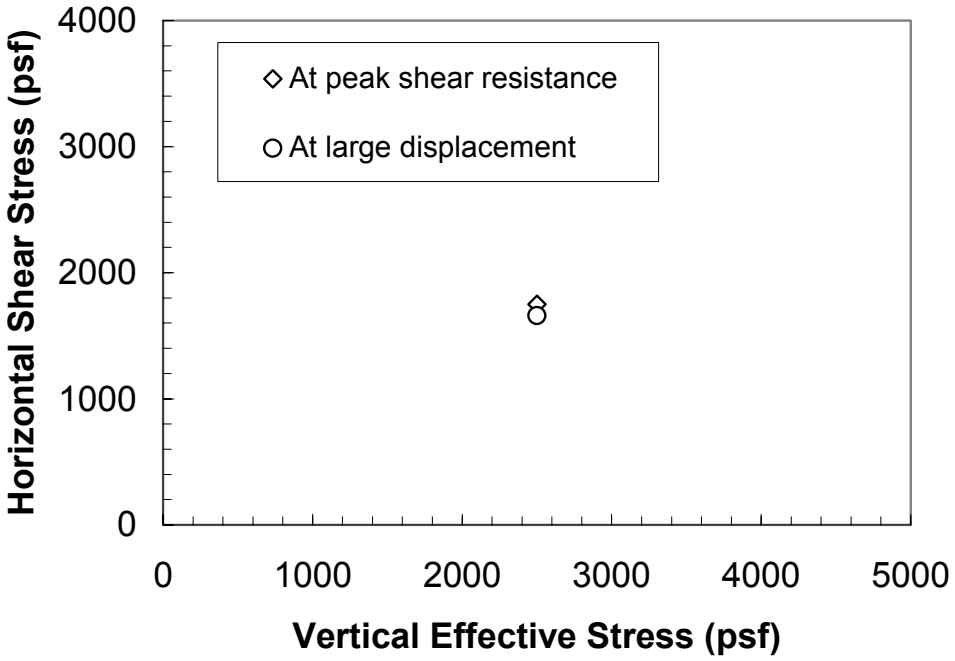

Figure 4.16 Measured horizontal peak and large displacement shear stress versus end of consolidation vertical effective stress for the Direct Shear tests on Tube B-3 [INCL#2] 19-21 ft.

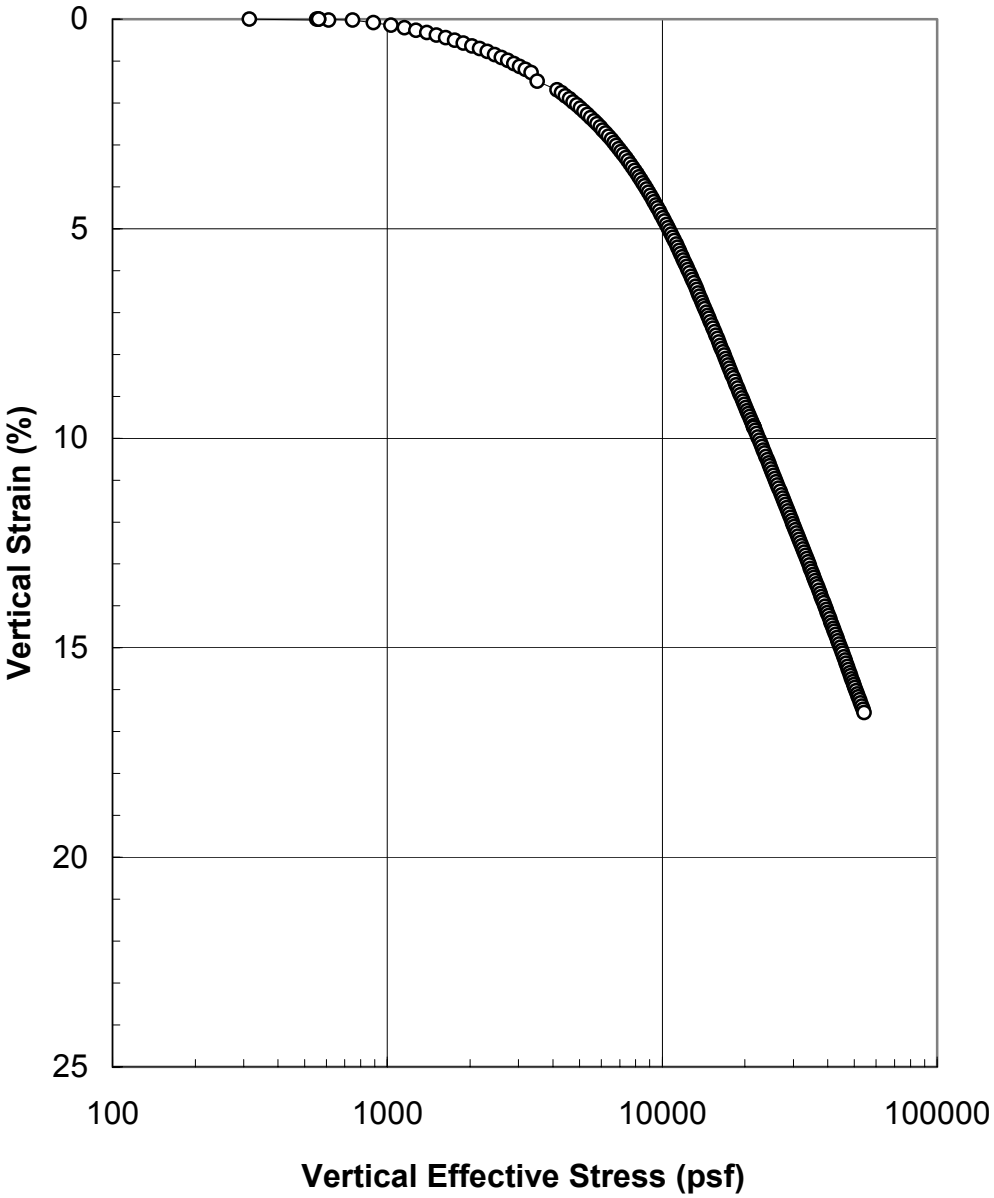

Figure 4.17 CRS compression curve from test CRS 110 on sample INCL#3 25-27 ft.

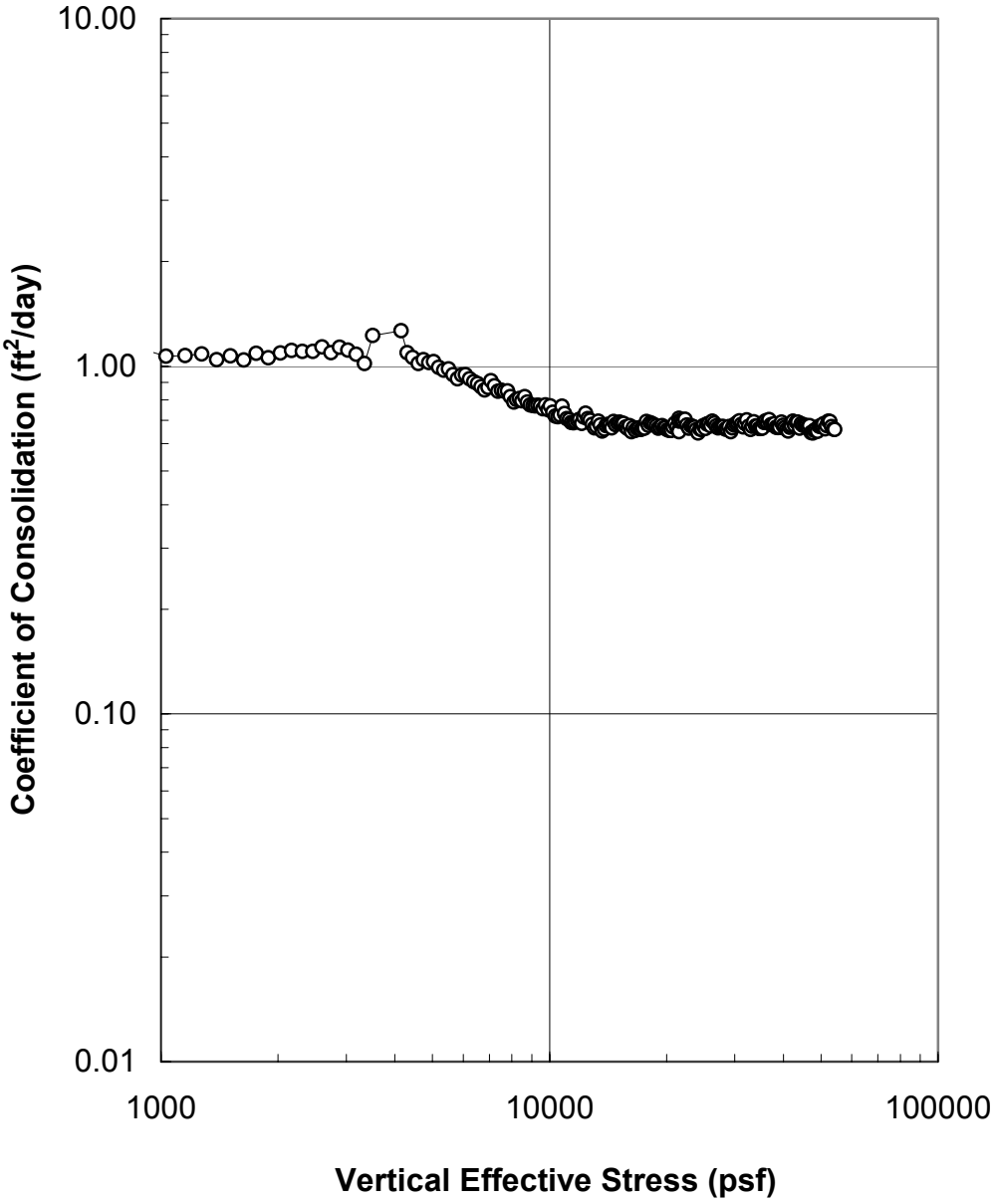

Figure 4.18 CRS coefficient of consolidation versus vertical effective stress from test CRS110 on sample INCL#3 25-27 ft.

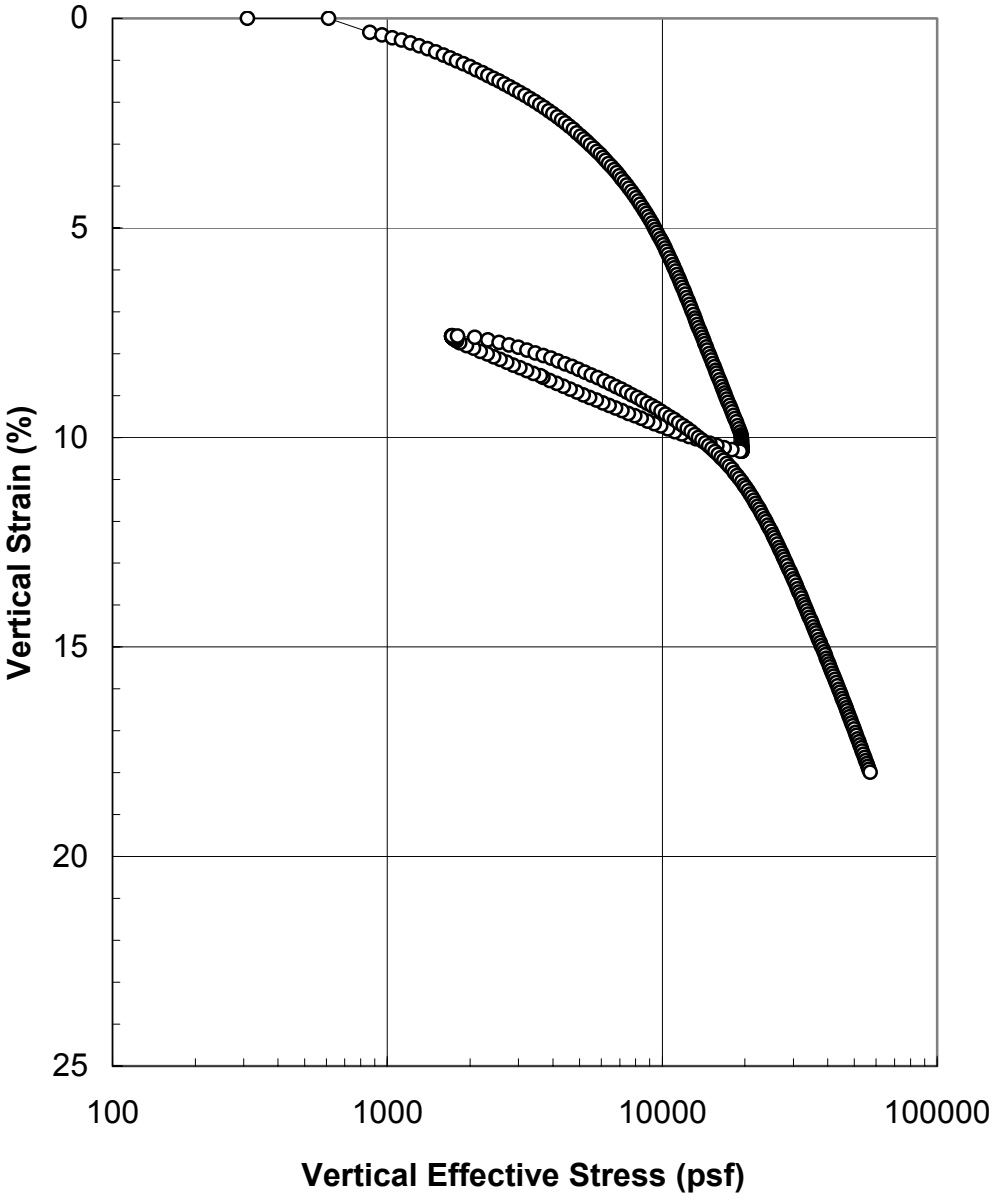

Figure 4.19 CRS compression curve from test CRS 111 on sample INCL#3 25-27 ft.

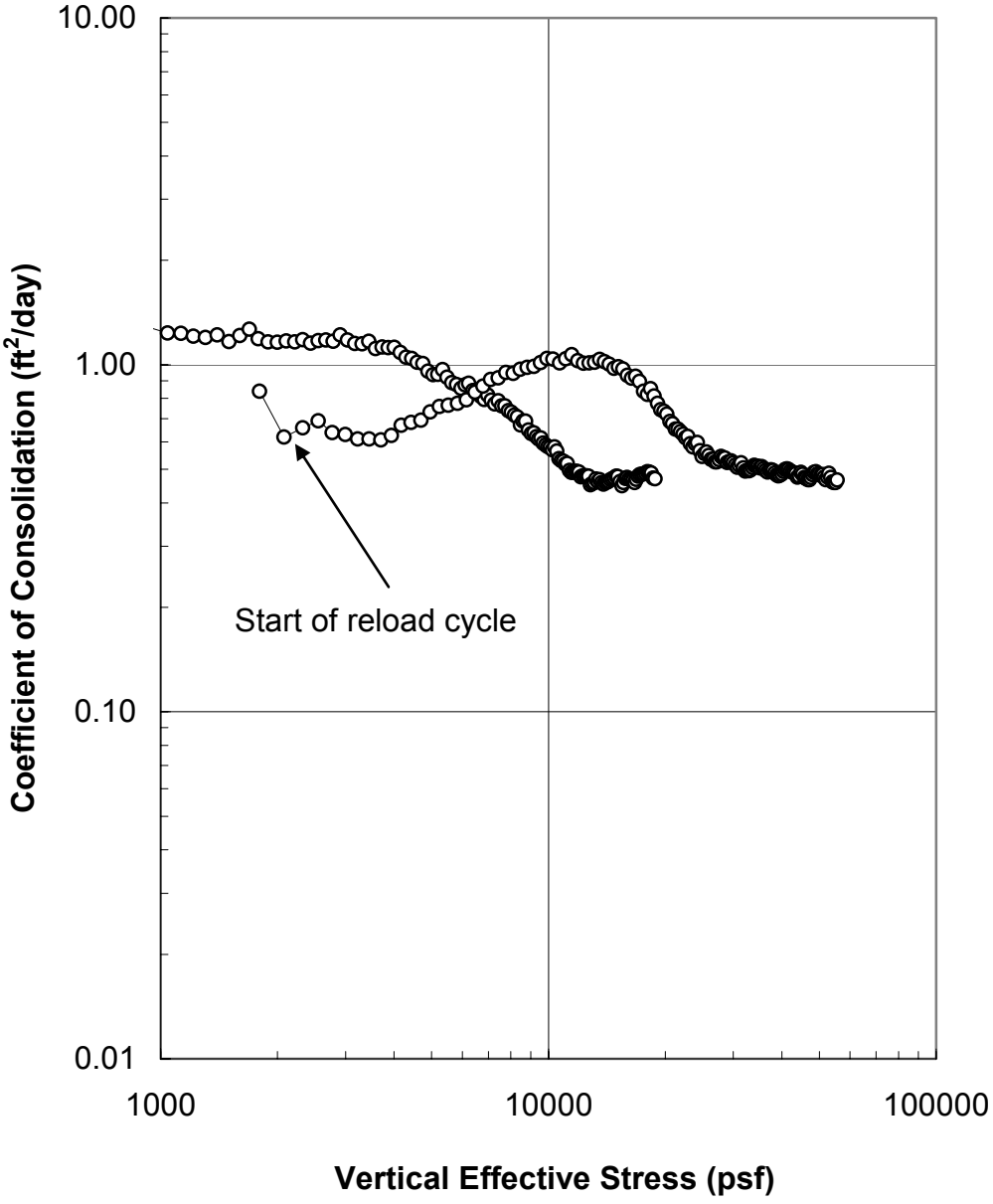

Figure 4.20 CRS coefficient of consolidation versus vertical effective stress from test CRS111 on sample INCL#3 25-27 ft.

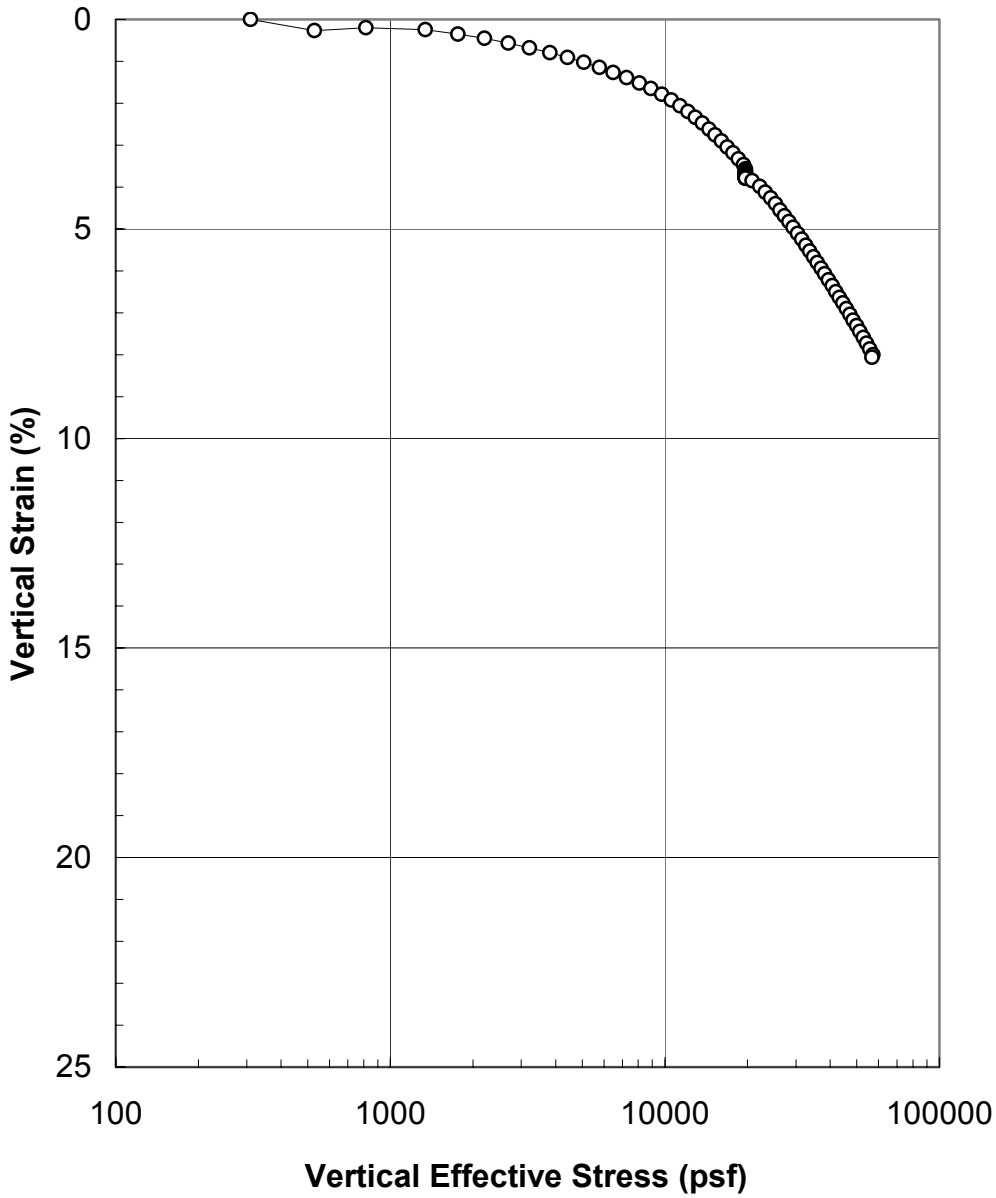

Figure 4.21 CRS compression curve from test CRS 113 on sample B-3 [INCL#2] 19-21 ft.

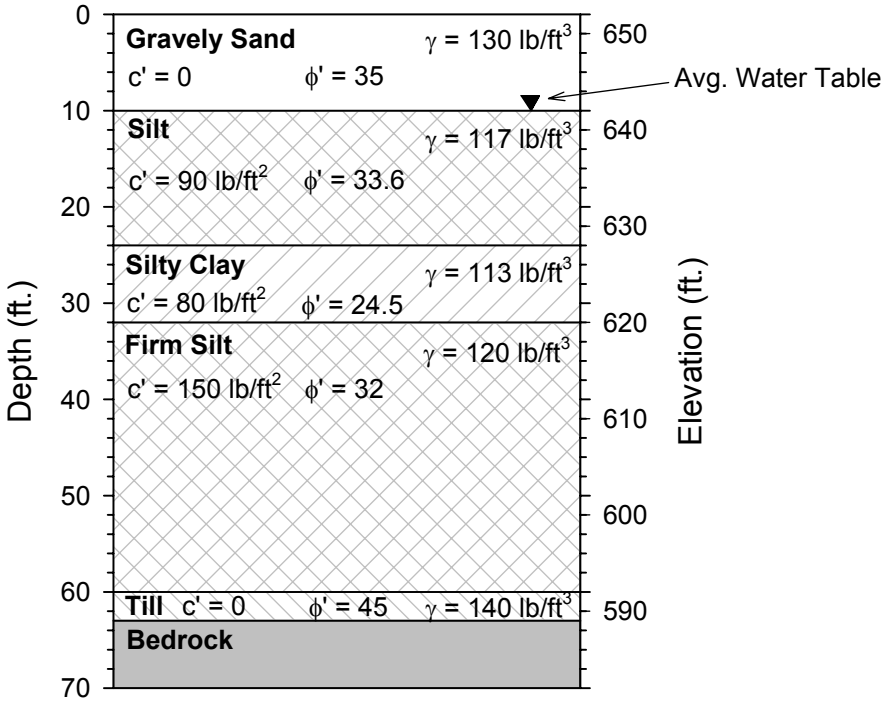

Figure 4.22 Graphical soil profile for Inclinometer 1 generated from Table 4.9.

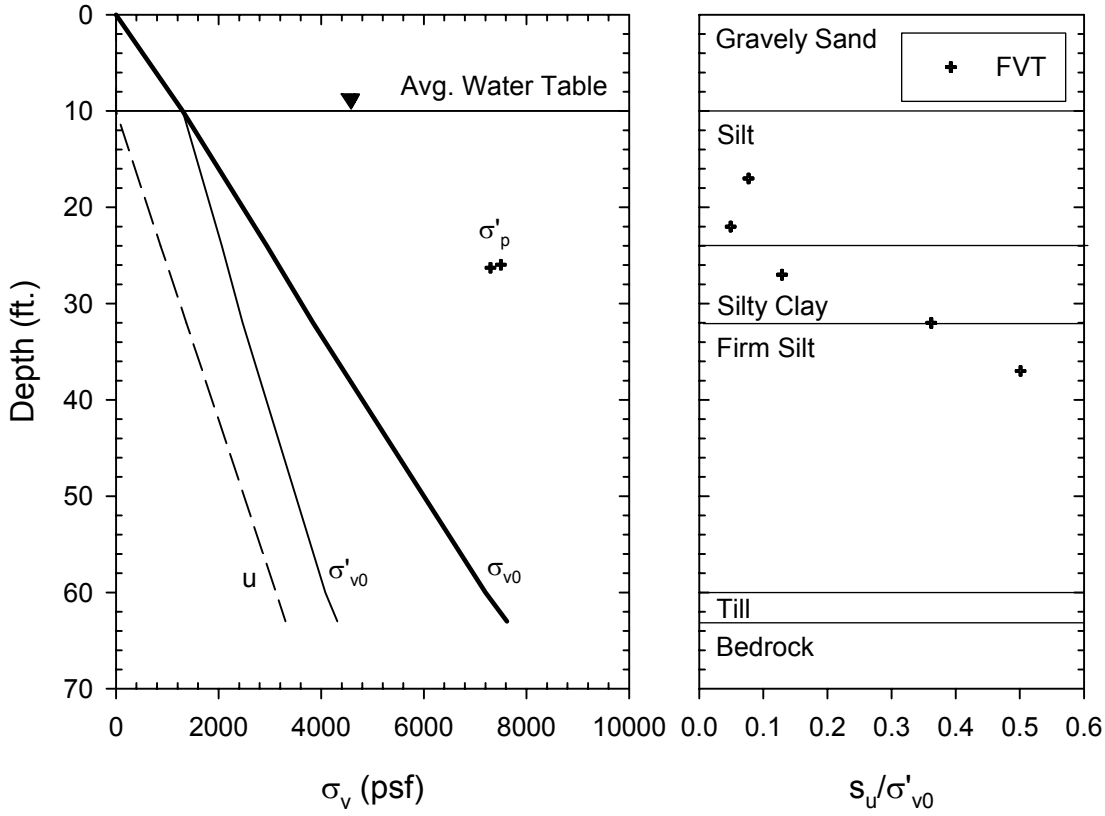

Figure 4.23 Vertical stress versus depth for Inclinometer 1 assuming hydrostatic pore pressures compared to the normalized undrained shear strength FVT results.

5.0 INSTRUMENTATION RESULTS

This chapter presents examples of data collected from the Waterbury site instrumentation and interpretation of that data. The instrumentation data is divided into three categories: precipitation and atmospheric, monitoring wells, and inclinometers. In general, data was recorded from January 25, 2006 to February 15, 2008.

5.1 PRECIPITATION AND ATMOSPHERIC DATA

Precipitation data at the site was recorded starting November 15, 2007, once the rain gauge was installed and operating properly. Therefore precipitation data from the National Weather Service/Federal Aviation Administration's Automated Surface Observing System at the Morristown-Stowe State Airport, approximately 13 miles northeast of the project site and at an elevation of 225 m (738 ft.), is also included. Figure 5.1 presents rainfall data for the full recorded-data time span and Figure 5.2 presents rainfall data from the installation of the rain gauge to February 15, 2008. Although the rain gauge includes an integrated heater for snow melting, this feature was not used due to the lack of available A/C power at the site. Since the data recorded for the rain gauge only occurred during late fall and winter of 2007/2008, the data may not reflect actual precipitation events but rather natural melting of accumulated snow, ice, and rain in the rain gauge itself.

The barometric pressure at the site was recorded to correct the VW piezometers for fluctuation in atmospheric pressure. Atmospheric pressure data from the Morrisville Airport is also included for comparison. Figure 5.3 presents atmospheric pressure data for the full time-span. The difference in pressure from the barometer and the airport before December 5, 2006, is most likely due to errors in the calibration factors and/or the zero reading. After December 5, 2006, the original barometer stopped working and the repaired barometer was reinstalled on May 19, 2007. Figure 5.4 presents atmospheric pressure data from the point that the barometer was reinstalled. The site barometer and airport data compare well, confirming that the repaired barometer was properly calibrated and thus the data can be used to correct the VW piezometer readings.

The battery voltage was recorded to monitor the battery and to verify that the solar panel was providing enough power for the system. Figure 5.5 presents the battery voltage over the full

time-span. The data show that the battery voltage is seasonally dependent and rarely drops below 12.0 Volts. During the two years that the datalogger was operating, a lack of power was never encountered.

5.2 MONITORING WELL DATA

The water table at two locations in the zone of slope movement was recorded through the use of open standpipe and VW piezometers. The measured pressure from a VW piezometer was converted to an equivalent height of the water column above it, and knowing the absolute elevation of the piezometer the elevation of the water table was calculated. To correct for the fluctuation of atmospheric pressure relative to the calibration pressure of the piezometer, the pressure recorded by the barometer was subtracted from the measured pressure of the piezometer prior to calculating the water table elevation. Figure 5.6 presents the corrected and uncorrected water table elevation for Monitoring Well #1. The large increase in uncorrected water elevation in April, 2007, coincides with a reported water line break along Reservoir Road inside the zone of slope movement. Figure 5.7 presents corrected and uncorrected water elevations for Monitoring Well #2. The large gap in data for the first part of 2007 is due to the piezometer not working. The data in these figures show that the water table generally fluctuates two to three feet with larger seasonal fluctuations. Monitoring Well #1 has larger fluctuations than Monitoring Well #2; this may be due to the top ten feet being gravelly sand and allowing more water to percolate down to the water table during precipitation events.

Figure 5.8 presents the Morristown Airport rainfall data superimposed on the corrected and uncorrected water elevation of Monitoring Well #1 for the entire time-span. When the time scale is reduced to June and July, 2006 (Figure 5.9), the data show that after prolonged precipitation events lasting almost half a day or longer, the water table elevation increases. For quick precipitation events, such as the possible thunderstorm in early July, 2006, the water table does not generally increase. A rapid increase in water table elevation in mid April (Figure 5.10), although proceeded by a prolonged precipitation event, coincides with a known water line break. Figure 5.11 shows that prolonged precipitation events occurring regularly can drive up the water table elevation gradually with little decrease. This figure also clearly shows the influence of correcting the piezometer readings for fluctuations in atmospheric pressure.

5.3 INCLINOMETERS

5.3.1 Inclinometer #3

The theory behind the in-place inclinometer is similar to that of a traditional inclinometer (Figure 5.12). Whereas a traditional inclinometer is moved a known distance from one reading to another, each IPI is fixed in the casing at known elevations by use of rigid connecting tubing. At the lower end of the tubing is a pivot and at the top end is the IPI and a second pivot. The gauge length is the distance from one pivot to another. The IPI measures its tilt angle relative to vertical and multiplying the gauge length by the sin of the angle results in the horizontal displacement of the top pivot relative to the bottom pivot. A sum of the horizontal displacements results in the cumulative displacement of the inclinometer casing at ground level assuming that the bottom pivot is prevented from moving. This is typically done by extending the inclinometer casing into bedrock and installing the bottom IPI below the bedrock surface.

Inclinometer #3 was located outside of the zone of slope movement as a reference. Figure 5.13 presents calculated displacement for each of the five IPIs installed in Inclinometer #3 for the entire time-span. All the IPIs give calculated positive displacements, indicating they were installed in the correct orientation and that the inclinometer casing is creeping downhill as expected at an average rate of 0.8 cm per year (0.3 in. per year).

Figure 5.14 presents the calculated deflection of the top IPI 05-14823. The deflection seems to be generally linear through most of the year with increasing deflection and relaxation occurring in late winter through spring. The second IPI, 05-14825 (Figure 5.15), also shows the same general movement but with a more damped reaction. IPIs 05-14827 (Figure 5.16) and 05-16366 (Figure 5.17) appear to show noise in the system. The bottom IPI 05-16370 (Figure 5.18), set in the bedrock, shows no movement over the entire time-span as expected.

Figure 5.19 presents an inclinometer profile of cumulative horizontal displacement versus depth. The increasing displacement followed by relaxation of the upper IPIs is evident as not all of the profile lines are in sequential order. The maximum recorded cumulative displacement over the project time span was less than one inch.

5.3.2 Inclinometer #2

Inclinometer #2 was located inside the zone of slope movement. Figure 5.20 presents the calculated displacement for each of the five VW IPIs installed in Inclinometer #2 over the full time-span. The figure shows that the third IPI, 05-16367, recorded significant displacement

approaching 1 foot in the uphill direction. Inspections of the site by UMass Amherst and VTrans have not shown actual deflections matching calculated deflections. A rotational-type slope movement could produce negative displacement values of the upper inclinometers as the soil mass essentially rotated out from underneath. This is consistent with measured negative displacements of the upper inclinometers. However, the large displacement of 05-16367 is not explained by this.

A typical IPI installation will have the inclinometers installed soon after the completion of the inclinometer casing. This insures that the inclinometers are installed in a near vertical orientation and that all future movement will be recorded. That was not possible for this project because of delays in getting the instrumentation. Hand inclinometer readings were taken at the project site for five months prior to the installation of the IPIs and show slope movement in the late fall of 2005 with a slip surface approximately at the intended elevation of IPI 05-16367 (Appendix B). During the installation of the IPIs in late December, 2006, it was noted that significant force was required to push the IPIs into the casing. This could have been due to the rigid connecting tubing coming into contact with the casing in zones of significant prior ground movement, causing the tubing to bend as it was inserted through the zone. Since the calculation for horizontal deflection assumes that the connecting tubing is not deformed and is free to move horizontally along its entire length, any point that the tubing comes into contact with the casing could produce incorrect horizontal displacement readings.

A full-scale profile drawing of the hand inclinometer readings from December 19, 2006, shows that the connecting tube could have been touching the casing wall at a point below IPI 05-16367 (Appendix C). This reduces the gauge length from 20 ft. to an effective length of less than 4 ft. and could result in calculated horizontal deflections that are much higher than in reality. This could explain the large deflections calculated for IPI 05-16367, but, since the effective gauge length is not known, and could change with further slope movement, a correction to the large deflections cannot be applied. Furthermore, since potential deflection of the tube occurs over 22 ft. below ground surface, it cannot be observed and verified.

A malfunctioning or out of calibration IPI could also cause large calculated deflections that do not match actual site observations. The VW instrumentation is very sensitive to shocks and could be forced out of calibration prior to installation in the casing. However, using the hand inclinometer readings from December 19, 2006, for reference it was concluded by Geokon and

UMass Amherst that IPI 05-16367 was most likely functioning correctly and that the factory determined calibration was valid.

Figure 5.21 presents the calculated displacements of all five IPIs over the entire time-span when the displacement scale has been fixed to show the movement of the four other IPIs. The topmost IPI, 05-14826 (Figure 5.22), shows generally negative displacements, consistent with rotation movement. IPI 05-14828 (Figure 5.23) also shows negative displacements until late April, 2007, and general positive displacements starting in September, 2007. Figure 5.24 presents IPI 05-16367, and with the exception of the magnitude of displacement, shows a general movement similar to 05-14828. IPI 05-16369, located below the estimated slip plane location, shows in Figure 5.25 almost no movement until April, 2007, with very little movement after. IPI 05-16372, located below the bedrock surface, shows (Figure 5.26) no movement over the entire time-span.

Figure 5.27 presents an inclinometer profile of horizontal cumulative displacement versus depth. The total cumulative displacement measured at the top IPI should reflect ground surface movement observed in the field, however the large displacements of IPI 05-16367 result in incorrect cumulative displacement. The first two profiles from early in 2006 do reflect the last hand inclinometer profile taken on December 19, 2005.

To correct the VW reading for temperature, each IPI includes a thermocouple. The datalogger itself also includes a thermocouple. Figure 5.28 presents temperatures of the datalogger and the three shallowest IPIs over the entire time-span. The sinusoidal seasonal variation in the temperature of the datalogger is apparent, as well as the progressively damped variation of the ground water temperature with depth.

5.3.3 Water Table Elevation and Inclinometer Movement

Relating an increase in water table elevation, and therefore an increase in pore water pressure, to slope movement gives the potential to develop an early warning methodology for possible slope movement. Figure 5.29 presents the water table elevation of Monitoring Well #1 superimposed with the cumulative horizontal displacement of Inclinometer #2 from March 1, 2007 to February 15, 2008. A clear correlation between water level and slope movement is not evident. A second rapid increase in the water table in July, 2007, shows only a slight change in horizontal deflection. A prolonged period of increased water table elevation around the 1st of November, 2007, shows no increase in movement until a second increase in the water table

occurs later in the month. The high seasonal water table in April, 2007, shows (Figure 5.30) increased movement, but the rapid increase in water table elevation due to a municipal water line break shortly thereafter on April 17 shows increased movement in the other direction. Plotting the individual IPIs superimposed over the water table elevation of Monitoring Well #1 show that movement at different depths can occur at different water table events. The topmost IPI, 05-14826 (Figure 5.31), generally moved with rapid increases in water table elevation. IPI 05-14828 (Figure 5.32) had significant movement in mid-May, 2007, at the same time the topmost IPI hardly moved. IPI 05-16367 (Figure 5.33) being located near the expected slip surface shows the greatest sensitivity to fluctuations in water table elevation, but although it responded to the mid-May water table increase, it was not as significant as for IPI 05-14828. The change in movement direction by IPI 05-16367 in April was assumed to be from movement occurring deeper due to the abnormally high water table caused by the broken municipal water line. Figures 5.34 and 5.35 show that IPI 05-16369 had movement, but this movement started prior to the water line breaking and ended around the time of the highest water elevation.

Figure 5.36 shows the same Inclinometer #2 cumulative displacement data over the same time-span as Figure 5.29 only superimposed over the water table elevation of Monitoring Well #2. There appears to be even less of a correlation between the two as expected since it is above the zone of slope movement. This lack of a correlation in both Figures 5.29 and 5.36 indicate that the relationship between ground water table elevation and slope movement is not linear. Since the slope does not move at a certain water table elevation, such as the first increase in late fall, 2007, but does move at the same water table elevation later, such as a few weeks later in the fall of 2007, it suggests that there might be a threshold value that must first be crossed to generate further movement. Further examination of Figures 5.29 and 5.36 show that during times of movement, not only is the ground water table high in Monitoring Well #1, but it is also high in Monitoring Well #2. At times with no movement, but high water elevation in Monitoring Well #1, Monitoring Well #2 is not high. In general, it seems if Monitoring Well #2 has a water elevation above approximately 199.5m (654.5 ft.) there is a good chance for movement to occur if the water table rises in Monitoring Well #1. If it is below 199.5m (654.5 ft.) there is a good chance no movement will occur regardless of the water table elevation in Monitoring Well #1.

Although neither monitoring well is located near Inclinometer #3, Figure 5.37 shows the cumulative horizontal displacement of Inclinometer #3 superimposed over the water table

elevation from Monitoring Well #1. Inclinometer #3 appears to move independent of water table elevation, which is consistent of it being outside the zone of slope movement. The rapid increase in water table elevation in July, 2007, however, does show a sudden jump in displacement. This increase in movement is also apparent in Figure 5.38 of Monitoring Well #2 superimposed over Inclinometer #3.

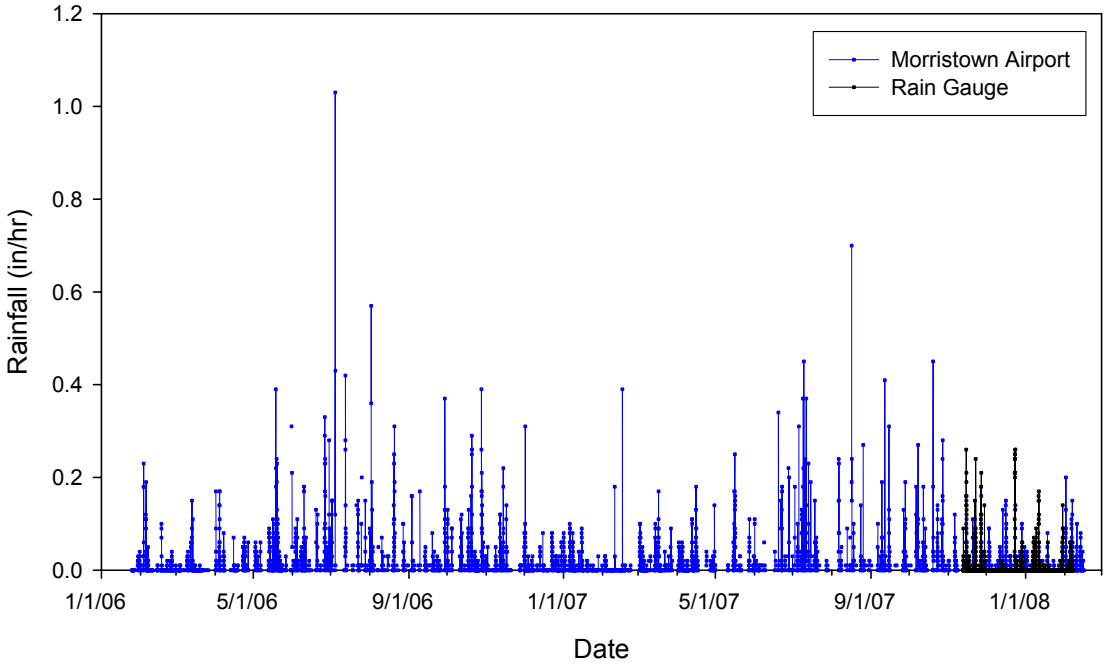

Figure 5.1 Rainfall data from Morristown Airport and the on site rain gauge.

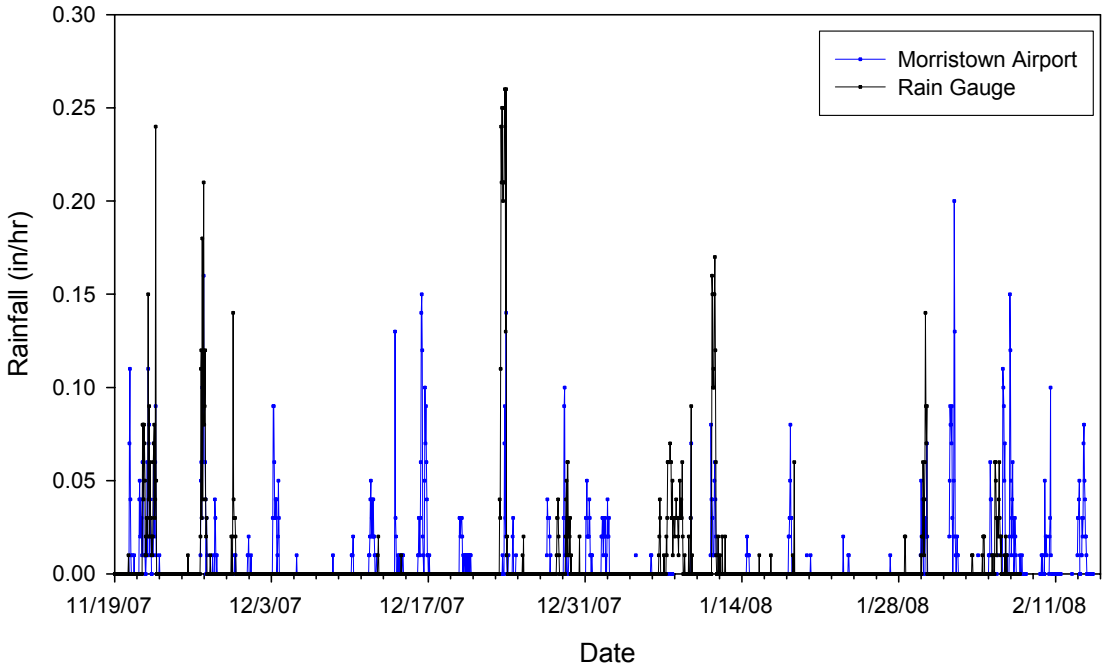

Figure 5.2 Rainfall data from Morristown Airport and the on site rain gauge after its installation.

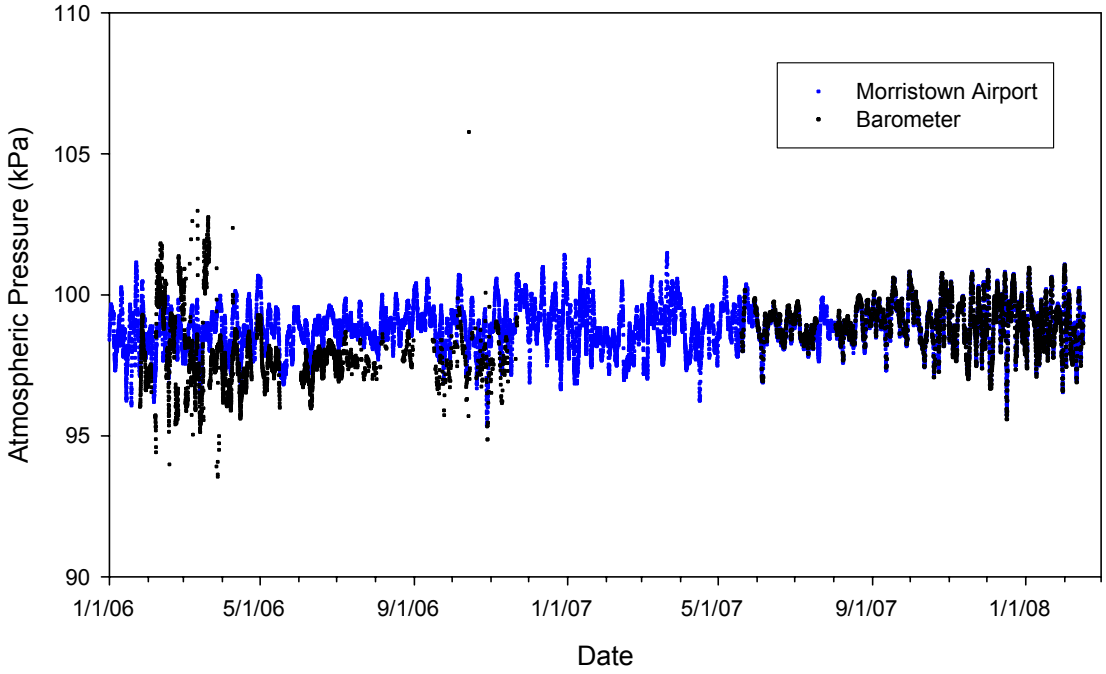

Figure 5.3 Atmospheric pressure measured at Morristown Airport (elev. 225m) and on the site barometer (elev. 200m).

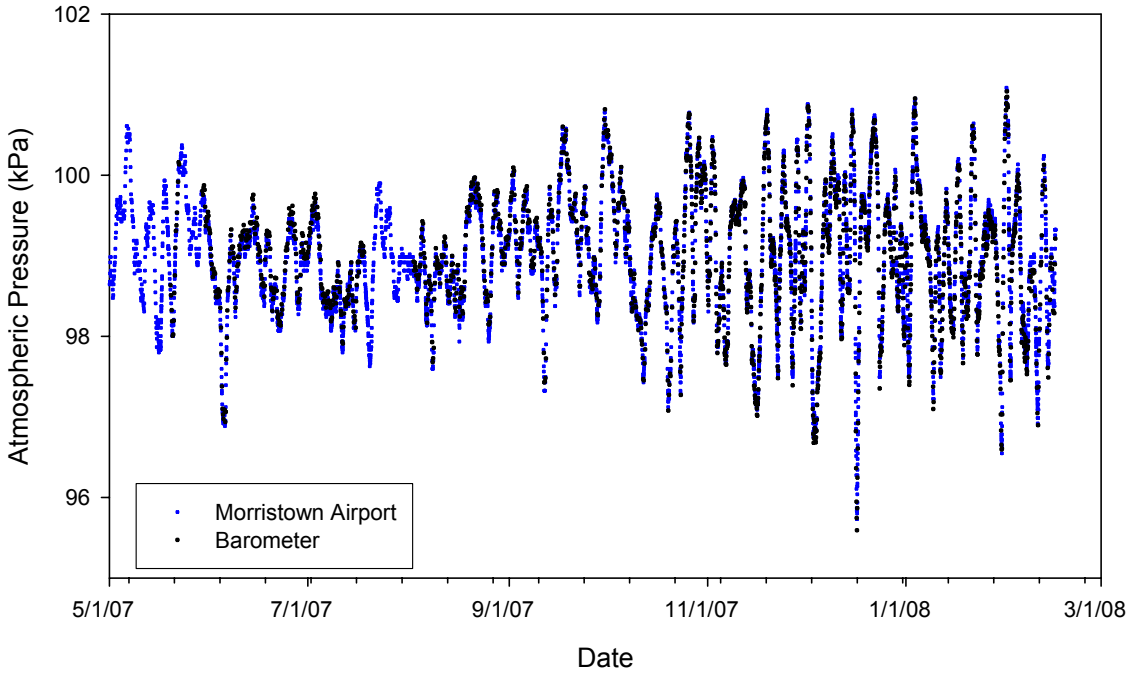

Figure 5.4 Atmospheric pressure measured at Morristown Airport (elev. 225m) and on the site barometer (elev. 200m) since the repaired barometer was reinstalled.

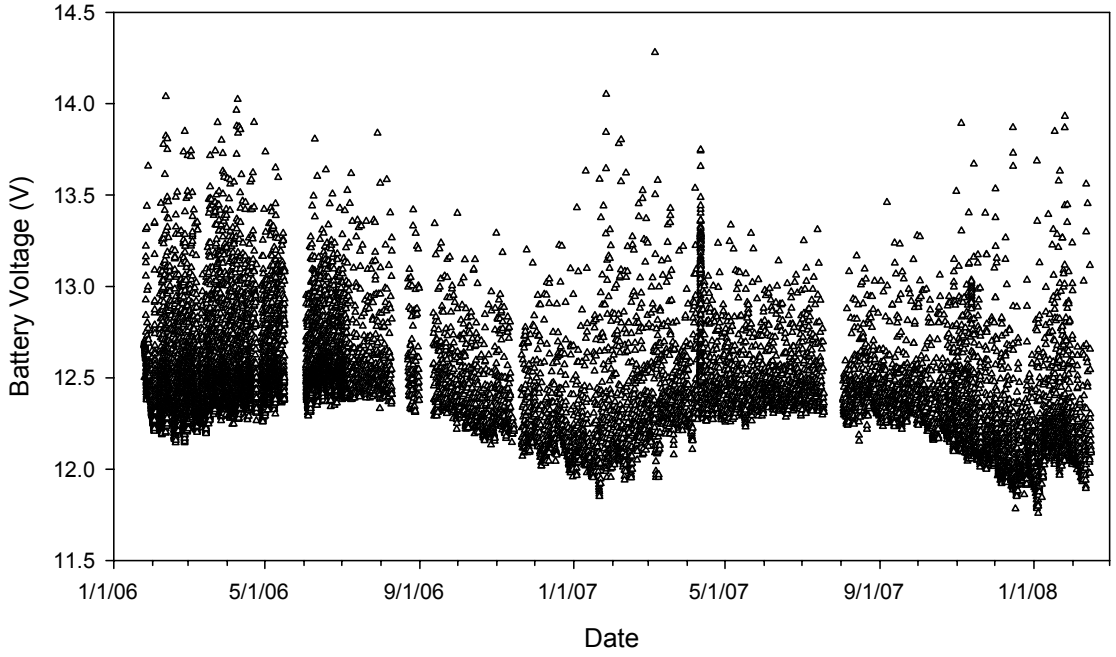

Figure 5.5 Recorded battery voltage showing seasonal dependence.

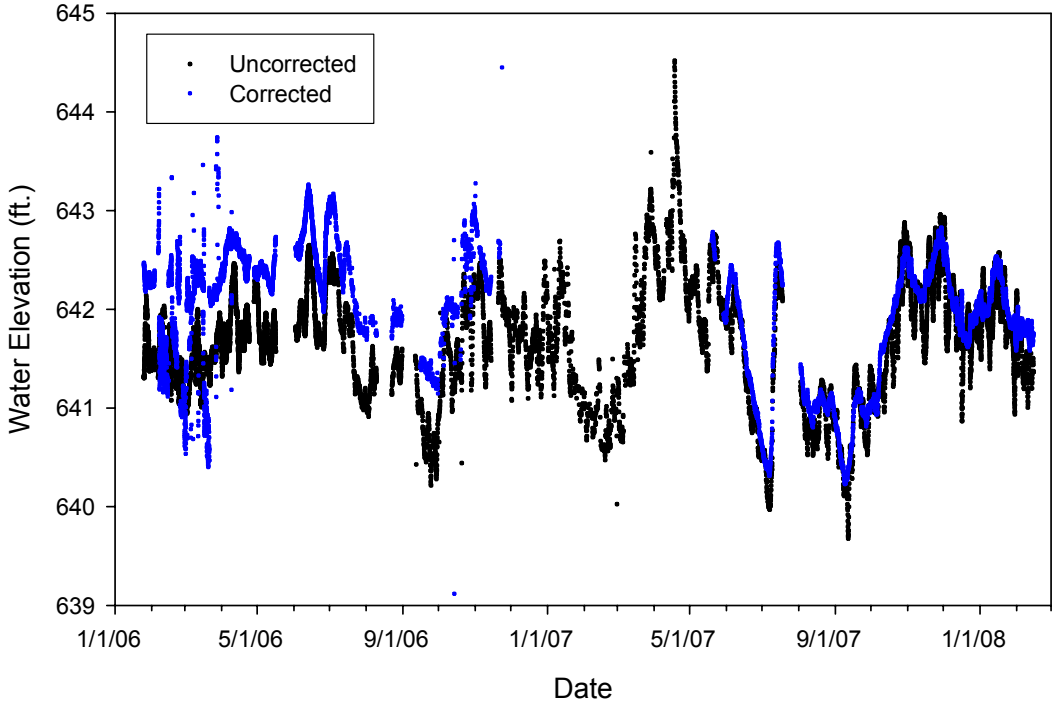

Figure 5.6 Corrected and uncorrected water table elevations for Monitoring Well #1.

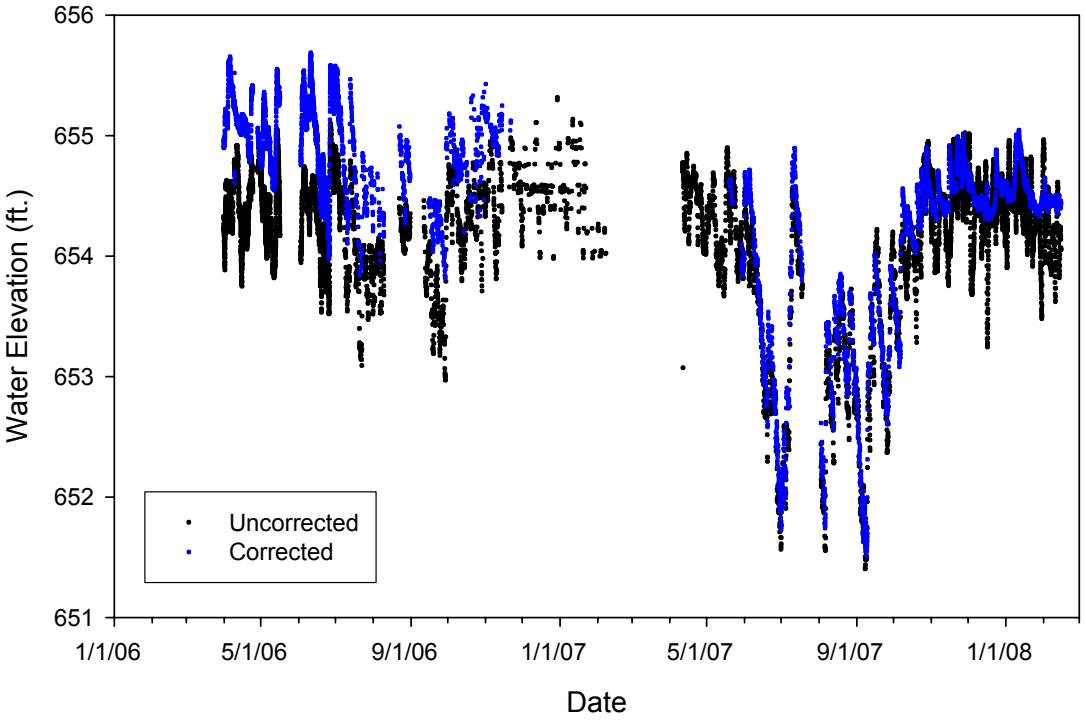

Figure 5.7 Corrected and uncorrected water table elevations for Monitoring Well #2.

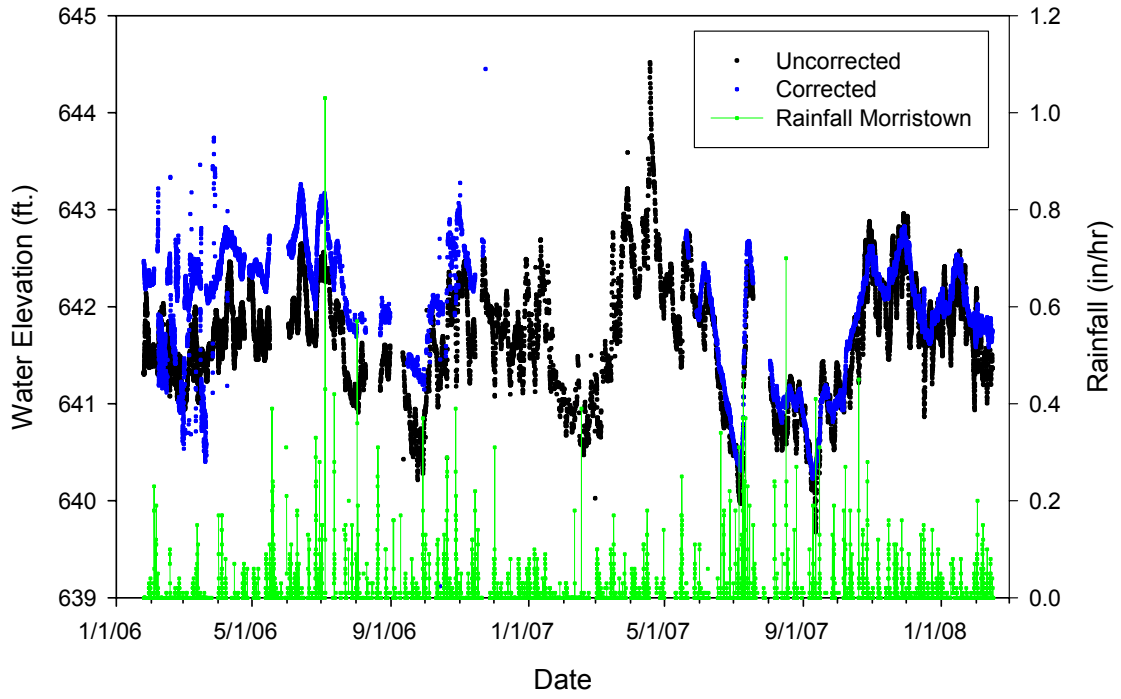

Figure 5.8 Corrected and uncorrected water table elevations for Monitoring Well #1 compared to measured rainfall at Morristown Airport.

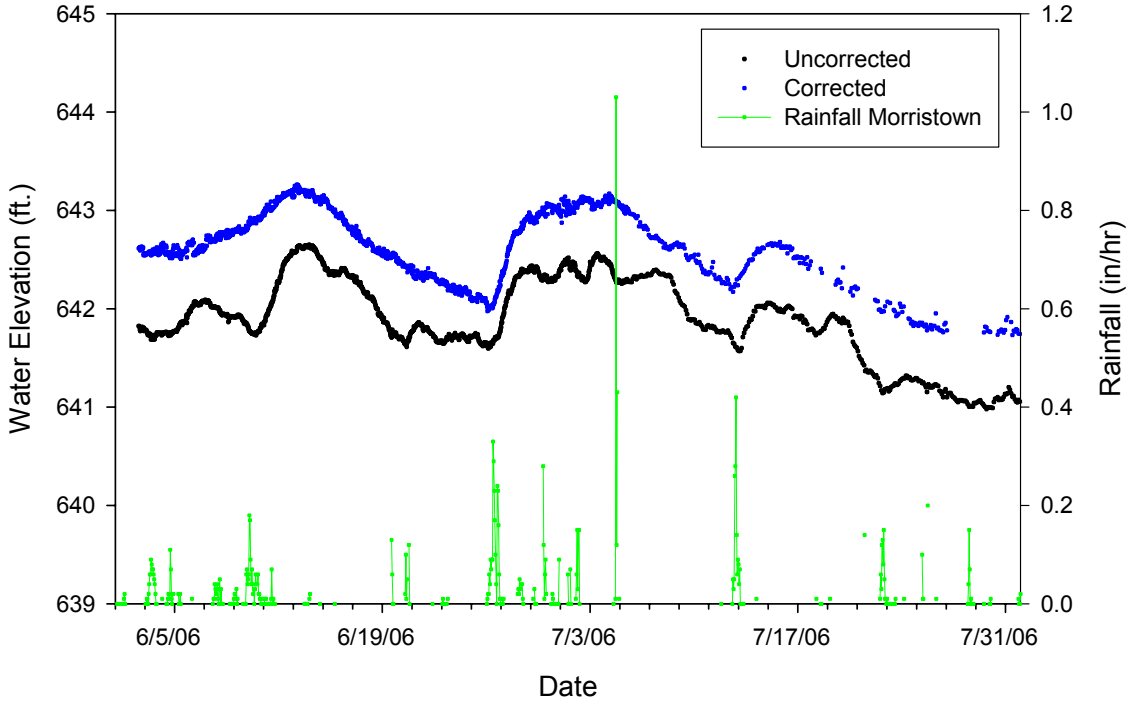

Figure 5.9 Corrected and uncorrected water table elevations for Monitoring Well #1 compared to measured rainfall at Morristown Airport for June and July, 2006.

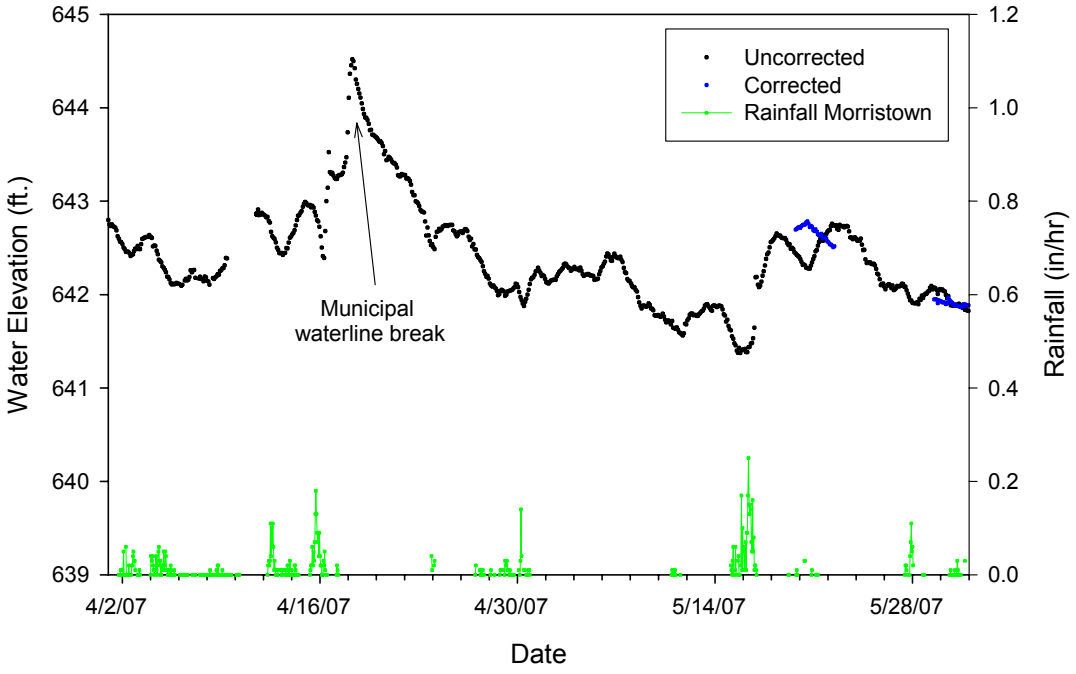

Figure 5.10 Corrected and uncorrected water table elevations for Monitoring Well #1 compared to measured rainfall at Morristown Airport for April and May, 2007. The large increase in water table elevation on April 17, 2007, coincides with a reported municipal water line break.

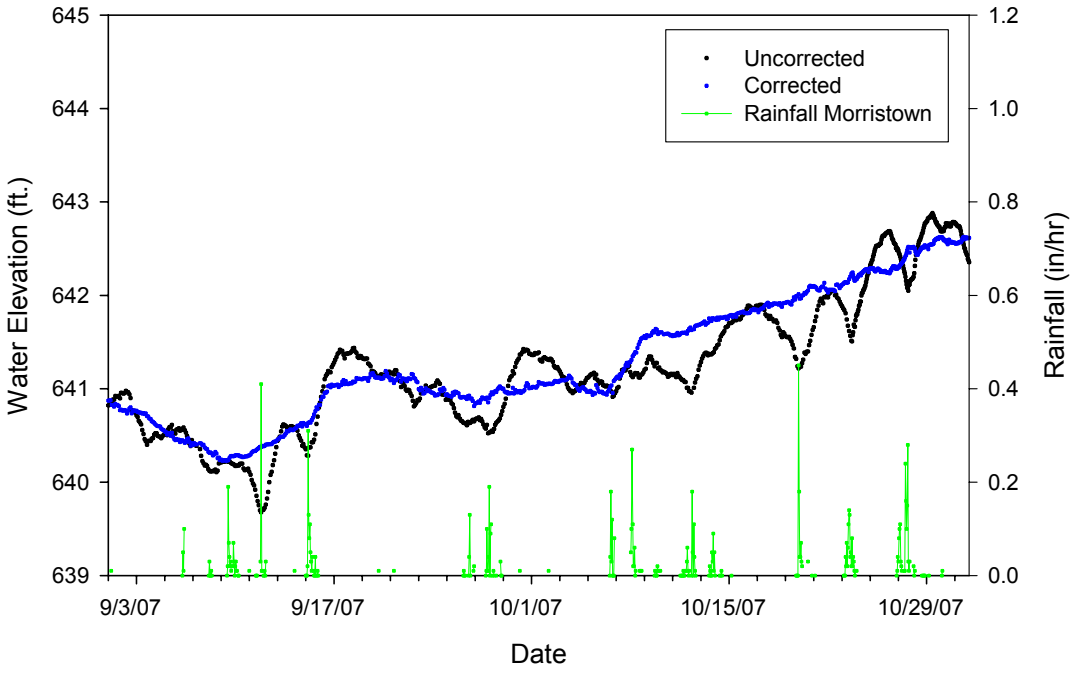

Figure 5.11 Corrected and uncorrected water table elevations for Monitoring Well #1 compared to measured rainfall at Morristown Airport for September and October, 2007.

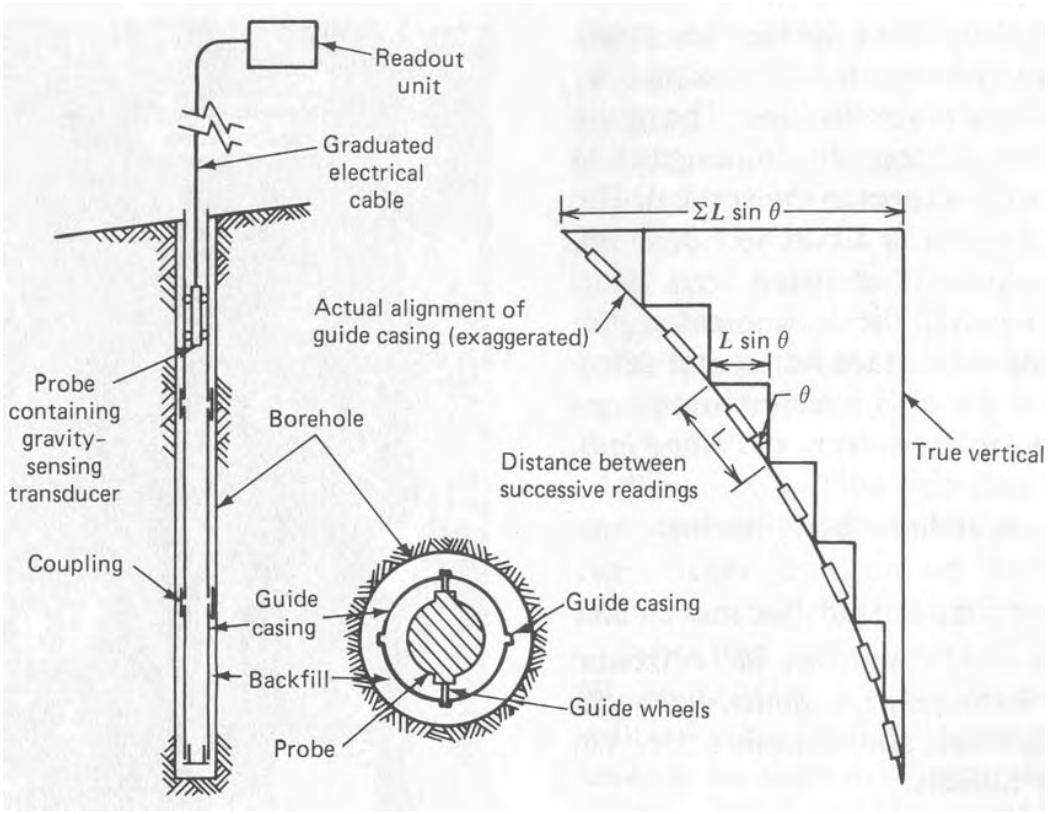

Figure 5.12 Principal of inclinometer operation (Dunnicliff, 1988)

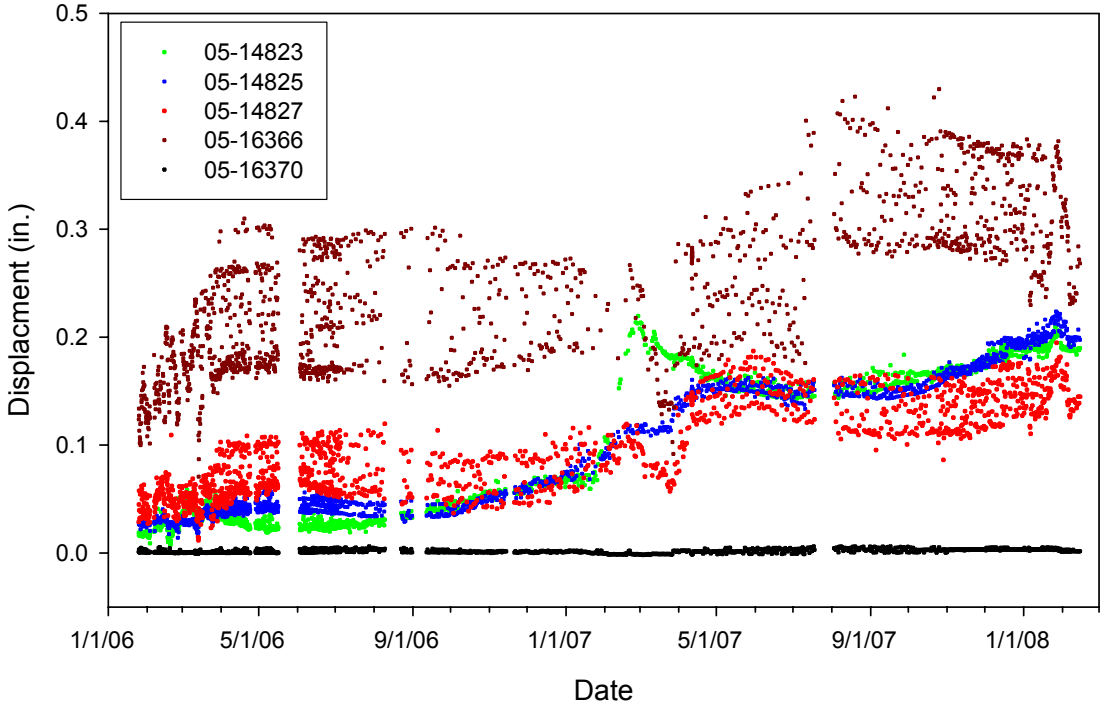

Figure 5.13 Calculated displacements for each IPI installed in Inclinometer #3.

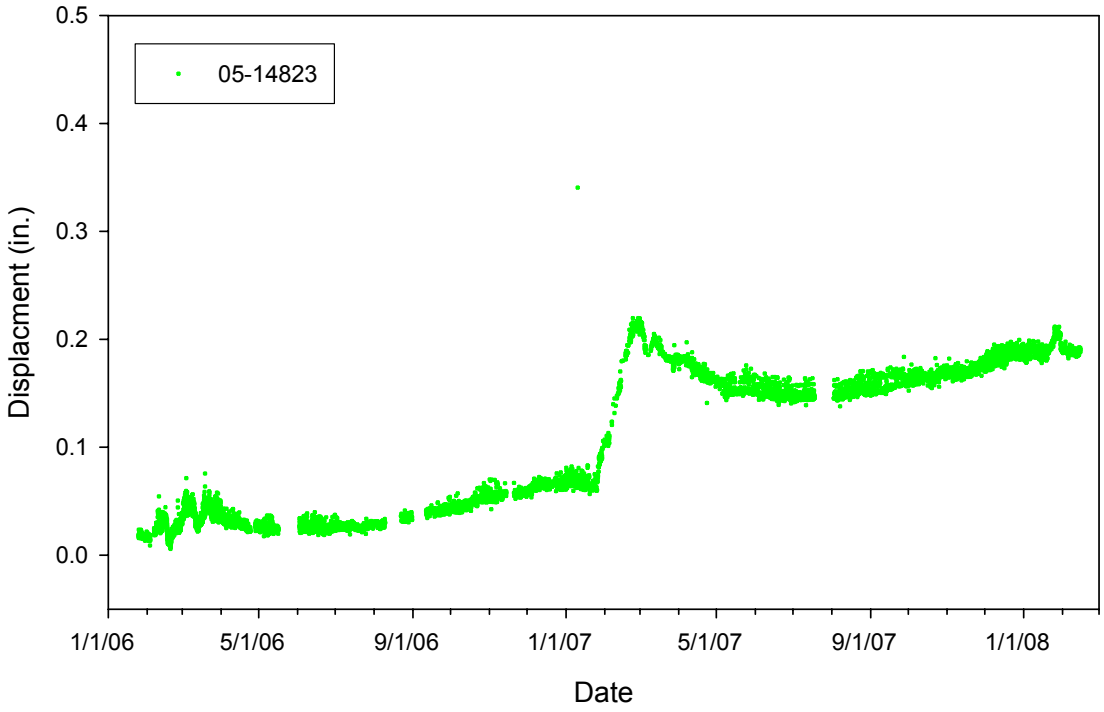

Figure 5.14 Calculated displacement for IPI 05-14823 installed at a depth of 0.76m (2.5 ft.) in Inclinometer #3.

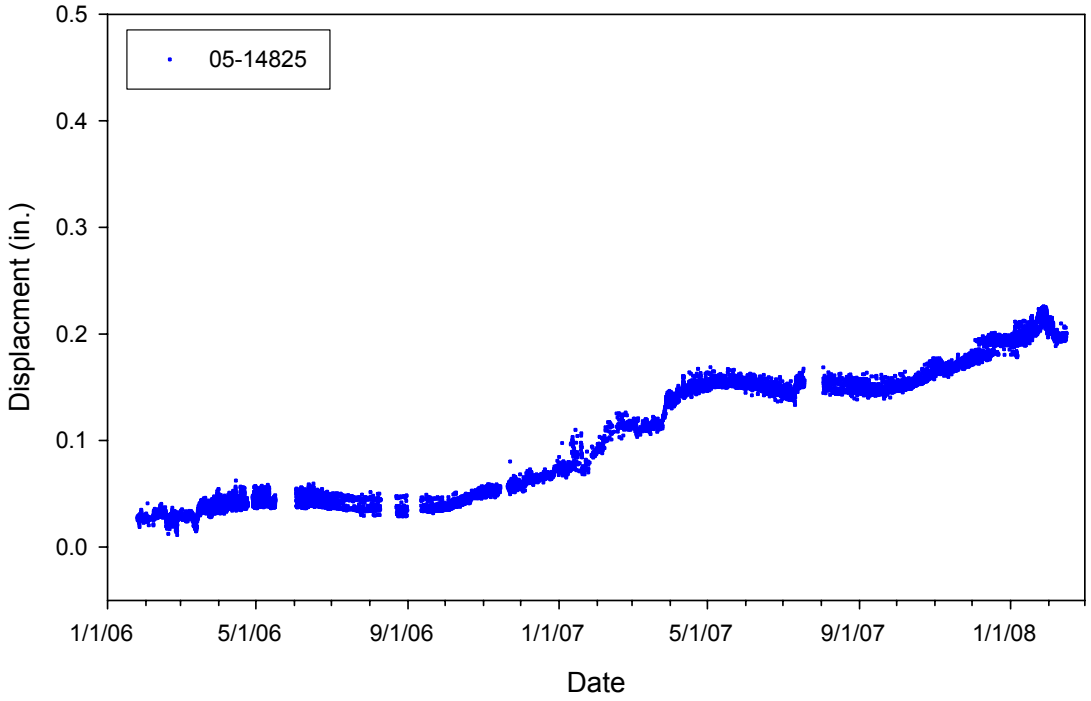

Figure 5.15 Calculated displacement for IPI 05-14825 installed at a depth of 2.29m (7.5 ft.) in Inclinometer #3.

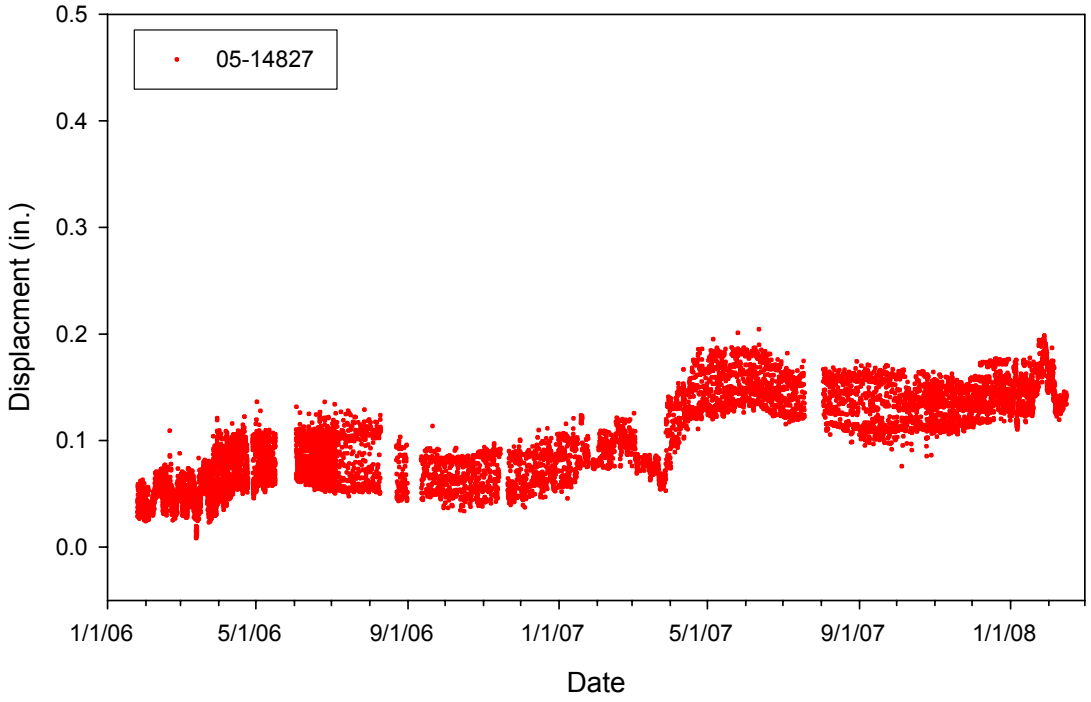

Figure 5.16 Calculated displacement for IPI 05-14827 installed at a depth of 3.81m (12.5 ft.) in Inclinometer #3.

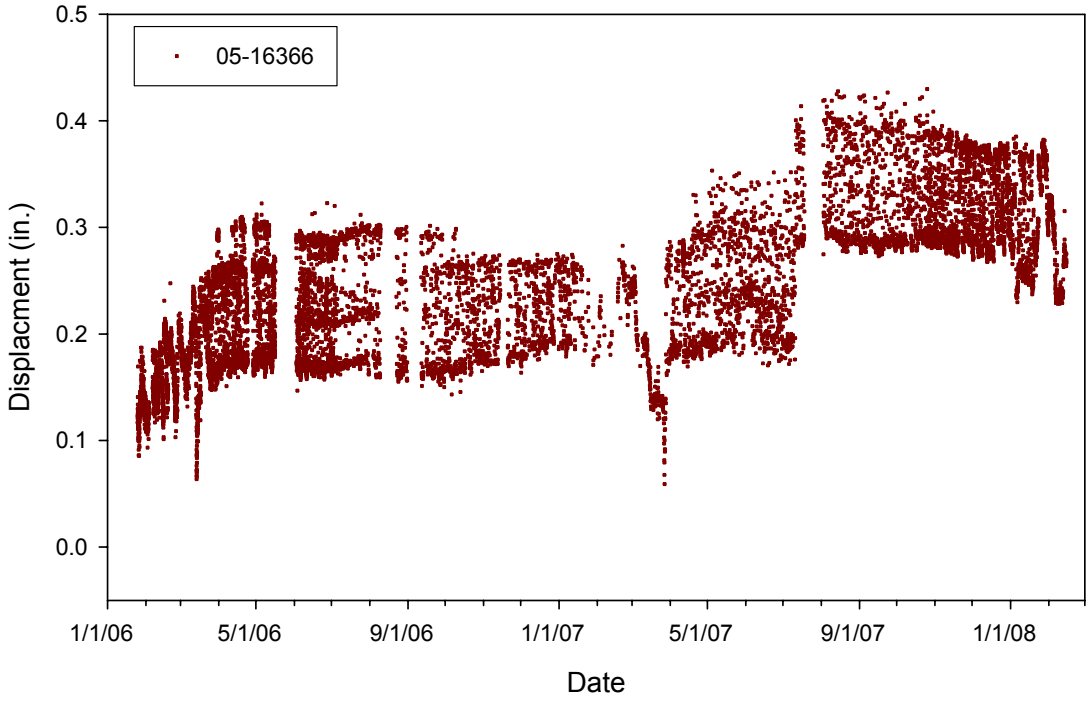

Figure 5.17 Calculated displacement for IPI 05-16366 installed at a depth of 6.86m (22.5 ft.) in Inclinometer #3.

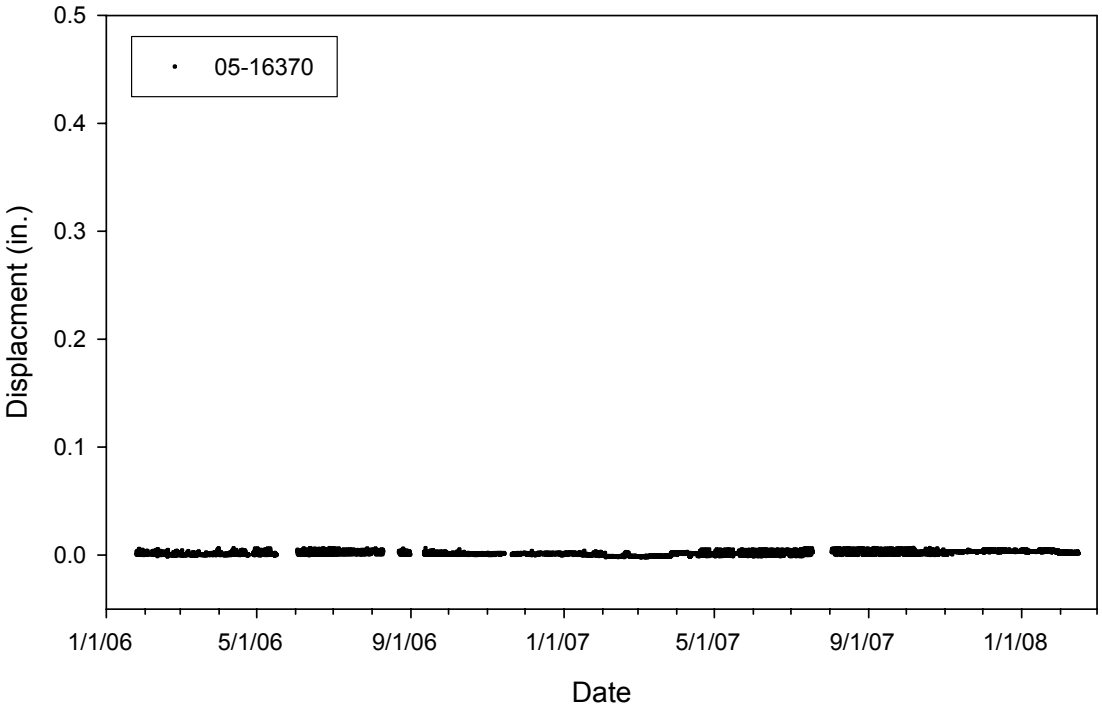

Figure 5.18 Calculated displacement for IPI 05-16370 installed at a depth of 12.95m (42.5 ft.) in Inclinometer #3.

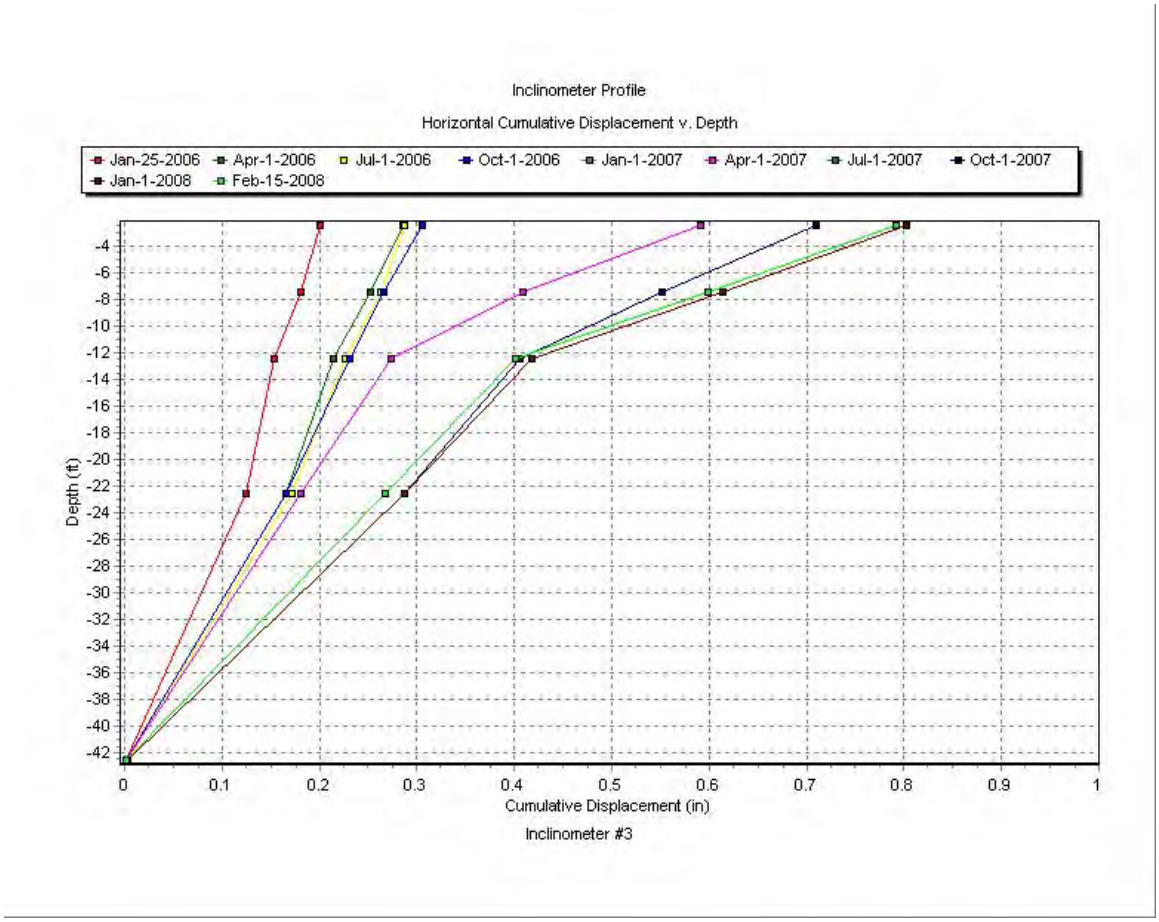

Figure 5.19 Inclinometer profile of horizontal cumulative displacement versus depth for Inclinometer #3.

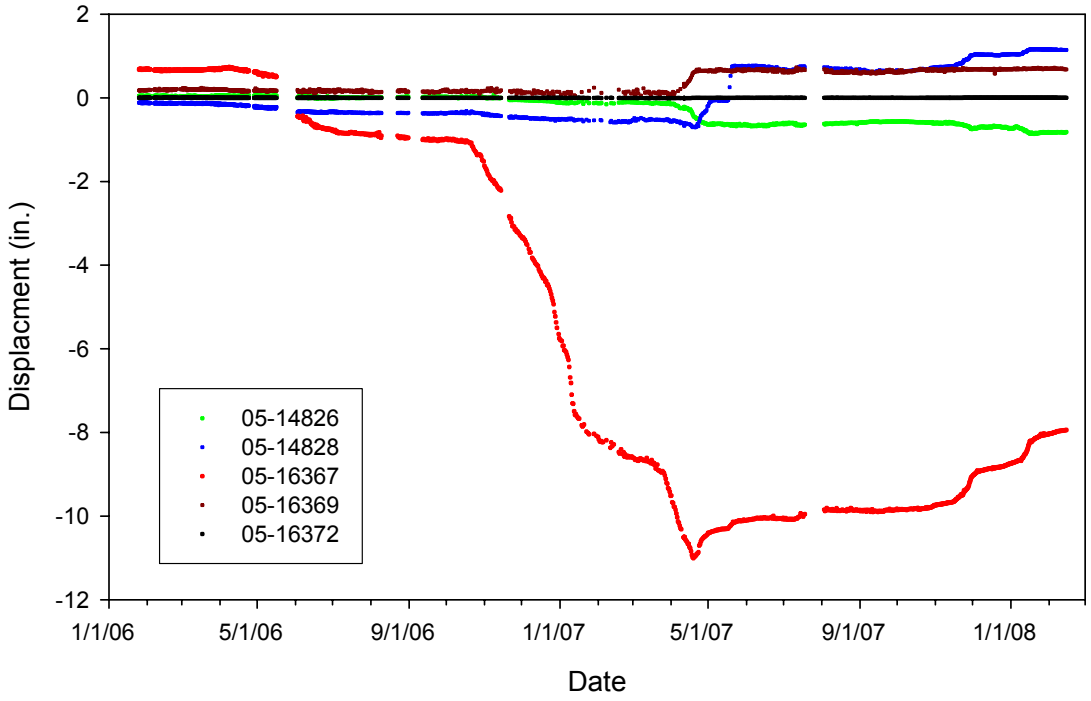

Figure 5.20 Calculated displacements for each IPI installed in Inclinometer #2.

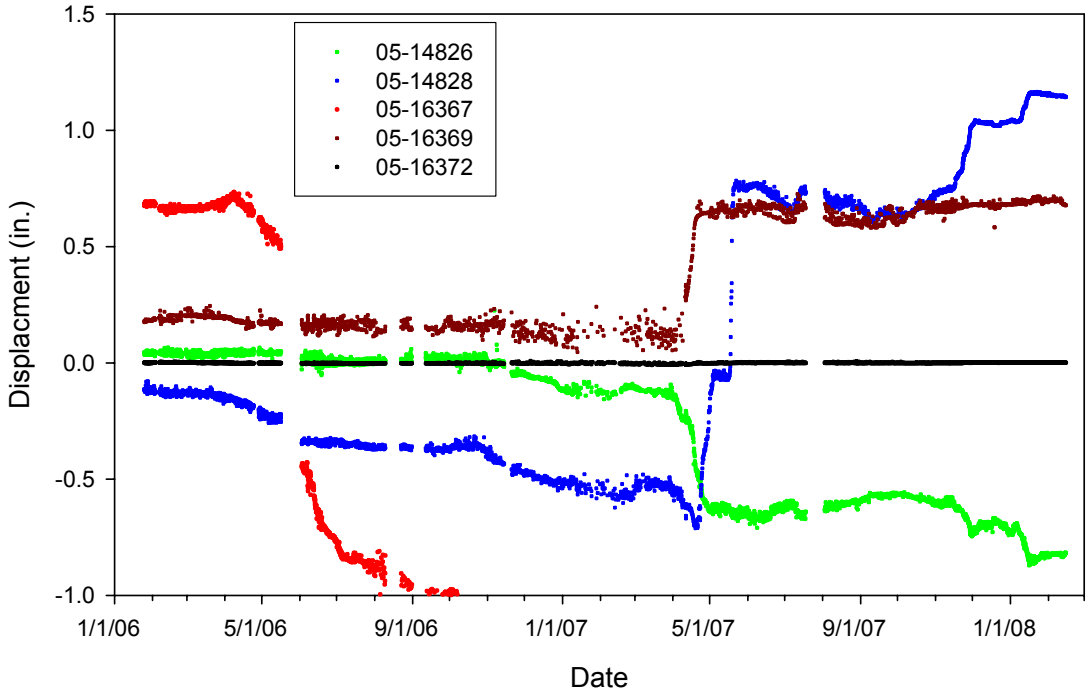

Figure 5.21 Calculated displacements for each IPI installed in Inclinometer #2 when the displacement scale has been reduced.

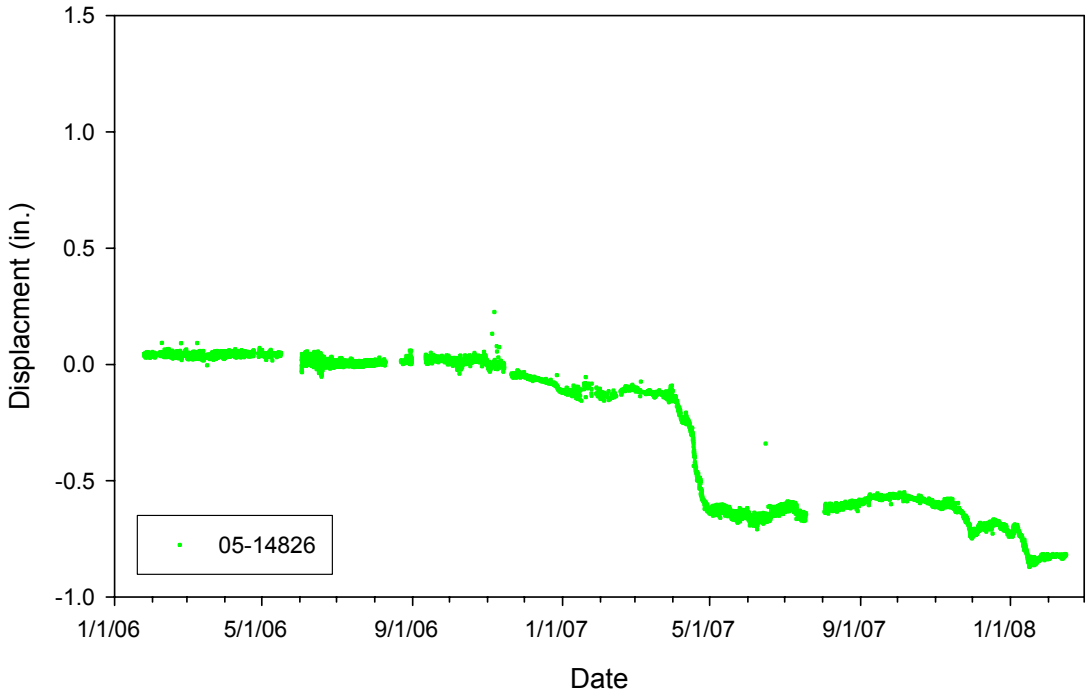

Figure 5.22 Calculated displacement for IPI 05-14826 installed at a depth of 0.76m (2.5 ft.) in Inclinometer #2.

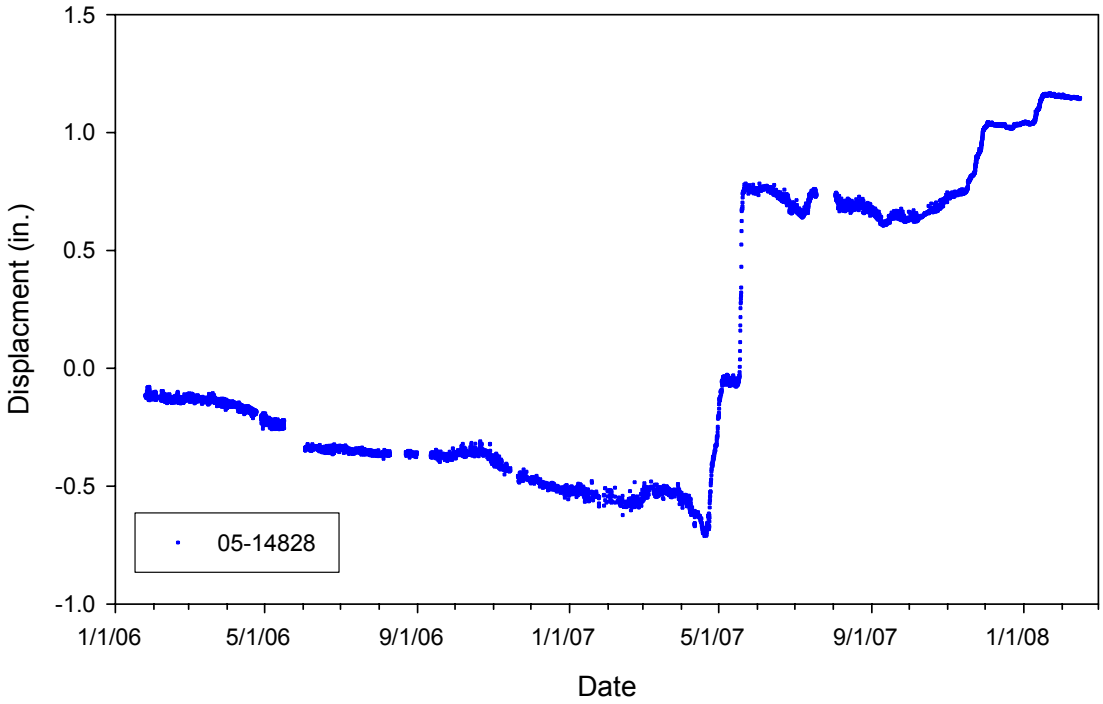

Figure 5.23 Calculated displacement for IPI 05-14828 installed at a depth of 3.81m (12.5 ft.) in Inclinometer #2.

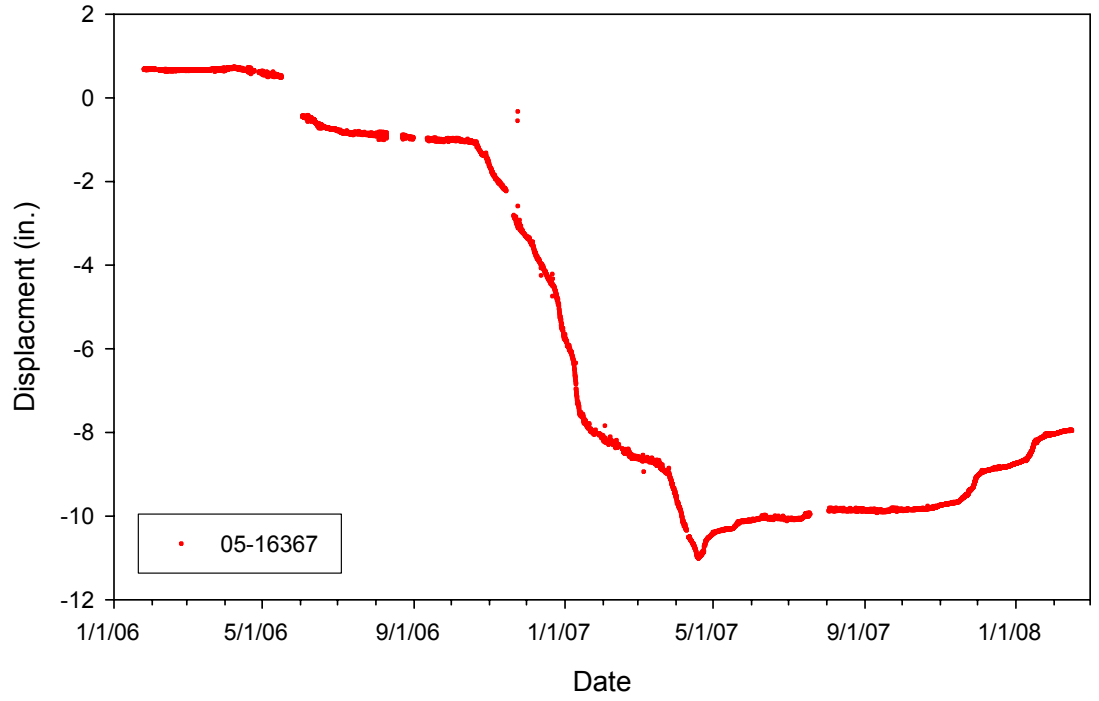

Figure 5.24 Calculated displacement for IPI 05-16367 installed at a depth of 6.86m (22.5 ft.) in Inclinometer #2.

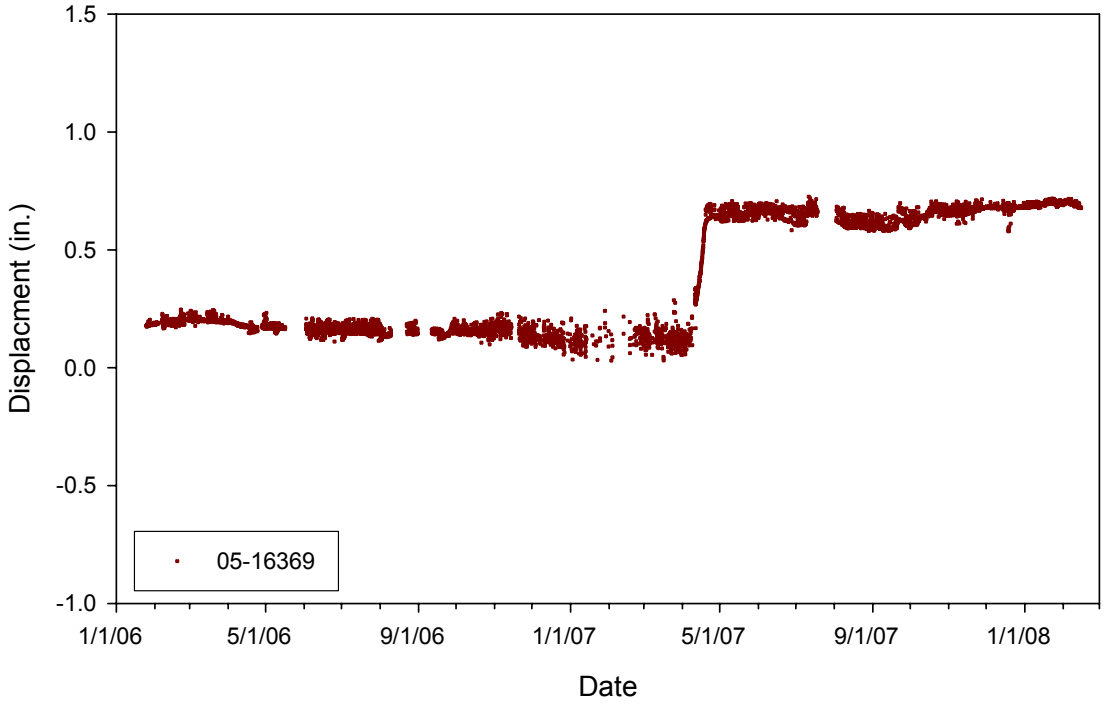

Figure 5.25 Calculated displacement for IPI 05-16369 installed at a depth of 12.95m (42.5 ft.) in Inclinometer #2.

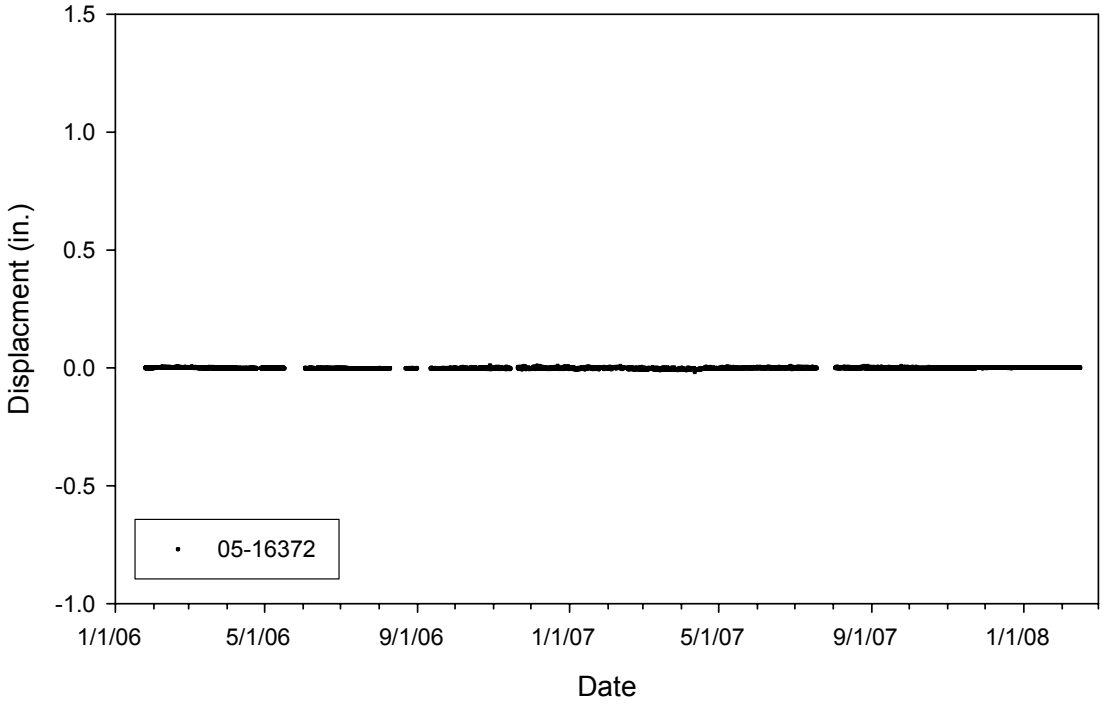

Figure 5.26 Calculated displacement for IPI 05-16372 installed at a depth of 19.05m (62.5 ft.) in Inclinometer #2.

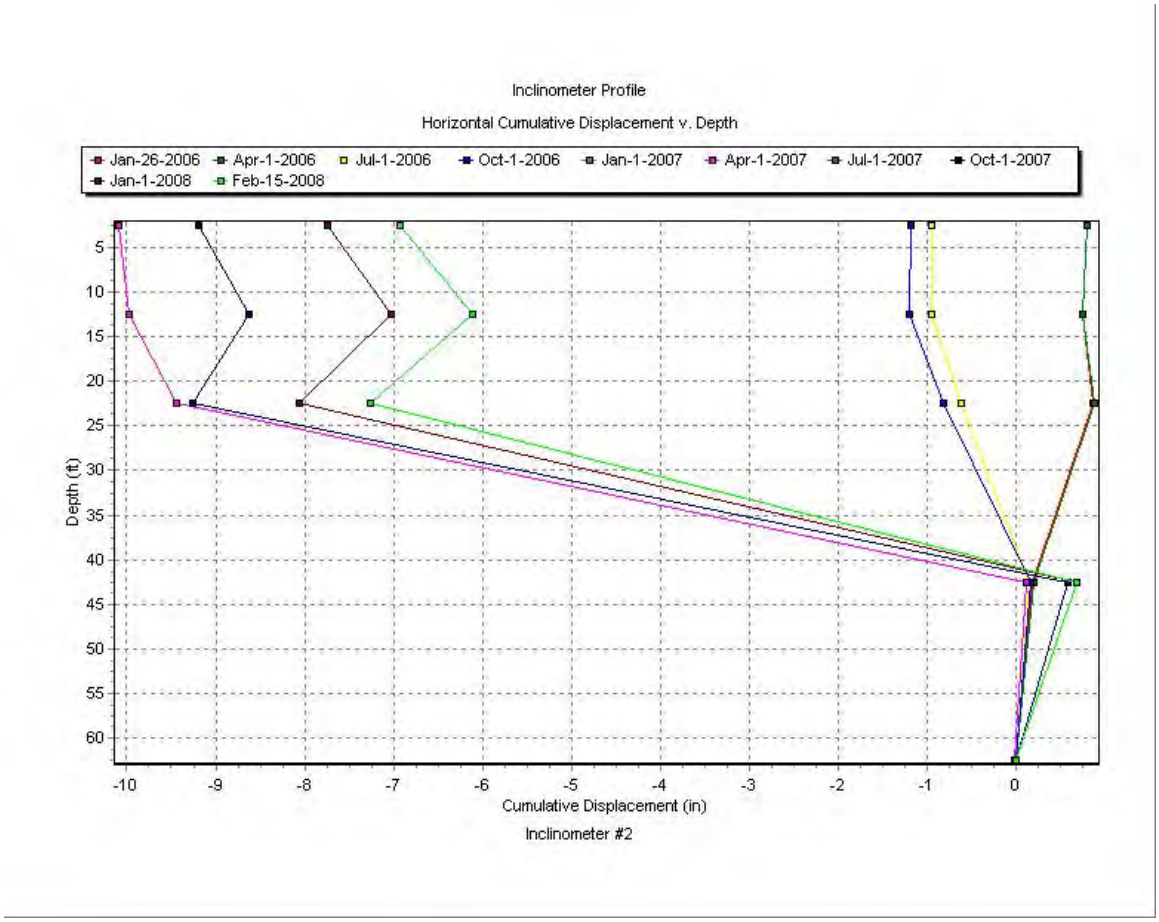

Figure 5.27 Inclinometer profile of horizontal cumulative displacement versus depth for Inclinometer #2.

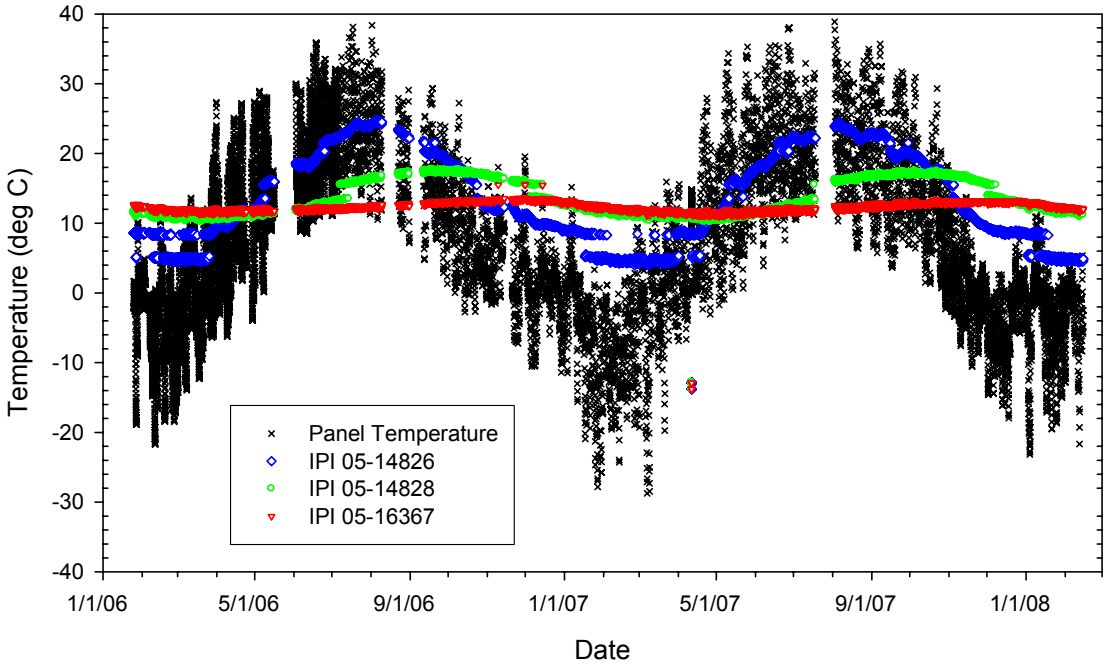

Figure 5.28 Temperature recordings of the datalogger and three shallowest IPIs in Inclinometer #2 showing seasonal variation and increasingly damped reaction of the ground water temperature with depth.

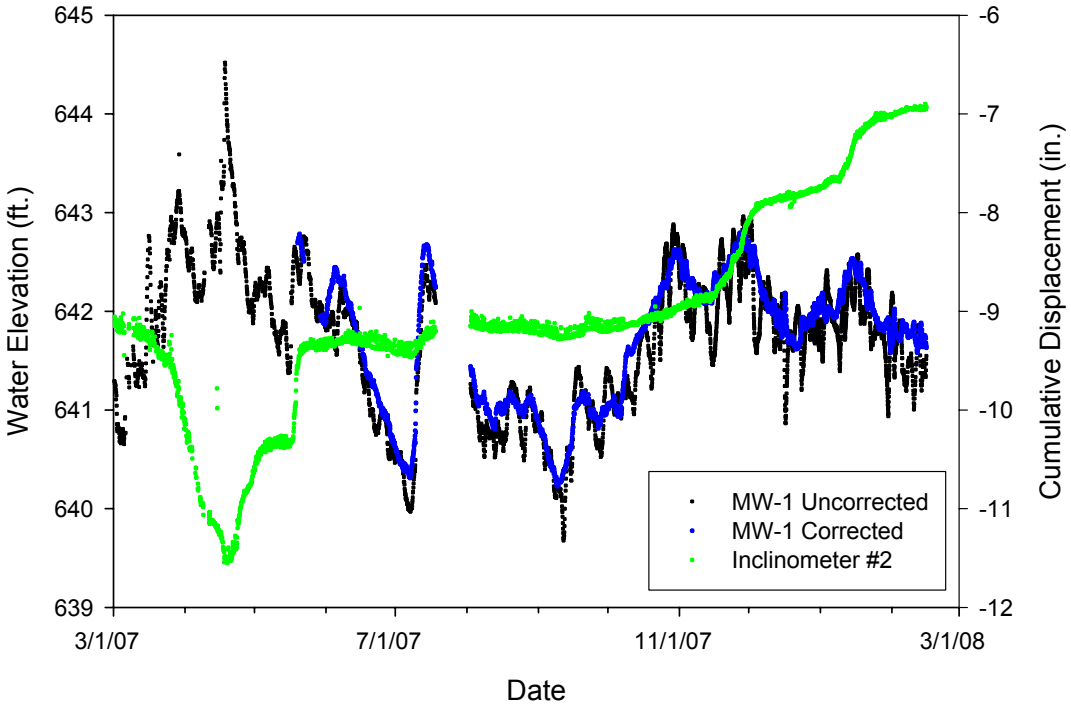

Figure 5.29 Corrected and uncorrected water table elevations for Monitoring Well #1 compared to horizontal cumulative displacement of Inclinometer #2.

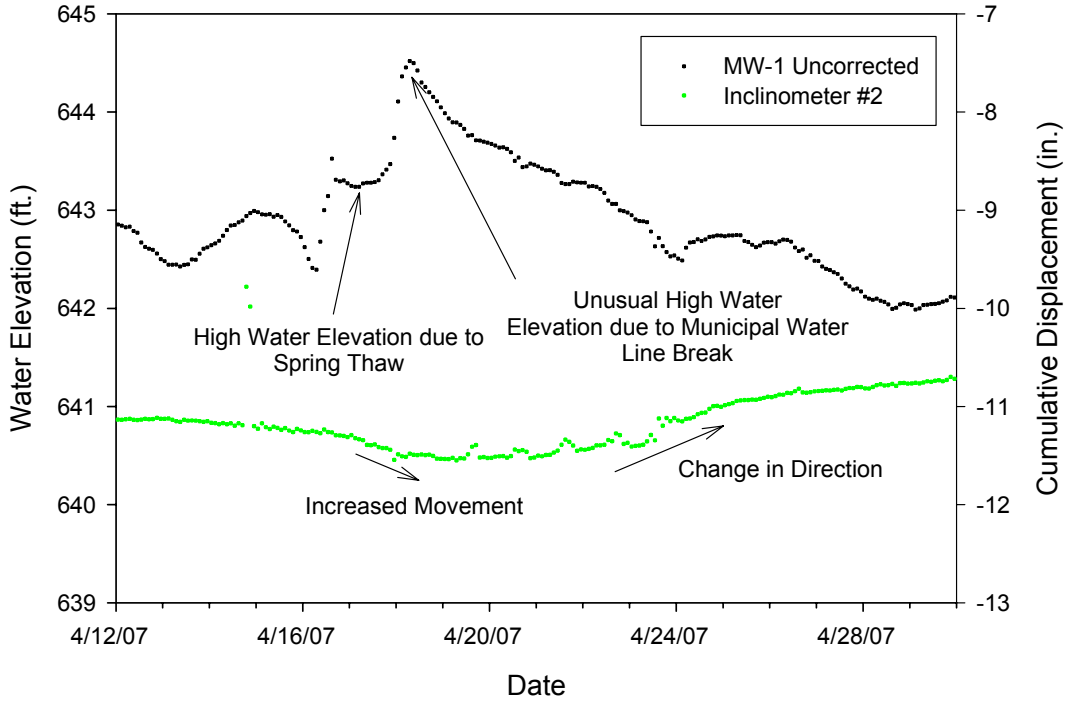

Figure 5.30 Uncorrected water table elevation for Monitoring Well #1 compares to the horizontal cumulative displacement of Inclinometer #2 for April, 2007.

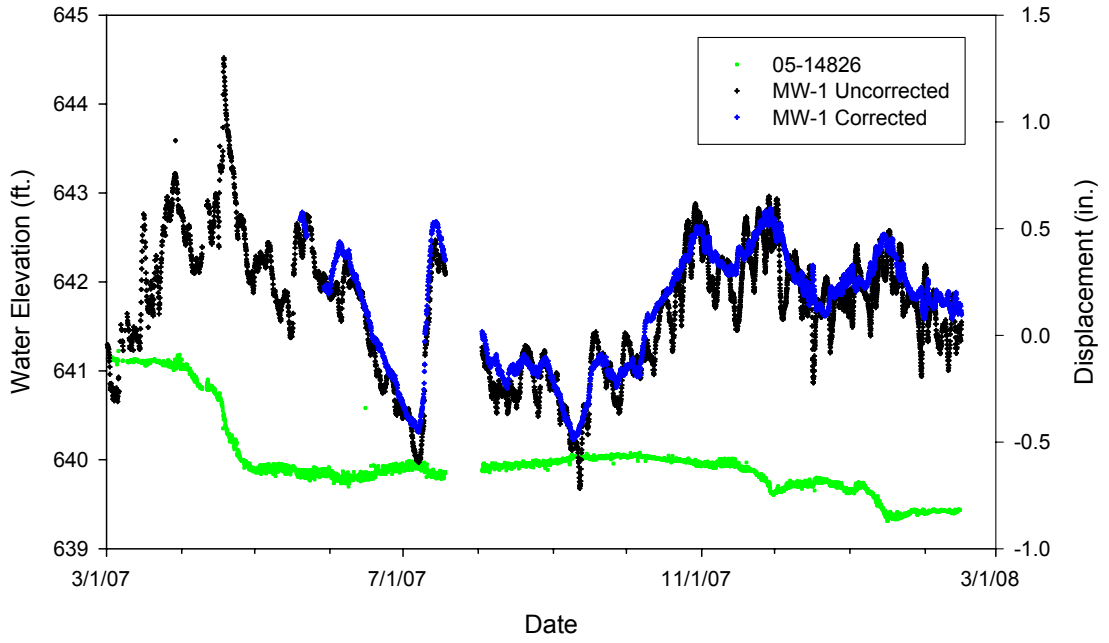

Figure 5.31 Corrected and uncorrected water table elevation for Monitoring Well #1 compared to the calculated displacement for IPI 05-14826 installed at a depth of 0.76m (2.5 ft.) in Inclinometer #2.

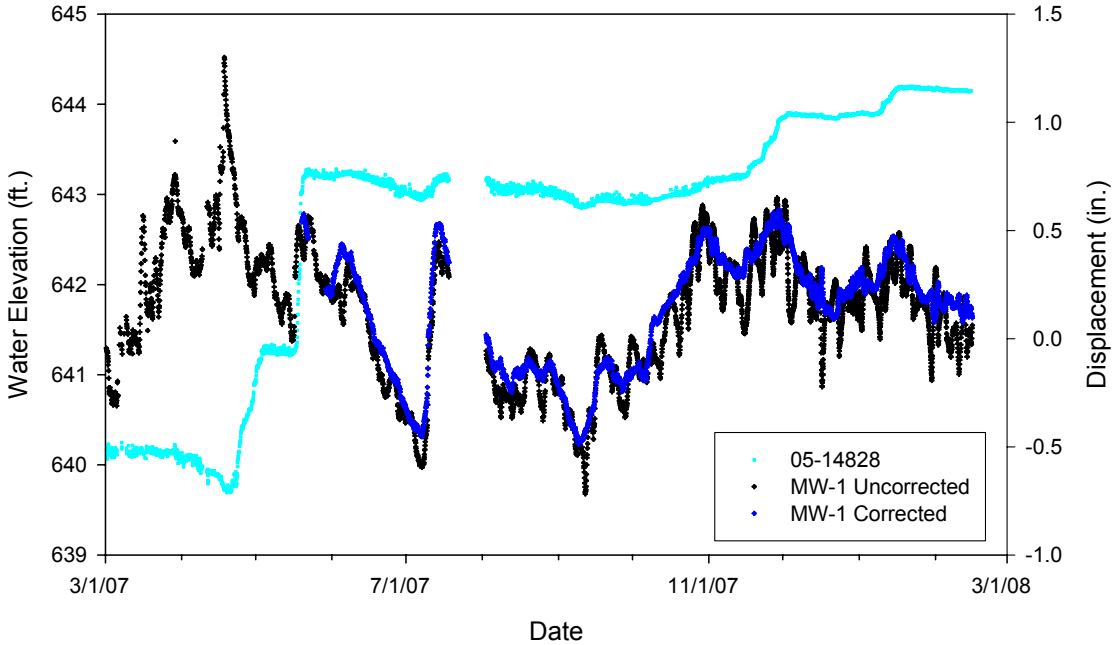

Figure 5.32 Corrected and uncorrected water table elevation for Monitoring Well #1 compared to the calculated displacement for IPI 05-14828 installed at a depth of 3.81m (12.5 ft.) in Inclinometer #2.

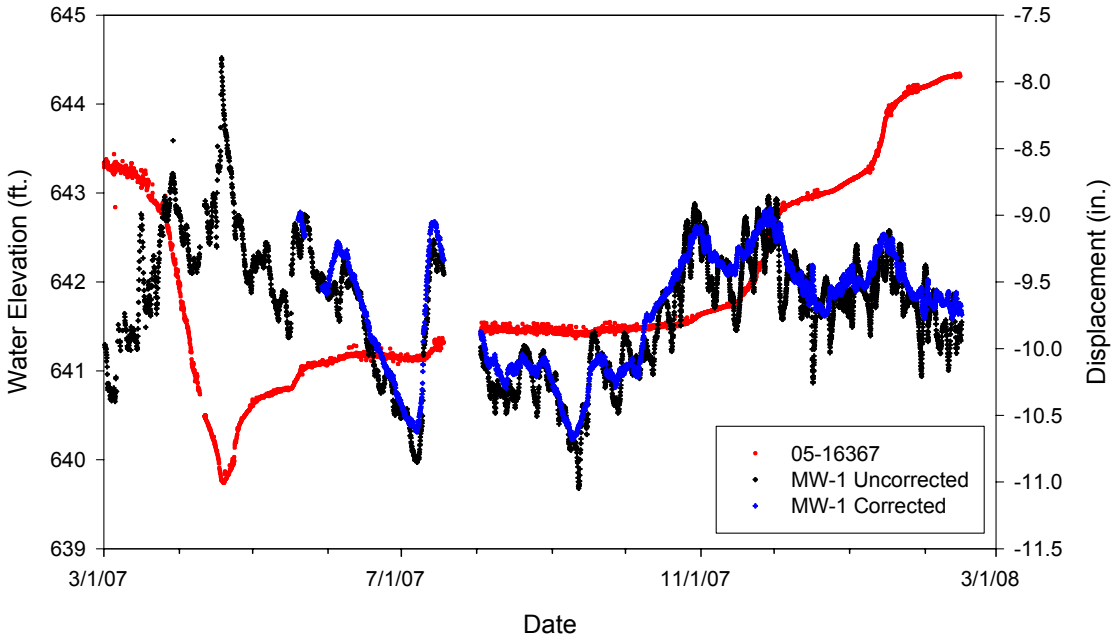

Figure 5.33 Corrected and uncorrected water table elevation for Monitoring Well #1 compared to the calculated displacement for IPI 05-16367 installed at a depth of 6.86m (22.5 ft.) in Inclinometer #2.

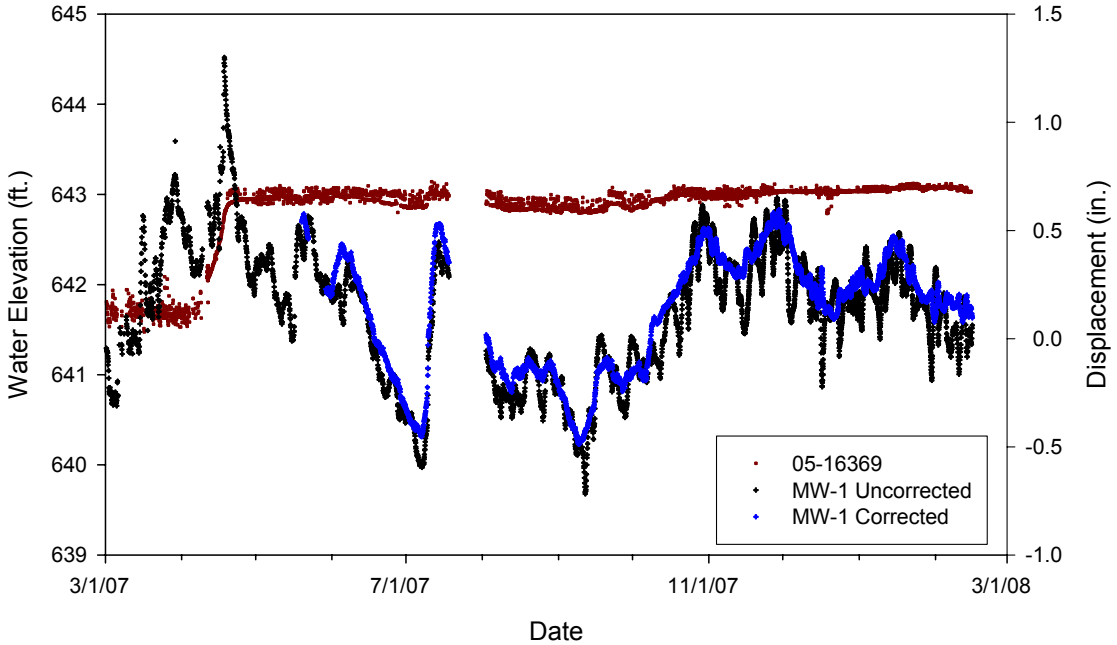

Figure 5.34 Corrected and uncorrected water table elevation for Monitoring Well #1 compared to the calculated displacement for IPI 05-16369 installed at a depth of 12.95m (42.5 ft.) in Inclinometer #2.

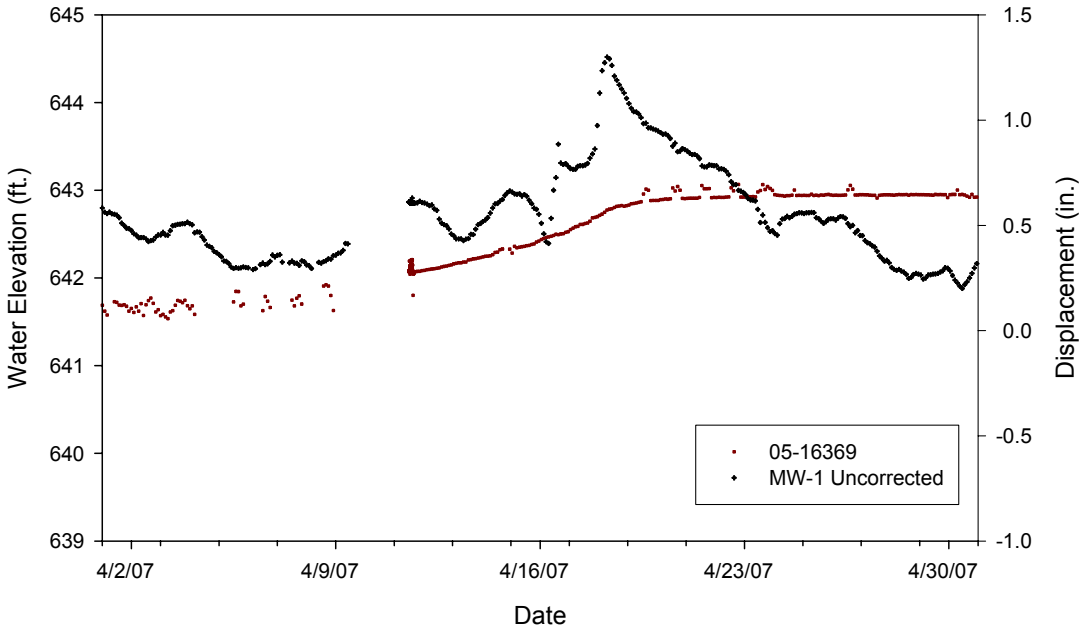

Figure 5.35 Uncorrected water table elevation for Monitoring Well #1 compared to the calculated displacement for IPI 05-16369 installed at a depth of 12.95m (42.5 ft.) in Inclinometer #2 for April, 2007.

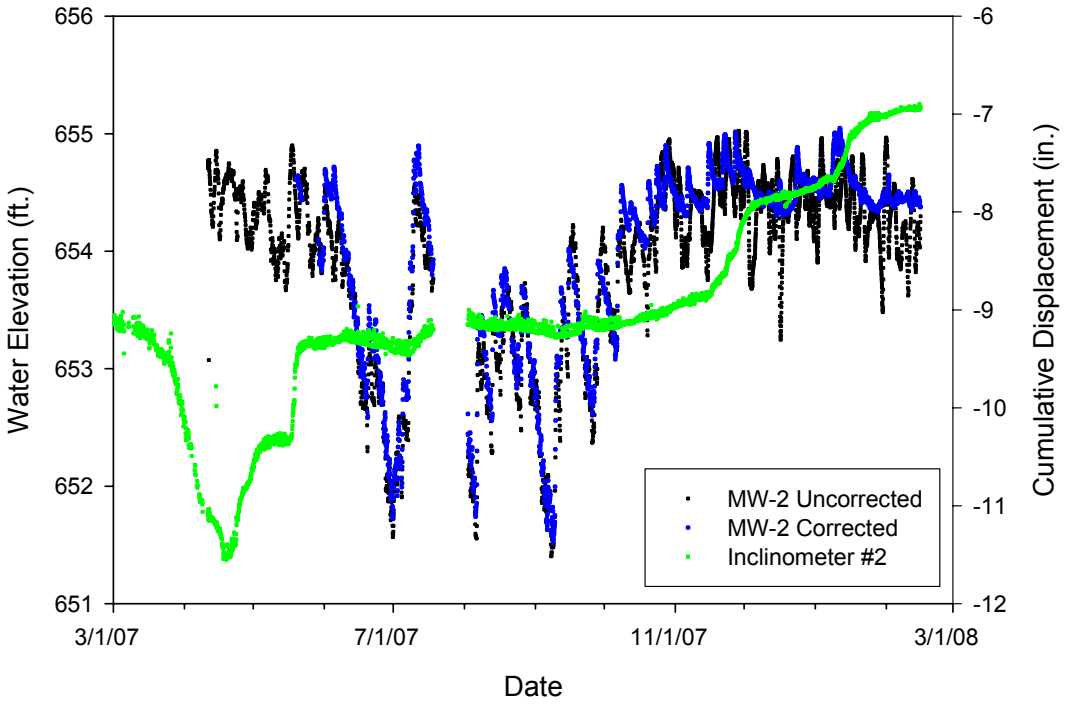

Figure 5.36 Corrected and uncorrected water table elevations for Monitoring Well #2 compared to horizontal cumulative displacement of Inclinometer #2.

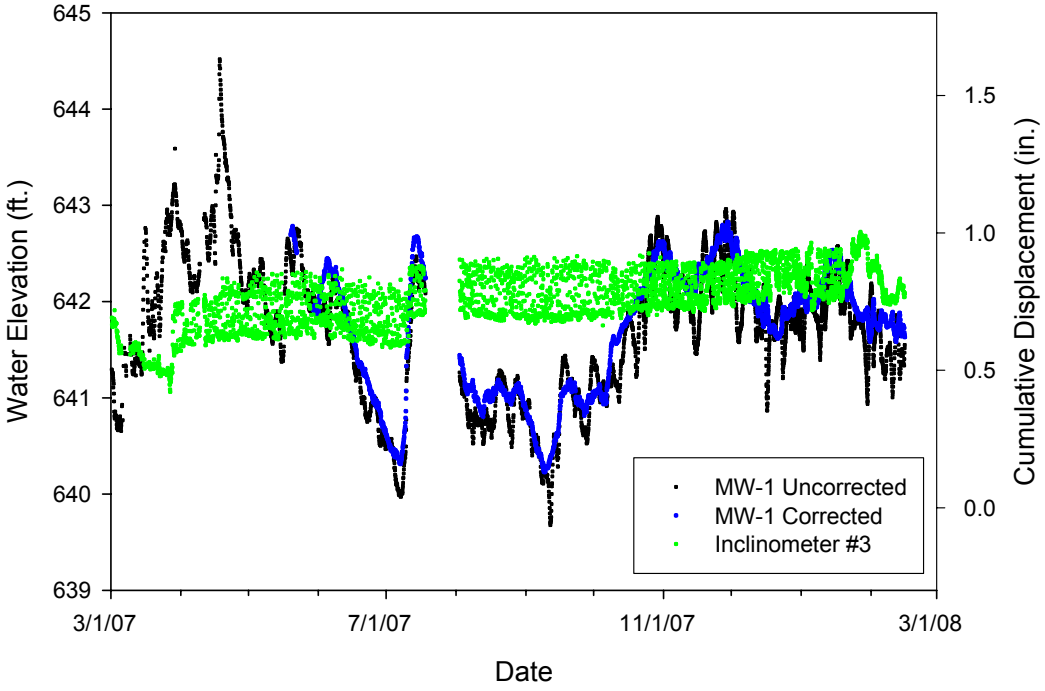

Figure 5.37 Corrected and uncorrected water table elevations for Monitoring Well #1 compared to horizontal cumulative displacement of Inclinometer #3.

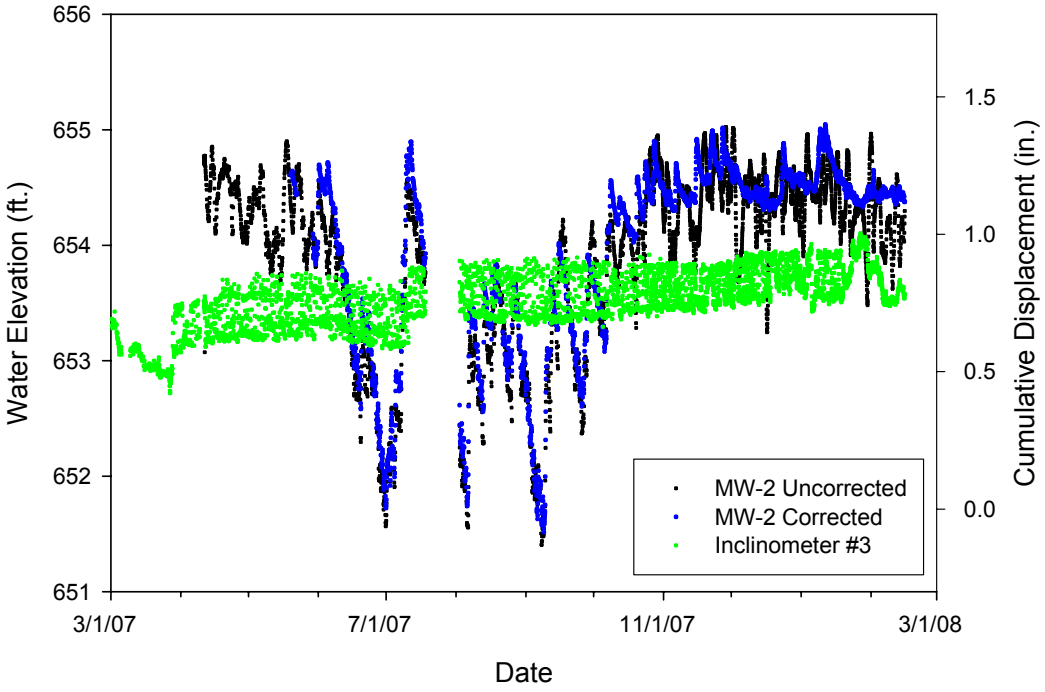

Figure 5.38 Corrected and uncorrected water table elevations for Monitoring Well #2 compared to horizontal cumulative displacement of Inclinometer #3.

6.0 NUMERICAL ANALYSIS

This chapter presents results of the slope stability analysis conducted using Slide 5.0 from Rocscience. Using the soil profile generated in Chapter 4 and water table elevations measured by the instrumentation (Chapter 5), the factor of safety for the slope was calculated. With known slope movement events detected by the in-place inclinometers, the model was back analyzed and refined through a series of iterations and sensitivity analysis. The effects of the water table elevation were further examined to determine "critical" elevations for potential slope movement. Potential remediation solutions using the refined soil model were analyzed to evaluate their effectiveness.

6.1 CREATING AND REFINING THE MODEL

A model of the Reservoir Road slope was created in Slide 5.0 using the soil profile generated in Chapter 4, as well as a cross section view of the slope generated from surveying data. Slide is a 2D limit equilibrium slope stability analysis program that does not take 3D end effects into account. The factor of safety or probability of failure for a soil or rock slope can be evaluated quickly and easily in a graphical interface. For this project an effective stress analysis was performed which assumes fully drained conditions. Seepage forces were not included. The method of analysis was Spencer's (1967) procedure. This is a complete equilibrium method which uses the method of slices and assumes that interslice forces are parallel and that the normal force acts at the center of the base of each slice. According to Duncan and Wright (2005), Spencer's method is "an accurate procedure applicable to virtually all slope geometries and soil profiles." The slip surface was defined as a circular failure and Slide's auto refine search was used to determine the critical slip surface.

Figure 6.1 presents the completed soil profile modeled in Slide. The initial model used estimates and measured results from the lab testing as described in Chapter 4 to assign unit weight and an effective stress cohesion intercept and friction angle to each material. Limits were placed on the model to force the failure surface to intersect with the ground surface in a certain area. From pictures taken of the site in the summer of 2005, the zone of slope movement was observed to cross the entire road.

Using monitoring well data, water elevations from the two monitoring wells were added to the model and the remaining location of the water table was estimated. Table 6.1 presents the maximum and minimum recorded ground water elevation in each monitoring well independent of the ground water elevation in the other monitoring well. The high water table associated with the break of the municipal water line which occurred around April 18, 2007, was not included. The two water table elevations were modeled in Slide using soil properties determined from the site characterization program as presented in Chapter 4 to calculate initial factors of safety. Figures 6.2 and 6.3 present the calculated factors of safety of 1.317 for the high and 1.461 for the low water table.

The direct shear tests showed that at large displacement, the silty clay material has an effective stress cohesion intercept value of zero. At times with a high measured water table, the slope had generally been moving and showing gradual inclinometer movement. Using the assumption that at these times of high water table, the soil may already be at its residual state, the Slide model was refined by setting the effective stress cohesion intercept values to zero for both the upper silt layer and the silty clay layer. Figures 6.4 and 6.5 present the resulting calculated factors of safety of 1.114 for the high and 1.255 for the low water table.

The inclinometer data provides information about slope movement, and although Slide does not analyze slope deformation, the water table elevation at times of slope movement can be input to the model. Assuming that when the slope was moving, the factor of safety was 1.0 or lower, the completed model with a known water table elevation could be analyzed to back calculate the corresponding soil property parameters, further refining the model. Some slope movement was recorded on April 17th, 2007, when the water table was naturally high due to the spring thaw, so the measured water table elevation on this date was used to refine the model.

Slide can be used to conduct a sensitivity analysis, in which individual input parameters are varied between defined minimum and maximum values. This creates a plot (Figure 6.6) of the factor of safety as a function of the individual input parameter value and allows the model to be refined. Generally, the sensitivity analysis showed that changes in the effective stress friction angle for the silty clay layer had the greatest impact on the factor of safety, consistent with a greater length of the critical slip surface occurring in this layer. However, since the silty clay material was tested in the lab more extensively than the silt material, there is more confidence in the effective stress friction angle of the silty clay than the silt. During refinement of the model,

the effective stress friction angle of the silt was reduced more than the silty clay. The firm silt and the till are below the critical slip surface and therefore their properties have no impact on the factor of safety.

For each refinement iteration, the effective stress friction angle for the silt was reduced by 0.5 to 1 degree and kept constant for the silty clay. A sensitivity analysis was run on the effective stress friction angle of the silty clay during each iteration to find the required friction angle to reach a factor of safety of 1.0. After 7 iterations, the resulting effective stress friction angles appeared reasonable and the model was thus considered fully refined. Table 6.2 presents the changes for each iteration and Table 6.3 presents the resulting material properties of the refined model. The effective stress friction angle of the silt was reduced from 33.6 to 28.5 degrees and from 24.5 to 23 degrees for the silty clay. Figure 6.7 shows the resulting critical slip surface. The critical slip surface computer by Slide intersects the location of Inclinometer #2 at roughly the same elevation as indicated by the inclinometers providing additional verification of the model.

6.2 MODELING MEASURED CONDITIONS

The water table elevations for several dates were analyzed to further verify the model. Table 6.4 present the maximum measured water table elevations from each monitoring well on some key dates. The factor of safety equaling 1.002 on April 17th, 2007, presented in Figure 6.7, corresponds to the naturally high water table elevation which was used to refine the soil model in the previous section. An additional high water table the next day on April 18th, 2007, shown in Figure 6.8, was a result of a municipal water line break, and the resulting factor of safety of 0.973 (Figure 6.9) confirms the subsequent inclinometer movement recorded shortly thereafter. It is possible that the slope movement occurring in conjunction with the natural high water table of around April 17, 2007, caused the municipal water line break of April 18, 2007.

During the late fall of 2007, the ground water table reached a peak on October 31, 2007, with no recorded slope movement. After a second peak on November 16, 2007, and a steady rise in the following days, slope movement was recorded on Inclinometer #2 (Figure 6.10). The resulting factor of safety on November 16th (Figure 6.11) is 1.029. Continued rise in the water table elevation to a peak on November 29, 2007, further decreased the factor of safety to 1.018. This shows that back-to-back high water table events can initiate slope movement compared to

isolated high water table events. There have been times when the water table elevation in Monitoring Well #1 has been high but no movement was recorded by the inclinometers. For example, Figure 6.12 presents a high water table on June 5, 2007, followed by a steady decline immediately after with no movement on the inclinometers. Modeling this water table in Slide (Figure 6.13) gives a factor of safety of 1.037, suggesting that the slope was close to moving. This is different than the back-to-back events of November, 2007, even though in both cases the high water table elevation was around 642.4 ft.

These analyzes indicate that water table elevation is an important trigger for slope movement and can therefore serve as a basis for developing a warning system. However, it is also clear that the time history of the water table elevation should also be taken into account.

6.3 FACTOR OF SAFETY AS A FUNCTION OF WATER TABLE

Knowing the elevation of the water table that may lead to a low factor of safety and potential slope movement is of use for setting alarm values in MultiloggerDB/Insite/MLWeb. Although the data presented in Chapter 5 do not show a direct relationship between water elevation and slope movement, modeling in Slide can give estimates of water table elevations that may be of concern.

Using the high and low water table elevation combinations presented in Table 6.1 and the fully refined model, Slide calculated a factor of safety of 1.116 for the low water table and 0.994 for the high water table.

The sensitivity analysis function of Slide can be applied to the water table. Assigning the low and high water tables in a model, Slide can calculate the mean water table elevation based on a normal statistical distribution. The normalized mean was set to 0.65 to reflect that the actual water table elevation has generally been closer to the high level than the low level. The resulting factor of safety using the mean water table elevation (Figure 6.14) is 1.041. Plotting the normalized water table elevation versus the factor of safety (Figure 6.15), the factor of safety equals 1.0 at a normalized water elevation equal to 95% of the range. This corresponds to a "critical" water table elevation at Monitoring Well #1 of 196.08 m (643.3 ft.) and 199.61 m (654.9 ft.) at Monitoring Well #2 using

$$\text{water table elevation} = F(\Delta H) + H_L \tag{6.1}$$

where

F = ground water table elevation factor from sensitivity analysis

$\Delta H = H_H - H_L$

H_H = highest ground water table elevation in monitoring well

H_L = lowest ground water table elevation in monitoring well.

One or both of these "critical" elevations are less than the actual water table elevations measured for the first two cases of slope movement modeled in Section 6.2. This is because the model was calibrated to get a factor of safety equal to 1.0 for the April 17, 2007, high water table elevations of 643.52 ft. in Monitoring Well #1 and 652.40 ft. in Monitoring Well #2. In the third case for November 16th, 2007, the water table elevation in Monitoring Well #2 was just below the "critical" value although slope movement was recorded, which is likely due to the back-to-back peaks in the water table elevation. In the case of the fourth model with an isolated high Monitoring Well #1 water table elevation on June 5, 2007, but yet both water table elevations were below these "critical" elevations and no slope movement was recorded.

6.4 EARLY WARNING SYSTEM

A benefit of automated instrumentation is the creation of alarm systems and early warning. Many dataloggers support alarm programming, allowing for the checking of instrumentation results for an alarm condition in real time, and with the addition of an auto dialer, the ability to page key personnel anytime. To reduce system complexity, data management and visualization software, such as the Multilogger/Insite/MLWeb package used on this project, support local alarms, allowing for alarm threshold values to be entered in engineering units. The instrumentation data is analyzed for alarm conditions each time it is downloaded from the datalogger. Local server-based alarm messages have the added benefit of being able to be sent out over a variety of medium, including sending of alphanumeric pages and email, or triggering a separate program on the server to run. In addition, local alarms are easy to implement and update and do not require datalogger programming. Some software packages also allow for more complex alarm types than are available on a datalogger, including low and high level alarms, rate of change alarms, and multi-stage alarms.

Once the decision is reached to implement an alarm system, the type of alarm and the relevant threshold values as well as the course of action during an alarm event need to be

determined. The course of action should be decided by the project engineer and other key personnel, and should be project specific.

For this project alarms can be implemented based upon one or more instruments and either using the measured values directly or some computed combination of measured values. The simplest alarm system would be to set a high level alarm for a monitoring well so that if the water table elevation reached a certain value, the alarm would be triggered. Using results from the ground water sensitivity function in Slide, such as that plotted in Figure 6.15, the project engineer can decide the minimum allowable factor of safety for the slope to activate a trigger, and set the corresponding water table elevation as the alarm threshold value.

Building on the high water table elevation alarm would be a two-level alarm, along the lines of a "green-yellow-red" system, where two separate threshold values are used. Green equals no action required, yellow equals slope and frequent monitoring of instrumentation required, and red equals immediate action required. Using the same ground water sensitivity function in Slide, factors of safety can be assigned by the project engineer to the yellow and red alarms and the corresponding water table elevations can be computed for the alarm threshold values.

Software packages like Multilogger allow for any instruments to be monitored for alarms, so the alarm does not have to be limited to just one instrument. Both monitoring wells could be assigned various alarm threshold values, and the same for the inclinometers. Precipitation measured by the rain gauge could theoretically be used as an alarm since the water table elevation is closely tied to that but consideration of the time of year would have to be built into the system (i.e., a heavy rain event in the winter might lead to mostly surface runoff in comparison to the summer where more water will infiltrate).

The rate of change in instrumentation readings is another type of alarm. If the change in value between the last reading and the current reading exceeds the alarm threshold, an alarm condition could be specified to be triggered. This type of alarm is available as a standard alarm in Multilogger in a "green-red" style, or with additional programming as a "green-yellow-red" style.

A third type of alarm relates to the time history of the instrument reading. If the reading is higher than a predefined threshold, and has been for more than predefined time period, then the

alarm condition will be trigged. With some additional programming, this type of alarm can be implimented in Multilogger.

Figure 6.16 and Table 6.5 present a summary of the alarm types. The alarm threshold values in Figure 6.16 are just to demonstrate the different types of alarms and were randomly chosen.

An early warning system that used alarms from the various instruments and sends out notification to key personnel whenever any of the alarms are triggered could be prone to excessive false alarms. For example, a rate of change alarm activating after a particularly heavy but short summer thunderstorm. An early warning system that uses an algorithm to combine the high level, rate of change, and time history alarms would be more robust and thus less likely to report a false alarm.

An algorithm that accommodated all three alarm categories could use weights assigned to each alarm type. Thus in the case of using the water table elevation data, the warning level would then be calculated as

$$WL = \alpha_{HL} \cdot AI_{HL} + \alpha_{RC} \cdot AI_{RC} + \alpha_{TH} \cdot AI_{TH} \quad (6.2)$$

where

WL = warning level

α_{HL} = high level alarm weight

AI_{HL} = high level alarm input

α_{RC} = rate of change alarm weight

AI_{RC} = rate of change alarm input

α_{TH} = time history alarm weight

AI_{TH} = time history alarm input

$(\alpha_{HL} + \alpha_{RC} + \alpha_{TH}) = 1.0$.

The input from the alarms can simply be -1 when a “green” condition is triggered, 0 for a “yellow” and 1 for a “red” condition. The weights should be between 0 and 1 such that the sum of all three weights equals 1. The values of the weights will need to be “tuned” by the project engineer based on past experience, project specific conditions, and to reduce false alarms. For the Waterbury Center slope, for example, the instrumentation and modeling results show that a

high water table elevation is a strong indication of potential slope movement and therefore the high level alarm could be given the largest weight in the early warning algorithm.

Depending on the status of the three alarms, the warning level will range from -1 to 1 such that in the event that all three alarms are in a "green" condition, the warning level will equal -1. For an overall early warning alarm, the "green" condition could be for a warning level value less than -0.5, the "yellow" condition could range from -0.5 to less than 0.5, and the "red" condition could be for warning level values above 0.5, although these threshold values should be decided upon and refined by the project engineer.

6.5 SEEPAGE ANALYSIS

Seepage forces were not included when creating and refining the Slide model because of the lack of information on the piezometric line upslope. The refined model uses only an estimated piezometric line based on the measured ground water table elevations in the two monitoring wells. Pore pressures for the stability analysis are calculated by multiplying the unit weight of water by the depth below the piezometric line assuming hydrostatic conditions, i.e., no flow.

According to Cedergren (1967), "water seeping in a generally horizontal [parallel to ground surface] direction destabilizes slopes, whereas water seeping in vertically downward produces no destabilizing forces and no pore pressures." Based on the geometry of the slope and the known water table elevation in the two monitoring wells, as well as Bryant Brook at the toe of the slope, it is probable that there is horizontal groundwater flow in the slope and that seepage forces should be analyzed.

Slide 5.0 includes a finite element method groundwater analysis function with the ability to use the computed pore water pressures directly in the slope stability analysis. Slide can also calculate negative pore water pressure in areas that are unsaturated, but for the stability analysis presented here it was assumed that pore water pressures were zero in the relatively shallow unsaturated zone above the water table. In situ hydraulic conductivity for the silty clay was estimated using the CRS data at e_0 as 1.4×10^{-7} cm/s (4.59×10^{-9} ft/s) and was assumed to be one order of magnitude higher in the silt layer, i.e., 1.4×10^{-6} cm/s (4.59×10^{-8} ft/s).

Conducting the stability analysis with seepage requires boundary condition information for the far left and right hand sides of the modeled region (Figure 6.17). On the far right, the

elevation of Bryant Brook was used as a total head boundary. For the far left (upslope) no information is available and a parametric approach was used. Extrapolation of the piezometric line upslope from Monitoring Well 2 relative to the ground surface suggests a total head at the far left of about 670 ft. Using these boundary conditions together with the same geometry and soil layers as the previous models and the measured ground water table elevations of the two monitoring wells on April 17th, 2007, the new model incorporating seepage forces was refined to reach a factor of safety equal to 1.0 (Figure 6.17). This was done by assuming no cohesion in the soil layers and modifying the effective stress friction angles. The resulting effective stress friction angles are 33 degrees for the silt layer and 24 degrees for the silty clay layer (Table 6.6). These compare well with the laboratory results of 33.6 and 24.5 degrees. Table 6.6 presents a comparison of the seepage analysis versus the piezometric line analysis. For the same soil properties, incorporating seepage forces reduces the calculated factor of safety of the project slope by approximately 10% in comparison to ignoring seepage.

The small reduction in effective stress friction angles of roughly 0.5 degrees from the measured lab results to the back calculated results indicate that the seepage analysis based model may be a more appropriate model to use rather than the piezometric line model. The uncertainty, however, in using the seepage analysis is the need to measure or estimate the pore water pressures at key points through the cross section of the slope. For this project, only the two monitoring wells and Bryant Brook provide ground water table elevations. Using the piezometric line analysis, the location of the ground water table upslope of Monitoring Well #2 has no effect on the calculated factor of safety and was added to the model parallel to the ground surface. For the seepage analysis, changing the ground water table upslope of Monitoring Well #2 will influence the magnitude of the seepage forces and hence the factor of safety. Without a third monitoring well or other piezometer installed upslope, it was necessary to estimate the location of the ground water table for this analysis.

Figures 6.18 and 6.19 presents results of a parametric analysis to determine the influence of the upper boundary condition in the seepage analysis model in comparison to assumed elevation of 670 ft. Starting with the same upper boundary elevation as used in the piezometric line analysis of 680 ft., Figure 6.18 shows the groundwater table meeting the ground surface above Monitoring Well #2, which has not been observed to occur. In contrast to this, lowering the upper boundary elevation to 660 ft., results in a ground water table that does not intercept

Monitoring Well #2 at its measured elevation (Figure 6.19) and gives a water table profile that does not look realistic. Whereas the assumption of 670 ft gives a water table profile that looks reasonable (Figure 6.17). The corresponding factor of safety for both of the two extreme cases of 660 and 680 ft. is about 4 to 5 % different than that of locating the upper boundary elevation at 670 ft.

6.6 MODELING POTENTIAL REMEDIATION SOLUTIONS

As part of their early recommendation for potential remediation methods, VTrans proposed three solutions. Using the refined Slide material properties, these three solutions were modeled to determine the resulting factor of safety for each. Table 6.7 presents the proposed remediation solutions and their factors of safety. The high water table elevations measured from the monitoring wells, combined with cohesion values of zero, produces the worse-case scenario to test the proposed solutions. The curtain drains were modeled as a granular material 0.15 m (0.5 ft.) wide and the ground water table was manually adjusted to reflect the effects of the drain.

The solution with two curtain drains but no rock fill (Figure 6.20) is the least effective as it does not really lower the ground water table much within the zone of the circular failure. Installing both curtain drains and the rock fill at the toe of the slope (Figure 6.21) gives the highest factor of safety, but is still limited by the high ground water table within the zone of failure. Figure 6.22 presents one curtain drain above the road and the rock fill at the toe of the slope.

Table 6.1 High and Low Water Table Elevations

	Monitoring Well #1 Elevation (ft.)	Monitoring Well #2 Elevation (ft.)
High	643.5	655.1
Low	639.6	651.3

Note: Water table elevation is the maximum or minimum recorded in the monitoring well independent of the elevation in the other monitoring well.

Table 6.2 Results of the Model Refinement Iterations

Iteration	Silt ϕ' Changed from 33.6° to	Resulting Factor of Safety *	Silty Clay ϕ' from Sensitivity Analysis to get FS = 1.0 (°)
1	-	1.123	20.6
2	32	1.099	21.5
3	31	1.084	21.9
4	30	1.070	22.4
5	29	1.055	22.8
6	28	1.041	23.3
7	28.5	1.048	23.1

Note: * with silty clay $\phi' = 24.5°$

Table 6.3 Summary of Refined Soil Profile Materials and Properties

Elevation	Name	Unit Weight	c'	ϕ' (°)
195.7-198.7 m (642-652 ft.)	Gravely Sand	20.4 kN/m^3 (130 lb/ft^3)	0	35
191.4-195.7 m (628-642 ft.)	Silt	18.4 kN/m^3 (117 lb/ft^3)	0	28.5
189-191.4 m (620-628 ft.)	Silty Clay	17.6 kN/m^3 (113 lb/ft^3)	0	23
180.4-189 m (592-620 ft.)	Firm Silt	18.6 kN/m^3 (120 lb/ft^3)	7.12 kPa (150 lb/ft^2)	32
179.5-180.4 m (589-592 ft.)	Till	22 kN/m^3 (140 lb/ft^3)	0	45
179.5 m (589 ft.)	Bedrock	-	-	-
-	Curtain Drain	18.6 kN/m^3 (120 lb/ft^3)	0	40
-	Rock Fill	22 kN/m^3 (140 lb/ft^3)	0	45

Note: Slip surface involves only the gravely sand, silt, and silty clay soil units (e.g., see Figure 6.7)

Table 6.4 Maximum Measured Water Elevations

Date Recorded	Monitoring Well #1 Elevation (ft.)	Monitoring Well #2 Elevation (ft.)
4/17/2007	643.52	652.40
4/18/2007	644.52	654.58
11/16/2007	642.39	654.82
11/29/2007	642.83	654.68
6/5/2007	642.45	652.72

Table 6.5 Summary of Alarm Conditions

Alarm	Green	Yellow	Red
High Level	$H_t \leq a_1$	$a_1 < H_t \leq a_2$	$H_t > a_2$
Rate of Change	$\frac{\Delta H_t}{\Delta t_c} \leq b_1$	$b_1 < \frac{\Delta H_t}{\Delta t_c} \leq b_2$	$\frac{\Delta H_t}{\Delta t_c} > b_2$
Time History	$\sum_{\Delta t_h} H_t \leq c_1$	$c_1 < \sum_{\Delta t_h} H_t \leq c_2$	$\sum_{\Delta t_h} H_t > c_2$

Notes:
1. H_t = ground water table elevation at time of current reading
2. a_1, a_2, b_1, b_2, c_1, and c_2 = alarm threshold values
3. Δt_c = time period for rate of change alarm
4. Δt_h = time period for time history alarm

Table 6.6 Comparison of Seepage and Piezometric Analyses

Material	Friction Angle (ϕ)	Seepage Analysis[1]	Piezometric Line Analysis[2]	Difference (%)
Lab Testing Results		1.018	1.123	10
Silt	33.6			
Silty Clay	24.5			
Piezometric Analysis Results		0.902	1.002[3]	11
Silt	28.5			
Silty Clay	23			
Seepage Analysis Results		0.998[3]	1.098	10
Silt	33			
Silty Clay	24			

Notes:
1. Seepage forces taken into account.
2. Seepage forces ignored.
3. Friction angle of silt and silty clay layers varied to give factor of safety equal to 1.0 for this case.

Table 6.7 Potential Remediation Solutions

Solution	Factor of Safety
Install 2 certain drains. One 14 feet east of centerline and 10 feet deep, and one 38 feet west of centerline and 8 feet deep.	1.121
Install 1 curtain drain 14 feet east of centerline and 10 feet deep, and install a counterberm at the toe of slope.	1.221
Install 2 certain drains. One 14 feet east of centerline and 10 feet deep, and one 38 feet west of centerline and 8 feet deep. Install a counterberm at the toe of slope.	1.280

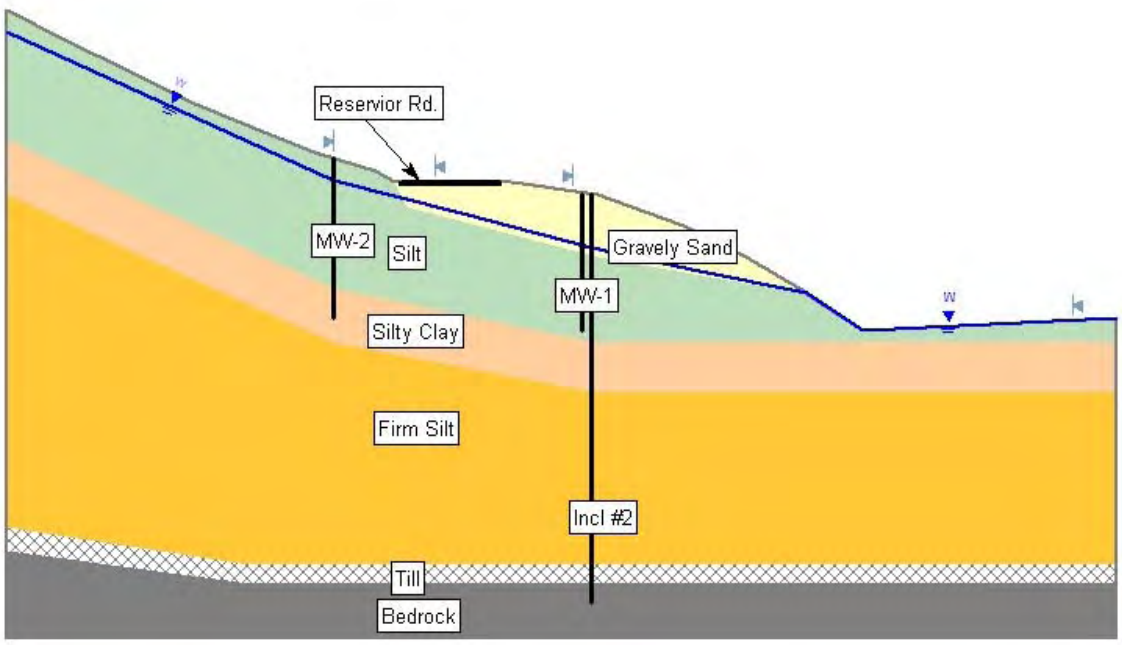

Figure 6.1 Completed Slide cross section and soil profile.

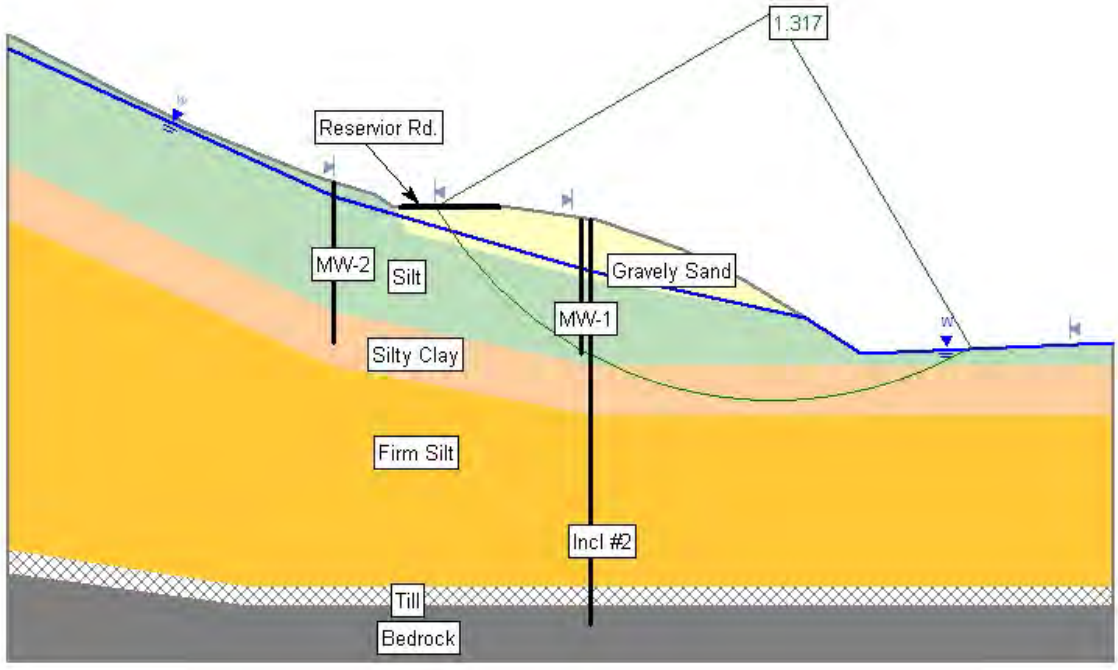

Figure 6.2 Factor of safety with a high water table and no refinement to the soil properties (presented in Table 4.9 and Figure 4.22).

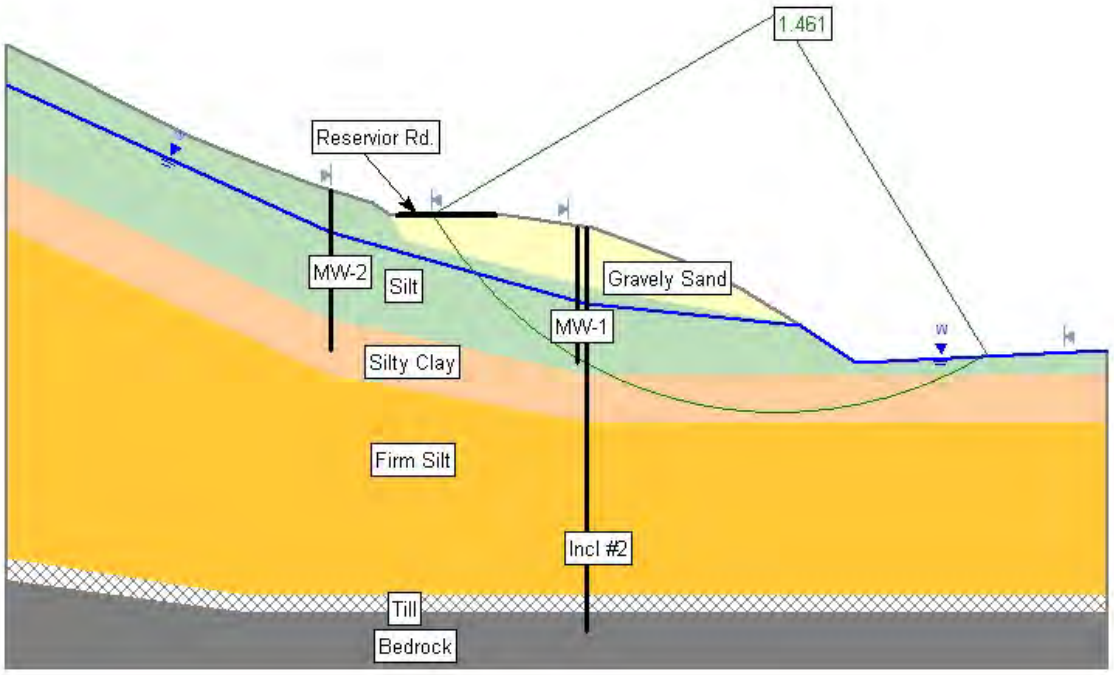

Figure 6.3 Factor of safety with a low water table and no refinement to the soil properties (presented in Table 4.9 and Figure 4.22).

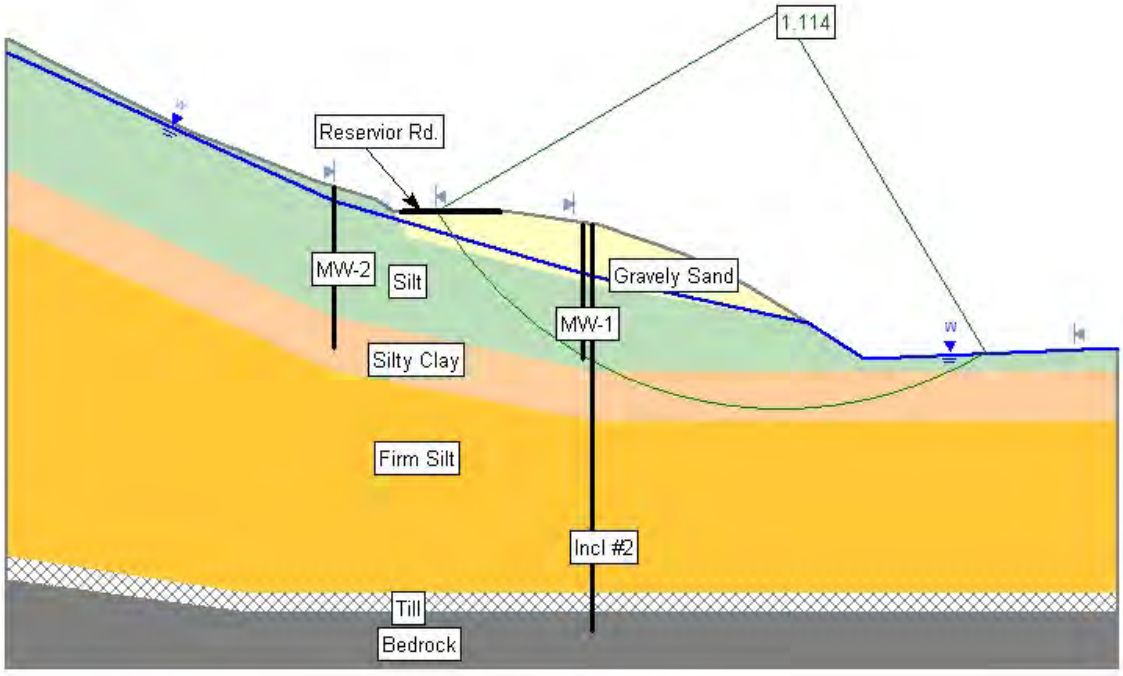

Figure 6.4 Factor of safety with a high water table and assumed zero effective stress cohesion intercept for the silt and silty clay soil properties (e.g., c' = 0).

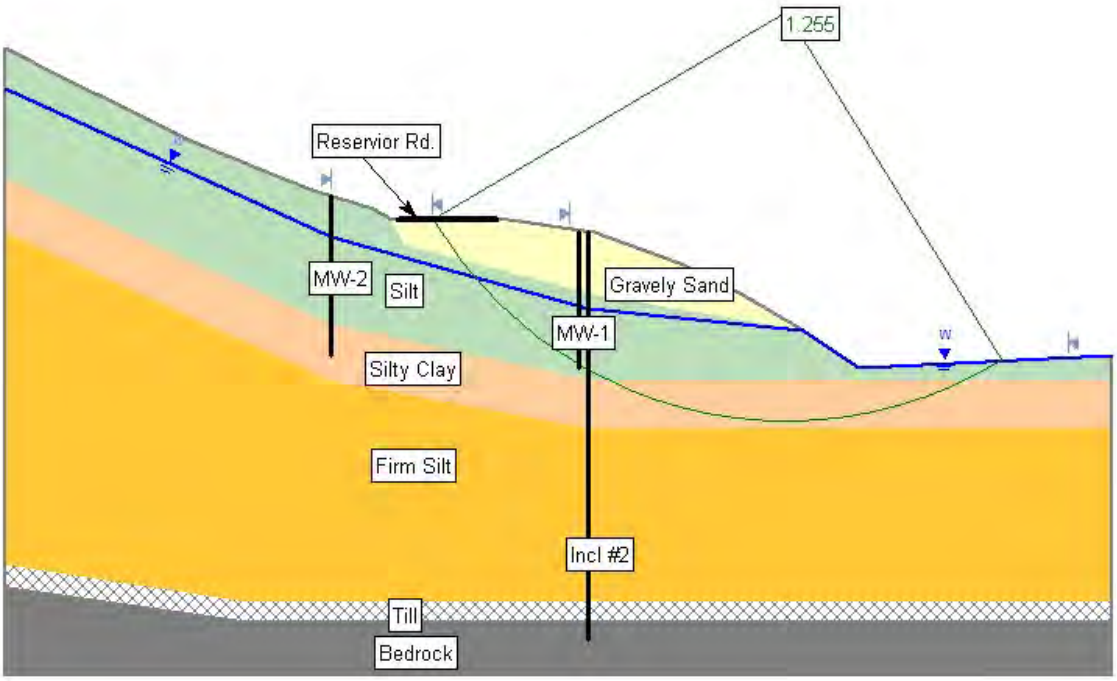

Figure 6.5 Factor of safety with a low water table and assumed zero effective stress cohesion intercept for the silt and silty clay soil properties (e.g., c' = 0).

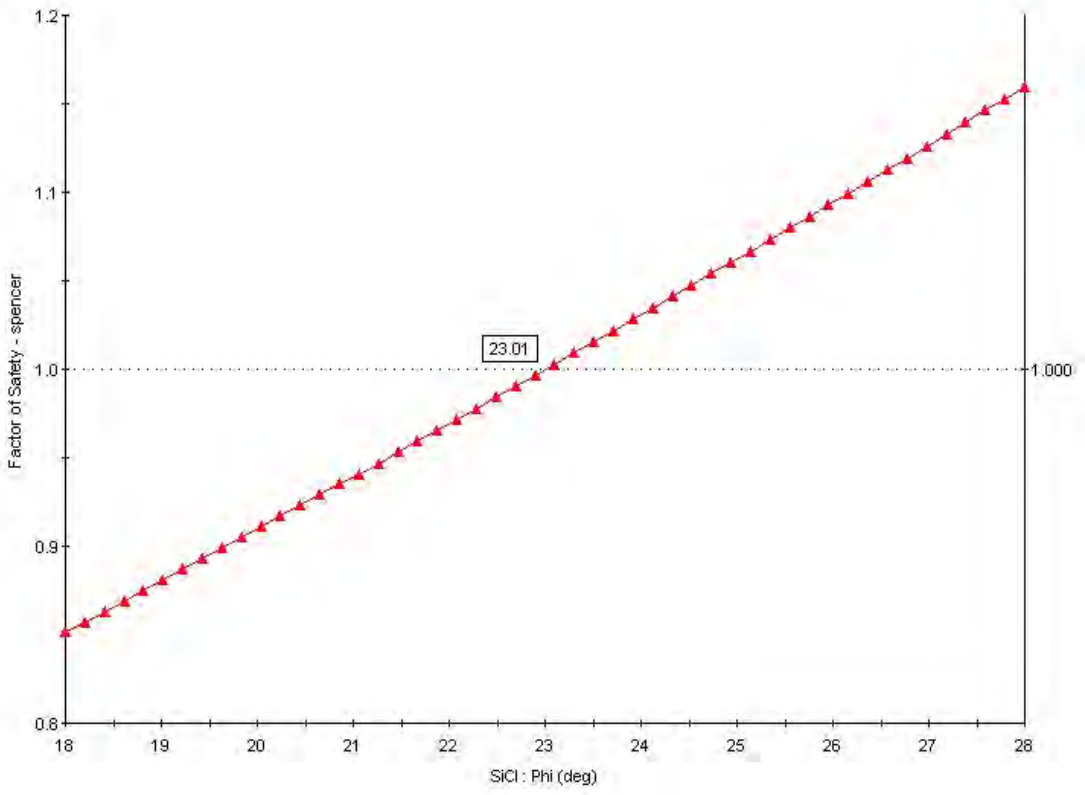

Figure 6.6 Sensitivity plot of friction angle of the silty clay layer versus factor of safety for iteration #7.

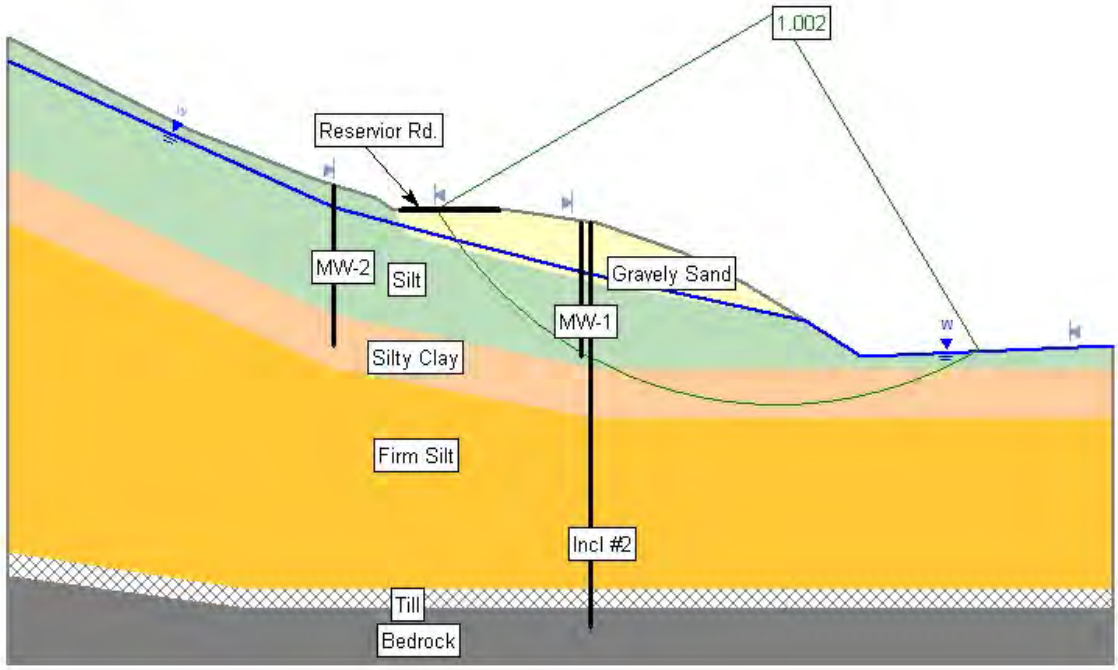

Figure 6.7 Factor of safety on 4/17/07 with conditions of high water table elevation and refined soil properties (Table 6.3).

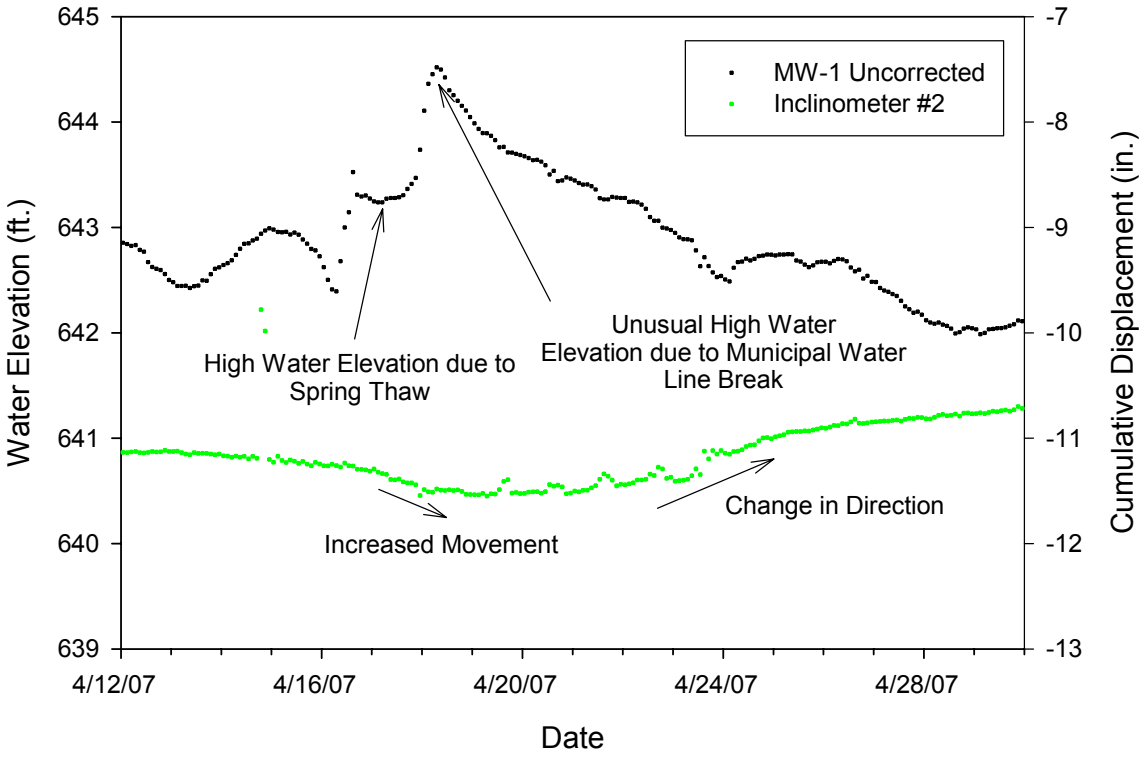

Figure 6.8 Measured water elevation and inclinometer movement, April, 2007.

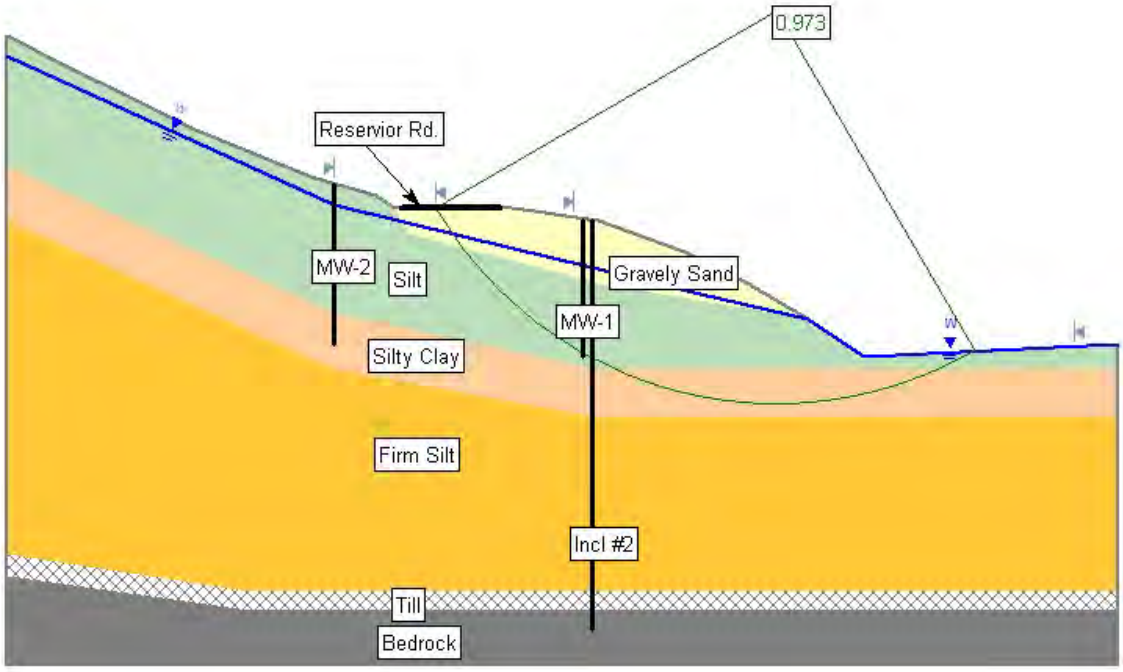

Figure 6.9 Factor of safety on 4/18/07 after municipal water line break (see Figure 6.8).

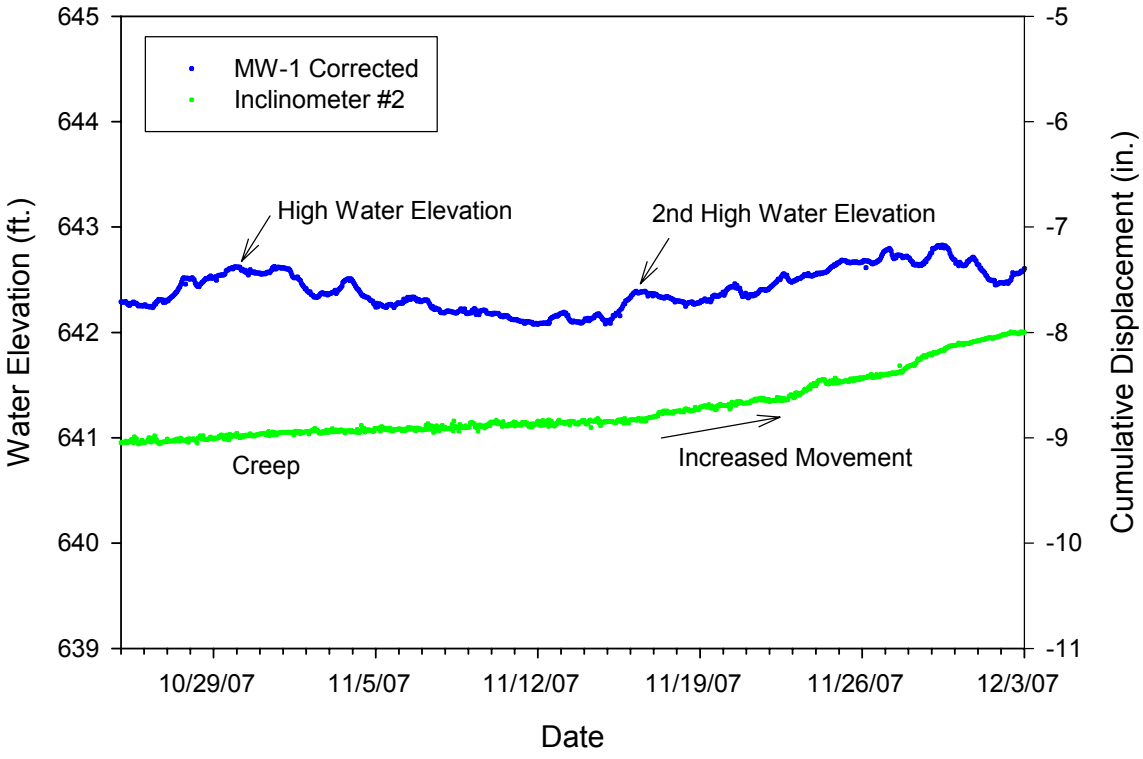

Figure 6.10 Measured water elevation and inclinometer movement, November, 2007.

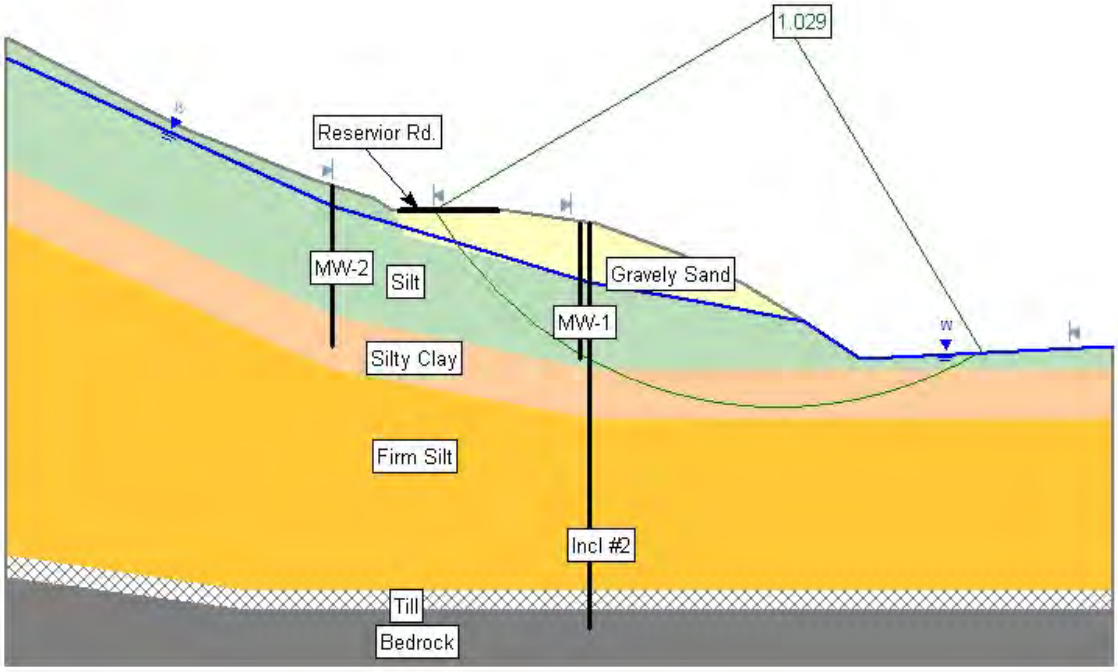

Figure 6.11 Factor of safety on 11/16/07 (see Figure 6.10).

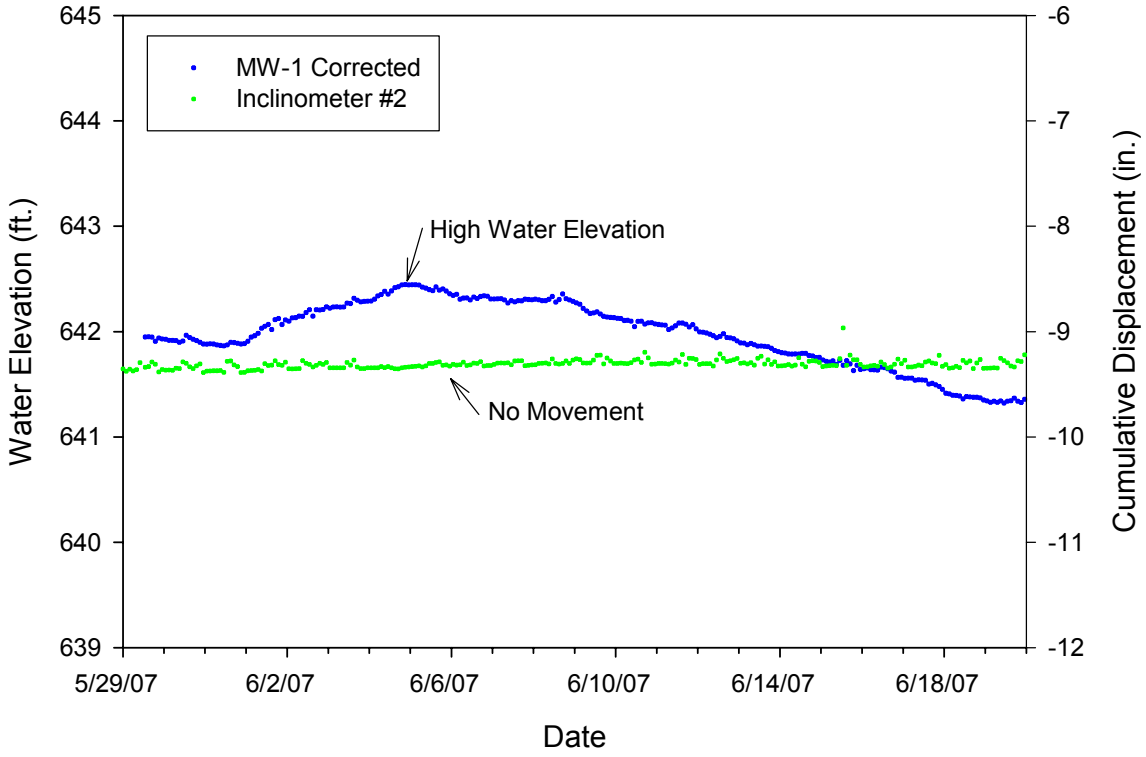

Figure 6.12 Measured water elevation and inclinometer movement, early June, 2007.

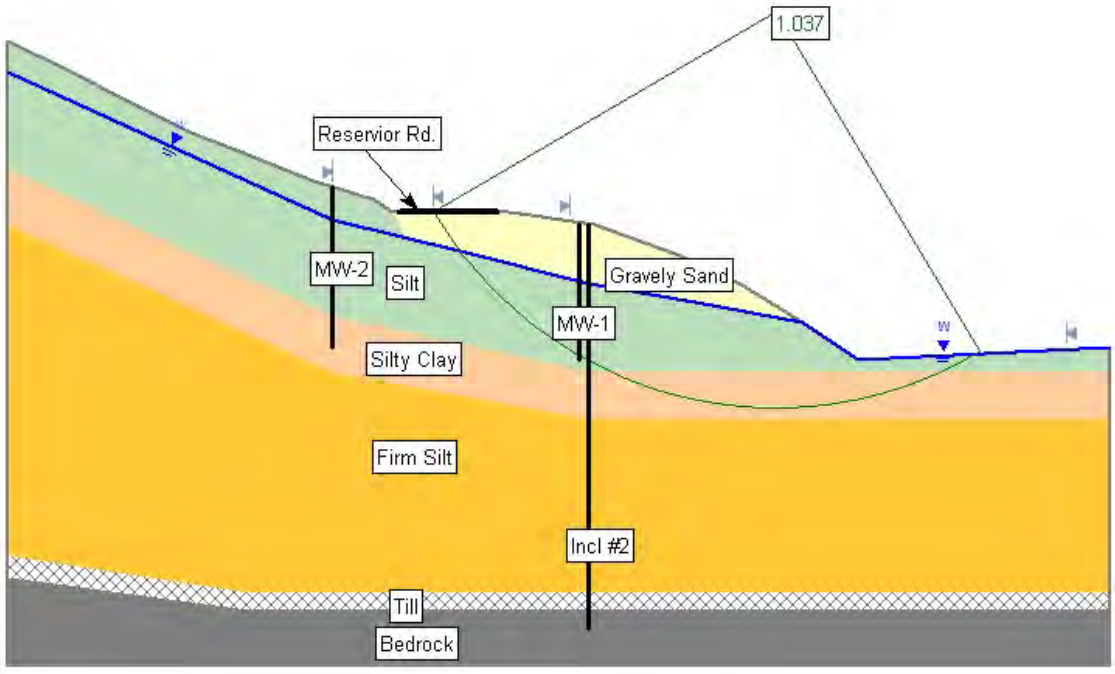

Figure 6.13 Factor of safety on 6/5/07 (see Figure 6.12).

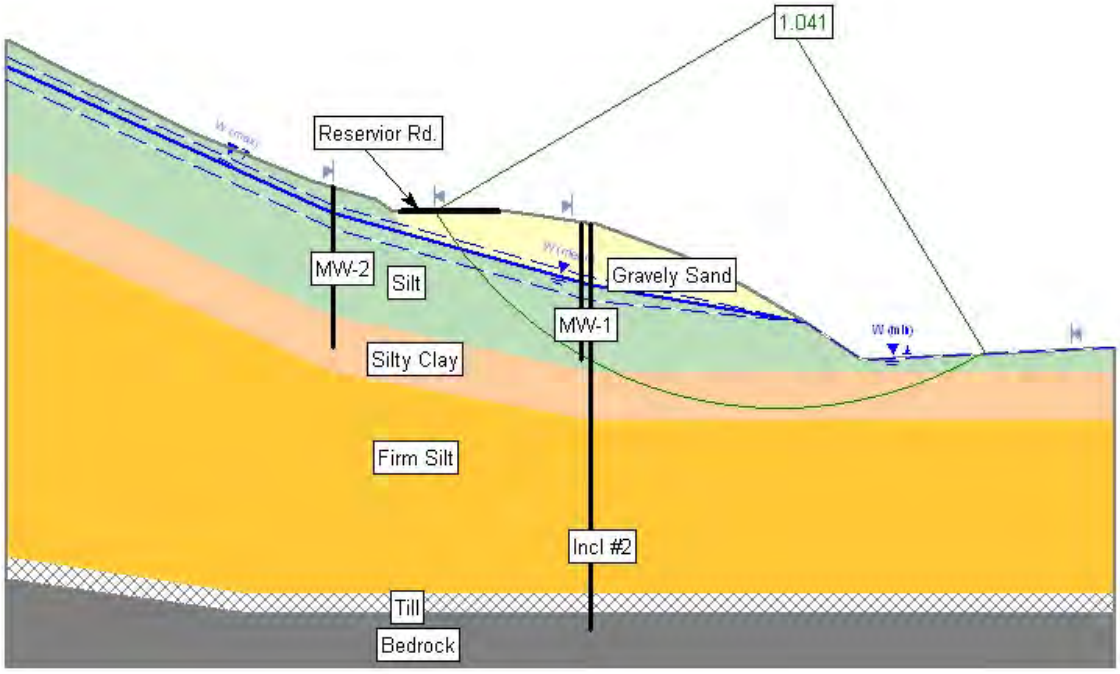

Figure 6.14 Factor of safety at mean water table elevation in MW #1 of 642.1 ft.

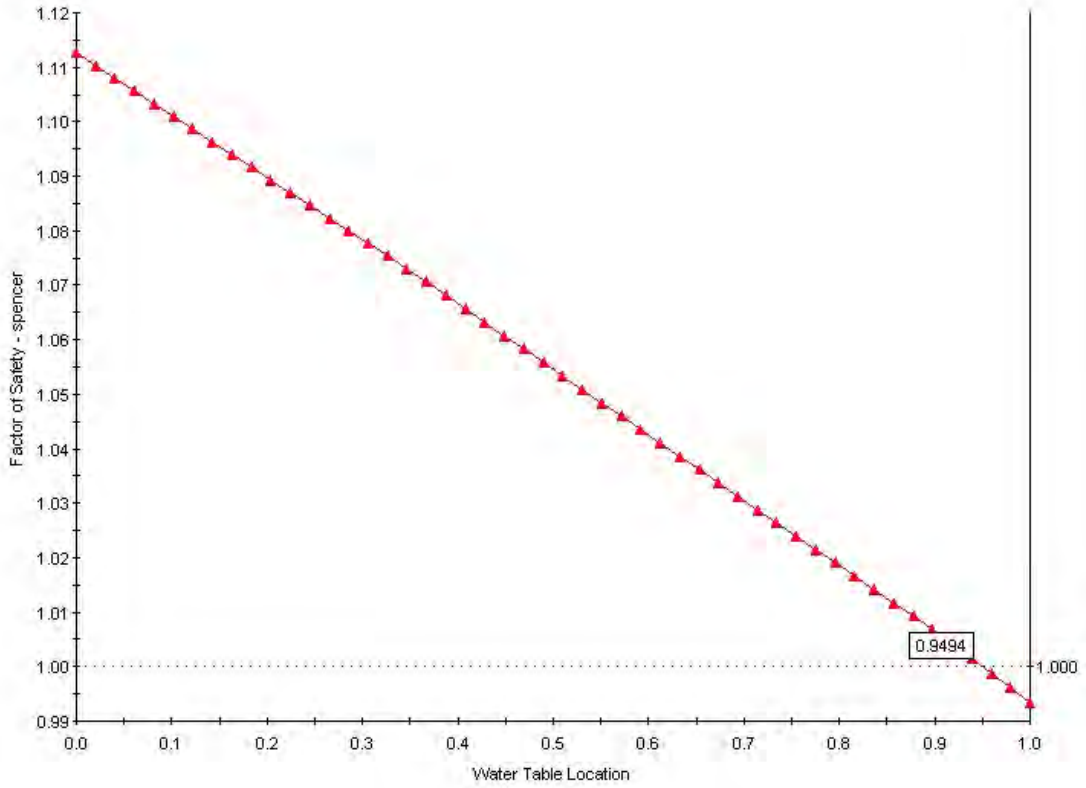

Figure 6.15 Sensitivity plot of normalized water table elevation versus factor of safety. For FS = 1.0, resulting ground water table elevation factor for use in Equation 6.1 is 0.9494.

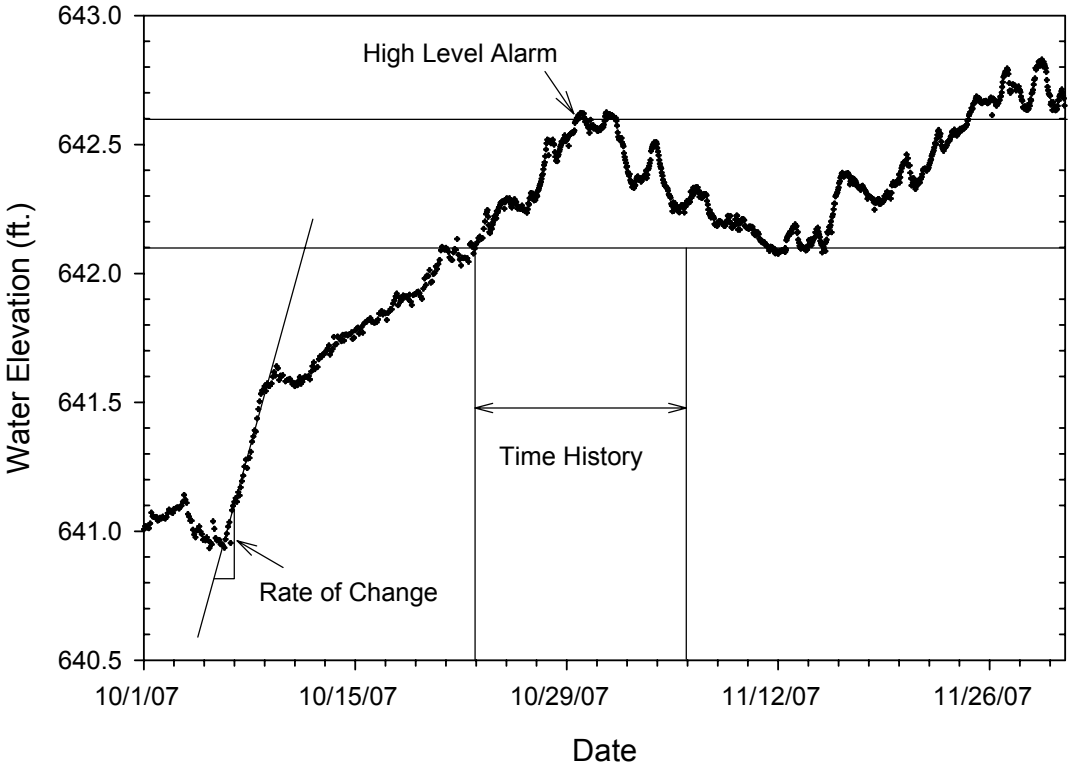

Figure 6.16 Summary of alarms. The high level alarm is activated whenever the current reading is above a threshold value, for this example 642.6 ft. The rate of change alarm is activated whenever the change from one reading to the next exceeds a threshold slope. The time history alarm is activated when the readings remain higher than a threshold value for longer than a set period of time, for this example two weeks.

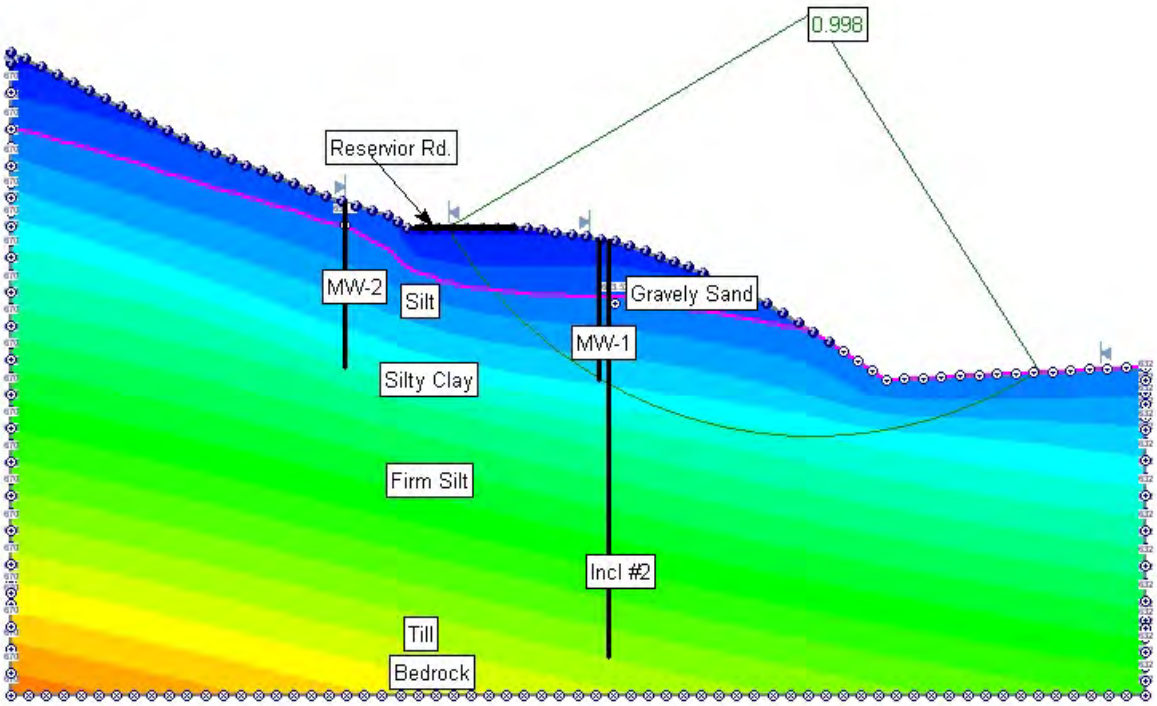

Figure 6.17 Factor of safety on 4/17/07 using the refined seepage analysis model with an assumed far left boundary condition of 670 ft. for the water table (purple line).

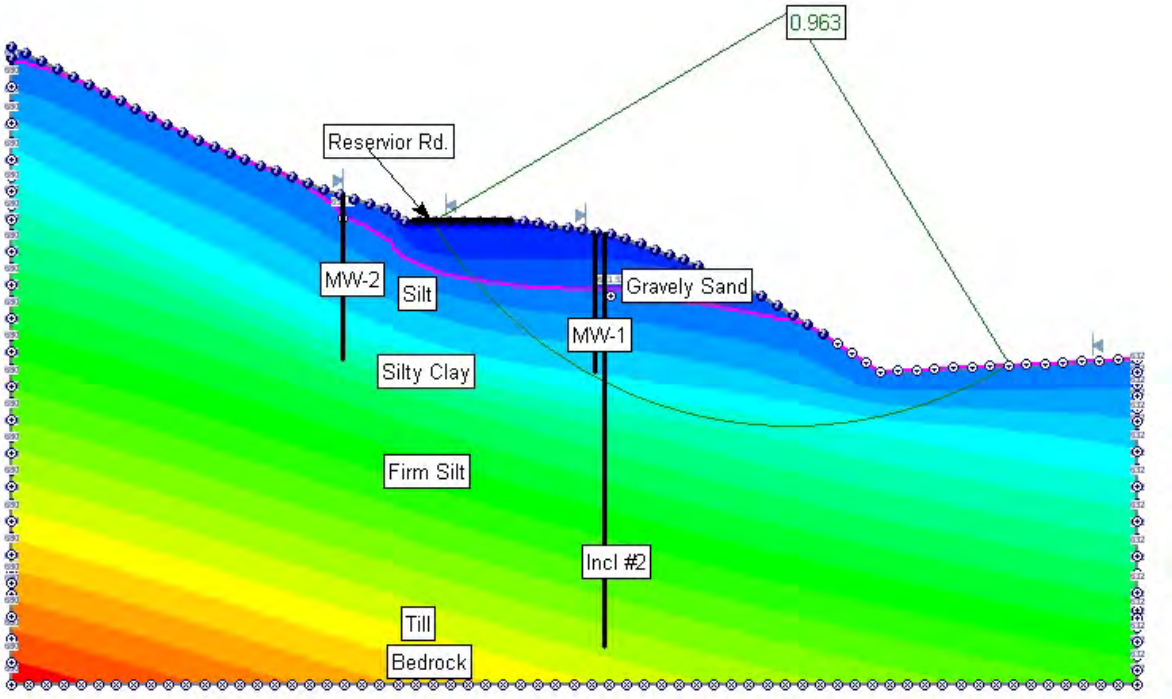

Figure 6.18 Factor of safety on 4/17/07 using the refined seepage analysis model with an assumed far left boundary condition of 680 ft. for the water table (purple line).

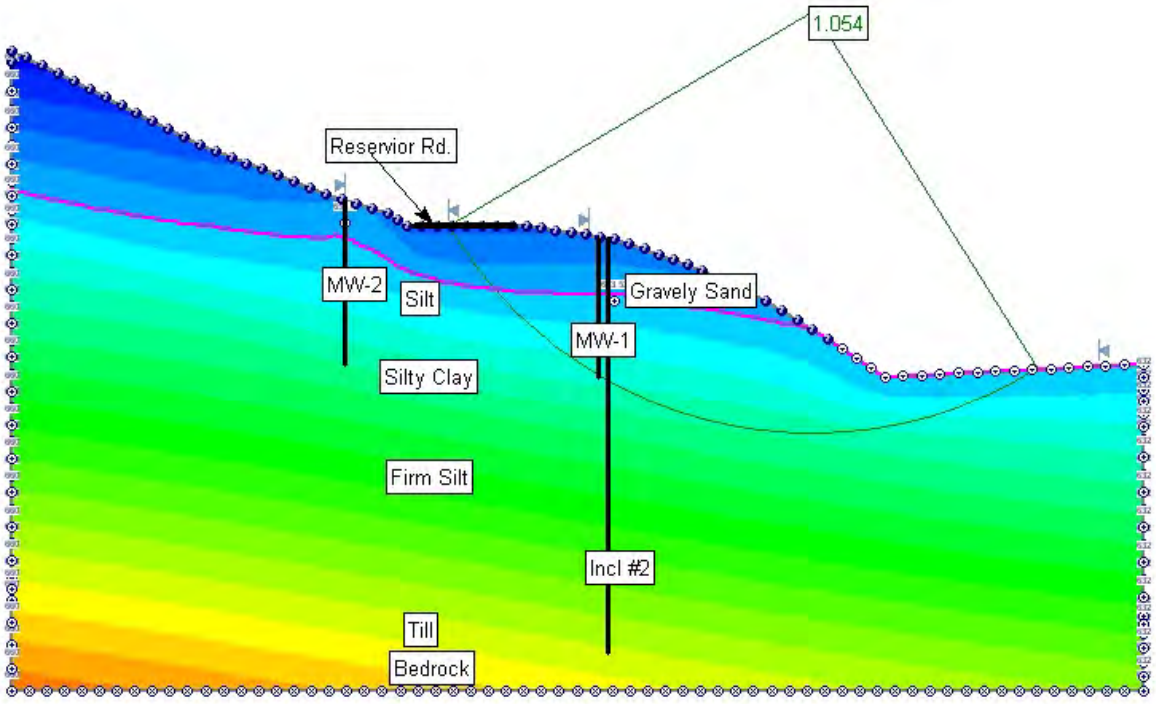

Figure 6.19 Factor of safety on 4/17/07 using the refined seepage analysis model with an assumed far left boundary condition of 660 ft. for the water table (purple line).

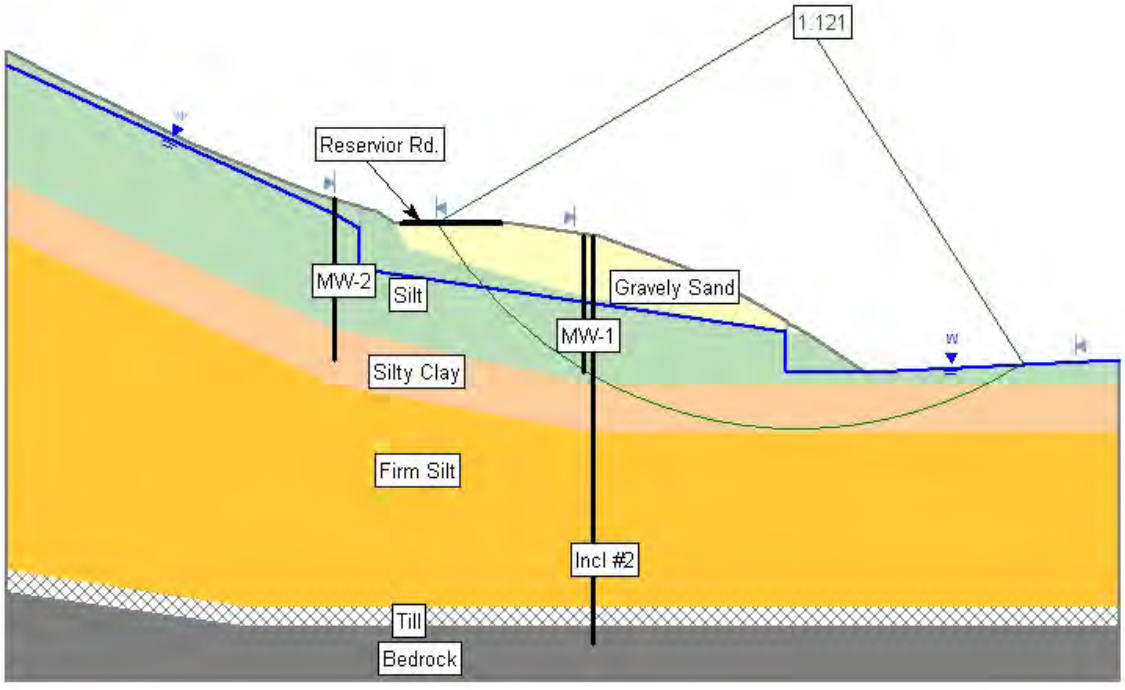

Figure 6.20 Factor of safety with 2 installed curtain drains.

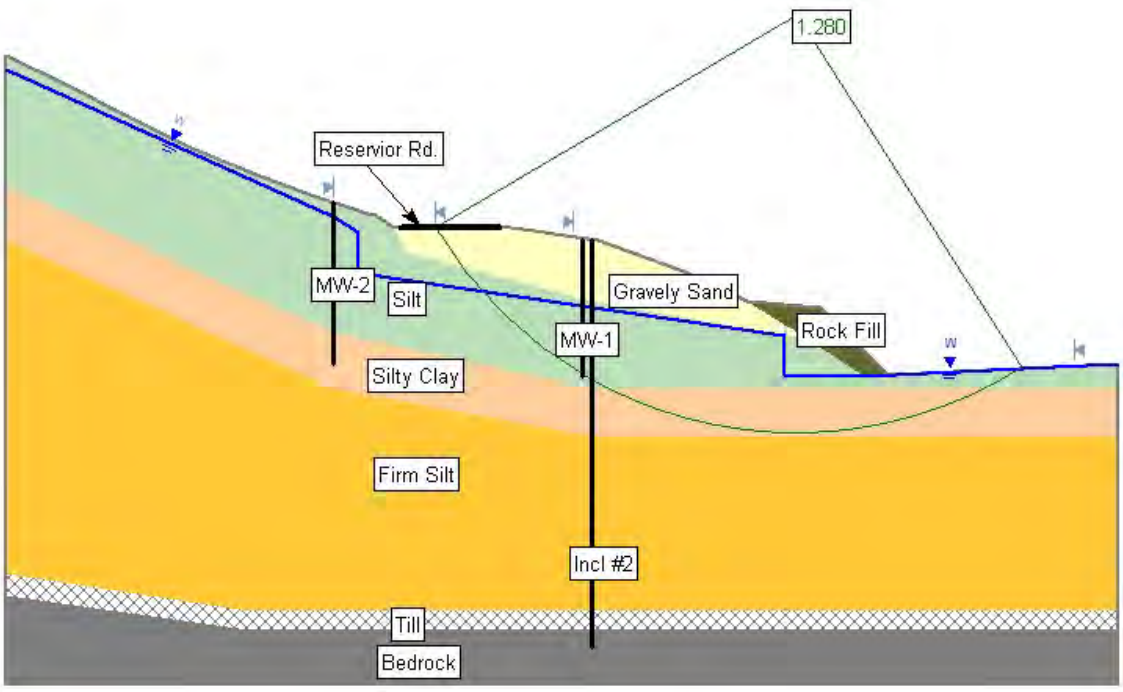

Figure 6.21 Factor of safety with 2 installed drains and rock fill at toe of slope.

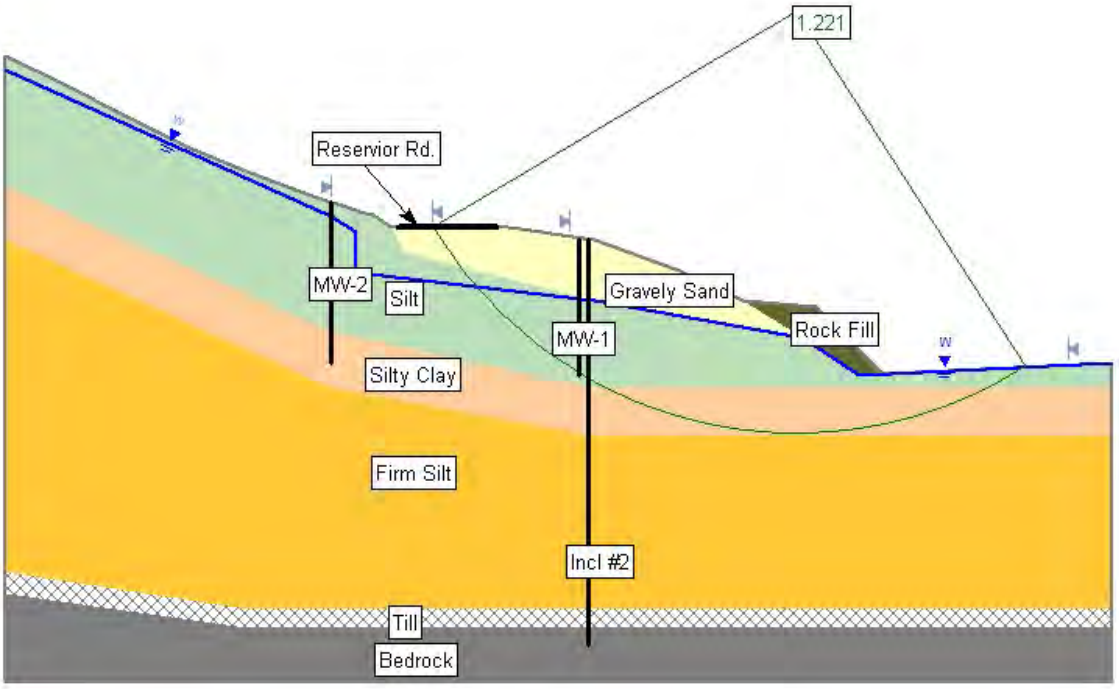

Figure 6.22 Factor of safety with 1 installed drain and rock fill at toe of slope.

7.0 CONCLUSIONS AND RECOMMENDATIONS

This chapter presents conclusions and recommendations based primarily on the experience gained on this project. Particular emphasis is given to documenting the lessons learned regarding the instrumentation, data logging, and data storage and visualization aspects so they can be applied to future VTrans projects. In addition, recommendations for future work, including information on recent advances in instrumentation technology, are presented.

Overall it is concluded that the instrumentation worked well and together with the data acquisition and database management software provides a good system for automated monitoring of slope movement. There were some periodic problems with the instrumentation but most of these were solved after a site visit to troubleshoot the problem. The analyzed instrumentation data coupled with results from the numerical analysis show good promise for implementing a robust and reliable early warning system with appropriate triggers (e.g., green, yellow and red) to active alarms when certain key instrumentation values or combination of values are reached. It will require some experience to determine what specific values to assign for the triggers and they will be project specific. It is likely that the triggers will have to be tuned during a project as data are collected and more is learned of the ground response to key events (e.g., heavy rain, construction, etc.).

The major problem in this project in terms of directly implementing and proof testing such an early warning system was that the inclinometers were installed after some significant slope movement had already occurred. This made it difficult to interpret readings from several of the key inclinometers that were located at or near the likely location of the slip surface as it is believed there was casing interference with the inclinometer tubing. Thus it was not possible to assign realistic trigger values for the inclinometers. However, from the instrumentation data and the stability analysis, the water table elevation was found to be a good indicator of slope movement and thus could serve as a basis for setting early warning alarms.

These general conclusions are based on a number of specific lessons learned in this project which are presented in the following section.

7.1 LESSONS LEARNED

The following lessons learned are based on the two years of remote monitoring at the Waterbury Center site and data analysis conducted for this project. These project specific lessons learned are supplemented with others based on UMass Amherst's experience with field instrumentation and remote data acquisition and monitoring for several other projects completed during the past decade. Most of these other UMass Amherst projects were focused on monitoring of groundwater conditions and involved the use of vibrating wire piezometers, conductivity probes, and datalogger systems.

7.1.1 Instrumentation and Data Logging

1. The instrumentation and datalogging system were relatively straight forward to install. The in-place-inclinometers are designed to be installed in standard inclinometer casing, allowing for drillers and field personnel familiar with inclinometer casing installation to prepare the test site. The piezometers were hung in standard open standpipe monitoring wells. Programming of the datalogger using Multilogger was done using a graphical interface. The program is well documented and relatively easy to use.

The instrumentation used in this project is mostly reusable providing it can be retrieved from the site, which might be an issue for the deep IPIs in Inclinometer #2 which has deformed a significant amount. All data acquisition equipment, including the datalogger, cabling, and multiplexers should be reusable.

2. In-place-inclinometer (IPI) resolution. With traditional manually operated probe inclinometers, one instrument is run up the inclinometer casing, usually at intervals of 0.61 m (2 ft.), allowing for a relatively high degree of resolution. The number of IPIs that can fit in a standard 70 mm (2.75 in.) inclinometer casing is approximately seven instruments because of the need to accommodate the rigid connecting tubing, a wire safety rope, and sensor cables from each IPI. For holes that are several tens of meters deep, this requires instruments to be installed with gauge lengths ranging from 1.5 to 6 m (5 to 20 ft.) and hence significantly less resolution than traditional probe inclinometers. In addition, large gauge lengths can result in undetected casing deformations between instruments and can also lead to significant bending of the semi-rigid tubing (and thus casing interference), as is believed to be the case for Inclinometer #2 at the Waterbury Center site.

The IPIs could be strategically placed to provide better resolution. For example, in this project the main slip surface at Inclinometer #2 is believed to be at around 7.62 m (25 ft.) below ground surface. Closer spacing of the IPIs in this region would have led to better data resolution. However, it is often not possible in projects to determine where critical zones of movement will occur prior to field drilling and instrumentation installation.

3. Instrument installation schedule. The in-place-inclinometers ideally should have been installed at the same time the inclinometer casings were installed. However, the instrumentation was not ready at that time and there was a several month delay. By the time of installation, significant deformation had already occurred to the point that traditional inclinometer probe readings in Inclinometer #1 were suspended shortly thereafter. The deformations made the physical installation of the IPIs difficult as the rigid connecting tubing had to be pushed past the bends in the inclinometer casing. In addition, the probable bending of the connecting tube associated with IPI 05-16367 mean that the deformation readings by that sensor have been suspect since the day of installation. Had the IPIs been installed in a near vertical casing, all the sensors would be expected to produce valid readings showing increased deformation. At such a point that the rigid tubing did indeed contact the side of the casing, the associated IPI would show a sudden and then gradual amplification of deformation as the effective gauge length was suddenly reduced and further deformation of the casing occurred.

4. Communication with the remote system using the cellular equipment was almost always successful. If a radio communication system is used the performance can be more erratic, as it can be affected by tree foliage, atmospheric events, and weather conditions. Cellular communications can also be affected by these same things, but often not to the same extent. On datalogger systems using a solar panel for power, low main battery power can affect communications as well. Frequent polling or extended communication sessions can drain the battery, eventually preventing further communications until the battery has been recharged.

Frequent polling of the cellular phone can also result in significant cellular charges depending on the type of plan and rates available for the cellular network being used.

5. Availability and reliability of cellular communication. Although cellular communication is preferred over radio for long distances, not all project sites have cellular service. To insure reliable communications and no dropped calls, a directional Yagi type of antenna was installed at the Waterbury Center site and this proved to work well as it was almost always possible to communicate with the datalogger from UMass Amherst.

One minor issue with the cellular modem used on this project was that when the new server was installed at UMass Amherst during the summer of 2007, it was discovered that its internal modem was too new to reliably communicate with the cellular modem at the site. This problem was solved by replacing the server's modem with an inexpensive modem that used an older communication protocol.

6. Protect components from the weather. The electronics of the datalogger and multiplexers are mounted inside weather-proof Nema enclosures, but other components of the system can be susceptible to weather. In addition to the water damaged barometer, the signal cable for Monitoring Well #2 passed under Reservoir Rd. through a drainage culvert. During the early spring of 2007, the signal cable was cut by ice moving in the culvert.

7. At other UMass Amherst projects, some vibrating wire pressure transducers have failed for unknown reasons. For those used in monitoring wells and open standpipe piezometers replacement was easy. However, for those buried in the subsurface using a drill rig, the instrument cannot be removed easily or at all, and if such instruments are used for critical measurements, redundancy of such instrumentation is important.

For the Waterbury Center site, the vibrating wire pressure transducers continued to work well after two years of service. The vibrating wire barometer was damaged by water infiltration caused by improper installation, and the instrument was simply removed and returned to the manufacturer for repair.

8. The solar panel-battery system used at the Waterbury Center site has performed remarkably well and sufficient power has always been available. For some UMass Amherst projects the solar panel-battery system was not reliable. Some instruments and devices, such as the cellular modem, can draw large amounts of power, and if the solar panel is not sized

correctly, the battery cannot be fully recharged. In addition, long-term degradation of the battery can lead to insufficient power. For maximum reliability, systems should be hard wired to grid power wherever available with an in-line battery for potential power outages.

9. For some UMass Amherst projects, rodents, and in particular mice, have eaten the sensor wires, leading to short circuits. Damage can range from individual sensors no longer working to failure of the entire data acquisition system. No damage from rodents occurred at the Waterbury Center project.

10. Lightening Strikes. Although lightening protection is installed on the various data acquisition system components and proper grounding is critical, no system is able to withstand a direct lightning strike. At one UMass Amherst project, the data acquisition system was destroyed by a lightening strike. No damage due to lightening was experienced at the Waterbury Center site.

11. Vandalism. Various instruments and components are exposed, such as the rain gauge, solar panel, and cellular antenna and all the major components of the data acquisition system need to be accessible to authorized personnel for maintenance and repair. This leaves the data acquisition system susceptible to vandalism, and in areas where vandalism could be expected, extra care should be taken to protect the system. For one UMass Amherst project, several instruments were pulled out of the ground and destroyed by vandals. No acts of vandalism were encountered at the Waterbury Center site.

7.1.2 Instrumentation Data Handling and Visualization

1. Volume of data. Fully automated data acquisition systems can produce enormous amounts of data. For smaller projects, with a few instruments and short project durations, spreadsheet-based data storage and visualization software (e.g., Excel) can be effectively used. Projects with a larger array of instruments or projects requiring monitoring over long time spans benefit the most from database-based data storage, and can incorporate near-real time early warning systems. Management of a database-based system can include a steep learning curve for initial setup, but after the software is configured, it virtually runs itself. Spreadsheet-based systems can require significant time throughout the life of the project as data is manually

imported and plots updated. Such files can also get very large and unstable, and become cumbersome to transfer among users.

2. Data visualization. The Canary Systems software used to set up the server based system for this project was found to be versatile and very useful. By setting up a user account and password based system, approved users can call-up and look at the project data from any internet connected computer. All instrumentation data can be inspected and a variety of tables and plots of user input time periods can easily be created. Furthermore, the software can handle multiple, independent, projects with separate user accounts for each project.

For this project the server simply consisted on a standard Dell desktop computer with a dedicated IP address and uninterruptible power supply (UPS) system. Although Canary Systems recommends the Microsoft Server operating system, for smaller projects such as the Waterbury Center project, Microsoft Windows XP Pro with the Internet Information Service tool kit installed was used and worked reliably.

3. Backup data. Automated instrumentation produces no paper backup and readings are not recorded in a field book. Care should be taken to regularly backup the spreadsheet or database files. Although no data was lost during the Waterbury Center project, updating of the Multilogger software to the current version often required restoring of database files from a backup copy.

7.1.3 Implementation of Early Warning System

1. The hardware and software used in this project all appeared well suited for implementation of a reliable early warning system for slope movement. Trigger values and hence alarms are easy to set in the Canary Systems software and a variety of messaging functions such as email and pager notification are available and easy to implement.

2. For most natural slopes rising in situ pore water pressure is usually the key trigger of slope movement. For a selected soil profile and corresponding soil properties, the factor of safety for the Waterbury Center slope is linearly related to the water table elevation (in the absence of any other influencing factors such as construction, undercutting by the base stream, etc.). Therefore the water table elevation can serve as a simple and reliable indicator of potential slope

movement. Alarms can be set making direct use of the water table instrumentation readings and/or in combination with other alarms for key inclinometers. Extending this further, developing a correlation between intensity and duration of rain events and water table rise can also serve as a useful trigger with possible exception of during winter months.

7.2 RECOMMENDATIONS FOR FUTURE WORK

In addition to the recommendations given in the previous section as part of the lessons learned on the Waterbury Center and other UMass Amherst projects, several other recommendations for future work are as follows.

7.2.1 Piezometers

The two open standpipe piezometers installed for the Waterbury Center project have continuous screens incorporating several soil layers and are therefore technically monitoring wells and not piezometers. Monitoring Well #1 is screened from 1.65 to 6.22 m (5.4 to 20.4 ft.) and includes both the gravely sand and the silt layer below. Monitoring Well #2 is screened from 3.05 to 7.62 m (10 to 25 ft.) and includes the silt layer and probably the silty clay layer. The two monitoring wells are sufficient for measuring the ground water table elevation and therefore for use in the slope stability analysis if the pore pressures are assumed to be hydrostatic. Given the geometry of the Waterbury Center slope this is unlikely to be the case. Since the pore water pressure in the silty clay layer has the greatest effect on the stability of the slope, buried or push in piezometers or open standpipe piezometers screened only in specific soil units such as the silty clay layer would allow the stability analysis to be more accurate.

This is of greater importance if seepage is included in the stability analysis. Knowing the pore pressures across the complete cross section is needed for accuracy in the model. Additional piezometers located upslope of Monitoring Well #2 are recommended. In addition, a piezometer located just upslope of the brook would allow for the location of the ground water table as it leaves the slope to be fixed rather than assumed in the slope stability model.

7.2.2 Deformation Based Early Warning

The work conducted in this project shows that stability of the Waterbury Center slope is most often directly related to the water table elevation. Conducting the stability analysis using Slide allowed for a direct correlation to be determined between water table elevation at the

monitoring well locations and the factor of safety. However, the key issue for safety is slope movement and thus similar such analysis should be conducted for slope movement. This cannot be done using limit equilibrium software such as Slide but rather has to be done using other numerical techniques such as finite elements. Such an analysis should be conducted using a parametric approach so that events such as rising water table and its impact on potential slope movement can be modeled and studied. This would indicate the locations of maximum slope movement and allow for trigger values to be selected for key inclinometers.

7.2.3 MEMS Based Sensors

The state-of-the-art in geotechnical instrumentation is constantly evolving and is currently dominated by micro-electro-mechanical-system (MEMS) based sensors. When the Waterbury Center project was created and instrumentation was selected, MEMS based sensors were not readily available commercially.

According to Sellers and Taylor (2008), the first MEMS based sensors for use in geotechnical instrumentation consist of accelerometers and are used in tilt sensors and inclinometers. The benefits of MEMS include:

- Inexpensive
- High shock tolerance (a 0.2 g sensor can withstand a 20,000 g shock)
- Low drift and thermal coefficients (~ 1 arc-second per degree C)
- Very good intrinsic linearity
- Stable, sensitive, and accurate
- Cable lengths up to 500 m
- Small size (as small as 13mm)
- Low power consumption (around 20 mW)

Replacement of accelerometer or vibrating-wire based in-place-inclinometers with MEMS based IPIs is now (2008) a commercially available solution for slope stability monitoring. In addition to the benefits listed above, MEMS based sensors have the ability to be addressed individually on a common communication cable by the datalogger. At one project in Boston, twenty MEMS based IPIs were installed in one borehole and connected together by one cable (Dunnicliff 2008). This increases the resolution available to IPI systems, which would be of great benefit for projects such as the Waterbury Center site.

The most impressive use of MEMS based sensors is the ShapeAccelArray (SAA, www.measurand.com) described by Abdoun and Bennett (2008), which is capable of measuring three-dimensional ground deformations at 30 cm (1 ft.) intervals to a depth of 100 m (330 ft.). Vibrations due to earthquakes or construction activities can also be measured. Because of the small size of MEMS, the SAA can fit into a 25 mm (1 in.) casing for installation and flexible enough to be rolled up on a reel for shipping and storage (Abdoun and Bennett 2008). Although the costs of an SAA can be high, the system was designed to be retrievable and reusable to offset the capital costs, and can be shortened or lengthened by the manufacturer depending on future project requirements (Abdoun and Bennett 2008). Two recent research projects on the use of SAA systems were conducted by Rensselaer Polytechnic Institute in collaboration with CalTrans and NYDOT.

8.0 REFERENCES

AASHTO (2004). Volume 2: Standard specifications for transportation materials and methods of sampling and testing. AASHTO, Washington D.C.

Abdoun, T. & Bennett, V. (2008). "A new wireless MEMS-based system for real-time deformation monitoring." Geotechnical News, 26(1), pp. 36-40.

ASTM (2006). Annual Book of Standards, Volume 04.08, Soil and Rock (1); D420-5611. ASTM, Philadelphia, PA.

Barendse, M.B. (2008). "Field evaluation of a MEMS-based, real-time deformation monitoring system." Geotechnical News, 26(1), pp. 41-44.

Becker, D.E., Crooks, J.H.A., Been, K., & Jeffries, M.G. (1987). "Work as a criterion for determining in situ and yield stresses in clays." Canadian Geotechnical Journal, 24(4), pp. 549-564.

Bennett, V., Abdoun, T., Danisch, L., Shantz, T., & Jang, D. (2007). Unstable slope monitoring with a wireless shape-acceleration array system. Geotechnical Special Publication, (175), pp. 38.

Campbell Scientific (2006). CR10X measurement and control system. Logan, UT: Campbell Scientific.

Cedergren, Harry R. (1967). Seepage, drainage, and flow nets. New York: John Wiley & Sons.

Dennis, N.D., Ooi, C.W., & Wong, V.H. (2006). "Estimating movement of shallow slope failures using time domain reflectometry." Proc. TDR 2006. West Lafayette, IN.

Ding, X., Ren, D., Montgomery, B., & Swindells, C. (2000). "Automatic monitoring of slope deformations using geotechnical instruments." *Journal of Surveying Engineering*, 126(2), pp. 57-68.

Duncan, J.M. & Wright, S.G. (2005). Soil strength and slope stability. New York: John Wiley & Sons.

Dunnicliff, J. (2008). "Geotechnical instrumentation news." Geotechnical News, 26(1), pp. 31-32.

Dunnicliff, J. (1988). Geotechnical instrumentation for monitoring field performance. New York: John Wiley & Sons.

Furlani, K.M., Miller, P.K., & Mooney, M.A. (2005). "Evaluation of a wireless sensor node for measuring slope inclination in geotechnical applications." Proc. 22nd International Symposium on Automation and Robotics in Construction. Ferrara, Italy.

Gale, M.H., Kim, J., King, S., Montane, P., & Orsi, C. (2006). "Bedrock geologic map of the southern Worcester Mountains watershed, Middlesex and Stowe 7.5 minute quadrangles, Vermont." Montpelier: Vermont Geological Survey.

Geokon (2007). Instruction manual: model 6300 vibrating wire in-place-inclinometer. Lebanon, NH: Geokon.

Hawkes, M. & Marr, W.A. (1999). "Data acquisition and management for geotechnical instrumentation on the central Artery/Tunnel project." Field Instrumentation for Soil and Rock, ASTM STP 1358, pp. 319.

Kane, W.F., & Beck, T.J. (2000). "Instrumentation practice for slope monitoring." Engineering Geology Practice in Northern California. Association of Engineering Geologists.

Kane, W.F., Holzhausen, G.R., & Constable, E. (2004). "Coastal bluff monitoring/alert system for railways." Geotechnical Special Publication, (126), pp. 2067.

Kosnik, D.E., Kotowsky, M.P., Dowding, C.H., & Finno, R.J. (2007). "Case studies in integrated autonomous remote monitoring." Geotechnical Special Publication, (175), pp. 95.

Kosnik, D.E. (2007). "Internet-enabled geotechnical data exchange." Geotechnical Special Publication, (175), pp. 88.

Ladd, C.C., & DeGroot, D.J. (2003). "Recommended practice for soft ground site chacterization: Arthur Casagrande Lecture." Proc. 12th Panamerican Conf. on Soil Mechanics and Geotechnical Engineering, Boston, MA, pp. 3-57.

Larsen, F.D., (1987a). "Glacial Lake Hitchcock in the valleys of the White and Ottauqueche Rivers, east-central Vermont." *Guidebook for Field Trips in Vermont Volume 2*. 79th Annual Meeting of the New England Intercollegiate Geological Conference, Montpelier, VT. pp. 29-52.

Larsen, F.D., (1987b). "History of glacial lakes in the Dog River Valley, central Vermont." *Guidebook for Field Trips in Vermont Volume 2*. 79th Annual Meeting of the New England Intercollegiate Geological Conference, Montpelier, VT. pp. 213-236.

Lollino, G., Arattano, M., Allasia, P. & Giordan, D. (2006). "Time response of a landslide to meteorological events." Natural Hazards and Earth System Sciences, 6, pp. 179-184.

Marr, W.A. (1999). "Uses of automated geotechnical instrumentation systems." Field Instrumentation for Soil and Rock, ASTM STP 1358, pp. 36.

Marr, W.A. (2005). “Automated collection of instrumentation data.” BSCES Geo-Institute One-Day Seminar. Waltham, MA.

O'Connor, K., Clark, R. J., Whitlatch, D.J., & Dowding, C.H. (2001). “Real-time monitoring of subsidence along I-70 in Washington, Pennsylvania.” Transit, 1772(-1), pp. 32-39.

O’Connor, K.M. (2006). “TDR Based Alarm Systems.” Proc. TDR 2006. West Lafayette, IN.

Sandbeakken, G., Berre, T. & Lacasse, S. (1986). “Oedometer Testing at the Norwegian Geotechnical Institute.” Consolidation of Soils: Testing and Evaluation, ASTM STP 892, pp. 329-353.

Sellers, J.B. & Taylor, R. (2008). “MEMS basics.” Geotechnical News, 26(1), pp. 32-33.

Simeoni, L. & Mongiovi, L. (2007). “Inclinometer monitoring of the Castelrotto landslide in Italy.” Journal of Geotechnical and Geoenvironmental Engineering, 133(6), pp. 653-666.

Spencer, E. (1967). “A method of analysis of stability of embankments assuming parallel inter-slice forces.” Géotechnique, 17(1), pp. 11-26.

Springston, G. & Dunn, R. (2006). “Surficial geologic map of the southern Worcester Mountains, Vermont.” Montpelier: Vermont Geological Survey.

Stewart, D.P., & Vermont Geological Survey. (1961). The glacial geology of Vermont. Montpelier: Vermont Development Dept.

Thorarinsson, A. (2007). “Methods for automatic storage, visualization, and reporting in datalogging applications.” Geotechnical Special Publication, (175), pp. 101.

Vermont Agency of Transportation (2005). “Reservoir Road Slide Failure.” Letter report.

Wissa, A.E.Z., Christain, J.T., Davis, E.H., & Heiberg, S. (1971). “Consolidation at constant rate of strain.” Journal of the Soil Mechanics and Foundations Division, 97(SM10), pp.1393-1413.

APPENDIX A

This appendix contains the boring and construction logs generated by VTrans during the drilling of Inclinometers #1, #2, and #3, and Monitoring Wells #1 and #2.

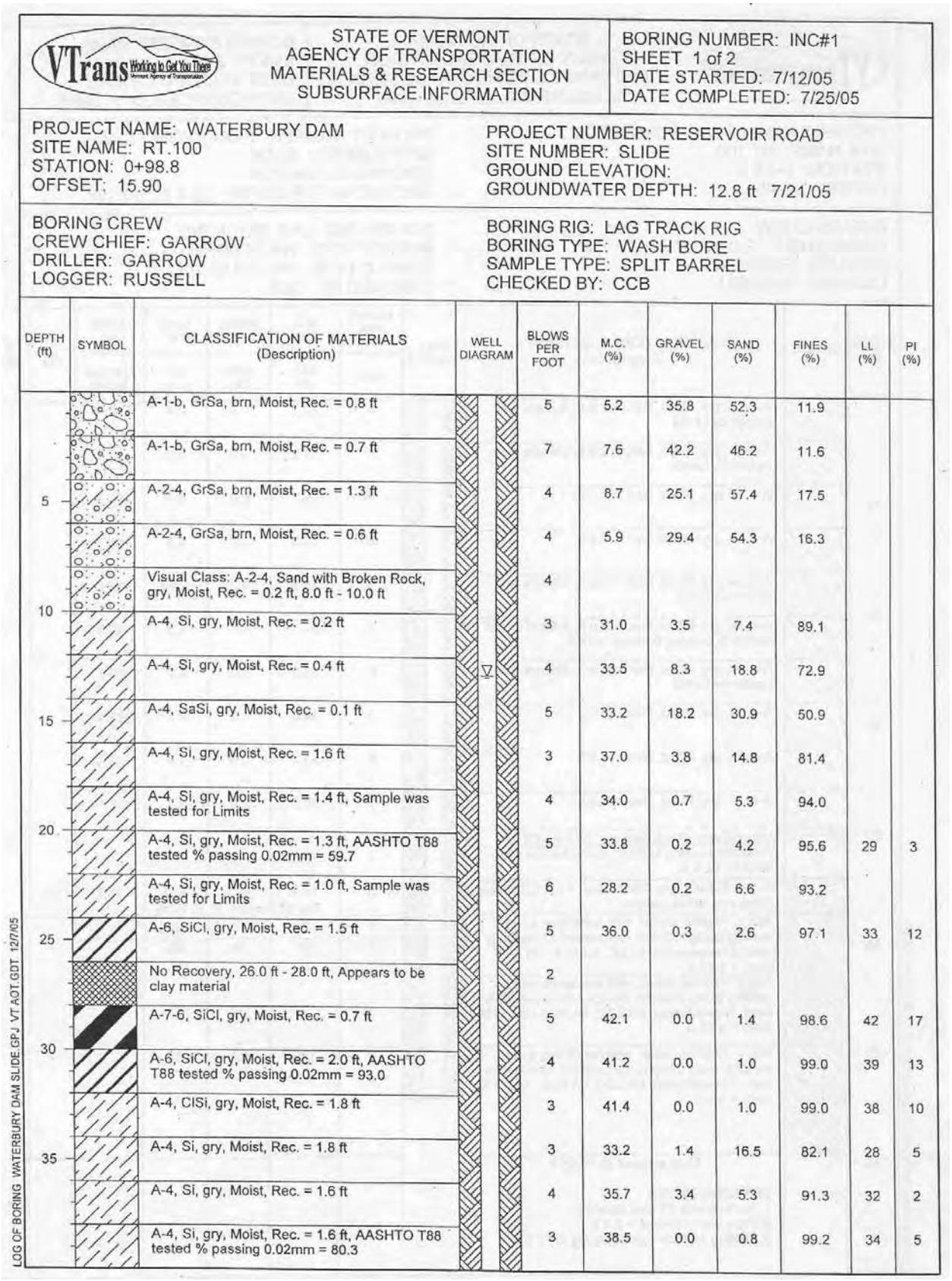

STATE OF VERMONT
AGENCY OF TRANSPORTATION
MATERIALS & RESEARCH SECTION
SUBSURFACE INFORMATION

BORING NUMBER: INC#1
SHEET 1 of 2
DATE STARTED: 7/12/05
DATE COMPLETED: 7/25/05

PROJECT NAME: WATERBURY DAM
SITE NAME: RT.100
STATION: 0+98.8
OFFSET: 15.90

PROJECT NUMBER: RESERVOIR ROAD
SITE NUMBER: SLIDE
GROUND ELEVATION:
GROUNDWATER DEPTH: 12.8 ft 7/21/05

BORING CREW
CREW CHIEF: GARROW
DRILLER: GARROW
LOGGER: RUSSELL

BORING RIG: LAG TRACK RIG
BORING TYPE: WASH BORE
SAMPLE TYPE: SPLIT BARREL
CHECKED BY: CCB

DEPTH (ft)	SYMBOL	CLASSIFICATION OF MATERIALS (Description)	WELL DIAGRAM	BLOWS PER FOOT	M.C. (%)	GRAVEL (%)	SAND (%)	FINES (%)	LL (%)	PI (%)
		A-1-b, GrSa, brn, Moist, Rec. = 0.8 ft		5	5.2	35.8	52.3	11.9		
		A-1-b, GrSa, brn, Moist, Rec. = 0.7 ft		7	7.6	42.2	46.2	11.6		
5		A-2-4, GrSa, brn, Moist, Rec. = 1.3 ft		4	8.7	25.1	57.4	17.5		
		A-2-4, GrSa, brn, Moist, Rec. = 0.6 ft		4	5.9	29.4	54.3	16.3		
		Visual Class: A-2-4, Sand with Broken Rock, gry, Moist, Rec. = 0.2 ft, 8.0 ft - 10.0 ft		4						
10		A-4, Si, gry, Moist, Rec. = 0.2 ft		3	31.0	3.5	7.4	89.1		
		A-4, Si, gry, Moist, Rec. = 0.4 ft	▽	4	33.5	8.3	18.8	72.9		
15		A-4, SaSi, gry, Moist, Rec. = 0.1 ft		5	33.2	18.2	30.9	50.9		
		A-4, Si, gry, Moist, Rec. = 1.6 ft		3	37.0	3.8	14.8	81.4		
		A-4, Si, gry, Moist, Rec. = 1.4 ft, Sample was tested for Limits		4	34.0	0.7	5.3	94.0		
20		A-4, Si, gry, Moist, Rec. = 1.3 ft, AASHTO T88 tested % passing 0.02mm = 59.7		5	33.8	0.2	4.2	95.6	29	3
		A-4, Si, gry, Moist, Rec. = 1.0 ft, Sample was tested for Limits		6	28.2	0.2	6.6	93.2		
25		A-6, SiCl, gry, Moist, Rec. = 1.5 ft		5	36.0	0.3	2.6	97.1	33	12
		No Recovery, 26.0 ft - 28.0 ft, Appears to be clay material		2						
		A-7-6, SiCl, gry, Moist, Rec. = 0.7 ft		5	42.1	0.0	1.4	98.6	42	17
30		A-6, SiCl, gry, Moist, Rec. = 2.0 ft, AASHTO T88 tested % passing 0.02mm = 93.0		4	41.2	0.0	1.0	99.0	39	13
		A-4, ClSi, gry, Moist, Rec. = 1.8 ft		3	41.4	0.0	1.0	99.0	38	10
35		A-4, Si, gry, Moist, Rec. = 1.8 ft		3	33.2	1.4	16.5	82.1	28	5
		A-4, Si, gry, Moist, Rec. = 1.6 ft		4	35.7	3.4	5.3	91.3	32	2
		A-4, Si, gry, Moist, Rec. = 1.6 ft, AASHTO T88 tested % passing 0.02mm = 80.3		3	38.5	0.0	0.8	99.2	34	5

LOG OF BORING WATERBURY DAM SLIDE.GPJ VT AOT.GDT 12/7/05

Figure A.1 Inclinometer #1 boring log, from the ground surface to a depth of 40 ft.

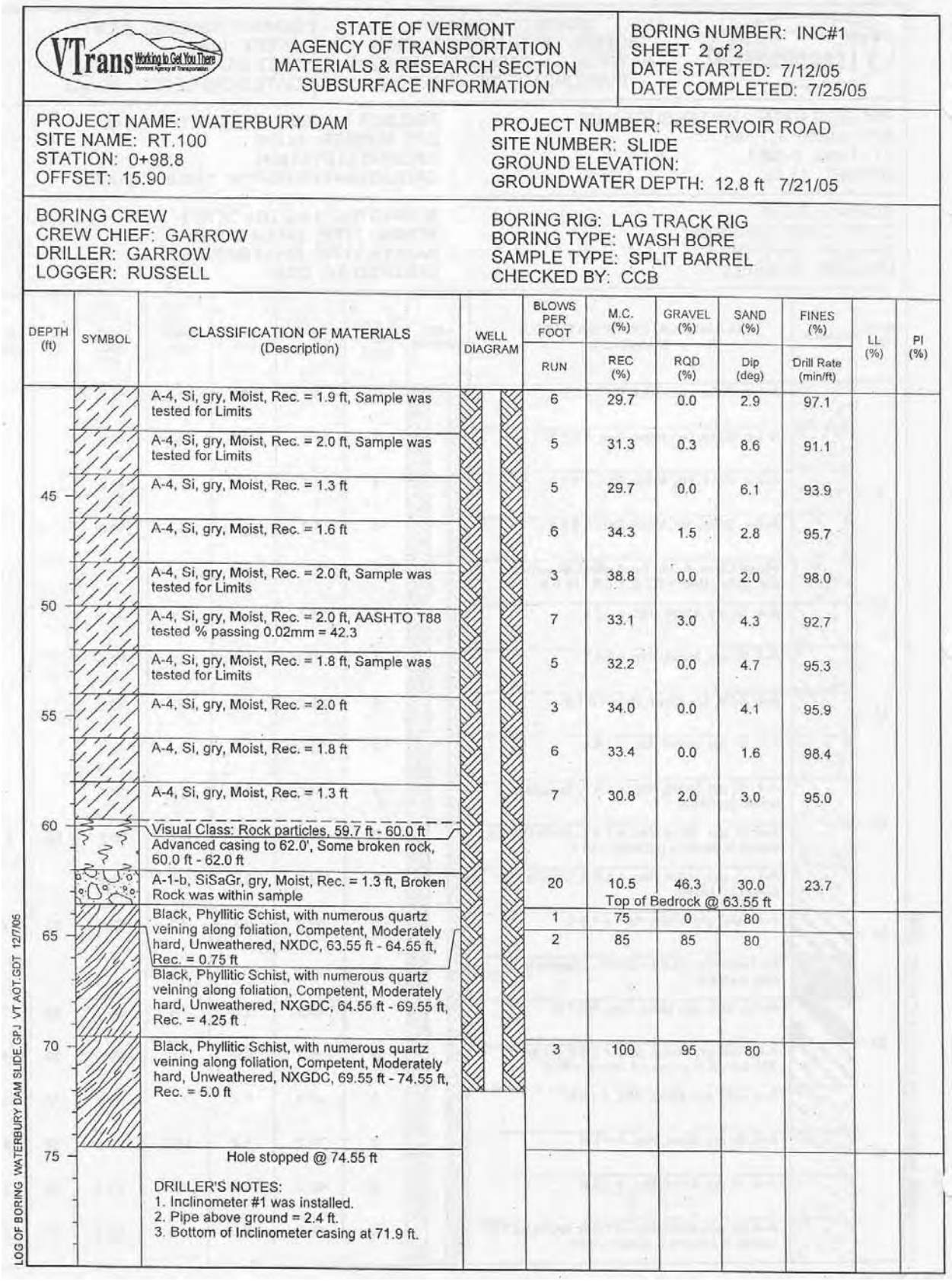

STATE OF VERMONT
AGENCY OF TRANSPORTATION
MATERIALS & RESEARCH SECTION
SUBSURFACE INFORMATION

BORING NUMBER: INC#1
SHEET 2 of 2
DATE STARTED: 7/12/05
DATE COMPLETED: 7/25/05

PROJECT NAME: WATERBURY DAM
SITE NAME: RT.100
STATION: 0+98.8
OFFSET: 15.90

PROJECT NUMBER: RESERVOIR ROAD
SITE NUMBER: SLIDE
GROUND ELEVATION:
GROUNDWATER DEPTH: 12.8 ft 7/21/05

BORING CREW
CREW CHIEF: GARROW
DRILLER: GARROW
LOGGER: RUSSELL

BORING RIG: LAG TRACK RIG
BORING TYPE: WASH BORE
SAMPLE TYPE: SPLIT BARREL
CHECKED BY: CCB

DEPTH (ft)	SYMBOL	CLASSIFICATION OF MATERIALS (Description)	WELL DIAGRAM	BLOWS PER FOOT / RUN	M.C. (%) / REC (%)	GRAVEL (%) / RQD (%)	SAND (%) / Dip (deg)	FINES (%) / Drill Rate (min/ft)	LL (%)	PI (%)
		A-4, Si, gry, Moist, Rec. = 1.9 ft, Sample was tested for Limits		6	29.7	0.0	2.9	97.1		
		A-4, Si, gry, Moist, Rec. = 2.0 ft, Sample was tested for Limits		5	31.3	0.3	8.6	91.1		
45		A-4, Si, gry, Moist, Rec. = 1.3 ft		5	29.7	0.0	6.1	93.9		
		A-4, Si, gry, Moist, Rec. = 1.6 ft		6	34.3	1.5	2.8	95.7		
		A-4, Si, gry, Moist, Rec. = 2.0 ft, Sample was tested for Limits		3	38.8	0.0	2.0	98.0		
50		A-4, Si, gry, Moist, Rec. = 2.0 ft, AASHTO T88 tested % passing 0.02mm = 42.3		7	33.1	3.0	4.3	92.7		
		A-4, Si, gry, Moist, Rec. = 1.8 ft, Sample was tested for Limits		5	32.2	0.0	4.7	95.3		
55		A-4, Si, gry, Moist, Rec. = 2.0 ft		3	34.0	0.0	4.1	95.9		
		A-4, Si, gry, Moist, Rec. = 1.8 ft		6	33.4	0.0	1.6	98.4		
		A-4, Si, gry, Moist, Rec. = 1.3 ft		7	30.8	2.0	3.0	95.0		
60		Visual Class: Rock particles, 59.7 ft - 60.0 ft Advanced casing to 62.0', Some broken rock, 60.0 ft - 62.0 ft								
		A-1-b, SiSaGr, gry, Moist, Rec. = 1.3 ft, Broken Rock was within sample		20	10.5	46.3	30.0	23.7		
					Top of Bedrock @ 63.55 ft					
		Black, Phyllitic Schist, with numerous quartz veining along foliation, Competent, Moderately hard, Unweathered, NXDC, 63.55 ft - 64.55 ft, Rec. = 0.75 ft		1	75	0	80			
65		Black, Phyllitic Schist, with numerous quartz veining along foliation, Competent, Moderately hard, Unweathered, NXGDC, 64.55 ft - 69.55 ft, Rec. = 4.25 ft		2	85	85	80			
70		Black, Phyllitic Schist, with numerous quartz veining along foliation, Competent, Moderately hard, Unweathered, NXGDC, 69.55 ft - 74.55 ft, Rec. = 5.0 ft		3	100	95	80			
75		Hole stopped @ 74.55 ft								

DRILLER'S NOTES:
1. Inclinometer #1 was installed.
2. Pipe above ground = 2.4 ft.
3. Bottom of Inclinometer casing at 71.9 ft.

LOG OF BORING WATERBURY DAM SLIDE.GPJ VT AOT.GDT 12/7/06

Figure A.2 Inclinometer #1 boring log, from a depth of 40 ft. to bottom of drilling.

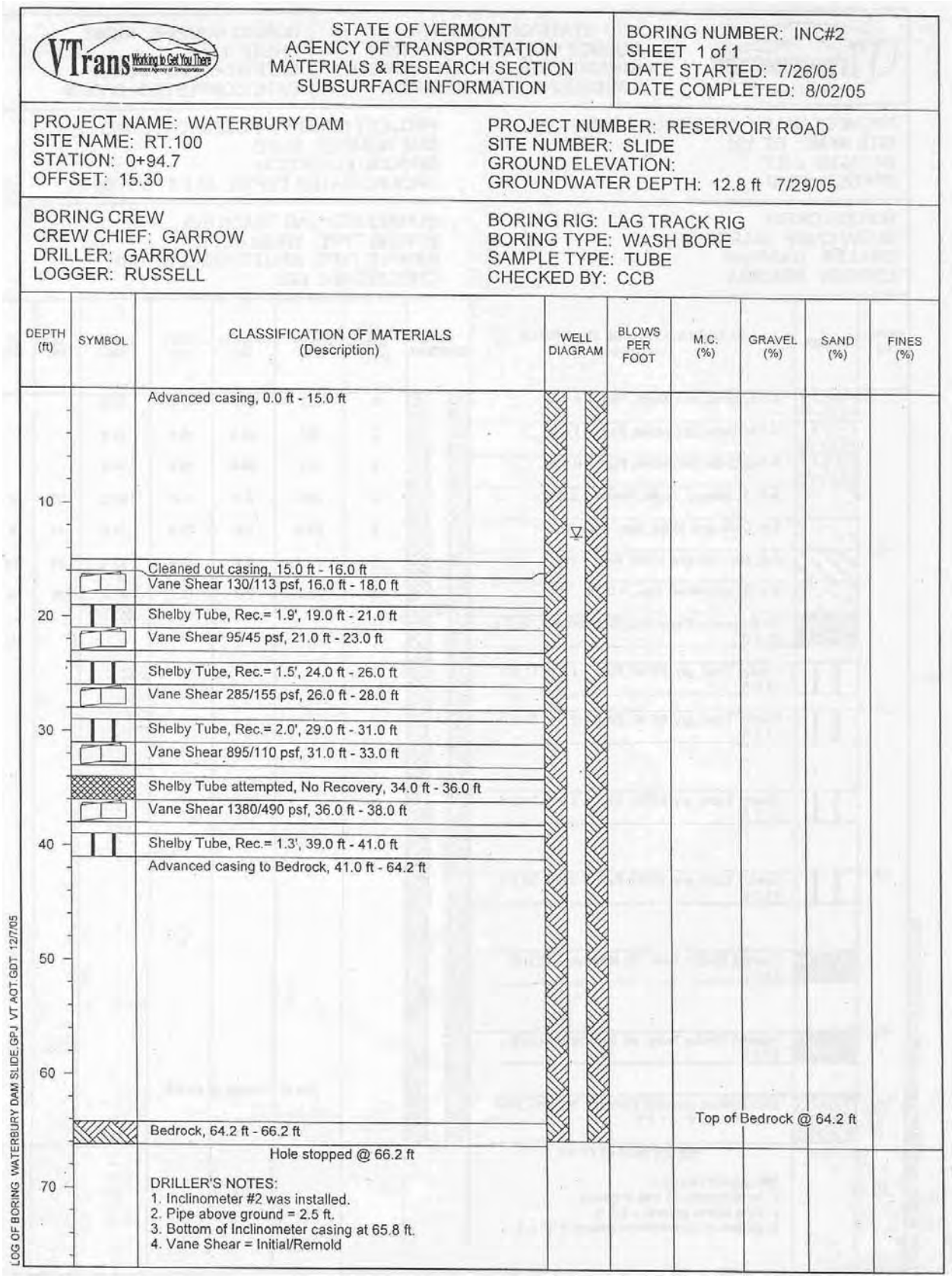

Figure A.3 Inclinometer #2 boring log

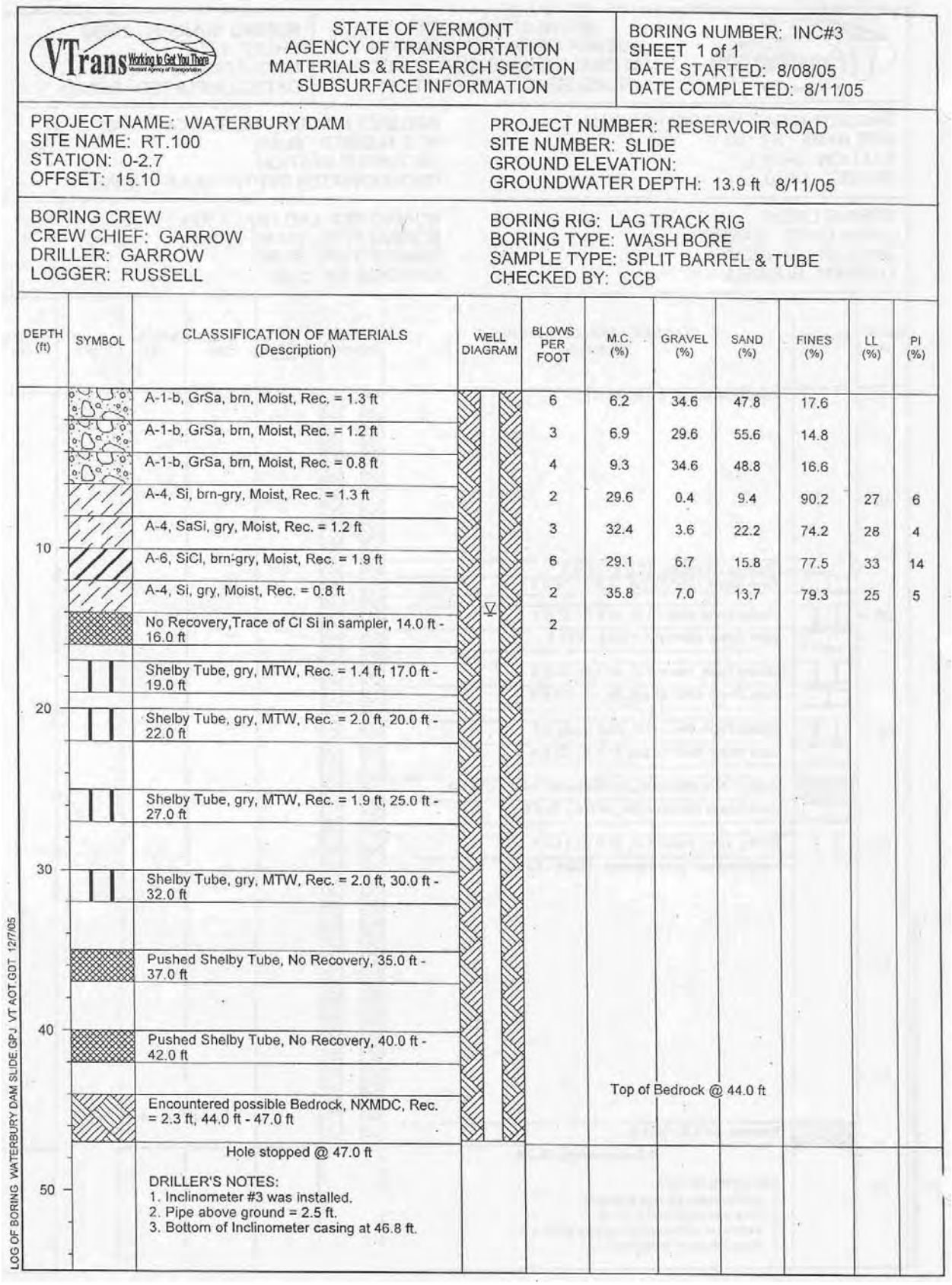

Figure A.4 Inclinometer #3 boring log.

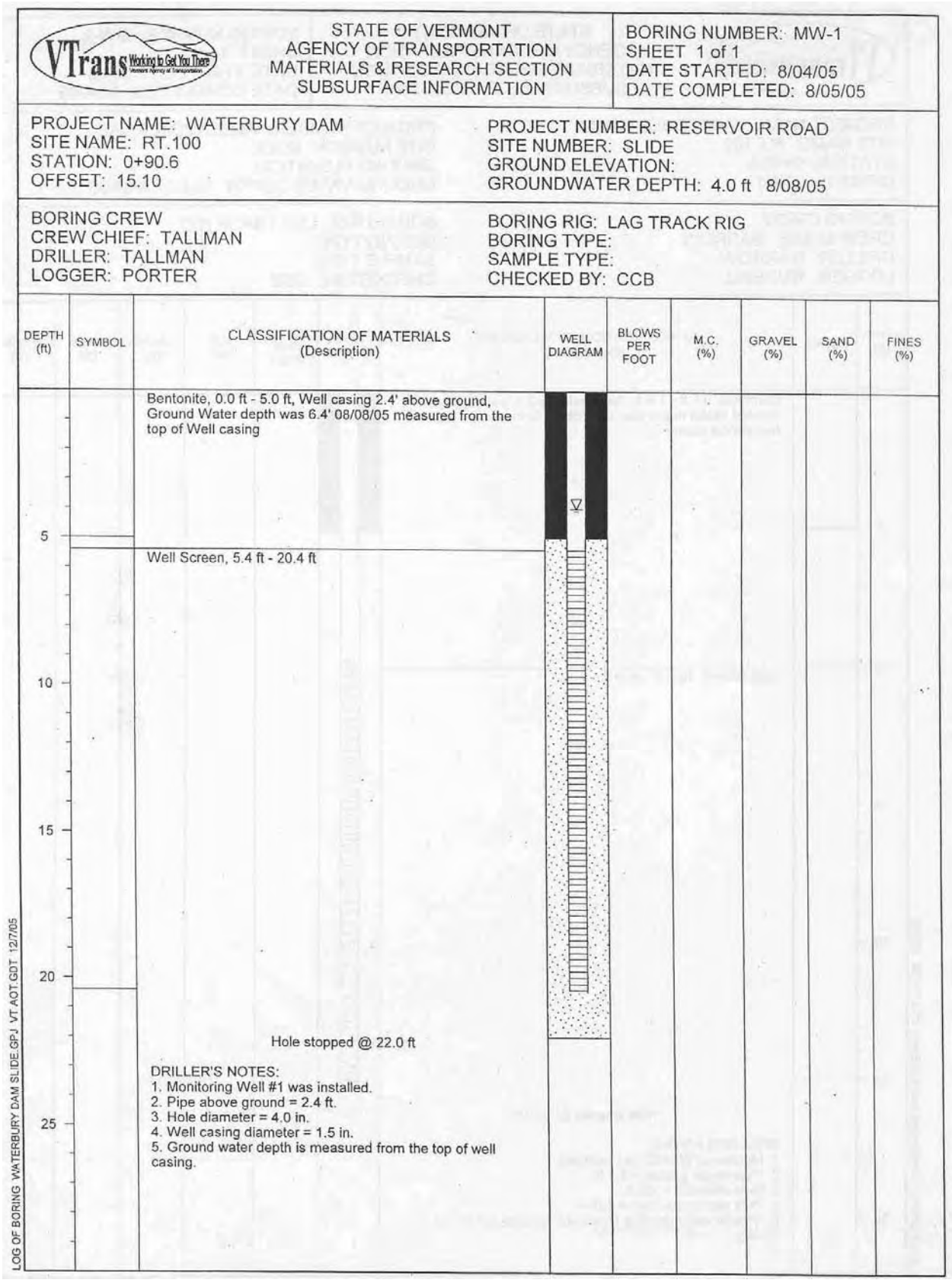

Figure A.5 Monitoring Well construction log.

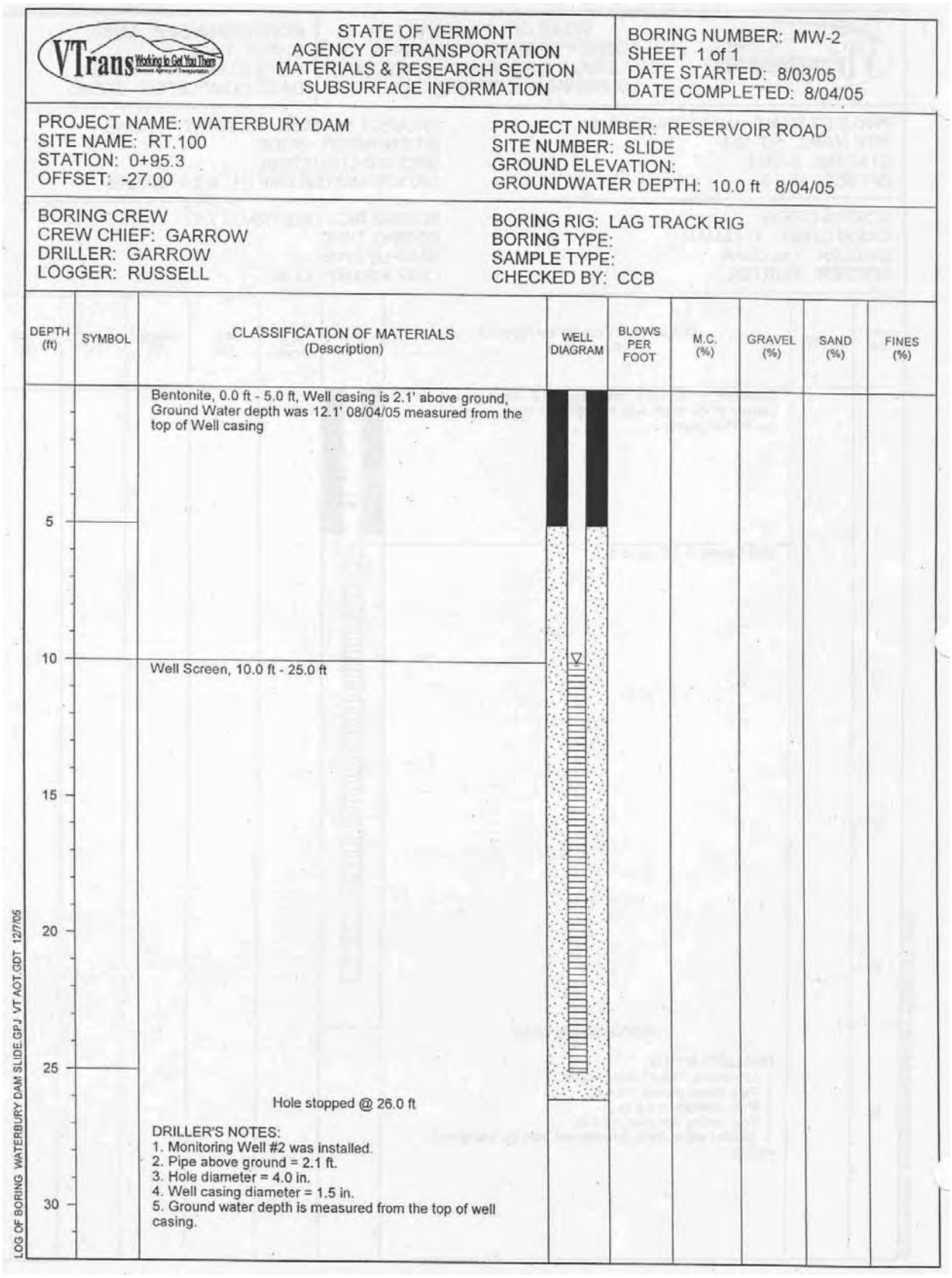

Figure A.6 Monitoring Well #2 construction log.

APPENDIX B

This appendix contains the cumulative displacement profiles generated by VTrans during manual inclinometer readings of Inclinometers #1, #2, and #3 prior to the installation of the in-place-inclinometers into Inclinometers #2 and #3.

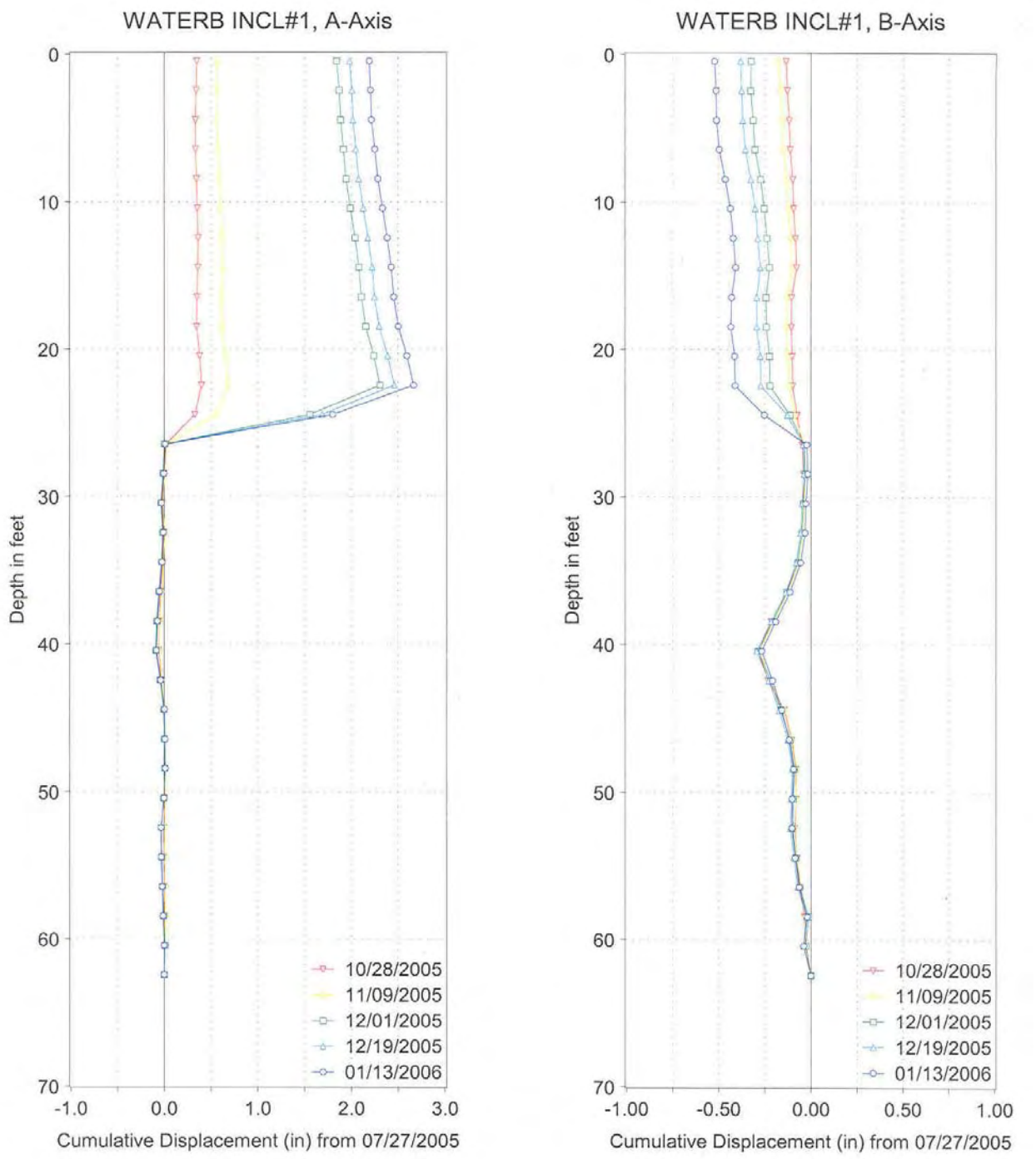

Figure B.1 Inclinometer #1 cumulative displacement profiles.

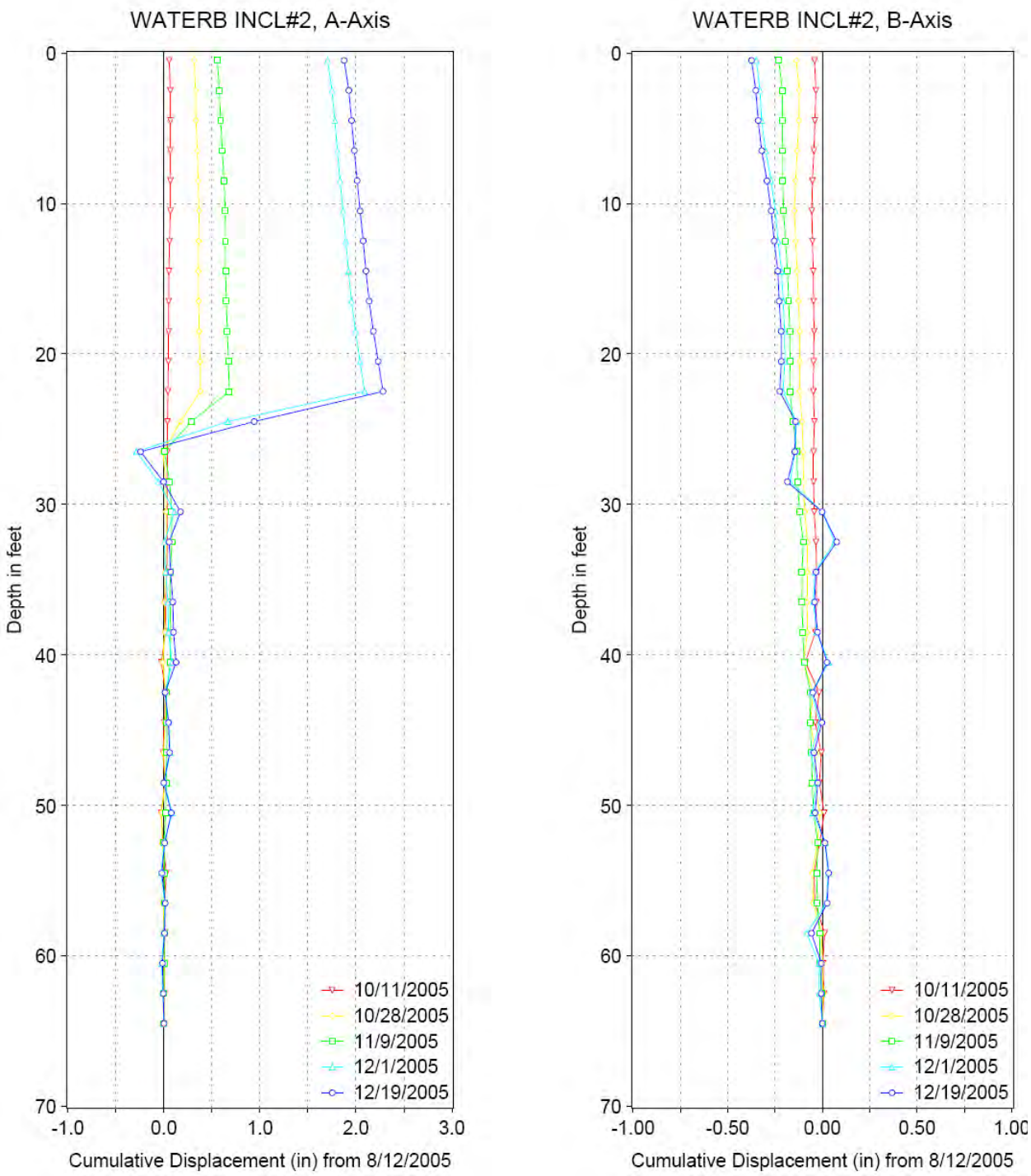

Figure B.2 Inclinometer #2 cumulative displacement profiles.

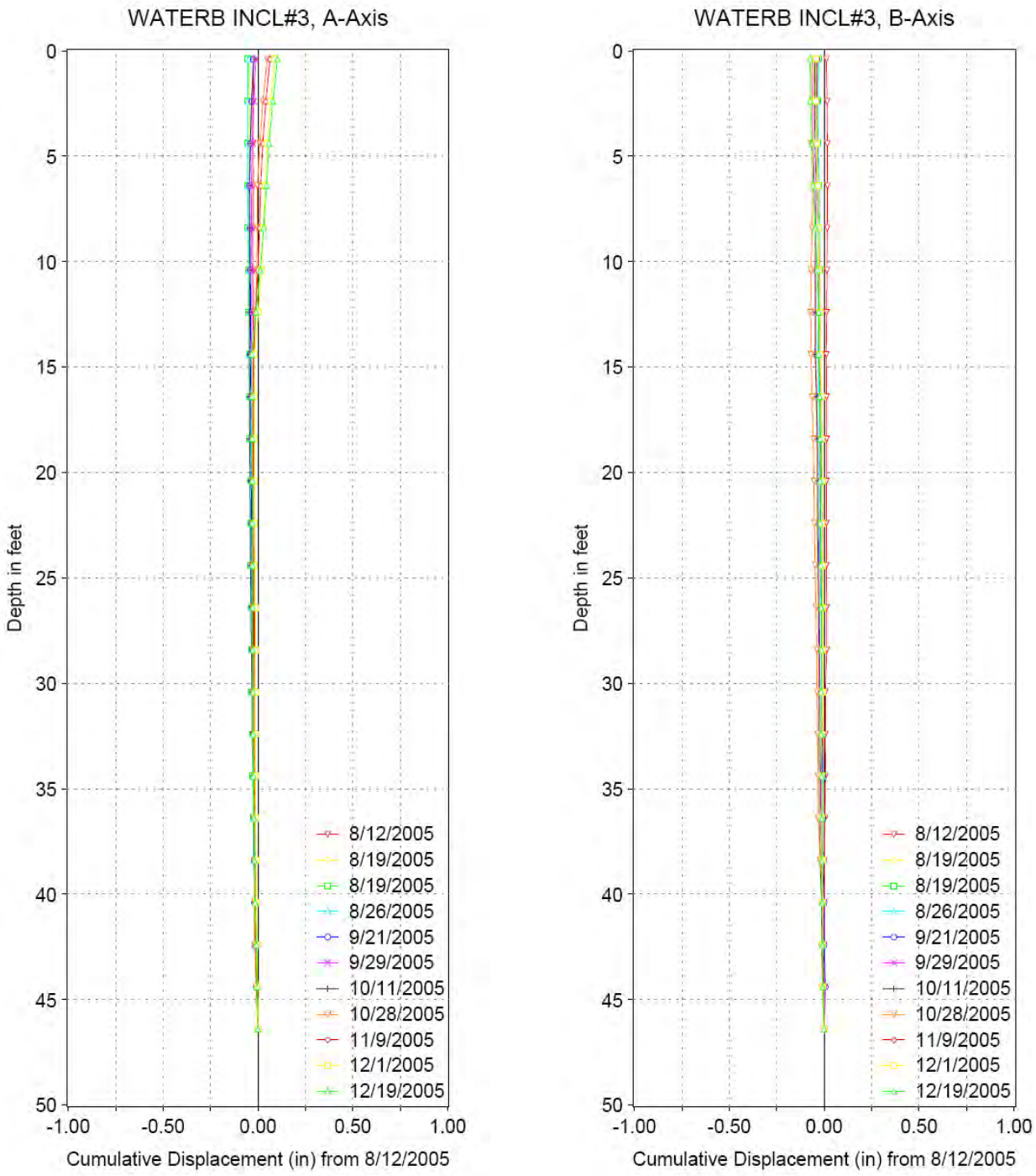

Figure B.3 Inclinometer #3 cumulative displacement profiles.

APPENDIX C

This appendix presents scale drawings showing the probable condition of the in-place-inclinometer string as installed in Inclinometer #2 on December 19, 2005. The deflection of the inclinometer casing was determined from results of the last manual probe inclinometer prior to the installation of the IPI string (Appendix B). The drawings show that the rigid connecting tubing between IPIs 05-16367 and 05-16369 was most likely contacting the side of the inclinometer casing, causing the effective gauge length to be less than the assumed length of 6.1 m (20 ft.).

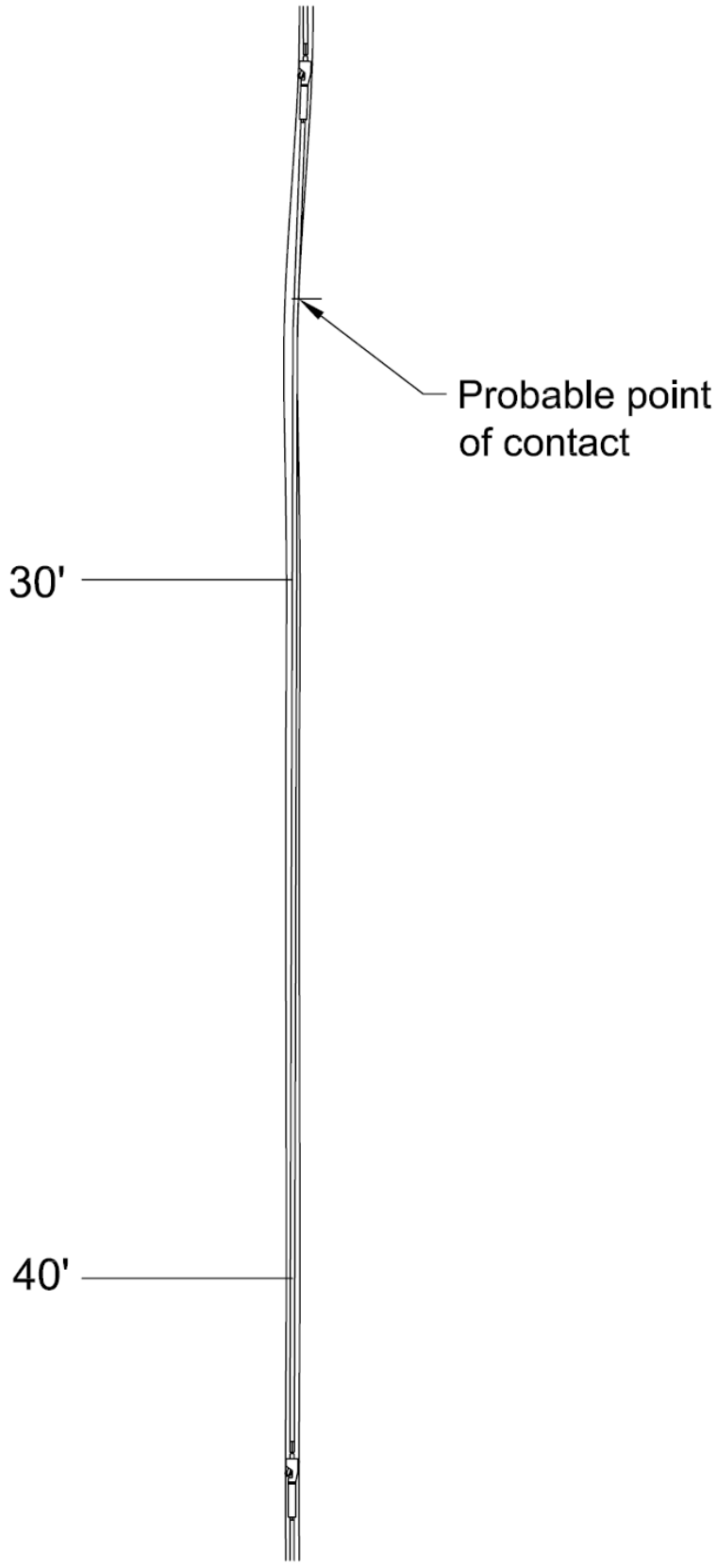

Figure C.1 Drawing showing rigid connecting tubing between IPIs 05-16367 and 05-16369.

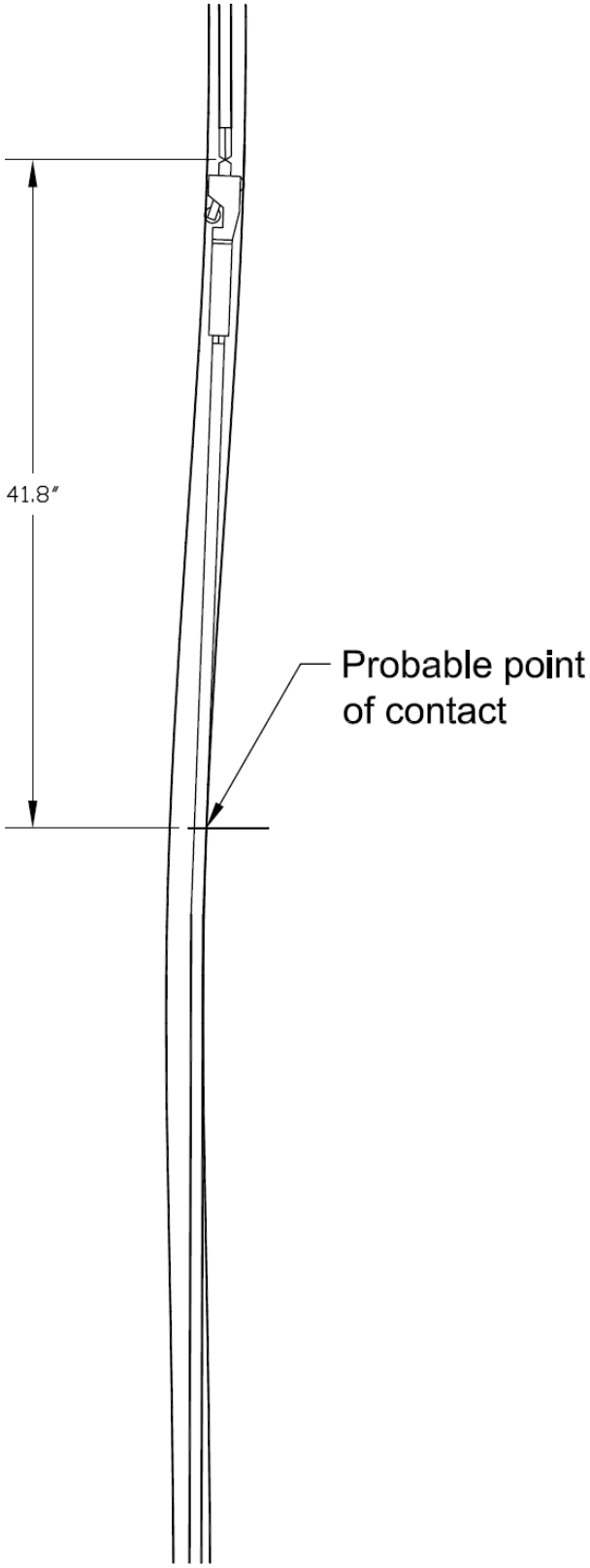

Figure C.2 Drawing showing the large deformation of the inclinometer casing in the vicinity of IPI 05-16367 and the probable point of contact between the casing and the rigid tubing.